TRACK/TRAIN DYNAMICS

by

WAGUIH HASSAN EL-MARAGHY, M.ENG.

A Thesis

Submitted to the School of Graduate Studies

in Partial Fulfilment of the Requirements

for the Degree

Doctor of Philosophy

McMaster University

April 1975

TRACK/TRAIN DYNAMICS

DOCTOR OF PHILOSOPHY (1975)   McMASTER UNIVERSITY
(Mechanical Engineering)   Hamilton, Ontario

TITLE: Track/Train Dynamics

AUTHOR: Waguih Hassan El-Maraghy, B.Sc. (Cairo
                              University)
                          M.Eng. (McMaster
                              University)

SUPERVISOR: Professor M.A. Dokainish

NUMBER OF PAGES: xxi, 240

ii

ABSTRACT

The dynamic response of the railway track modelled as a continuously supported beam on a Kelvin type foundation and subjected to an axial force and time dependent moving loads is studied. The transient and steady state solutions are found for the general case including all linear effects. This study shows the effects of axial force and damping on the dynamic response. The results also show that the effect of the velocity of the moving load on the dynamic response is small, and hence it is not necessary to consider the wave type expression to study the effect of track elasticity on the dynamics of railway vehicles.

An analysis for the dynamics of a railway vehicle including the effect of vertical track elasticity is presented, with particular emphasis on the lateral stability and the response to vertical track irregularities. The model used in the analysis is that of a six-axle locomotive of the type commonly used in North America. Wheel tread profile parameters, gravity stiffness effects and creep forces are included in the mathematical model.

The results show that an increase in vertical track elasticity results in a small increase in the

critical speed at which hunting instability occurs. The increase in track elasticity results in appreciable increase in the amplitude of the response to track irregularities especially at high frequencies.

A method for the minimization of the vibrations transmitted due to track irregularities using the minimax principle and mathematical programming techniques is suggested. The method is demonstrated by considering the minimization of the lateral cab acceleration within the frequency range of interest.

The analyses and digital computer simulations are viewed as analytical tools for studying the effect of changing the vehicle and/or track parameters on the dynamic response of both the vehicle and the track. The methods developed are general and can be used in the design stage to adjust geometry and/or suspension characteristics for any proposed design of a railway vehicle.

ACKNOWLEDGEMENTS

TABLE OF CONTENTS

LIST OF SYMBOLS

a
- constant for the beam ($\sqrt{EI/m}$)
- length of major axis for wheel/rail contact area

A
- constant depending on the magnitude of the principal curvatures of the surfaces in contact and the angles between the planes of principal curvature of the two surfaces

[Ã]
- mass matrix before elimination of internal reactions

[AD]
- mass matrix in generalized coordinates, for longitudinal modes (27 x 27)

[AT]
- mass matrix in generalized coordinates, for lateral modes (15 x 15)

b
- constant proportional to axial force in beam (N/2EI)
- length of minor axis for wheel/rail contact area

B
- constant depending on the magnitude of the principal curvatures of the surfaces in contact and the angles between the planes of principal curvature of the two surfaces

[B̃]
- stiffness matrix before the elimination of internal reactions

viii

[BD] — stiffness matrix in generalized coordinates, for longitudinal modes (27 x 27)

[BT] — stiffness matrix in generalized coordinates, for lateral modes (15 x 15)

c — coefficient of viscous damping per unit length of beam

— constant related to the dimensions of the wheel/rail contact area ($\sqrt{ab}$)

c_{cr} — coefficient of critical damping ($\sqrt{2km}$)

c_e — damping coefficient for lumped parameter model of the track

c_j — damping coefficient ($j = 1,\ldots,18$)

c_R — damping coefficient for rotational shock absorber

c_V — damping coefficient for lateral shock absorber

[C] — damping matrix

[C'] — damping matrix depending on the instantaneous prevailing values of $\{x\}$ and $\{\dot{x}\}$

[$\bar{C}$] — damping matrix of forcing function

[CD] — damping matrix in generalized coordinates, for longitudinal modes (27 x 27)

[CT] — damping matrix in generalized coordinates for lateral modes (15 x 15)

d — positive real root of equation (A.2.9)

D — differential operator

ix

$[D]$	– transformation matrix relating all the displacements to the independent displacements, for the longitudinal modes (Table B.2)
e_0	– half the lateral distance between the wheel/rail contact points, wheelset in central position
e_ℓ, e_r	– distance from center of track to left and right wheel/rail contact points respectively
E	– modulus of elasticity
f	– creep coefficient
$f(x)$	– initial displacement of beam
$f(\vec{x})^p$	– lateral acceleration at the cab
f_ℓ, f_u	– lateral acceleration at the cab for the lower and upper bounds of the frequency range of interest
$\{f_k(\vec{x})\}$	– vector of maximum lateral cab acceleration
f_0	– natural frequency for beam on elastic foundation $(\omega_0/2\pi)$
f_1	– coefficient relating longitudinal creep force to longitudinal creepage
f_2	– coefficient relating lateral creep force to lateral creepage
f_3	– coefficient relating creep torque to spin
f_{23}, f_{32}	– coefficients relating spin to lateral creep force and lateral creepage to creep torque
F	– Fourier transform of $f(x)$

$\mathcal{F}$ – Fourier transform operator

$\{F\}$ – forcing function

$\{\bar{F}\}$ – complex amplitude of forcing function

$g(x)$ – initial velocity of the beam

G – modulus of rigidity ($\frac{E}{2(1+\nu)}$)

     – Fourier transform of $g(x)$

$[G]$ – matrix whose eigenvalues give the natural frequencies of an n-degree of freedom dynamic system ($2n \times 2n$)

i – imaginary unit ($\sqrt{-1}$)

$I_\alpha, I_\beta, I_\gamma$ – mass moment of inertia about x, y and z-axis respectively

$[I]$ – unit matrix

J_ν – Bessel function of the first kind and order ν

k – track modulus

K_e – stiffness coefficient for lumped parameter model of the track

K_j – stiffness coefficient ($j = 1, \ldots, 12$)

$[K]$ – stiffness matrix

$[K']$ – stiffness matrix depending on the instantaneous prevailing values of $\{x\}$ and $\{\dot{x}\}$

$[\bar{K}]$ – stiffness matrix of forcing function

ℓ_e – effective length of rail

ℓ_j – length ($j = 1, \ldots, 35$)

$\mathcal{L}$ – Laplace transform operator

m – mass

     – mass of beam per unit length

M_z - creep torque

$[M]$ - mass matrix

$[\bar{M}]$ - mass matrix of forcing function

N - axial force in beam

    - normal force between two bodies in contact

N_{cr} - Euler buckling load

N_0 - reactions between wheels and rails, wheelset in central position

$N_{\ell j}, N_{rj}$ - reaction between rails and left and right wheels respectively for the laterally displaced wheelset number j

P - applied concentrated load

q - external load per unit length of the beam

Q - Fourier transform of q

$\bar{Q}$ - Laplace transform of Q

r_0 - wheel tread radius, wheelset in central position

r_ℓ, r_r - radii of left and right wheel tread circle, wheelset displaced laterally

RA,RB,RM   - internal reaction between frame and wheelset in the x, y and γ directions respectively

RV,RW,Rγ   - internal reaction between motor and wheelset in the v, w and γ directions respectively

s   - propagation velocity of travelling wave train

s_j - j^{th} eigenvalue (j^{th} root of matrix G)

.S   - forward speed of the railway vehicle

t   - time

T_x, T_y – longitudinal and lateral creep forces respectively

$[T]$ – transformation matrix relating all displacements to the independent displacements, for the lateral modes (Table B.1)

u – linear displacement of a mass center of gravity in the longitudinal (x) direction

U – objective function of optimization

v – linear displacement of a mass center of gravity in the lateral (y) direction

– velocity of moving load

v_{cr} – critical velocity for track

w – linear displacement of a mass center of gravity in the vertical (z) direction

W – gravity force per wheelset

x – distance along the beam

$\{x\}$ – generalized displacements

$\vec{x}$ – vector of design variables

$\vec{x}_{opt}$ – vector of optimum design variables

$\{\bar{X}\}$ – complex amplitude of response

y – transverse displacement of the beam

$\{y\}$ – input displacement due to track irregularities

Y – Fourier transform of y

Y_1 – amplitude of travelling wave train

$\bar{Y}$ – Laplace transform of Y

$\{z\}$ – vector of displacements

$[Z]$ — complex matrix $((K - \Omega^2 M) + i\Omega C)$

α — angular displacement about x-axis

α_1 — constant related to the beam on foundation subjected to an axial force and a moving load ($\frac{1}{2} \sqrt{\frac{N + mv^2}{EI}}$)

α_1, α_2 — angles made by the lateral and rotational shock absorbers respectively with the x-axis

β — angular displacement about y-axis

— damping ratio (c/c_{cr})

γ — angular displacement about z-axis

Γ — gamma function

δ — Dirac delta

ϵ — rate of change of contact plane slope with lateral displacement of wheelset

— infinitesimal increment

$\epsilon(t)$ — error function due to track irregularities

ζ — constant for beam ($c/2m$)

η — rate of change of distance between track center line and contact points with lateral displacement of wheelset

η_0 — ratio of axial force in beam to buckling load (N/N_{cr})

θ — velocity ratio (v/v_{cr})

θ_0 — angle between contact plane and horizontal, wheelset in horizontal position

xiv

θ_ℓ, θ_r — angle between contact planes and horizontal, after movement of wheelset

λ — effective conicity of wheel tread defined as the rate of change of rolling radius with lateral displacement of wheelset

— constant depending on track parameters $(\sqrt{\omega^2 - \zeta^2 - a^2 b^2})$

μ — coefficient of friction

μ_j — real part of jth eigenvalue

ν — Poisson's ratio

ξ_x, ξ_y — longitudinal and lateral creepages respectively

ξ_γ — spin

(ξ, η, ζ) — moving reference coordinates

ρ — acceleration of moving load

$\{\upsilon\}$ — displacement and velocity vectors for free vibrations $(\{x, \dot{x}\}^T)$

$\{T\}$ — complex amplitude of $\{\upsilon\}$

ϕ — constant for beam $(c_{cr} v_{cr}/8EI)$

Φ, Ψ_1 — constants function of the ratio of major to minor length of axes for wheel/rail contact area (a/b ratio) and Poisson's ratio

ψ — rate of change of the angle of the wheelset centerline to the horizontal with the lateral displacement of the wheelset

ω — constant for beam on elastic foundation $(\sqrt[4]{k/4EI})$

ω_0 - fundamental natural frequency for infinite beam on elastic foundation ($\sqrt{k/m}$)

ω_j - j^{th} natural frequency

ω_{dj} - j^{th} damped natural frequency

Ω - forcing frequency

Ω_ℓ, Ω_u - lower and upper range of forcing frequency respectively

Subscripts

a   - body

bf   - front frame

br   - rear frame

c   - motor

d   - wheelset

de   - track/wheelset

j   - index indicating motor or wheelset number ($j = 1, 2, \ldots, 6$)

ℓ - left

r   - right

t   - partial derivative with respect to time ($\frac{\partial}{\partial t}$)

Superscripts

$\cdot$ - first derivative with respect to time ($\frac{d}{dt}$)

$\cdot\cdot$ - second derivative with respect to time ($\frac{d^2}{dt^2}$)

$'$ - first derivative with respect to x ($\frac{d}{dx}$)

"   — second derivative with respect to x $(\frac{d^2}{dx^2})$

-1   — inverse of matrix

T   — transpose of matrix

—   — Laplace transform of the corresponding

variable

LIST OF FIGURES

LIST OF TABLES

xxi

CHAPTER 1

INTRODUCTION

"Engineering may be described as the art of
applying science to the advantage of some business purpose.
The opportunities offered by modern science have been
variously grasped by different industries and railways are
generally held to be among the more backward in this
respect. The situation has advanced considerably in recent
years..." [1]*. Expanded and improved rail service is
required worldwide to meet the needs of growing populations.
Throughout the world, high-speed rail passenger and freight
service has grown. Concern with congestion, ecology,
energy and safety is at the root of the growing emphasis on
improvement and expansion of public transportation
facilities.

Research and/or the identification of research needs
is being stressed by governmental agencies and industry.
High on the list of research priorities are numerous issues
concerned with the dynamics, control, and mechanical design
of transportation vehicles, components and guideways.
Academic work in the field of Applied Mechanics can be of

---

*Numbers in square brackets designate references in
the Bibliography.

direct and immediate relevance to these problems and to much of the research work in the future.

Because of the increased use of heavier trains moving at higher speeds, new and more serious operating problems have arisen. These problems manifest themselves in a variety of ways such as the rock and roll problem, track buckling and derailment. It is becoming more and more apparent that many of the problems encountered have their roots in the dynamic characteristics of railway vehicles and tracks. In most of the research work in the area of railway vehicle dynamics reported so far, the contribution of the track to the total system was minimized to the extent that it is regarded simply as a structure providing a reaction to the loads of passing vehicles.

The present practice of welding rails together to lengths of about 1400 feet has significant advantages in maintenance and in the running of trains, but on the other hand new potentially dangerous problems have arisen. There is the risk of failure under tension loading in the winter time and the possibility of summer buckling especially under the influence of moving loads.

Hunting, which is a sustained lateral oscillation experienced by the wheelsets and/or bogies is an important aspect of the dynamics of railway vehicles, it is still one of the major factors limiting vehicle speeds. For safe

operation the speed at which hunting occurs should be greater than the maximum operating speed. In the absence of instability, when the speed at which hunting occurs is above the operating speed range, the lateral and vertical motions of the railway vehicles are determined by track geometry. For new high performance systems, passenger compartment accelerations should be much less than the gravitational acceleration, and a study of the dynamic response to track imperfections and the minimization of the response transmitted to the vehicle due to track irregularities is necessary.

The subject is of growing importance because of the trend towards higher speeds and higher payloads and the alarming increase in the number of serious problems attributable to track/train dynamics. Currently several research centres are undertaking ambitious research programs on track/train dynamics. The railroad industry in North America has embarked on intensified research efforts in this area.

The first objective in the present investigation is to review and make systematic presentation of the most significant contributions. In the review, attention is concentrated on analytical research and experimental research performed in conjunction with analytical efforts.

The second objective of the present investigation is to study the dynamic response of railway tracks to moving forces. This is necessary in order to develop more insight into the dynamic behaviour of the railway track when subjected to time dependent and constant moving loads. This is also important because for the case of new high speed, high-comfort systems (vibrational accelerations much less than g) inertia effects can be neglected. The characterization of the track and roadbed should be sufficiently realistic to allow the successful prediction of vehicles and track motions. All possible linear effects including damping in the rail and the foundation, and axial force in the rails due to temperature changes of the continuously welded rails is included. This study is intended to show the effect of axial load and damping on the dynamic response and buckling of the railway track, and to determine the effect of the velocity of the moving loads on the dynamic response.

The third objective in the present investigation is to study the dynamics of a railway vehicle model including the effect of vertical track elasticity, with particular emphasis on lateral stability and response to vertical track irregularities. The solutions are intended to provide a better understanding of some of the problems encountered in the area of track/train dynamics,

and to illustrate the adequacy or inadequacy of models on rigid track.

The analyses and computer simulations developed are to be viewed as analytical tools for studying the effect of changing vehicle and/or track parameters and the design on the coupled track/train dynamics in order to achieve stable running conditions with maximum comfort.

CHAPTER 2

LITERATURE SURVEY OF TRACK/TRAIN DYNAMICS RESEARCH

Over the last few years an extensive amount of research dealing with different aspects of railway vehicle dynamics, railway track mechanics and track/train dynamics has appeared in the literature. In addition many papers on creep, rolling contact, vibrations of beams on elastic foundations, vibrations of beams and structures under the effect of moving loads,...,etc., have been published. These are also important and relevant to the study of track/train dynamics.

In the present survey of the literature, attention is concentrated on analytical research and experimental research performed in conjunction with analytical efforts. The survey is primarily concerned with the dynamics of single, conventional railway vehicles including locomotives on rigid and flexible tracks. A review of track dynamics and coupled track/train dynamics is also presented.

For convenience, this review is divided into several sections, in such a manner, that in each section a different aspect of the problem is discussed. These sections are:

6

2.1 Train Dynamics

    2.1.1 Kinematic Oscillations

    2.1.2 Creep

    2.1.3 Dynamic Stability

    2.1.4 Dynamic Response to Track Irregularities

2.2 Track/Train Dynamics

    2.2.1 Track Dynamics

    2.2.2 Coupled Track/Train Dynamics

2.1 <u>Train Dynamics</u>

      Over the past few years, there has been an
increasing effort devoted to development and design of
trains. An attempt shall be made here to review the
significant research concerned with the dynamics of
conventional railway vehicles. The wheels for such
vehicles are coned or tapered to provide static stability,
self-centering action of the vehicle, in order to prevent
the continuous rubbing of one flange or the other against
the rail. With the original cylindrical wheel treads,
guidance was largely achieved by the lateral forces
exerted by the flanges, and the contribution of the tread
forces was secondary. Until a few years ago almost all
scientific work on the behaviour of railway vehicles in
curves ignored the coning of the wheels and assumed that
the guiding forces were obtained completely by the action
of the flanges.

Recently, it has been recognized that guidance, dynamic response to rail irregularities and dynamic stability are intimately related, and a new approach to vehicle design was possible. This approach recognizes that in the first instance the aim should be to design the vehicle and its suspension so that guidance is achieved by the forces acting between the wheel tread and the rails, thus avoiding flange contact in normal running conditions. With this approach it has been possible to develop a theory for the dynamics of railway vehicles based on a linearized analysis.

The application of this theory enables the analysis of a given vehicle and its suspension as well as the systematic consideration of new ranges of values of the parameters involved in the problem.

The main functions of the suspension in addition to support the vehicle are:

(i)   to provide guidance to the vehicle so that it follows the track without flange contact in normal running conditions.

(ii) to stabilize the motion of the vehicle so that the critical speed will be outside the operating range.

(iii) to provide effective vibration isolation to track irregularities over the entire speed range.

The requirements to fulfill these various functions have always conflicted to various degrees. The severity of these conflicts have increased recently in view of the trend towards higher payloads and speeds. The problem is how to design a railway vehicle which is stable and has optimum damping so that the response to economically attractive track imperfections is satisfactory up to very high speeds.

2.1.1 Kinematic Oscillation

Consider a single pair of tapered wheels that are rigidly joined by an axle and that roll on rails having rounded heads, (Figure 2.1(a)). If the axle is initially aligned with the track and if no external disturbances are applied, the axle will roll uniformly along the track. The path of the centre of the axle will coincide with the centre-line of the track. Next, consider the same axle starting from an initial condition in which the axle is displaced in the transverse direction toward the right rail (Figure 2.1(b)). In position 1 the left wheel is rolling on a smaller radius than the right wheel. The effect of this difference is to cause the left wheel to slow down and the right wheel to speed up. The axle yaws toward the left rail (position 2), and soon is displaced as far to the left (position 3) as it was initially to the right (position 1). Now the left wheel speeds up and

left rail
(1)   (2)   (3)   (4)
right rail
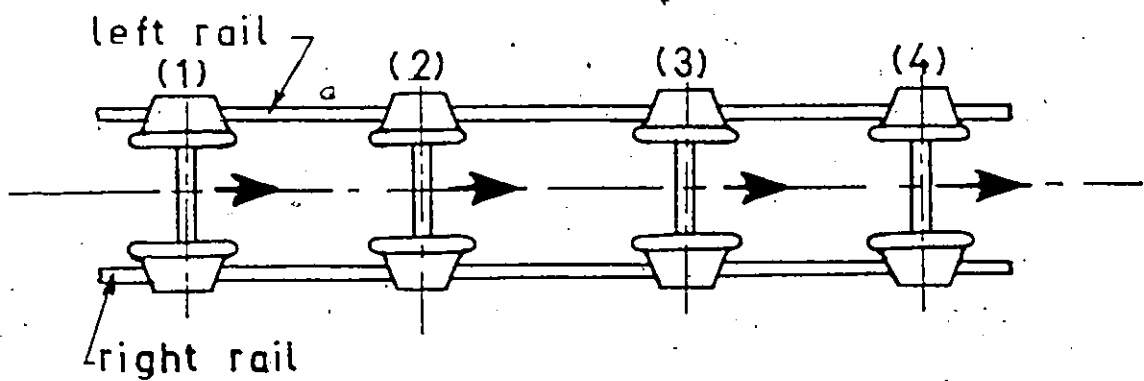
(a) Motion of wheelset initially aligned
    with track

track centerline
(1)   (2)   (3)   (4)

path of center of axle
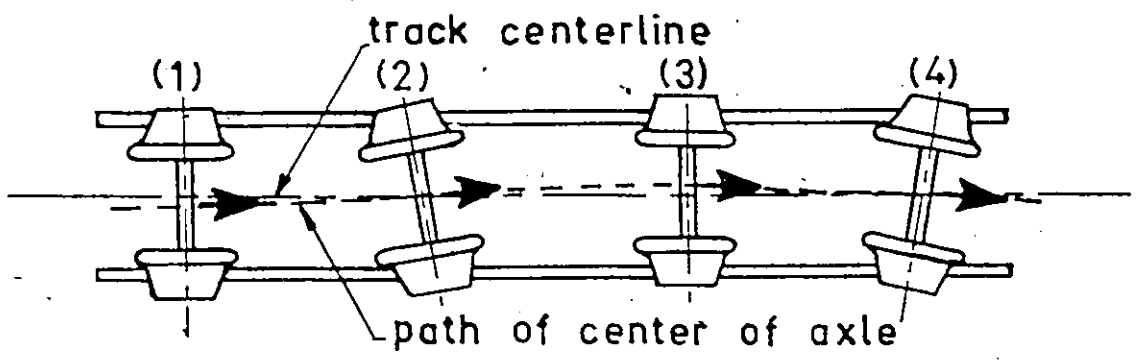
(b) Motion of wheelset initially displaced
    in transverse direction
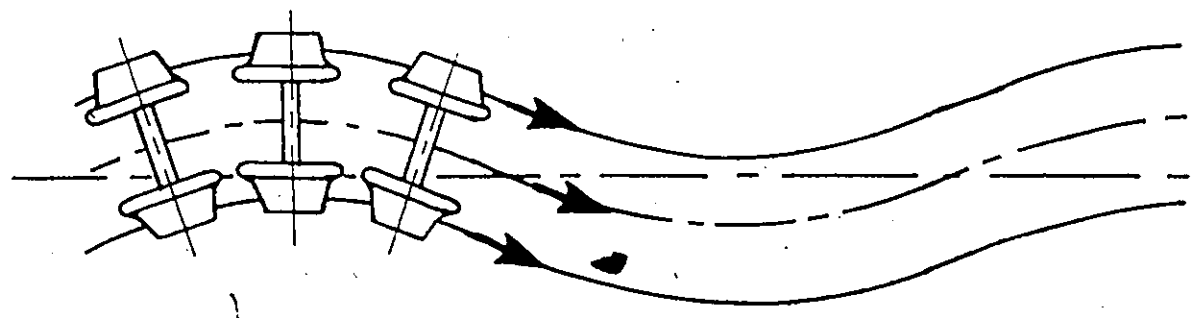
(c) Path of wheeset in kinematic mode

Figure 2..1 The kinematic oscillation of a wheelset

the right wheel slows down, the axle turns back toward the right rail (position 4). For small displacements the flanges do not come into play and therefore the coning of the wheels dominates the motion.

If pure rolling is maintained the wheelset traces out a more or less sinusoidal path as it proceeds down the track as shown in Figure 2.1(c). This motion is referred to as the kinematic oscillation. Klingel [2] showed that the frequency of oscillation is proportional to speed and to the square root of the cone angle (as cited by Wickens [3]).

$$\text{Frequency of kinematic mode} = S\sqrt{\frac{\lambda}{e_0 r_0}}$$

where S is the forward speed of the vehicle

λ the coning angle

e_0 one half the rail gauge

and r_0 the nominal rolling radius .

Klingel's description of the wheelset oscillation assumed that pure rolling is maintained throughout the motion of the wheelset. In reality this is not the case because of the phenomenon of creep, first described in the present application by Carter [4].

For a truck, the rigid frame restrains the axles from following their sinusoidal paths independently. The motion of a truck initially displaced toward the right

rail is shown in Figure 2.2. In the initial position the front axle has a tendency to turn back toward the right rail while the rear axle has a tendency to turn further toward the left rail. The rigid truck frame restrains the axles from turning in opposite directions. As a result, tangential forces are developed at the wheel-rail inter- faces and elastic strains exist in both the wheel and the rail. Consequently the wheel is subject to a slipping or "creep" displacement in the direction of the creep force which arises from the difference in elastic strains of the wheel and rail.

Generally speaking lateral slipping of the wheel occurs when a vehicle is moving over curves or when a "nosing" of the vehicle, which is actually a movement with alternating radii, occurs. On the other hand the longitudinal slipping results from the difference between the actual distance travelled by the centre of the wheel along a tangent rail and the calculated distance on the basis of the number of revolutions of the wheel.

2.1.2 Creep

The phenomenon of creep between wheel and rail is of fundamental importance in the study of railway vehicle dynamics. Complete slip of wheel on rail, which is the limiting case of creep, is important for studies of traction and braking. When two bodies are pressed together
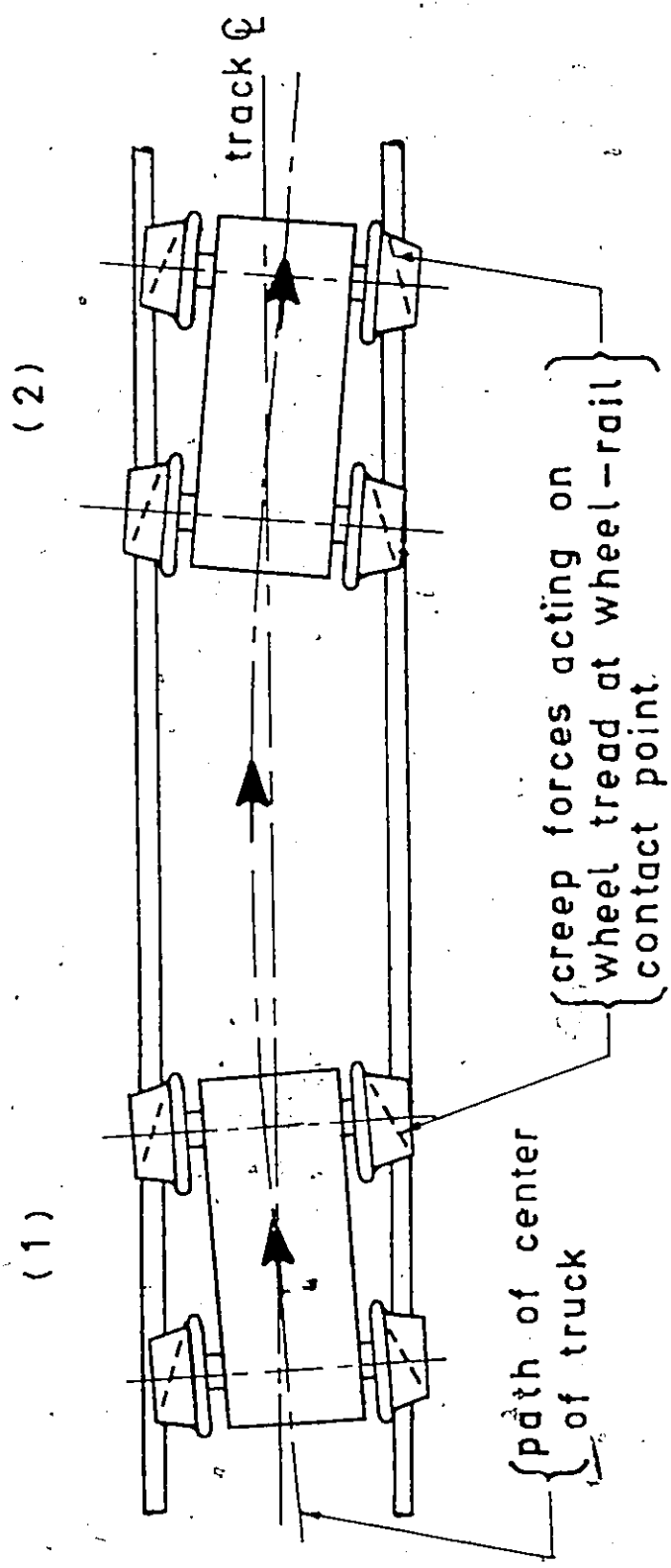
Figure 2.2 Motion of truck initially displaced in transverse direction

13

by a force and one is made to roll on the other by means of appropriate forces or moments, rolling contact is said to take place. A theory of rolling contact is one which explains how forces are transmitted from one body to another during rolling.

Creep may be described as the part-elastic part-frictional behaviour, in which the elasticity of the two bodies in contact accommodates regions of complete slip and no-slip within the rolling contact area. Creep will be present between a wheel and a rail when the contact pressure is insufficient to maintain friction adhesion.

When an elastic body rolls over another elastic body, contact takes place over an area. Small deviations from a pure rolling motion induce tangential forces acting in the common area of contact; and conversely, externally applied tangential forces cause deviation from the steady rolling motion. For example, when a wheel exerts a tractive effort, the distance travelled by the wheel is less than the pure rolling displacement as calculated by combining the number of revolutions made with the perimeter of the wheel. This effect is termed "longitudinal creep", so that creep is a mode of progression intermediate between pure rolling and pure sliding. Similarly, if a wheel is rolling along a rail and a lateral force is applied, a lateral displacement of

the wheel occurs which is proportional to the distance travelled. This is "lateral creep".

The deviation from the pure rolling velocity during rolling is referred to as the "creep". Considering the rigid body velocity of the contact area around the wheel (velocity attributable to pure rolling) and the actual velocity of the contact area with the rail, creep is defined as the difference between these velocities. The "longitudinal creepage" is defined as the ratio of the creep to the mean rolling velocity of the wheel. The "lateral creepage" is similarly defined as the difference between the actual velocity at the contact area of the wheel and rail in the lateral direction and the rigid body velocity divided by the mean rolling velocity. In addition, there may be angular velocities of wheel and rail about an axis normal to the contact area, giving rise to "spin", defined as the difference between these angular velocities. Longitudinal creep, lateral creep and spin, define the relative motion between wheel and rail as illustrated in Figure 2.3.

The problem of creep was first treated by Carter [4,5] who recognized its importance in the railway field. He was the first to appreciate that the wheel-rail forces are due to "creepage". Carter [4] defined creepage as the ratio between creep and rolling velocity. Poritsky's

angular velocity = $\hat{\dot{\beta}}$

$(\dot{\beta}\, r_0 + \xi_x\, S)\, dt$

r_0

(a) longitudinal creep

$\xi_y\, S$

S

$\mathcal{J}$

(b) lateral creepage

$\xi_\gamma = \dfrac{\dot{\gamma}}{S}$

$\dot{\gamma}$

(c) spin
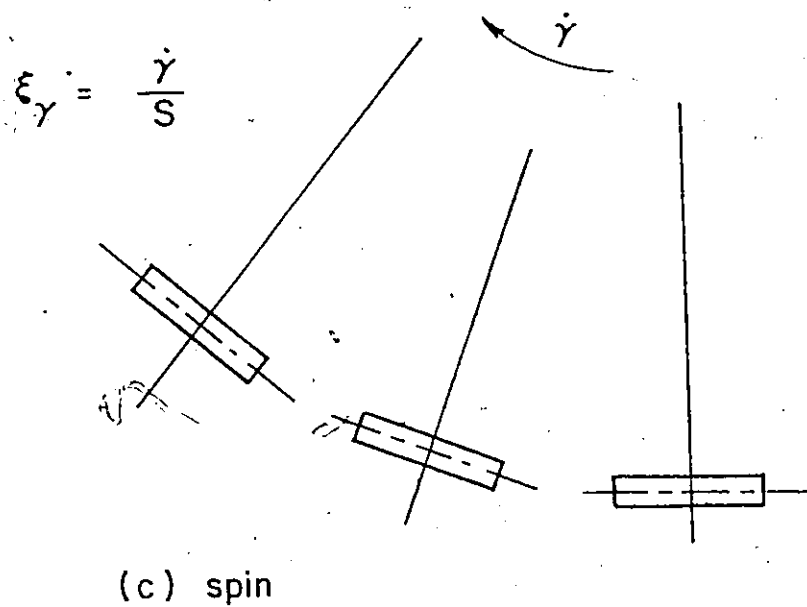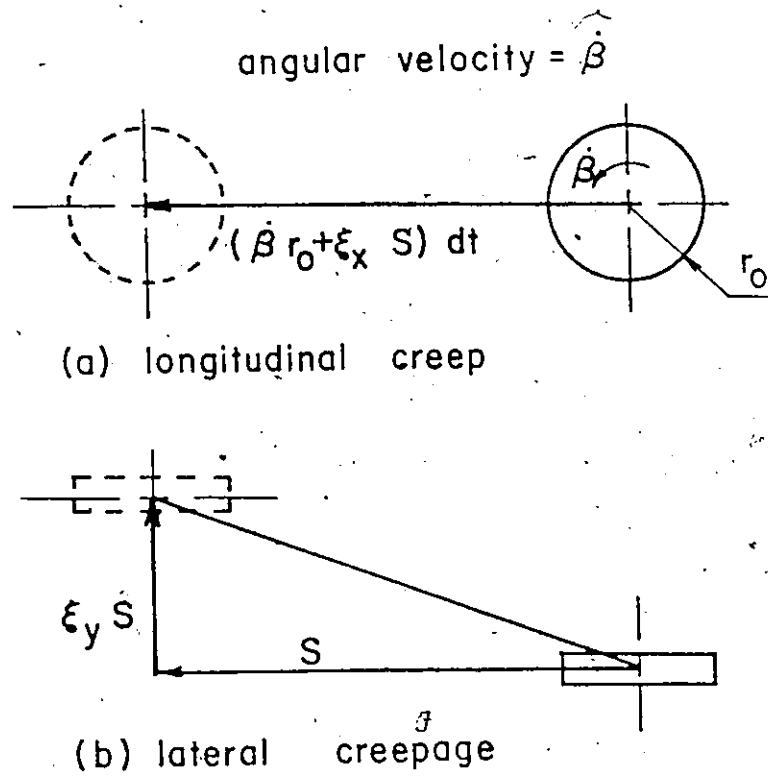
Figure 2.3   Relative motions between wheel and rail

[7] work is similar to Carter's, both treated the two dimensional case of two cylinders with parallel axes rolling together with creep in the direction of rolling. Johnson [8] proposed an approximate solution for longitudinal and transverse creep. His solutions are essentially extensions of the two dimensional solution obtained by Carter and Poritsky. In the two dimensional solution, the contact region considered is an infinite strip. The locked region is an infinite strip adhering to the leading edge. In the contact of a sphere and a plane, the contact region is a circle. Johnson then assumed that the locked region is a circle symmetric about the x-axis.

Johnson [9] provided also a solution to the creep problem which for the first time includes spin, the theory is only valid for vanishing creep and spin and for circular contact area. Johnson also performed experiments and his results agree reasonably well with his theory. The assumption of a circular no-slip region, tangential with the contact circle at its leading point was apparently a reasonable approximation for the case of rolling spheres or a rolling sphere on a plane. This work was extended later to consider the case of an elliptic contact area.

An approximate theory for the three dimensional problem was given by Vermeulen and Johnson [10], who approximated the area of adhesion by an ellipse similar

to the contact ellipse. The theory treats the case of longitudinal and transverse, or lateral, creep for all values of creepage.

Another treatment is given by Haines and Ollerton [13] for the three dimensional case of elliptical contact, but for creep in the direction of rolling only. This solution amounts to dividing up the contact region into strips parallel to the direction of rolling, and then applying the two-dimensional theory (Carter solution) to each strip separately. Perhaps one of the most positive achievements in that paper is the demonstration, for the first time, of the validity of the assumption that the tangential traction in the slip region is a constant proportion of the normal pressure at any point. All theoretical work in the field so far has been based upon that proposition.

Kalker's [11,12] work is perhaps the most mathematically rigorous work reported. He has developed theories for the most general cases of arbitrary values of creep and spin. Kalker [11] also indicated that Johnson's theoretical results compared with the experimental ones show that the theory can very well be used as an approximate theory. Johnson [27, p.59] indicated that creep measurements show large variations with both the theory and with each other, and that further refinements

to the theories are unlikely to change the predictions of
creep coefficients by more than a few percent; he also
presented a comparison between results from his theory
with Müller's [28] experimental results. The comparison
is reasonable (Figure 2.4) although creep measurements
are lower than predictions, this is believed to be due to
surface contamination.

Nayak et.al. [14,15] reviewed experimental and
analytical studies of friction and creep in rolling contact
and examined the influence of different factors on friction
(adhesion) and creep. Their findings indicate that the
creep coefficients are insensitive to rolling velocity or
normal vibrations, and that surface roughness does not
influence the creep coefficients at operating loads. They
also found that dynamic loads due to suspension resonances
do not appear to influence the friction or creep
coefficients significantly.

As the magnitudes of the creepages and spin
increase, only part of the contact area remains locked
together, relative slipping taking place over part of the
trailing edge, in accordance with the law of coulomb
friction. Because of this, a departure from the linear
relationship as indicated in Figure 2.5 exists. The
increases in the value of the creepages and spin cause
slipping over an increasingly large part of the contact

(a) longitudinal creep

(b) lateral creep
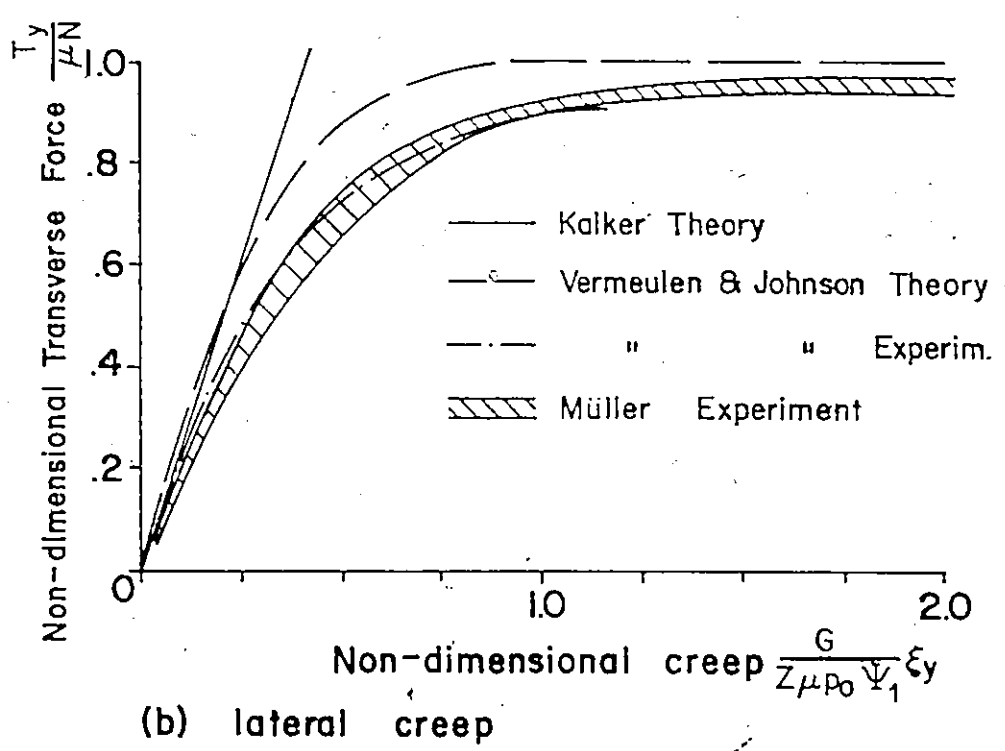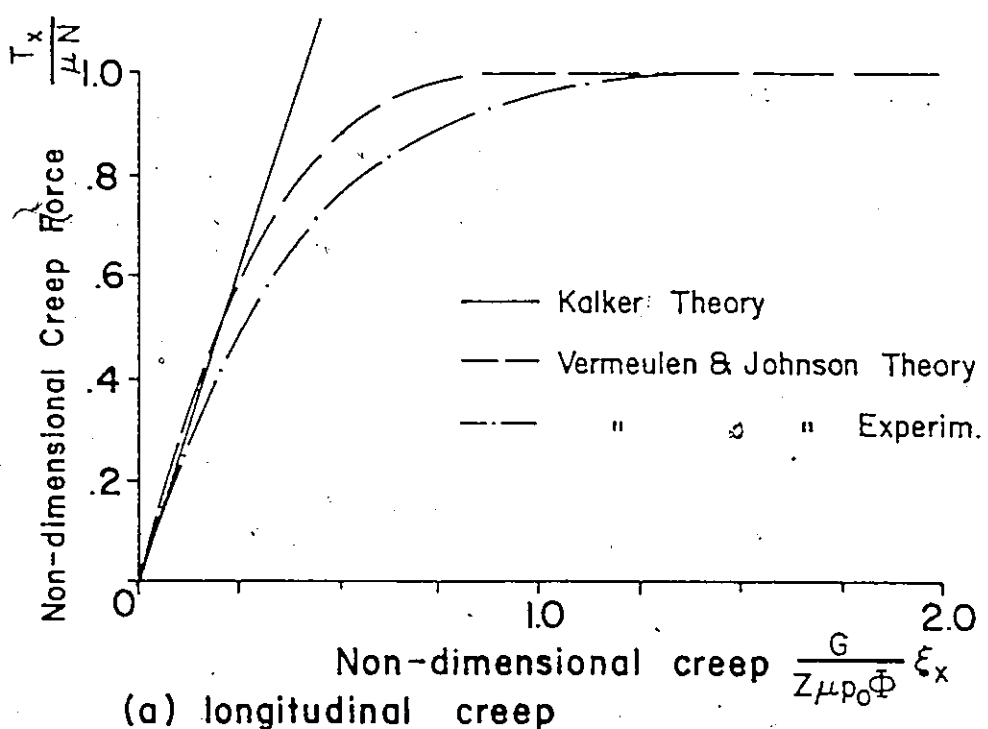
Figure 2.4   Comparison of full-scale data and
experimental results with elastic
theory.
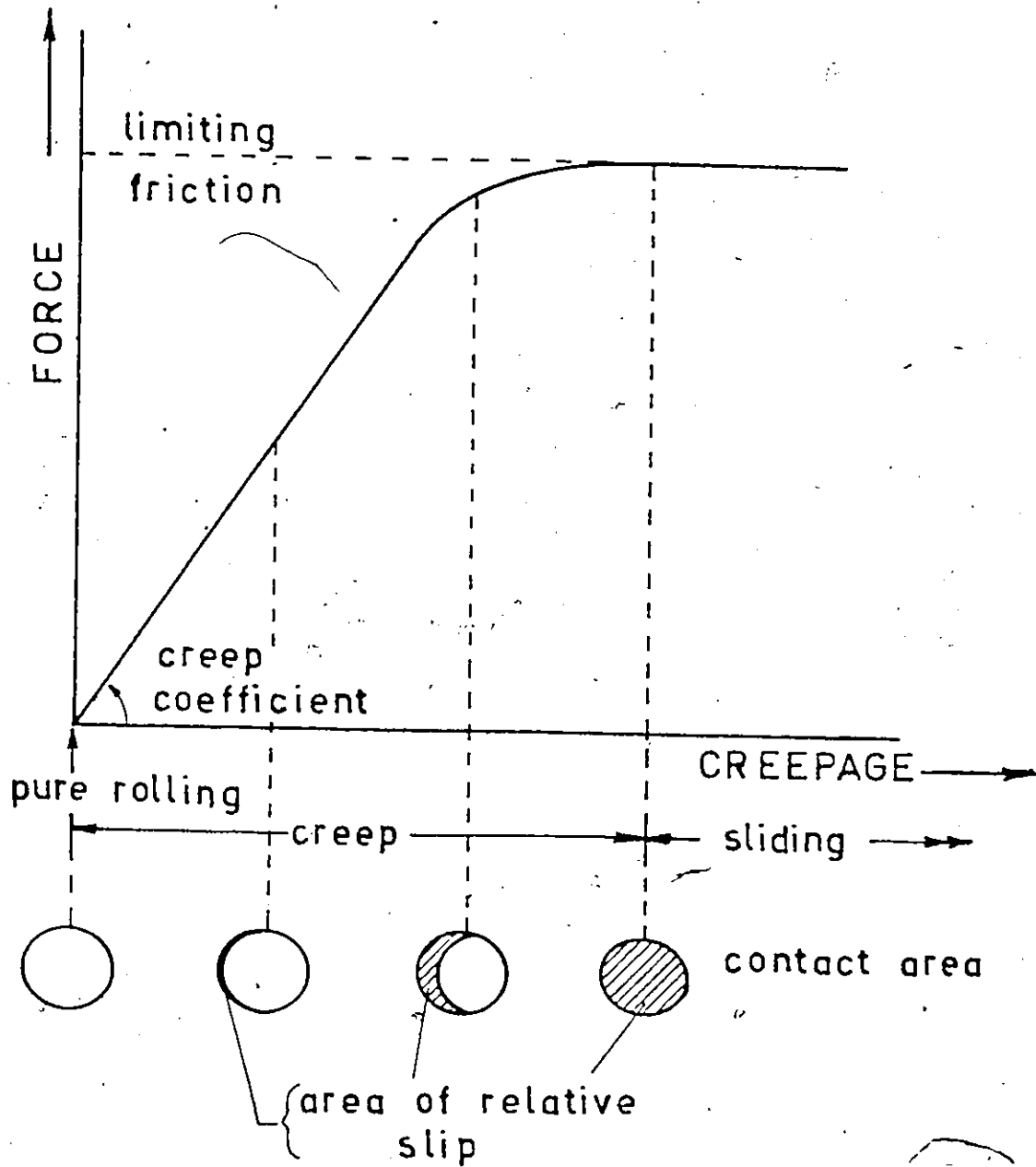
Figure 2.5   Relationship between longitudinal creep
and longitudinal creep force

area until ultimately there is gross sliding of the wheel over the rail.

2.1.3 Dynamic Stability

An important aspect of the dynamics of railway vehicles is the sustained oscillation in the lateral plane experienced by the vehicles and which is usually referred to as hunting. The existence of this oscillation has been a matter of experience since the early days of railways, but it is only in the last decade that an increasing scientific work on hunting has been published. This has been motivated firstly by a recognition of the inadequacy of the old empirical cut-and-try approach to suspension development, and by the needs of current and future high speed train projects.

This behaviour occurs only above a certain critical forward velocity, known as "critical speed". This generally determines the maximum safe speed which the vehicle concerned is able to attain, because the hunting oscillations have a number of practical consequences which tend to limit the maximum speed of trains. In addition to human discomfort arising from high vibrational acceleration levels, the large lateral forces which can occur contribute to derailment proneness and to structural fatigue damage to both the track and the vehicle. It follows that the elimination of hunting is an important requirement for safe

running at high speeds.

The hunting oscillation, in which the wheel flanges bang from one rail to the other arises from the dynamic instability of the wheelsets and bodies caused by the interaction between the conicity of the wheels, the forces acting between the wheels and the rails, and the action of the suspension.[3] It will be described later how the forces acting between the wheels and rails are non-conservative in nature.

The truck hunting, or secondary hunting, is inherent in the vehicle design. Unless the wheel profile is cylindrical, truck hunting will always occur above a certain critical speed.

Another hunting mode, known as body hunting or primary hunting, may occur if the suspension between the trucks and car body is such that relative yaw and roll motion is allowed. This is reported in reference [16] which considers a dual axle vehicle. Body hunting which usually occurs at low speeds is characterized by violent motions of the car body, and less distinct truck and/or wheelsets motions. Body or primary hunting usually occurs in a limited speed range (see Figure 1.6, reference [16]). This hunting mode is similar to a resonance phenomenon in several ways. First, the hunting usually begins when the frequency of the truck motion equals one of the natural

frequencies of car body motion. The dominant truck frequency is caused by the coned or hollowed profile of the wheel tread, and increases nearly proportionally with vehicle speed. Thus when the dominant frequency reaches one of the car body frequencies, hunting may occur. Like resonance behaviour, body hunting can be controlled by damping. If the car body is adequately damped, body hunting can be eliminated entirely [17].

In the case of truck hunting, when it begins it will continue to grow more violent as vehicle speed increases. While below the critical speed the motion of the vehicle is determined by track features, above the critical speed the continuously growing hunting oscillations are limited only by the action of the flanges, slipping of the wheels, and suspension non-linearities.

In the design of the railway vehicles, the aim should be to achieve guidance by the creep forces acting on the wheel tread, thus avoiding flange contact in normal running conditions. For this reason linearized analyses of the stability of railway vehicles have been used to predict the critical speeds. Considerable research work related to the development of a realistic linearized stability theory is reported in the literature, and significant effort has been devoted to correlating these linear stability analyses with actual rolling stock

behaviour, especially in Great Britain and Japan. This work has utilized roller stands on which scale model and full scale vehicles are placed. The vehicle wheels are driven by the rollers at speeds equivalent to the operating speed range. Qualitative agreement has been obtained in many cases. Good correlation between experimental results and those obtained using the linear theory was achieved by Wickens [16]. Successful attempts to correlate the results from the developing stability theory with performance on actual rails are few. Gilchrist, et.al. [18] have obtained good agreement between the predicted results and the results of actual running tests for British four-wheeled vehicles. Blader and Kurtz [19] have obtained agreement between analytically predicted results using the linearized stability theory and the results of running tests for freight cars.

Attempts to include non-linearities such as that due to wheel-flange contacts have been made by some authors [20,21,22,23]. These studies have indicated that hunting oscillation occurs in a limit cycle. While the linear theory cannot describe the eventual motion it has proved to be very useful in predicting critical speeds, and has in fact dominated the practical design of high speed vehicles. Surely it is more important to know how to avoid instability rather than to describe it. In view of that, the remainder

of the discussion here will concentrate on the review of the significant achievements reported in literature on the linear stability theory.

Carter's modelling [4,5] is the forerunner of all modern dynamic stability analyses. His work resulted from the requirement for a discussion of the relative merits of locomotives so far as their riding qualities and tendency to derail were concerned. Using a modelling of the wheel-rail forces which for the first time included creep terms, but omitting the components of rail reactions in the horizontal plane (now referred to as "the gravitational forces"), Carter established the differential equations and the characteristic polynomials for a number of locomotive types, and investigated their stability. Unlike his predecessors and some authors who followed him, Carter [5] understood from his modelling that the lateral oscillations could be self-excited.

Langer and Shamberger [6] misrepresented Carter's work by stating that it "... discussed forced oscillations the life of which depended upon the application of some periodic force, such as from cylinder action or rail joints ...", and claiming their modelling to be the first of a self-induced nature. Their conclusion that the critical speed is dependent on roll frequency is not borne out in more recent experience.

Cain [24,25] established energy balance equations using Carter's modelling of the creep phenomena. Like Langer and Shamberger [6] he also assumed that the roll frequency was an important factor.

The analysis of the dynamic stability of railway vehicles took new importance with the advent of modern computers. Since the 1960's many investigators have analyzed the linearized multi-degree of freedom equations of motion of railway wheelsets and trucks using both analog and digital computers. Some of these analyses have included degrees of freedom of the car body while others have assumed the car body to translate uniformly along the track as the truck and wheelsets undergo various dynamic motions. All investigations have shown that the taper ratio or coning angle significantly affects the stability of the secondary hunting mode. All of these linear analyses result in eigenvalue problems. The solution of the eigenvalue problem for various design parameters and speeds indicate the effects of these parameters on the stability of the railway vehicle.

Wickens [26] published a very useful study on the subject of dynamic instability of wheelsets and bogies. In his paper, the instability is investigated for the case of profiled wheel tread (worn wheels) rather than purely conical. Using the root-locus and parametric

studies Wickens shows that the instability is due to the combined action of the shape of the wheel tread profile and the creep forces acting between the wheels and rails. Wickens' most significant contribution both in this paper and in his later work lies in the clarity of the presentation and discussion of the concepts and parameters involved in such analyses.

In November 1965, a joint Convention on the "Interaction between Vehicle and Track" was organized by the Institution of Mechanical Engineers. Papers presented and published in the proceedings of that conference [27] are to that date widely used as a reference for those working in the field of car design. The Convention was arranged to show how scientists and engineers were cooperating together in order to help the railways to make full use of its advantages, and use the new and better skills now available to them to this end. The discussion of the papers presented at the Conference are published in the Proceedings and are as interesting to read as the papers themselves. Notable amongst the matters discussed and relevant to the present discussion are the papers by Bishop [28], Wickens [16], Matsudaira [17], and Gilchrist et.al. [18].

Bishop [28] demonstrated the hunting phenomenon using a model vehicle, and noted that during bogie hunting,

the motion exhibits a limit cycle. He emphasized the value of development of a linear theory and throughout his paper compared hunting of railway vehicles with the flutter of aircraft.

Wickens [16] presented an improved gravitational stiffness model but neglected the spin terms and the lateral creep due to spin and his paper contains a misinterpretation discussed by Blader [29]. Wickens discussed existing and recently developed theories of the lateral motion of railway vehicles in relation to experimental work on both models and full-scale vehicles. He showed that a linear theory taking into account a significant number of degrees of freedom and the influence of wheel rail profiles, yield values for the critical speeds which are consistent with experimental results. The influence of various parameters on the stability is also discussed in the paper using the root-locus curve.

A discussion of the appropriateness of the modelling and the values for creep by Gilchrist [27, p.104], Johnson [27, p.69] and Wickens [27, p.150] confirms the importance of the spin term in the dynamic stability analysis of railway vehicles. In the discussion of his paper Wickens [27, p.150] showed that for the numerical example considered [16], the quantitative error due to the neglect of spin is significant; but that qualitatively,

however, the behaviour remains unchanged.

Matsudaira [17] reported comparisons between the theoretical predictions and results for models on a roller test track. The value of the critical speed reported is much higher than that found by Wickens [16]. The wide discrepancy may be attributed to the different vehicle designs and to the fact that Matsudaira considered a conical tread whereas Wickens used a worn tread (the effect of tread wear was shown to decrease the critical speed), and although in his paper Matsudaira does not refer to it, the tread profile has appreciable influence on hunting.

Gilchrist et.al. [18] illustrated comparisons between the theoretical predictions and the results obtained using an experimental vehicle. Their experiments have shown a reasonable degree of accuracy for the theoretical predictions of hunting motion, and they conclude that it is desirable and possible to remove the problem of lateral instability at the design stage. Then the lateral problem, like the vertical, would become one of response to rail irregularities.

At the "High-Speeds" Symposium in Vienna in 1968, Wickens [30] reviewed theoretical and experimental aspects of lateral dynamics of railway vehicles, with particular reference to the problems of dynamic stability and response to track features. The paper includes the description and

modelling of the creep-spin terms.

Wickens [31] published a further study on the lateral dynamics of railway vehicles with particular reference to dynamic stability, dynamic response and curving. The paper contains a comprehensive analysis of the basic problems, but his analysis and experimental data, as in his previous work, deal primarily with single axle suspensions.

Matsudaira et.al. [32] gave the derivation of the equations of motion for a car model, the prediction from which are compared with experiments on the roller rig developed at the Railway Technical Research Institute of the Japanese National Railways. The authors conclude their paper by making remarks on the validity of the stand test as a means of experimental research on the hunting of railway vehicles; in brief the test is recommended but it comprises several points to be checked with particular reference to the railway vehicle model and scale.

Blader [29] showed that the prediction of the linear critical speed remains substantially unaffected by the consideration of other cars coupled to it, and that a group of cars under tension is no less stable than a single uncoupled car.

Clark and Law [33], Cooperrider [23] and Matsudaira [17] have found that the critical speed of hunting for

conventional, dual axle trucks increases with increasing suspension stiffness. Cooperrider also found that the primary stiffness has a more dominant effect than the secondary stiffness on the critical speeds of truck hunting. Wickens [16,26] found that the critical speed for a dual axle vehicle increases initially with suspension stiffness, but beyond a certain point will decrease as stiffness is increased further.

The influences of wheel conicity, mass distribution, suspension damping and vehicle geometry on the secondary hunting are shown by Clark and Law [33], Cooperrider [23] and Matsudaira [17] for conventional trucks and by Wickens [16,26] for dual axle vehicles and by Blader and Kurtz [19] for freight cars.

A dynamic stability analysis for a proposed high speed passenger car including the control unit and the tilting mechanism was performed by Dokainish and Siddall [34]. The number of degrees of freedom considered is realistically large; in addition the equations for the active suspension are included in the analysis. The work also includes the effect of the wheel tread profile and the variation of the suspension parameters on the dynamic stability performance of the vehicle.

In the case of linear analyses, the dynamic stability is investigated by studying the character of the

solutions, more precisely by studying the roots of the
characteristic equation associated with the equations of
motion of the system. In the case of a multi-degree of
freedom system the problem is an eigenvalue problem, its
solution in the presence of damping in the system results
in complex conjugate eigenvalues with negative real part
for all roots if the system is stable. The stability is
then investigated using root-locus plots for various system
parameters.

2.1.4 Dynamic Response to Track Irregularities

Below the critical speed, above which hunting occurs,
the lateral and vertical motions of railway vehicles are
determined by track geometry. In studies of dynamic response,
three general quantities of interest exist: the definition
of the input, the determination of the transfer function
and the assessment of the resulting output.

Motions of the vehicle symmetric about the
longitudinal plane of symmetry are excited by vertical
track irregularities, while transverse motions are excited
by lateral track irregularities and cross-level.

Track irregularities can be considered to be
distributed randomly, in which case the techniques of random
process theory can be used; thus, the input is described
by a power spectral density function which gives a
distribution of the mean-square value of the input in terms

of its frequency content. Track irregularities can also be treated as deterministic imperfections. The sinusoidal irregularities are in particular worth considering because power spectra and auto-correlation functions obtained from field measurements indicate the existence of periodic functions [35]. Periodic excitation of the vertical vehicle oscillations results also from evenly spaced rail joints or rail welds.

Hobbs [35] studied the effect of track alignment on the response of a restrained wheelset. The wheelset has two degrees of freedom (lateral, and yaw motion) and is restrained by springs in the lateral and longitudinal directions. The model assumes that the vehicle body is running at a constant speed with negligible body oscillation. The forcing functions due to rail irregularities are derived and the response of the wheelset were obtained.

In [37] the authors have studied the dynamic response of a railway vehicle to track irregularities both theoretically and experimentally. This work has shown that the response of a wheelset of a vehicle is a maximum when the wave length of imperfection is equal to the kinematic wave length of the wheelset. For wave length of imperfections longer than the kinematic wave length, the wheelset tends to follow the imperfection. For wave length of imperfection shorter than the kinematic wave length the displacement of

of the wheelset is reduced.

Research work describing the lateral irregularities of rails in a statistical sense was done by Stassen [38] and by Sewall et.al. [39]. Stassen studied the dynamic response of a simplified model of a bogie with two degrees of freedom having the lateral deviations as input, and the generalized coordinates which describe the movements of the bogie as output. Sewall et.al. [39] used four-degrees-of-freedom models for lateral response to lateral or rolling (cross-level) inputs from the rails. They also considered the case of deterministic (including sinusoidal) and random input functions, and their results were obtained in both the frequency and time domains.

La Buschagne and Scheffel [40] described briefly some aspects of experimental research in the South African Railways and the conditions affecting the riding quality of railway vehicles. Parameters which influence the vertical riding quality of railway vehicles are given with reference to the theory of forced vibrations. For the six degrees of freedom model, the assumption that wheel-rail contact is being maintained at all times (which is the case generally) with the wheels following the longitudinal rail profile is made. The authors consider a sinusoidal excitation of vertical vehicle oscillations resulting from the evenly spaced rail joints or rail welds. Results recorded during

tests were found to be in good agreement with the theory,
and it is concluded that the vertical vehicle oscillations
can be simulated on digital computers using the rail
profile as input function. The authors note however that a
more rigourous mathematical model of the path of the wheel
on the rail should include the vertical vibrations of the
rails as an additional degree of freedom of the whole
system.

The most recent advance for the case of dynamic
response of railway vehicle to track irregularities was
done by ElMaraghy [41]. He studied the dynamic response
of models for a six-axle locomotive due to sinusoidal
lateral and/or vertical track irregularities. Two
mathematical models were set up, a full model for the
"stationary" vehicle in which creep between wheels and rails
was neglected, and a full model for the "moving" vehicle
in which creep forces, gravity stiffness effects and wheel
tread profiles were considered. The results obtained show
the effect of creep forces and the condition of the wheels
on the steady state response. The analysis is general and
for the method used there is no restriction on the number
of degrees of freedom or the modes to be considered, and
the inputs can be in-phase or out-of-phase, with or
without the same forcing frequency. Virtually all previous
studies did not allow rigid body pitch motion of the car,

consequently out-of-phase vertical inputs could not be considered.

2.2   Track/Train Dynamics

Because of the increased use of heavier trains moving at higher speeds, it is becoming more and more apparent that the dynamic characteristics of the railway track and roadbed can influence appreciably the dynamic response of railway vehicles. In almost all of the research work on railway vehicle dynamics reported so far, the contribution of the track to the total system is minimized to the extent that it is regarded simply as a structure providing a reaction to the loads of passing vehicles.

With the present practice of welding rails together to lengths of about 1400 feet significant advantages in maintenance and in running of trains are achieved, but on the other hand new serious problems have arisen. There is the risk of failure under tension loading in the winter time or the possibility of summer buckling or "kinking" especially under the influence of moving loads; Koci [46] indicated that in a number of cases buckling of the track was observed, by locomotive crews, occurring ahead of the moving train.

Assuming that instability of railway vehicles can

be eliminated up to very high vehicle speeds, consideration
should be given to the limitation due to wave generation
and propagation. Generally, to a body moving in a medium,
the propagation velocity of wave in the medium sets a speed
limit to the moving body. The sound velocity in the air
provides a barrier for an airplane. This situation is
applicable to a train too. Let us also examine the wave
propagation due to the rolling of a wheel on the rail. The
rail deflects under the wheel load and the deflected shape
propagates with the translation of the vehicle. "As the
vehicle speed increases and approaches the wave propagation
velocity in the rail, an extraordinary resistance will be
produced as in the case of sound in the air..." [47]. The
wheels will be accompanied by large-amplitude stationary
waves, which will eventually destroy the rail. This means
that the propagation velocity of deflection wave of the
rail sets a speed limit to the train running on it. For
assumed values of foundation and rail parameters, Timoshenko
[48] found that the "critical speed" is more than fifteen
times the speed of the fastest locomotive at that time.
In the presence of axial load in the rails due to temperature
changes however, the critical speed for the track may be
reduced to within the range of the operating velocities of
modern-high speed trains, and Kerr [49] demonstrated that
this is indeed a possibility.

To obtain more insight into the dynamic behaviour
of the railway track an analysis for the static and dynamic
response of the railway track to time dependent and constant
moving loads should be undertaken as a first step. Very
few studies on this subject have been published in the
literature. In some cases models have been used without
justification. Most investigators have considered the
railway track system modelled as a continuously supported
beam on a foundation subjected to concentrated moving loads.
A concentrated moving load represents the force due to a
wheel load, inertia effects being neglected on the
assumption that comfort specifications placed on new systems
are stringent (vibrational accelerations much less than g).

Much of the research work on the coupled dynamics
of transportation vehicles and guideways deal with the case
of beam-type elevated guideways. In this case the dynamic
motion of the vehicle is computed by standard transfer
function methods using the guideway deflection as a known
input to the vehicle suspensions. This was the subject of
a recent survey paper [50] and will not be discussed in the
present review; the interest here is in the case of a
railway track on a "foundation".

2.2.1 Track Dynamics

The dynamic effects of moving loads and vehicles
on beams has been, for more than one hundred years, the
subject of numerous mathematical and experimental studies.

Some of the early investigations were concerned with the construction of railway bridges and later on the highway bridges. Recently, the present and future high speed ground transportation systems have motivated a new interest in the problem of the track dynamics due to moving loads. The track is usually modelled as a beam on a foundation. The characterization of the track and roadbed should be sufficiently realistic to allow the successful prediction of vehicle motions, but not needlessly complex. If the model is too complex, the utility of the model will suffer due to the difficulties in supplying accurate data, solving the resulting equations, and interpreting the results.

Timoshenko [48] was the first to conduct a study on the response of the railway track modelled as a continuously supported beam on a foundation and subjected to a moving load. Actually, in the crosstie systems only ties are continuously supported by the roadbed, while the rail itself rests on the ties, that is on closely spaced elastic supports as shown in Figure 2.6. Investigations have shown however, that an equivalent continuous elastic foundation can be substituted with good approximation for such supports [51], and in this way the theory of beams on elastic foundations can be applied to the analysis of the rails themselves.

The usual approach in formulating problems of beams

RAIL

TIE

BALLAST

SUBGRADE

K_1

RAIL
PAD

K_2

TIE

K_3

BALLAST

K_4

SUBGRADE
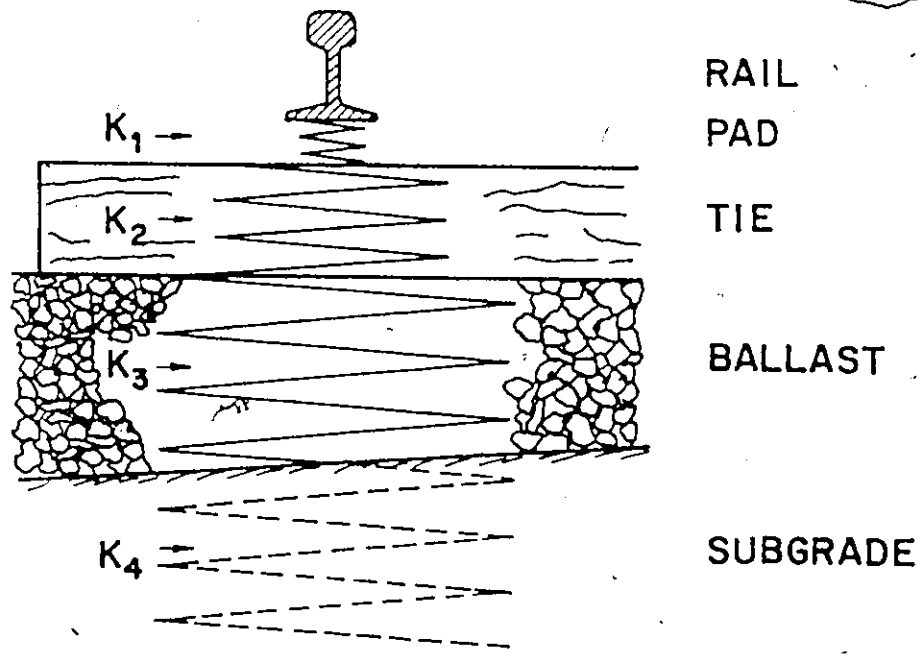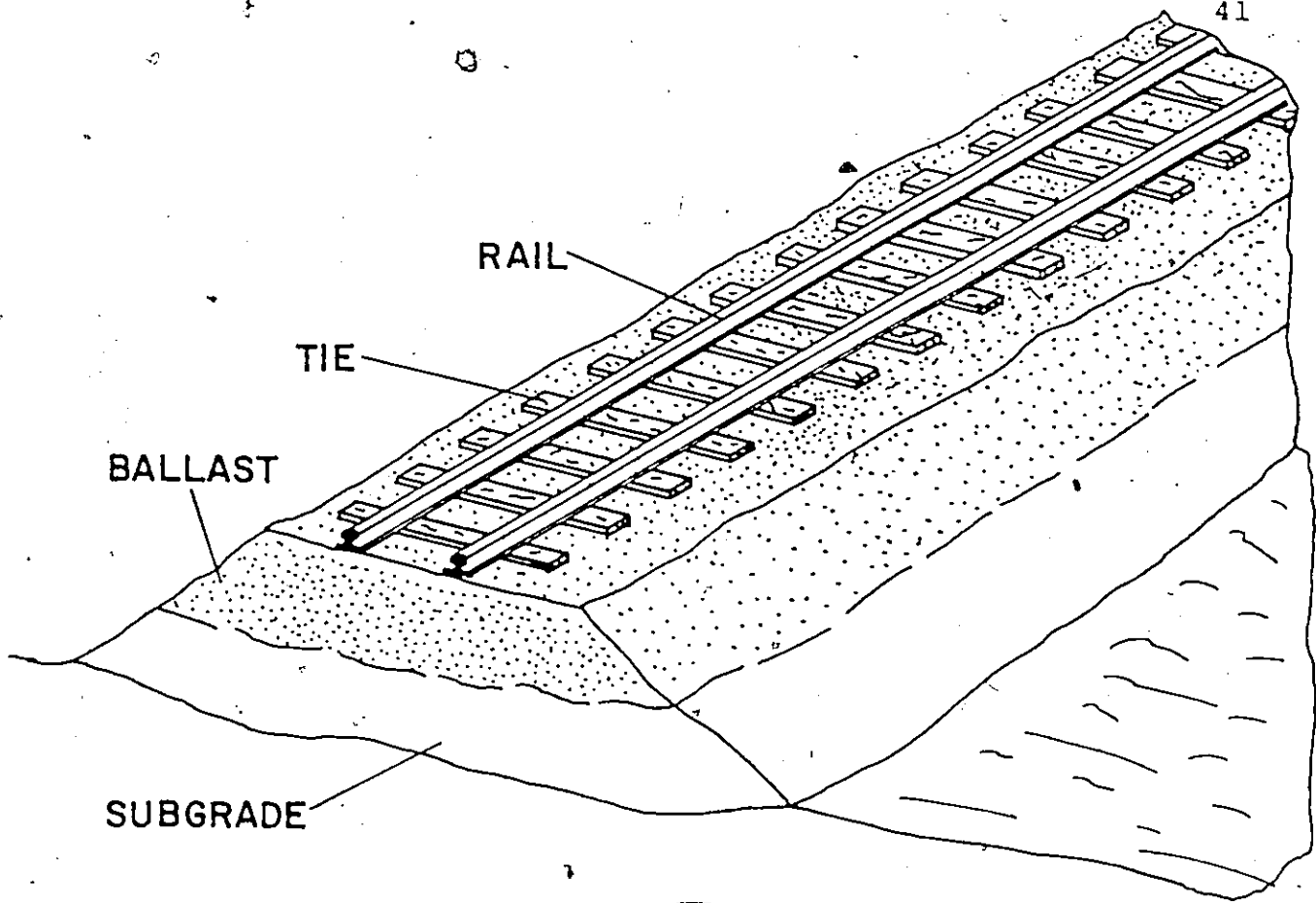
Figure 2.6 The conventional railway track and its representation as a system of springs as suggested by Birmann [53]
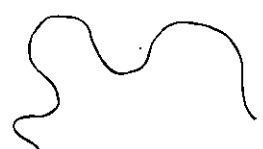
(or plates or shells) on foundation is to include the reaction from the foundation into the corresponding differential equation of motion. The foundation is rather a complex medium. The ballast material for example (as all soils) is not elastic. But since interest here is in the response of the foundation at the contact area (actually at the top of the crossties) and not in the stresses or displacements inside the ballast or the soil, the problem reduces to finding a relatively simple mathematical expression which should describe the response of the foundation at the contact area with a reasonable degree of accuracy.

The simplest representation of a continuous elastic foundation was provided by Winkler, who assumed it was composed of closely spaced, independent linear springs. "The Winkler assumption, in spite of its simplicity, does often more accurately represent the actual conditions existing in soil foundations than do some of the more complicated analyses where the foundation is regarded as a continuous isotropic elastic body..." [51]. For this reason Hetényi in his book [51] devotes nine chapters out of ten in analyses of problems arising in connection with this type of foundation. Railway tracks have almost always been modelled for the purpose of analyses as beams supported on Winkler type foundation with or without

damping; various investigators, however, have used different end conditions. Other types of elastic and visco-elastic foundations (e.g., Filonenko-Borodich, Hetényi, Pasternak, Vlasov, Reissner, semi-infinite elastic half space,...,etc.) were used for different physical applications, depending on the properties of the supporting medium. This was reviewed in a paper by Kerr [52].

Birmann [53] conducted an experimental and analytical study for the static and dynamic track parameters. The model used for the track is a rail on elastic foundation (see Figure 2.6), and Birmann measured the deflections of the track and roadbed by the aid of deeply buried probes. Birmann found that even at high speeds, the behaviour of the foundation is quasi-static, and that the vertical track elasticity is a very important factor in the analysis.

Indeed, a principal factor in track analysis and design is the modulus of track elasticity more commonly known as track modulus (and sometimes foundation modulus). The track modulus is the ratio of applied load to track depression; the load per unit length of each running rail required to depress the track one unit. The track modulus is usually calculated by one of the following three expressions.

$$k = \frac{p}{y} \qquad (2.1)$$

This is illustrated in Figure 2.7(a) where p is a uniform load per unit length of rail and y the track depression.

Another way is to symmetrically apply loads to ties and find the deflection ordinates of the rail measured at every tie (Figure 2.7(b)), then calculate the track modulus k from

$$k = \frac{\Sigma P_i}{s \ \Sigma \ Y_i} \tag{2.2}$$

where P_i is the wheel load at tie number i,

Y_i deflection of tie number i

and   s   the tie spacing

The third method is based on the analysis of beam on elastic foundation

$$k = \sqrt[3]{\frac{P^4}{64 \ EI \ Y_0^4}} \tag{2.3}$$

This is illustrated in Figure 2.7(c),

where P is the magnitude of single wheel load,

Y_0 rail deflection under load point

E modulus of elasticity of rail

and   I the moment of inertia of the rail section.

The relationship between the maximum bending stress and the applied load P is given by:
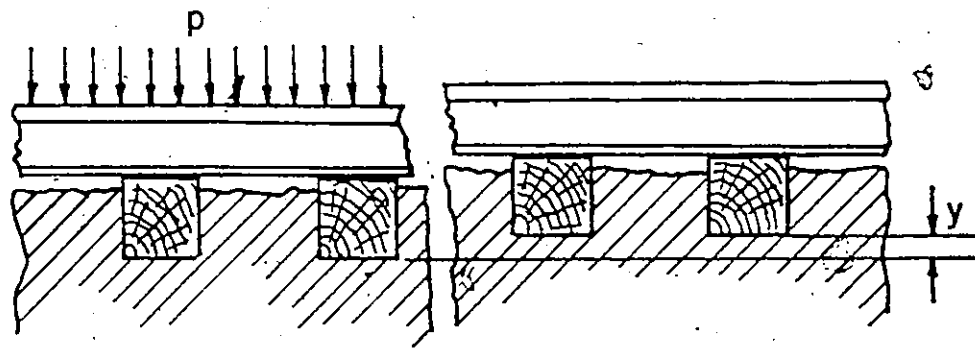
(a) for a uniformly distributed rail load
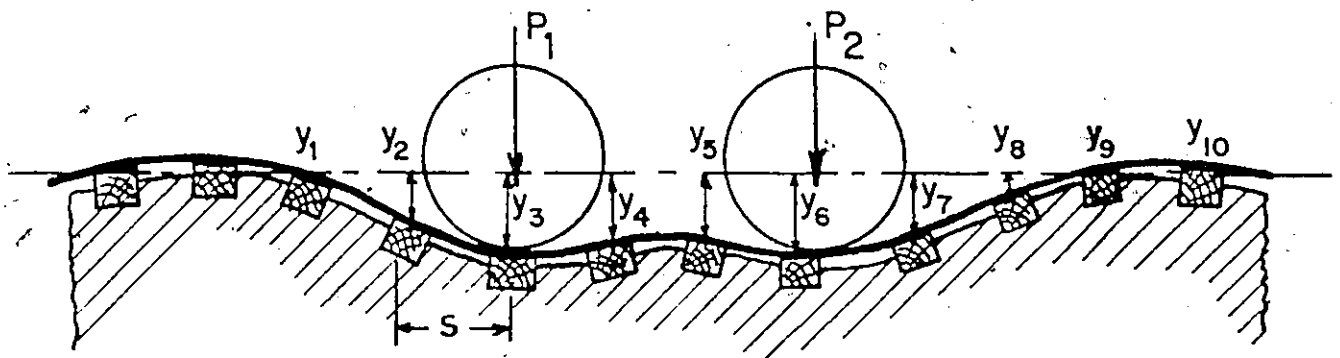
(b) for the track under wheel loads
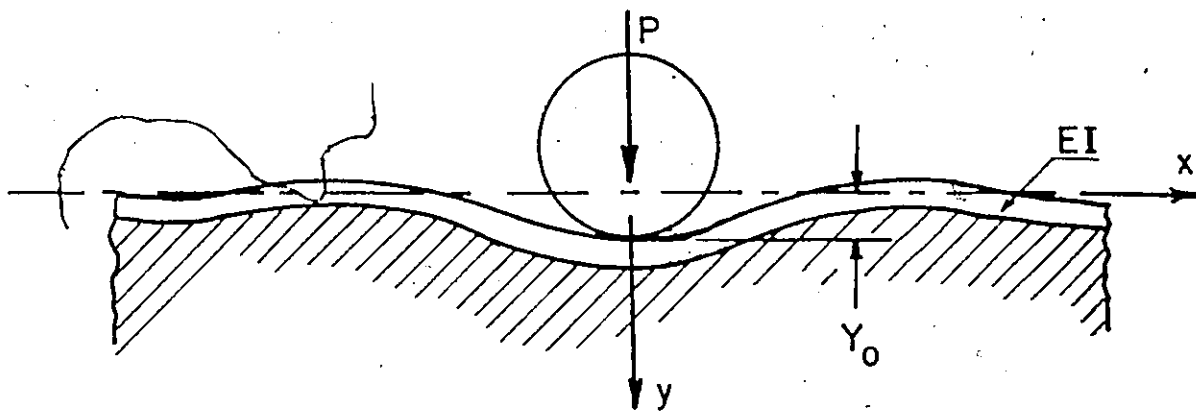
(c) for the track modeled as a beam on
elastic foundation

Figure 2.7   Illustration of the methods for the determination
of the track modulus

$$\sigma_{max} = \frac{M_{max}}{Z} = \frac{P}{4Z} \sqrt[4]{\frac{4EI}{k}} \qquad (2.4)$$

where Z denotes the section modulus of the rail.

It is seen from equation (2.4) that an error in the determination of the modulus k will not influence substantially the value of σ_{max}. Putting for instance, 2k instead of k into (2.4), we find that a 100 percent increase introduced in k causes only 16.5 percent deviation in the value of the maximum bending stress. A comparison of measured and calculated deflections as well as stresses is given in Figure 24 of reference [51]. It can be observed that the stresses measured usually check more closely with the theoretical results than do the deflection measurements.

Timoshenko and Langer [54] utilized the beam on Winkler foundation theory to develop an experimental method for the determination of forces produced in rails by moving locomotives. Their experiments show that the magnitude of the track modulus can be determined in such a manner that the deflection of the rail calculated on the assumption of the continuous foundation is in good agreement with the deflection of the actual rail supported by ties.

The problem of the response of an infinite beam continuously supported on a Winkler type foundation and subjected to constant velocity moving load as shown in Figure 2.8 was investigated in connection with the response
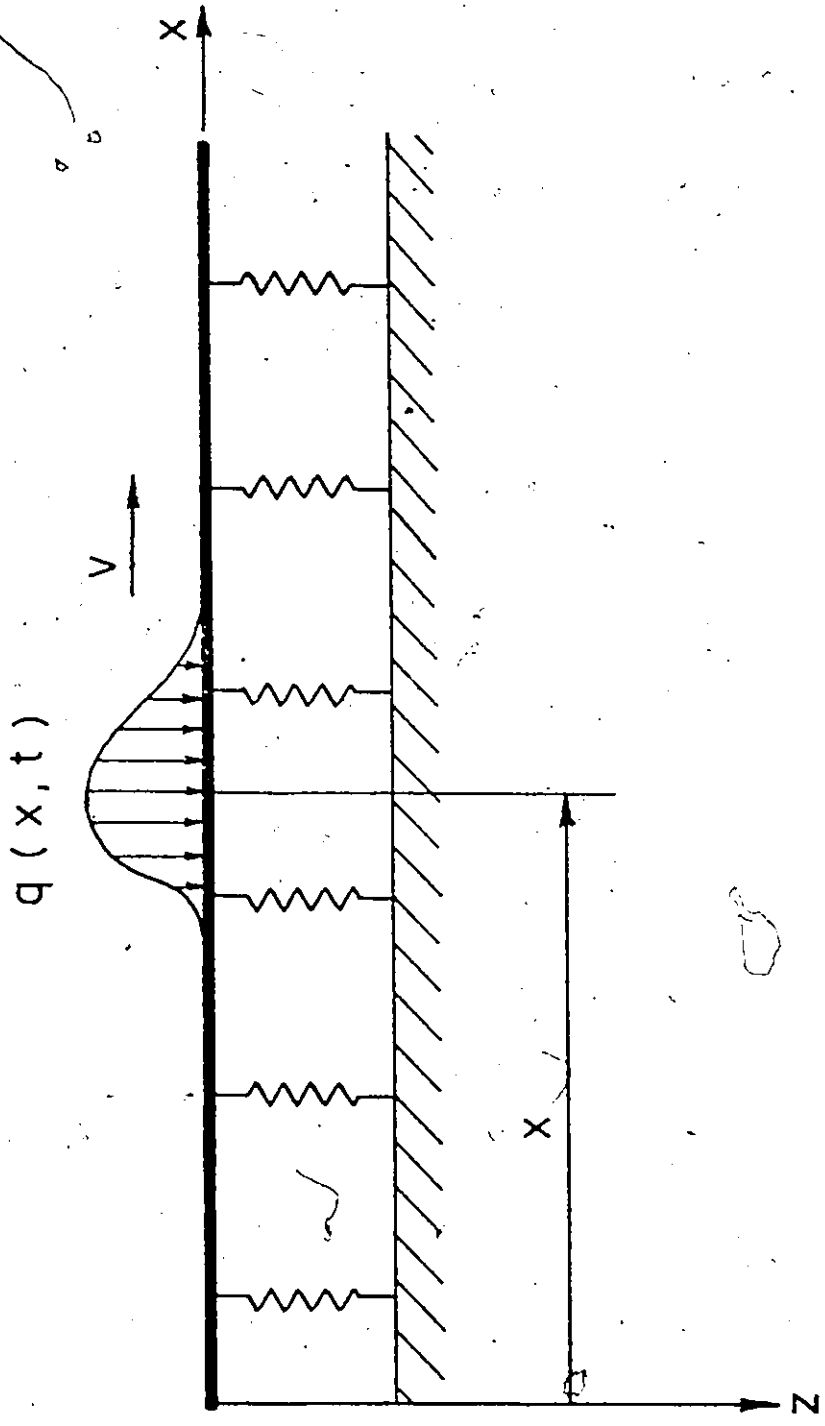
Figure 2.8   Infinite beam on a Winkler foundation and subjected to a general moving load q (x,t)

of a railroad track by several authors. The differential
equation which describes the response of the beam
subjected to a moving load q(x,t) is:

$$EI \frac{\partial^4 y}{\partial x^4} + m \frac{\partial^2 y}{\partial t^2} + k\,y = q(x,t) \qquad (2.5)$$

where y(x,t) is lateral displacement of the beam axis

   EI   the flexural rigidity

   m   the beam mass per unit length

   k   modulus of the Winkler foundation

When the load on the beam is a concentrated load P
equation (2.5) is rewritten as:

$$EI \frac{\partial^4 y}{\partial x^4} + m \cdot \frac{\partial^2 y}{\partial t^2} + k\,y = P\,\delta(x,t) \qquad (2.6)$$

where $\delta(x,t)$ is the Dirac delta function.

   To find the dynamic response due to a moving load
when the beam and the base are of infinite extent, the
properties are constant, and constant velocity of the
moving load, it appears reasonable to assume that after a
period of time the transient motions will become negligibly
small and that the beam displacements will approach the
steady state. This assumption was made by several authors.

   When a beam rests on a continuous foundation and
subjected to a dynamic load, the caused deformations are
associated with dissipation of energy in the beam as well

as in the foundation. Therefore when analyzing such problems it is more realistic to introduce the damping effects in the formulation of the problem.

In the most common approach, the viscous damping term is included in the differential equation by assuming that the damping force is proportional to the lateral velocity. Differential equation (2.5) becomes:

$$EI \frac{\partial^4 y}{\partial x^4} + m \frac{\partial^2 y}{\partial t^2} + c \frac{\partial y}{\partial t} + k\, y = q(x,t) \qquad (2.7)$$

where c is the damping coefficient. It should be noted that in the above equation the added term $(c \frac{\partial y}{\partial t})$ represents the damping of the beam as well as of the foundation. The corresponding mathematical model is that of a beam on a Winkler foundation of the Kelvin type as shown in Figure 2.9.

Equation (2.7) was solved by Criner and McCann [55] for an infinite beam subjected to a moving load P, using an electrical analog computer. The results are presented as graphs in terms of dimensionless parameters. Some non-linear characteristics as beam lift-off were considered, but for none of the cases could more severe conditions be produced than indicated by the linear solutions.

Equation (2.7) was solved analytically by Kenny [56] for an infinite beam subjected to a constant load which moves with a constant velocity. Because of damping the
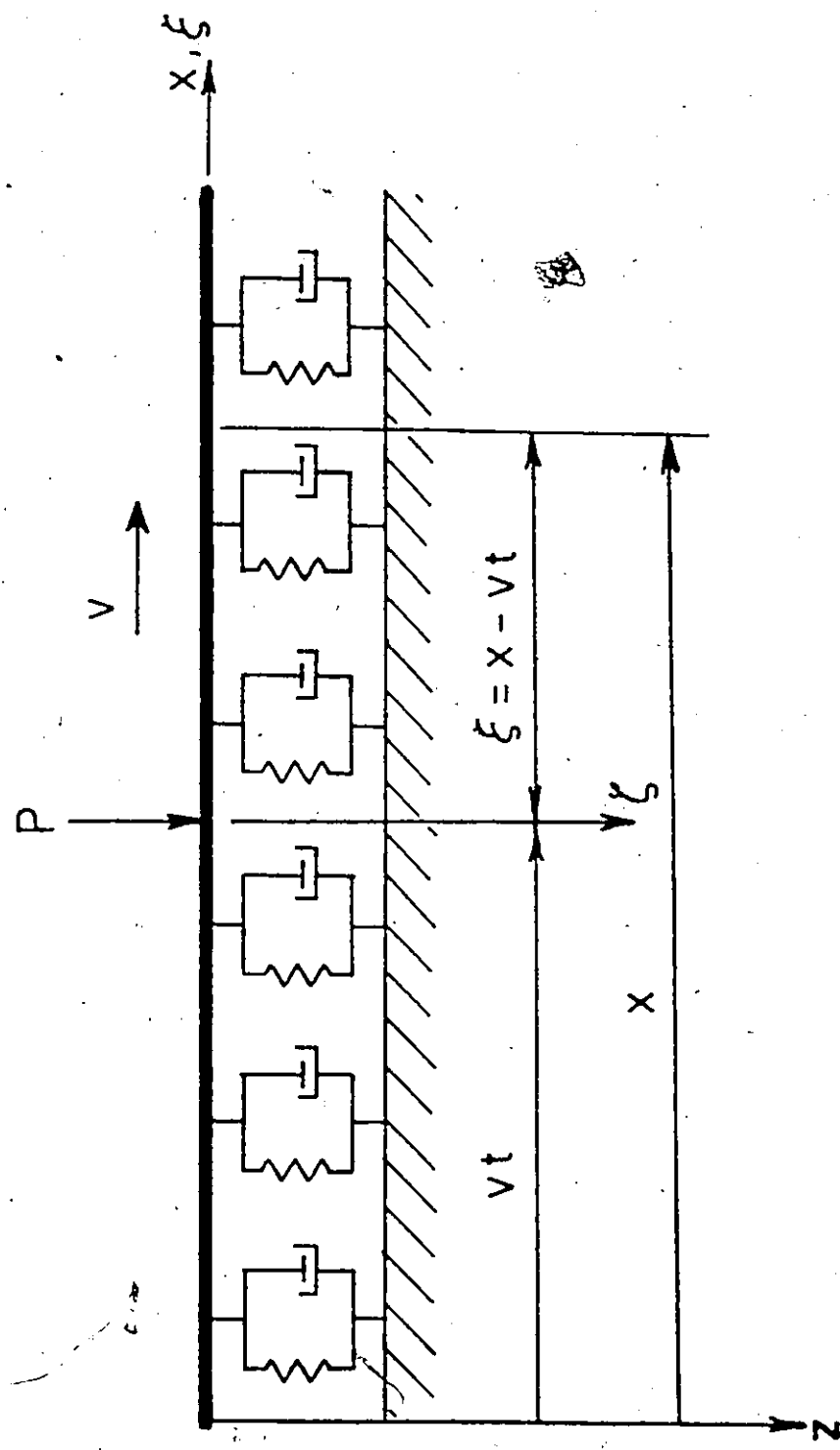
Figure 2.9 Infinite beam on a Winkler foundation of the Kelvin type and subjected to a concentrated moving load.

moving deflection profile is not symmetric. Due to the phase shift the position of largest deflection takes place at a position slightly behind the position of the moving load.

Mathews considered the steady state response of the railway track as a beam on a Winkler type foundation with [57] and without [58] damping. The analysis is for the case of an infinite beam subjected to an alternating load whose point of application moves with constant velocity along the beam and is of the form $P \cos \Omega t \, \delta(x-vt)$ where Ω is the frequency of the sinusoidally fluctuating load. This load is supposedly due to forces exerted by the wheels of vehicles and locomotives on a continuously supported rail. These periodic fluctuations may be caused, for example, by the vertical component of forces of oscillating parts in the moving vehicle or due to vertical sinusoidal track irregularities. Using this approach, and for vanishing frequency of fluctuation of the moving load, Mathews [58] duplicated Kenney's [56] results.

The recent practice of welding railroad rails to each other suggests that considerable axial compression forces may be induced in the rails due to thermal strains. This axial force affects the critical speed as well as the response of the rail to a moving load. Timoshenko [48] found that for assumed values of rail and foundation

parameter the critical speed is more than fifteen times the highest speed of a locomotive at the time, and he concluded that the static equations are sufficient for the analysis of stresses in railroad rails.

Recently, Kerr [49] treated the problem for an infinite beam on a Winkler type foundation including the axial load; the mathematical model he considered is shown in Figure 2.10. It was shown that the critical speed increases with an axial tension and decreases with compression, v_{cr} approaching zero when the axial force approaches the buckling load. This is shown in Figure 2.11 which is an illustration of $v_{cr} = \sqrt{\sqrt{\frac{4kEI}{m^2}} - \frac{N}{m}}$. And it was concluded that in the absence of expansion joints in the rails, the critical velocity may be reduced to within the operational velocities of trains. The response of the beam due to a moving concentrated load was found based on the following differential equation:

$$EI \frac{\partial^4 y}{\partial x^4} + N \frac{\partial^2 y}{\partial x^2} + m \frac{\partial^2 y}{\partial t^2} + k\,y = P\,\delta\,(x,t) \qquad (2.8)$$

where N is the axial force.

The relation between the speed (s) of propagation of free waves in the beam and the axial force (N) was found in a non-dimensional form to be

$$\frac{s}{s_{min} \mid N = 0} = \sqrt{\frac{1}{2}\left(\gamma^2 + \frac{1}{\gamma^2}\right) - \frac{N}{N_{cr}}} \qquad (2.9)$$
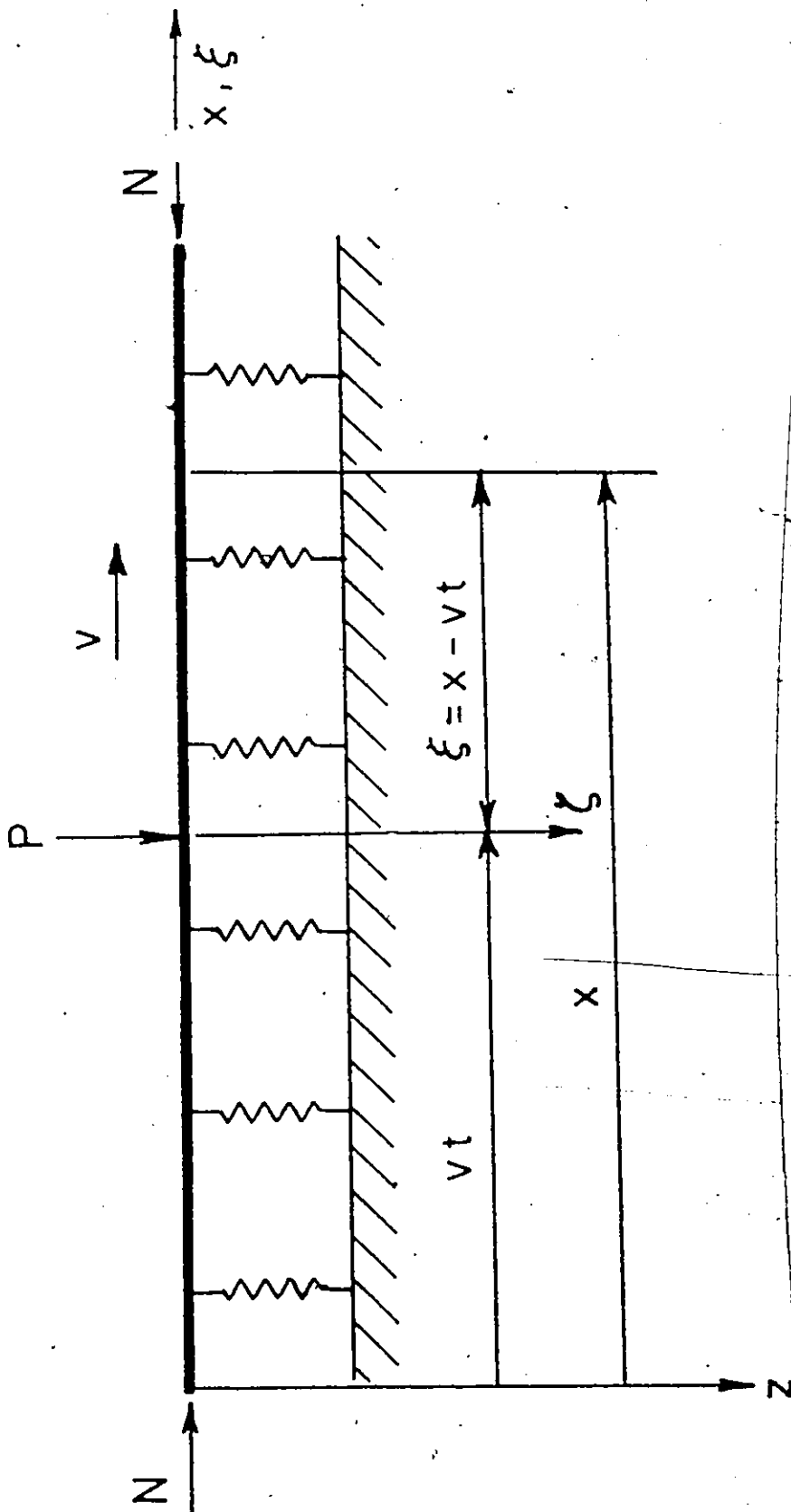
Figure 2.10 Infinite beam on a Winkler type foundation and subjected to an axial force and a moving load.
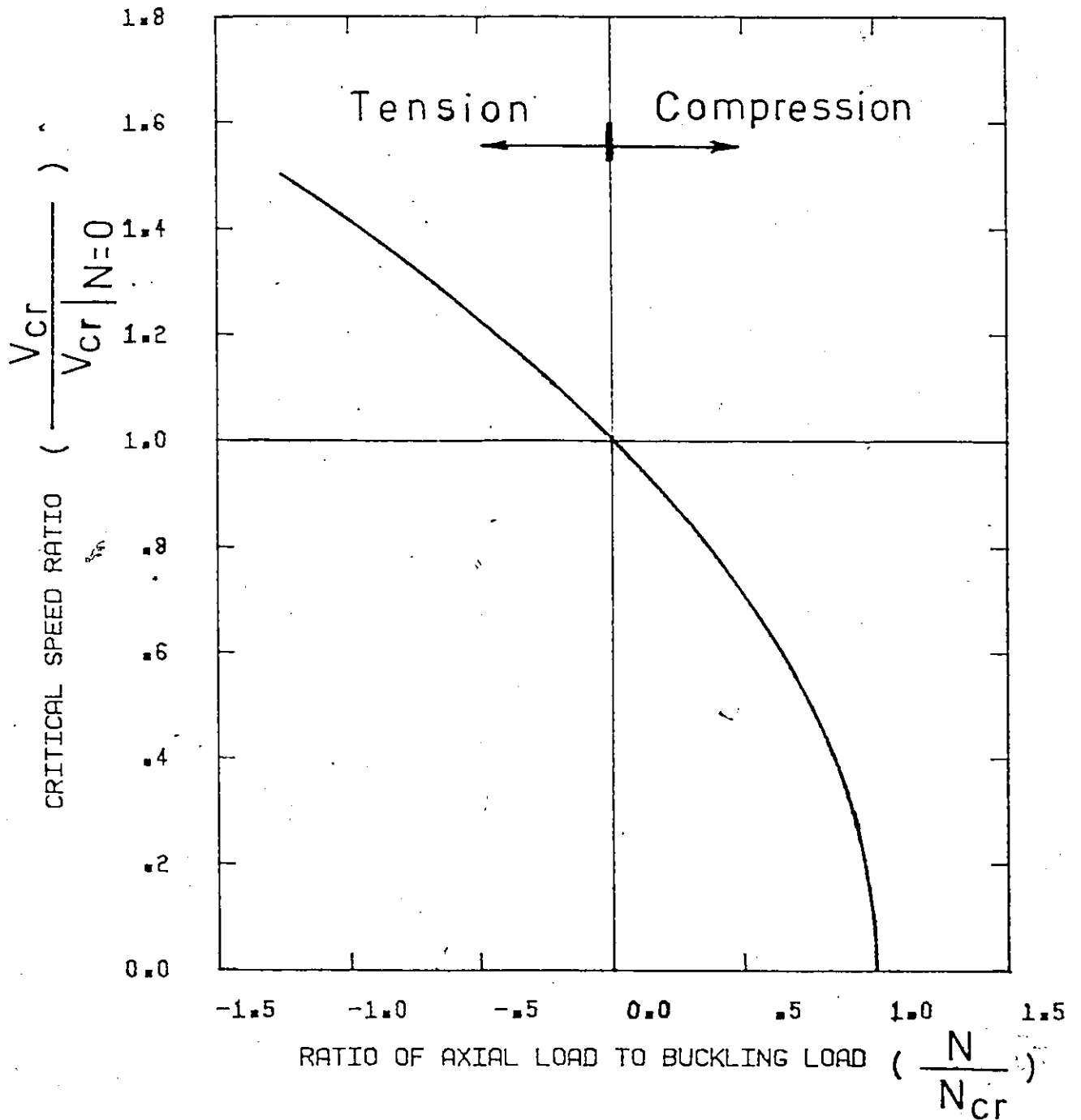
Figure 2.11   Effect of axial force on the critical
velocity of the track (v_{cr})

where
$$\gamma = \frac{2\pi}{\lambda} \sqrt[4]{\frac{k}{EI}}$$

k is the foundation modulus

λ the wave length of wave train

and N_{cr} the buckling load

A three dimensional illustration of equation (2.9) is given in Figure 2.12.

Kerr did not include damping in his model and considered only the case of a constant concentrated moving load at constant speed.

Newland in a short Research Note [59] has studied the possibility of lateral buckling of a continuously welded rail due to a moving load. His modelling for the beam motion in the horizontal plane is similar to that of Kerr, given by equation (2.8), for the motion in the vertical plane.

2.2.2 Coupled Track/Train Dynamics

Dynamic coupling occurs between a vehicle and its guideway due to the suspension forces acting on the guideway and the guideway deflection profile acting on the suspension. The two systems may be strongly coupled dynamically with vehicle body and suspension dynamics exerting a major influence on guideway deflection or may be weakly coupled
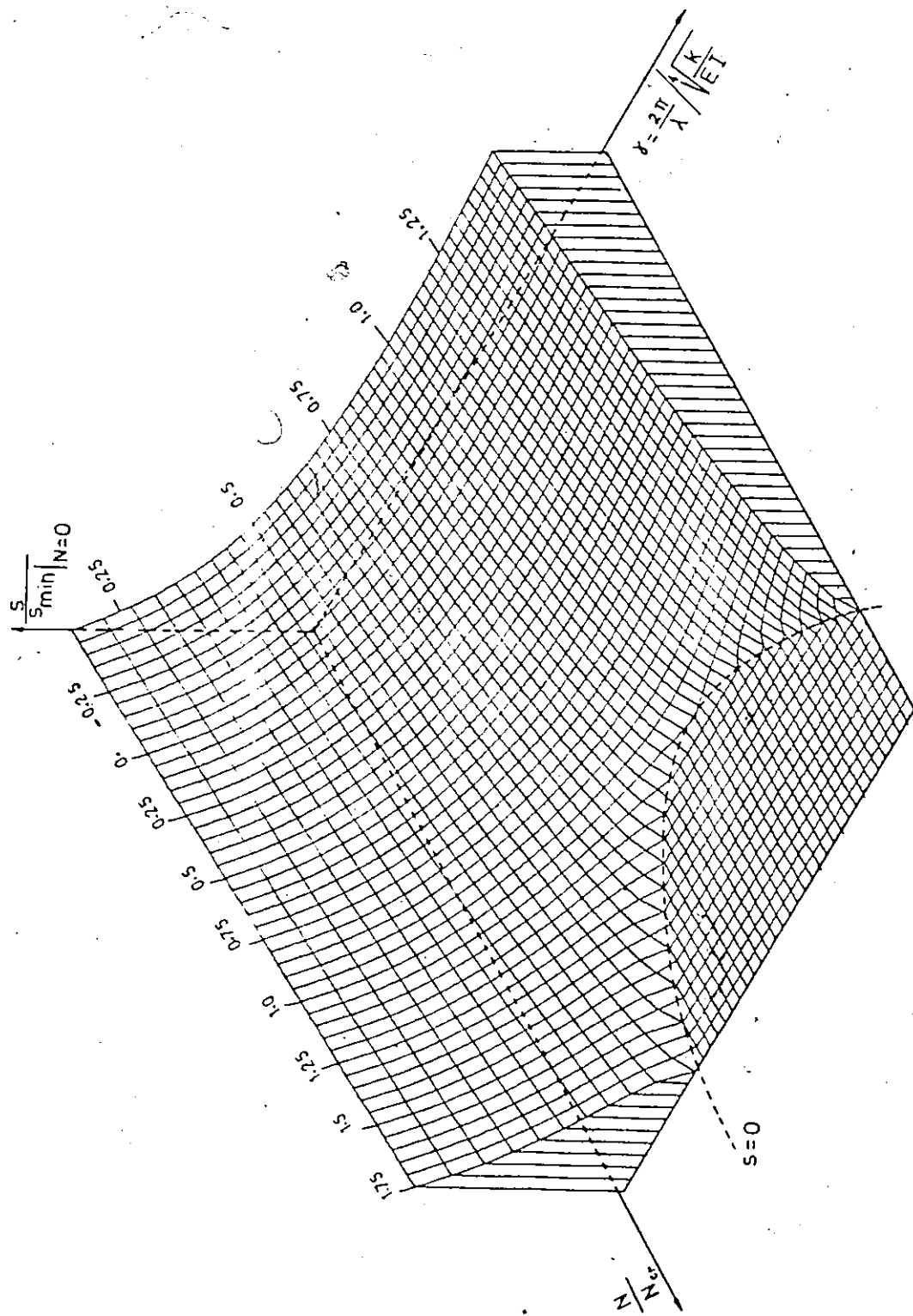
Figure 2.12   Three dimensional computer plot for the relation between
the ratio of axial force to buckling force, the ratio
of speed to critical speed and γ (given in Equation (2.9).)

if the dynamic suspension forces acting on the guideway are
small compared with the static forces due to vehicle weight.

After the high speed digital and electronic analog
computers came into wide use in the mid-1950's, the study
of more complete and realistic vehicle/guideway models
became feasible, and since 1970 several important
investigations have been published for vehicles with
vertical degrees of freedom only or with vertical as well
as pitch motion (one and two dimensional vehicles). Most
of these investigations however were for vehicle/elevated
guideway of the single, multiple or continuous span types.
Virtually all of these studies were based on the modal
analysis using the Bernoulli-Euler beam equation. Other
methods of solution included the lumped mass methods and
the finite difference and other direct methods [50]. The
simplest model for a vehicle/guideway system consist of
constant concentrated or distributed forces equal to
vehicle weight which crosses the guideway at constant
velocity (see Figure 2.13). Studies of constant forces
moving along the guideway are considered to be important
because they represent good limiting approximations for
vehicle-guideway systems in which passenger compartment
accelerations are less than about 0.05 g [50].

The coupled dynamics of transportation vehicles
and beam type elevated guideway was the subject of a recent
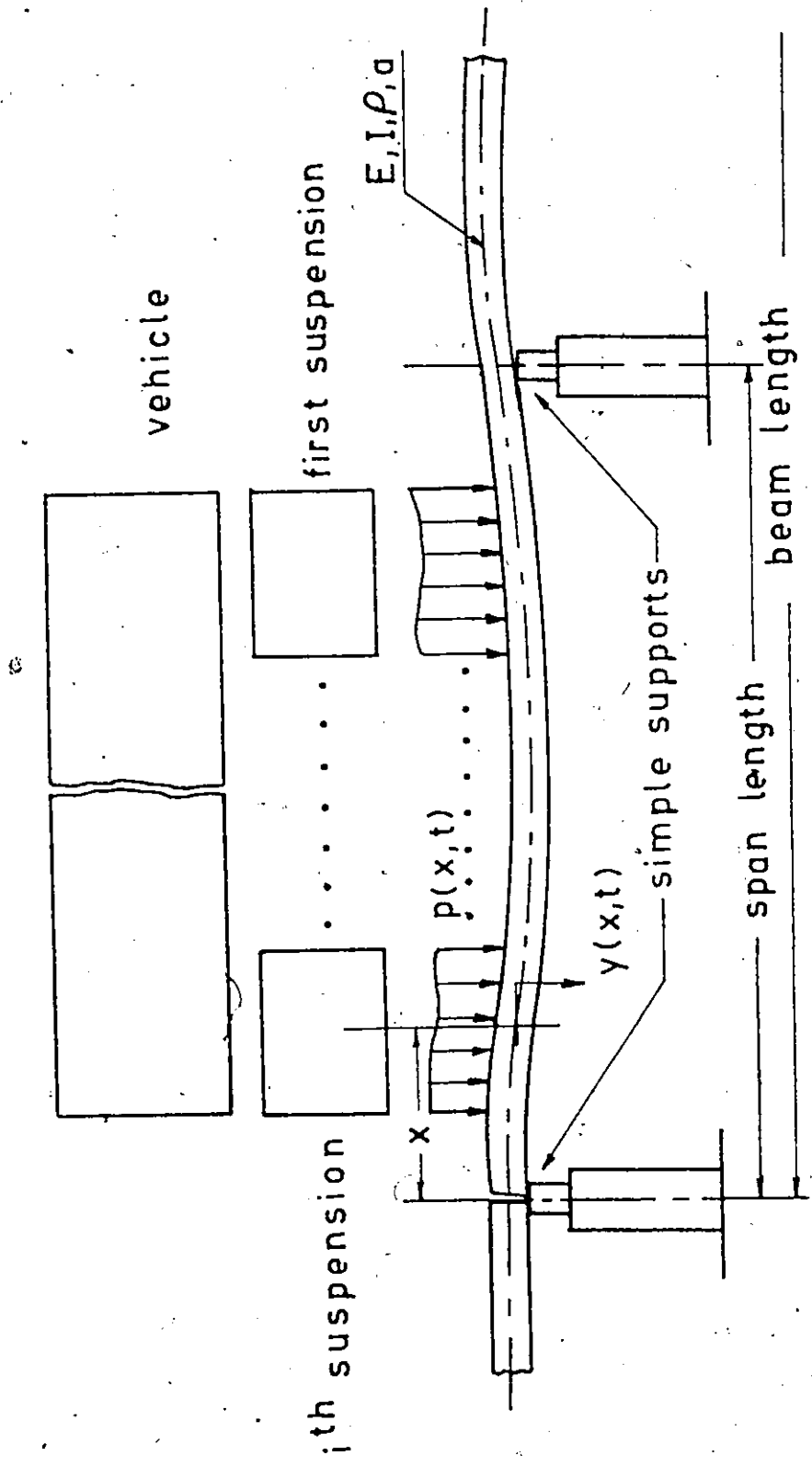
Figure 2.13   General vehicle/elevated-guideway dynamic model

review [50] and will not be further discussed here. Present
and future high speed ground transportation systems have
activiated a new interest in the problem of moving loads
and mass-spring systems on beams continuously supported on
elastic foundation. As vehicle speeds for proposed systems
increase, the dynamic interactions between the vehicles and
their guideway become an increasingly important potential
problem.

Nelson and Conover [60] appear to be among the
first investigators to consider the problem of the trans-
verse response of a beam subjected to a continuous sequence
of moving mass loads. More specifically, the problem they
treated was not explicit determination of the transverse
response but rather the determination of the behaviour
(stable and unstable) of the transverse response for a
finite, simply supported, Bernoulli-Euler beam resting on
a uniform elastic foundation and loaded by a continuous
sequence of identical, equally spaced, constant speed mass
particles. They determined the boundaries separating the
regions of stable and unstable response for various values
of the physical system parameters. This was done by
utilizing Floquet theory and an iterative computational
procedure on a digital computer.

Benedetti [61] studied the problem of the
determination of the coupled transverse response of a finite

Bernoulli-Euler beam loaded by one or several spring-mass vehicles travelling across the beam at a constant speed. The beam is uniform, simply supported and rests on a massless uniform elastic foundation. The vehicles which are identical, equally spaced and attached to the beam consist of a wheel mass and a viscously damped spring-supported mass.

Studies [62,63] on the vehicle-guideway dynamics were performed in conjunction with the proposed designing of tracked air cushion vehicles (TACV). The vehicle-guideway system is modelled as an arbitrary number of lumped sprung vehicle mass travelling along single simply supported Bernoulli-Euler beams on a foundation. Biggers and Wilson [63] found the dynamic response of the vehicles and guideway using an iterative procedure. The end conditions used in these studies, which are simple supports, are not realistic for modelling a railway track as a continuously supported beam on a foundation. It appears that it was used by most authors for reasons of mathematical simplications, namely to use the normal modes method for the solutions.

In reference [37] the authors have studied analytically and experimentally the dynamics of four wheeled railway vehicles including the effect of vertical track elasticity. This effect was introduced by assuming the

mass of a wheelset to be supported by a spring and the anchorage of this spring follows the rail irregularities profile. This model does not represent the actual case and is more applicable to the modelling of the elasticity of the tires of a vehicle and not the vertical elasticity of the railway track.

The dynamic variation of wheel load attributed to vertical deformation of rail end due to unevenness profile of running surface of rail at weld was studied by Kuroda [64]. The vehicle/track model assumes that the wheel and the rail are mass points and that they remain in contact without separation (Figure 2.14) which is the case in normal running conditions. But it is further assumed that the deviation of truck and body of vehicle motion is negligibly small and that they can be considered moving at the constant speed of the vehicle, while motionless in the vertical direction.

Meacham [65,66] as a result of several years of active research in the field of track/train dynamics interaction developed a more realistic model for the conventional track structure which is not too complex. Meacham used this model to study the freight car-rocking problem. The computer study included the use of analog as well as digital and hybrid computers. Laboratory and field tests results gave good correlation with the computer
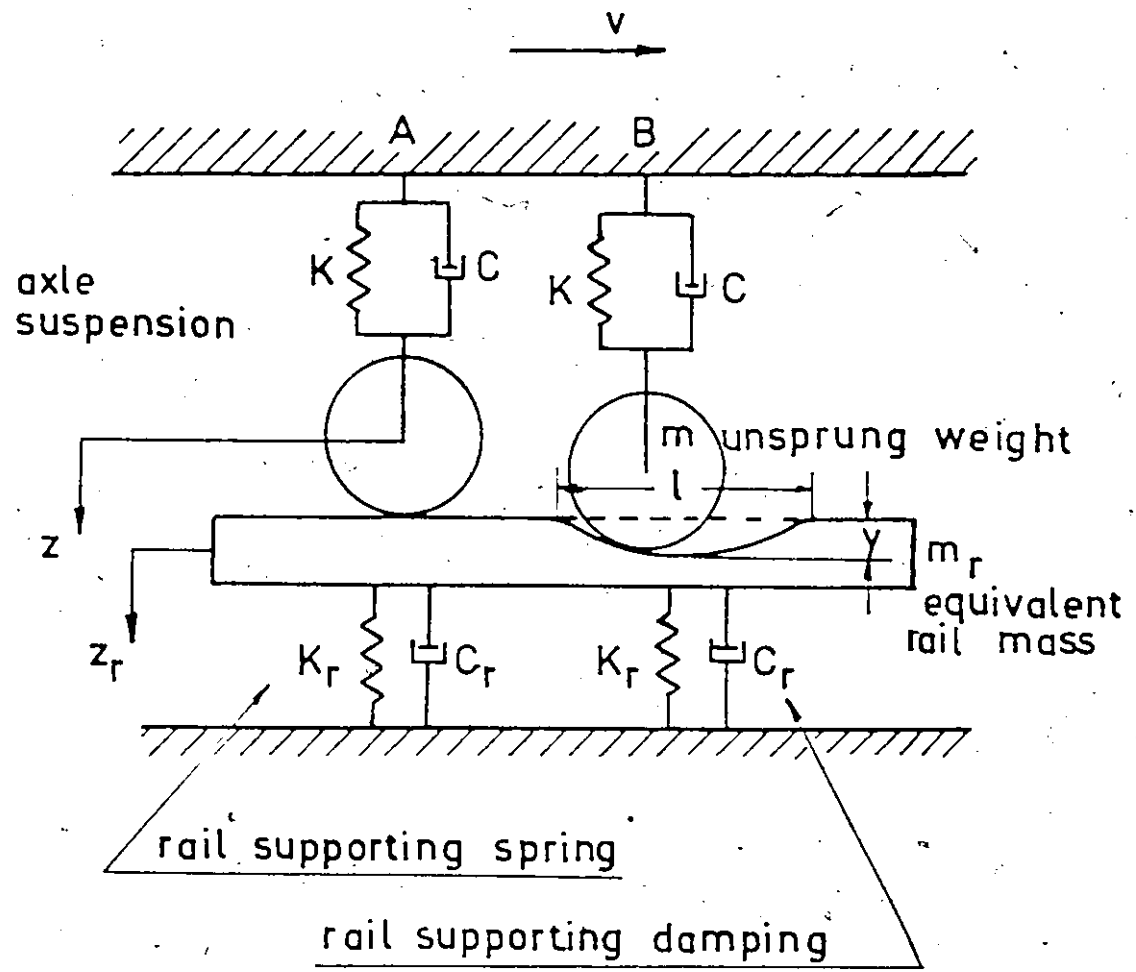
Figure 2.14   A simplified vibration model for a
             vertical deformation of rail used by
             Kuroda [64]

results. The model of a conventional tie-type structure is converted to a mathematical model that can be incorporated in the analysis of the vehicle motions. For this purpose the track system is discretized. Meacham's studies indicate that for the mathematical representation of the railway vehicle and the track for computer studies, the vehicle can be represented by a spring-mass system supported by another spring-mass system representing the track. The input to the system is usually a displacement representing the vertical profile of the track. The wheel-track force generated represents a force travelling at vehicle speed and located at the wheels. "For studies of vehicle response, this is a perfectly proper system giving as it does the continuous force exciting the vehicle..." [55]. For a study of the track, however, it is obvious that this force is a transient one with respect to any fixed point on the track. The force directly over any point reaches a maximum only when the wheel is directly over that point.

In the discussion at the "Interaction between Vehicle and Track" Conference [27, p.49] Professor Bishop says "That the track is essentially a passive thing; it has no source of energy built into it. There are thus good reasons, I think, for asserting that it cannot change the motion qualitatively. It can only change it quantitatively. So we really need to know, how sensitive is this

quantitative adjustment that can be expected from the track?".

Actually one should also say in which direction will the effect be. If a vertical track flexibility is assumed how (in which direction)will this affect the lateral stability? How will it affect the response of the railway vehicle due to rail irregularities?... etc.

In this thesis an attempt shall be made to answer some of these questions and to illustrate the adequacy or inadequacy of models on rigid tracks.

CHAPTER 3

TRACK DYNAMICS

Studies on the response of the continuously supported beam subjected to moving loads were conducted first, in connection with the determination of stresses in railroad tracks, by Timoshenko [48]. The problem of the response of beams on foundations subjected to moving loads has been treated by several authors [49, 55, 56, 57, 58]. However, the models used for these analyses neglected important factors and considered only special cases of loading.

As the tendency is toward heavier loads and higher speeds for railway vehicles, the forces exerted by the wheels may cause excessive dynamic deflections of the track. These deflections, if large, may cause permanent distortions or buckling of the track, which in turn can result in costly accidents.

In this chapter the problem of the dynamic response of the railway track modeled as a beam on Kelvin type foundation and subjected to time dependent moving forces is analyzed. The principal analytical techniques and simplifying assumptions which may be used for physically realistic forcing functions are discussed.

The analysis takes into consideration all possible

65

linear effects including damping in the beam and the foundation and axial load in the beam. The effect of damping, axial load in the beam, velocity and acceleration of the moving forces on the dynamic response are discussed.

3.1 Description of Mathematical Model

In all analyses for the response of railway tracks reported so far, the track has been modeled as a beam on an elastic foundation of the Winkler type with or without damping. In the crosstie systems only the ties are continuously supported by the roadbed, while the rail itself rests on the ties. Investigations [51, 54] have shown, however, that an equivalent continuous elastic foundation can be substituted with good approximation for such supports. In this way, the theory of beams on elastic foundations (which had its first application in the calculation of stresses and deflections of railroad tracks [51] can be applied to the analysis of the railway track itself. Various investigators, however, have used different end conditions when modeling the track and the roadbed as a continuously supported beam on an elastic Winkler type foundation with or without damping. The infinite beam, the semi-infinite and the finite beam with simply supported ends have all been considered. It is believed that the infinite beam represents a more realistic representation of the physical situation, and

thus is the model which is used in the present research.

Current practice is to weld the rails together into lengths of about 1400 feet. Significant advantages in the maintenance of the track and trains are achieved by this technique. Because of the lack of expansion joints, changes in temperature may cause considerable axial forces in the rails. In the present analysis, this effect is taken into account by including an axial load N in the model of the railway track. This load will be compressive if there is a rise in temperature or tensile if there is a drop in temperature; the reference temperature being the one at which the axial thermal strains or stresses vanish.

In view of the above discussion, the model considered in this research is that of an infinite Euler beam on a Kelvin type foundation subjected to an axial load and a time dependent moving load as shown in Figure 3.1.

The differential equation of a beam subjected to a load w may be obtained by first considering the bending of an elemental segment of a beam subjected to an axial force N. For the uniform beam having a moment of inertia I and a modulus of elasticity E we get:

$$EI \frac{\partial^4 y}{\partial x^4} + N \frac{\partial^2 y}{\partial x^2} = w \qquad (3.1)$$

The loads applied (w) when the beam rests on an elastic viscously damped foundation are:
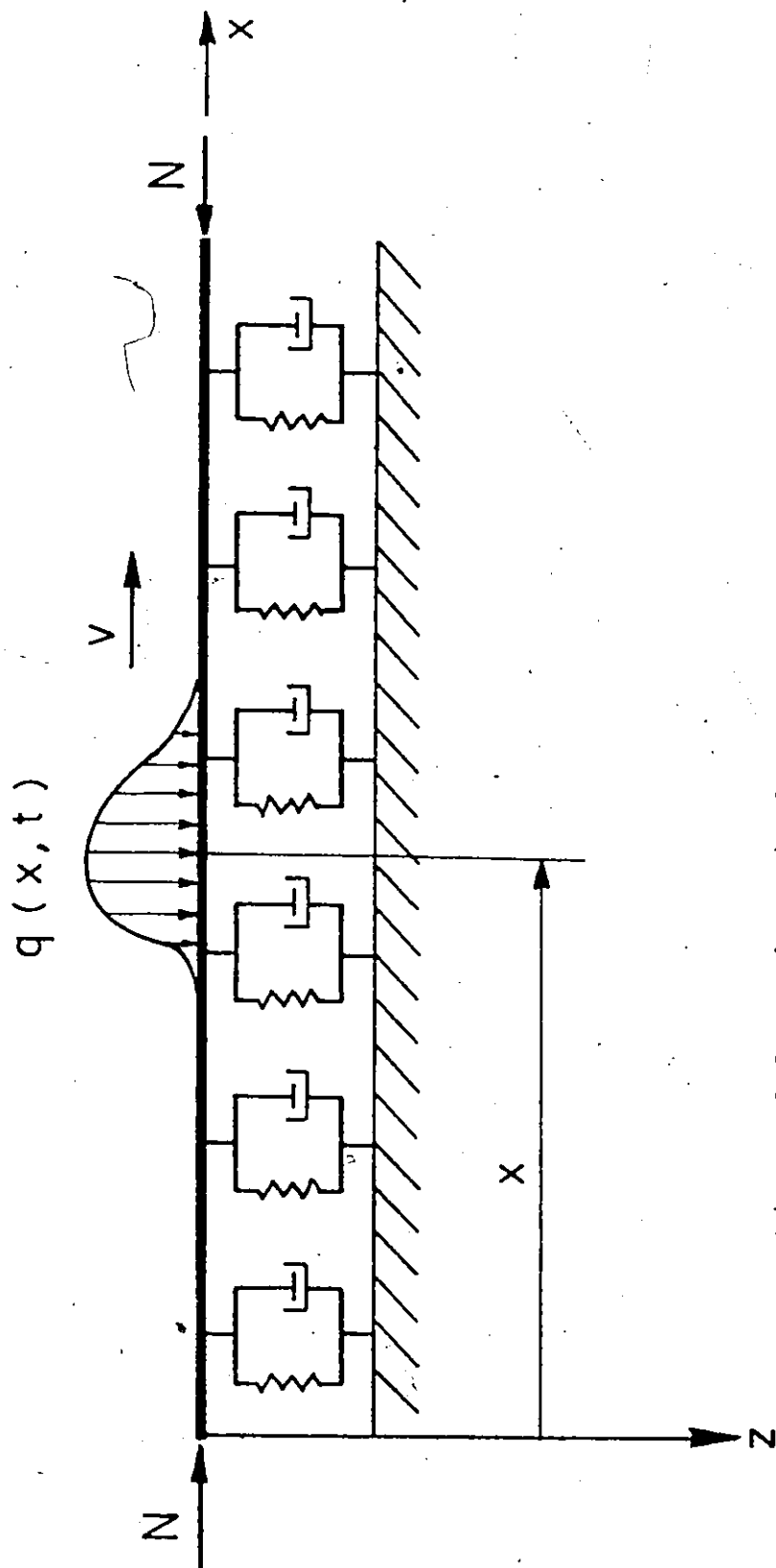
Figure 3.1 Mathematical model for the railway track as a beam on a Kelvin type foundation subjected to an axial force and a time dependent moving load

Inertia force: $m \frac{\partial^2 y}{\partial t^2}$

Force due to viscous damping: $c \frac{\partial y}{\partial t}$

Spring force: $k y$

Applied force: $q(x,t)$

where

m = mass of beam per unit length

k = modulus of the foundation

c = the coefficient of viscous damping

Substituting for w into equation (3.1) produces the differential equation of motion of the continuously supported beam on a foundation of the Kelvin type subjected to an axial load and a moving time-dependent forcing function $q(x,t)$.

$$EI \frac{\partial^4 y}{\partial x^4} + N \frac{\partial^2 y}{\partial x^2} + m \frac{\partial^2 y}{\partial t^2} + c \frac{\partial y}{\partial t} + ky = q(x,t) \qquad (3.2)$$

$$- \infty < x < \infty, \ t > 0$$

The present investigation is based on the solution of this partial differential equation.

3.2 Derivation of Solutions

Before proceeding with the solution of equation (3.2) the possibility of propagation of free waves in the infinite beam should be considered.

3.2.1 Propagation Velocity of Free Waves

.To study the propagation of free waves in the

infinite beam, we consider the undamped case with no forcing function:

$$EI \frac{\partial^4 y}{\partial x^4} + N \frac{\partial^2 y}{\partial x^2} + m \frac{\partial^2 y}{\partial t^2} + ky = 0 \qquad (3.3)$$

This equation was previously solved by Kerr [49] who found the critical velocity of the beam subjected to the axial compression force N to be:

$$v_{cr} = \sqrt{\sqrt{\frac{4kEI}{m^2}} - \frac{N}{m}} \qquad (3.4)$$

3.2.2 Response to General Moving Load

Very little work on the response of beam to time dependent forces is reported in the literature. Nowacki [67] is one of the few authors who considered the transient problem; the particular case studied is the response of an infinite Bernoulli-Euler beam on an elastic foundation (without axial force or damping) due to a transient load P $\delta(x)\delta(t)$. . The transient response of an infinite beam on a foundation was considered in [69]. Solution in integral form is obtained, without its evaluation in closed form.

For the general case the initial-boundary value problem is solved using integral methods. In addition to equation (3.2) we have the following initial and boundary conditions. The initial conditions will be given by the prescribed displacement and velocity (at t=0):

$$y(x,0) = f(x) \text{ and } \frac{\partial y(x,0)}{\partial t} = g(x) \qquad (3.5)$$

The boundary conditions for all times (t>0) are:

$$\left. y(x,t) \right|_{|x| \to \infty} \longrightarrow 0$$

and

$$\left. \frac{\partial^n y(x,t)}{\partial x^n} \right|_{|x| \to \infty} \longrightarrow 0 \quad (n=1,2,3)$$

(3.6)

Integral transform methods are used to solve the partial differential equation (3.2) with initial and boundary conditions given by (3.5) and (3.6) respectively. The usual assumptions concerning the existence of the Laplace and Fourier transforms are made.

Laplace and Fourier transforms are defined by [68]:

$$\bar{Y}(\alpha,p) = \frac{1}{\sqrt{2\pi}} \int_{-\infty}^{\infty} e^{-i\alpha x} \, dx \int_{0}^{\infty} e^{-pt} \, y(x,t) \, dt \qquad (3.7)$$

Where the capitalization of the respective letters implies the Fourier transformation and the overbar indicates the Laplace transformation.

The transformed form of equation (3.2) becomes:

$$\bar{Y}(\alpha,p) = \frac{(\zeta F+G) + (p+\zeta) \; F + \frac{1}{m} \bar{Q}}{(p+\zeta)^2 + a^2 (\alpha^2+b)^2 + \lambda^2} \qquad (3.8)$$

where

$$\zeta = \frac{c}{2m} \qquad a^2 = \frac{EI}{m} \qquad \omega_0^2 = \frac{k}{m}$$

$$b = \frac{N}{2EI} \qquad \lambda^2 = \omega_0^2 - \zeta^2 - a^2 b^2$$

The inversion theorem for the Laplace transform together with its convolution property are first used,

followed by the use of the convolution theorem for the Fourier transform. The integral representation of the displacement field $y(x,t)$ is given by Appendix (A):

$$y(x,t) = e^{-\zeta t} \left\{ \int_{-\infty}^{\infty} [g(\xi) + \zeta f(\xi)] \; h(x-\xi, \; t) \; d\xi \right.$$

$$\left. + \int_{-\infty}^{\infty} f(\xi) \; h_t(x-\xi, \; t) \; d\xi \right\}$$

$$+ \frac{1}{m} \int_0^t e^{-\zeta(t-\tau)} \int_{-\infty}^{\infty} q(\xi,\tau) \; h(x-\xi, \; t-\tau) \; d\xi d\tau$$

$$\text{(3.9)}$$

where

$$h(x,t) \quad = \frac{1}{\sqrt{4\pi a}} \int_0^t J_0 \left(\lambda\sqrt{t^2-u^2}\right) \frac{1}{\sqrt{u}} \; \cos\left(\frac{x^2}{4au} - abu - \frac{\pi}{4}\right) du$$

and

$$h_t(x,t) \quad = - \frac{\lambda t}{\sqrt{4\pi a}} \int_0^t \frac{J_1\left(\lambda\sqrt{t^2-u^2}\right)}{\sqrt{t^2-u^2}} \; \frac{1}{\sqrt{u}} \; \cos\left(\frac{x^2}{4au}\right.$$

$$\left. - abu - \frac{\pi}{4}\right) du$$

$$+ \frac{1}{\sqrt{4\pi a}} \; \frac{1}{\sqrt{t}} \; \cos\left(\frac{x^2}{4at} - abt - \frac{\pi}{4}\right) \qquad \text{(3.10)}$$

For zero initial conditions the result is

$$y(x,t) = \frac{1}{m} \int_0^t e^{-\zeta(t-\tau)} \int_{-\infty}^{\infty} q(\xi,\tau) \; h(x-\xi, \; t-\tau) \; d\xi d\tau \qquad \text{(3.11)}$$

For physically realistic situations, the applied loading function is non-zero over a region $x_1 \leqslant x \leqslant x_2$

$$y(x,t) = \frac{1}{m} \int_0^t e^{-\zeta(t-\tau)} \int_{x_1}^{x_2} q(\xi,\tau) \; h(x-\xi, \; t-\tau) \; d\xi d\tau \qquad \text{(3.12)}$$

Although (3.9)., (3.11) and (3.12) represent the complete integral solutions of the problem, they cannot, in general, be evaluated exactly. Even in simple cases of interest, evaluation of solutions in closed-form is very difficult, and it is necessary to resort to asymptotic and/or numerical methods. In the following discussion the term "transient response" will be used to designate the solution of the initial-value problem along with a forcing function. The steady-state response can be obtained from a formal passage to the limit as t tends to infinity. In general the steady state solution can be obtained from the transient solution for large values of t.

Some special cases for the forcing function of physical interest and relevance to the area of railroad track deflection and vibrations are:

(i) $q(x,t) = P \delta(x)$

(ii) $q(x,t) = P \delta(x) \delta(t)$

(iii) $q(x,t) = P \delta(t); \quad x_1 \leqslant x \leqslant x_2$

(iv) $q(x,t) = P \delta(x-vt)$

(v) $q(x,t) = P \cos \Omega t \, \delta(x-vt)$

(vi) $q(x,t) = P f(t) \, \delta(x-vt \pm \rho t^2)$

In all the above cases the initial conditions will be assumed to be equal to zero, and hence the integral representation of the solution given by equations (3.11) or (3.12) will be used.

(i) <u>Deflection of the beam due to a concentrated static</u>
<u>load q(x,t) = P δ(x)</u>

.For the case of no axial force (N=0, h=0) the
transient solution is:

$$y(x,t) = \frac{P}{m\sqrt{4\pi a}} \int_0^t e^{-\zeta r} \int_0^r J_0(\lambda\sqrt{r^2-u^2}) \frac{1}{\sqrt{u}}$$

$$\cos\left(\frac{x^2}{4au} - \frac{\pi}{4}\right) du\ dr \qquad (3.13)$$

The steady-state solution is obtained from a formal
passage to the limit as t tends to infinity.

$$Y_{st}(x) = \frac{P}{m\sqrt{4\pi a}} \int_0^\infty e^{-\zeta r} \int_0^r J_0(\lambda\sqrt{r^2-u^2}) \frac{1}{\sqrt{u}}$$

$$\cos\left(\frac{x^2}{4au} - \frac{\pi}{4}\right) du\ dr \qquad (3.14)$$

The integration may be performed by interpreting
(3.14) as the Laplace transform of the inner integral.
Let $\lambda u = v$, $\lambda r = \nu$ and $\chi = (\lambda x^2/4a)$, getting

$$Y_{st}(x) = \frac{P}{m\sqrt{4\pi a}} \mathcal{L}\left[\frac{1}{\sqrt{\lambda}} \int_0^\nu J_0(\sqrt{\nu^2-v^2}) \frac{1}{\sqrt{v}} \cos\left(\frac{\chi}{v} - \frac{\pi}{4}\right) dv\right] \quad (3.15)$$

From Erdélyi's [70] table of Laplace transform we have

$$\mathcal{L}\left[\int_0^\nu J_0(\sqrt{\nu^2-v^2}\ f(v)\cdot dv;\nu\to p\right] = \frac{1}{\sqrt{p^2+1}}\ \bar{f}(\sqrt{p^2+1}) \qquad (3.16)$$

where $\bar{f}(p) = \mathcal{L}[f(v);\ \nu\to p]$

Also let $\sigma = 1/\sqrt{v}$

But

$$\mathcal{L}\left[\frac{1}{\sqrt{v}}\cos\left(\frac{\chi}{v}-\frac{\pi}{4}\right)\right]=\frac{\sqrt{2}}{2}\left\{\mathcal{L}\left[\frac{1}{\sqrt{v}}\cos\frac{\chi}{v}\right]+\mathcal{L}\left[\frac{1}{\sqrt{v}}\sin\frac{\chi}{v}\right]\right\}$$

$$=\sqrt{2}\left[\int_{0}^{\infty}e^{-\frac{p}{\sigma^2}}\cos(\chi\sigma^2)\;\frac{d\xi}{\xi^2}\right.$$

$$\left.+\int_{0}^{\infty}e^{-\frac{p}{\sigma^2}}\sin(\chi\sigma^2)\frac{d\sigma}{\sigma^2}\right] \qquad (3.17)$$

From Gradshteyn's Ryzhik's [71] table of integrals:

$$\int_{0}^{\infty}e^{-\frac{\beta^2}{\xi^2}}\sin(\Delta^2\xi^2)\frac{d\xi}{\xi^2}=\frac{\sqrt{\pi}}{2\beta}\,e^{-\sqrt{2}\,\Delta\beta}\;\sin(\sqrt{2}\,\Delta\beta) \qquad (3.18a)$$

$$\int_{0}^{\infty}e^{-\frac{\beta^2}{\xi^2}}\cos(\Delta^2\xi^2)\frac{d\xi}{\xi^2}=\frac{\sqrt{\pi}}{2\beta}\,e^{-\sqrt{2}\,\Delta\beta}\;\sin(\sqrt{2}\,\Delta\beta) \qquad (3.18b)$$

Using equations (3.16), (3.17) and (3.18a&b) as well as letting $\zeta\to0$,

$$Y_{st}(x)=\frac{P\omega}{2k}\,e^{-\omega|x|}(\cos\omega|x|+\sin\omega|x|) \qquad (3.19)$$

where

$$\omega=\sqrt[4]{\frac{k}{4EI}}$$

which is the result given by Hetényi [51] in a slightly different form.

(ii) **Response to an instantaneous loading**

$$\underline{q(x,t)=P\,\delta(x)\,\delta(t)}$$

By substituting for $q(x,t)=P\,\delta(x)\,\delta(t)$ in equation (3.12) the transient response due to the

instantaneous loading is obtained as:

$$y(x,t) = \frac{P}{m\sqrt{4\pi a}} e^{-\zeta t} \int_0^t J_0(\lambda\sqrt{t^2-u^2}) \frac{1}{\sqrt{u}}$$

$$\cos(\frac{x^2}{4au} - abu - \frac{\pi}{4}) \, du \qquad (3.20)$$

To compare the result with the one obtained by Nowacki [67], the transient response at the origin is obtained for the case of no damping ($\zeta=0$) and no axial force ($N=0$, $b=0$ and $\lambda = \omega_0$):

$$y(0,t) = \frac{P}{m\sqrt{4\pi a}} \cos(-\frac{\pi}{4}) \int_0^t J_0(\omega_0\sqrt{t^2-u^2}) \frac{1}{\sqrt{u}} \, du \qquad (3.21)$$

The integral can be evaluated by making the change of variables $u = t \cos\theta$, hence

$$y(0,t) = \frac{P}{m\sqrt{4\pi a}} \cos(-\frac{\pi}{4}) \int_0^{\pi/2} J_0(\omega_0 t \sin\theta) \sqrt{\frac{t}{\cos\theta}} \sin\theta \, d\theta$$

$$(3.22)$$

$$= \frac{P}{m\sqrt{4\pi a}} \cos(-\frac{\pi}{4}) \frac{1}{\sqrt{\omega_0}} \int_0^{\pi/2} J_0(\omega_0 t \sin\theta) \sqrt{\omega_0}t$$

$$\frac{1}{\sqrt{\cos\theta} \sqrt{\sin\theta}} \, d\theta \qquad (3.23)$$

Noting that this result is a special case of Sonine's first finite integral (see Watson [72]), we get

$$\int_0^{\pi/2} J_0(\omega t \sin\theta) \frac{\sin\theta}{\sqrt{\cos\theta}} \, d\theta = \frac{2^{-3/4} J_{1/4}(\omega_0 t) \; \Gamma(1/4)}{\sqrt[4]{\omega_0 t}}$$

and hence

$$y(0,t) = \frac{\sqrt{k/m}\ P\ \Gamma(1/4)}{2\sqrt{\pi}(4EI)^{1/4}(2k)^{3/4}}\ [\sqrt{k/m}\ t]^{1/4}$$

$$J_{1/4}\ (\sqrt{k/m}\ t) \qquad\qquad (3.24)$$

This result differs slightly from the result obtained by Nowacki [67]. This difference is apparently due to the difficulties encountered by Nowacki in calculating an inverse Laplace transform.

3.2.3 Response to Moving Load of Constant Amplitude

Most researchers were essentially concerned with the investigation of the steady state problem which takes into account certain specific physical cases. Of course, neglecting certain effects leads to mathematical simplifications and the resulting steady state problem is solved as a boundary value problem.

Mathews [57, 58] analyzed the problem of vibrations of an infinite beam on an elastic foundation (without axial force) subjected to an alternating load whose point of application moves with constant velocity along the beam. Application of the results to problems of deformations of railway track is briefly indicated.

Kenney [56], Kerr [49] and others analyzed the steady state vibrations of beams on foundations subjected to a constant moving concentrated load but their models for the beam, usually considered as a Bernoulli-Euler beam do not include all possible linear effects. In the

following steady state solution all linear effects included
in the present analysis,will be considered for the case of
a concentrated load moving at a constant velocity as shown
in Figure 3.2.

The right hand side of equation (3.2) is of the
form P δ (x-vt), and the governing equation of motion
becomes

$$EI \frac{\partial^4 y}{\partial x^4} + N \frac{\partial^2 y}{\partial x^2} + m \frac{\partial^2 y}{\partial t^2} + c \frac{\partial y}{\partial t} + ky = P\, \delta(x-vt) \quad (3.25)$$

Because of the infinite extent of the beam as well
as the steady-state assumption, for an observer moving with
the load along the beam, the deflections of the beam will
appear static. This observation suggests that it is
desirable to transpose the coordinate system to the moving
reference axes (ξ, η, ζ) where $\xi = x-vt$; $\eta = y(\xi) =$
$y(x-vt)$, $\zeta = z$.

This transformation of coordinate systems will
transform the partial differential equation given by
equation (3.25) to an ordinary differential equation in the
moving reference axes. Because interest here is in
the case of load and velocity invarient with time, all
partial derivatives with respect to time become equal to
zero, and the differential equation becomes:

$$EI\, \eta^{iv} + (N+mv^2)\, \eta'' - cv\, \eta' + k\, \eta = P\, \delta(\xi) \quad (3.26)$$

Because of the steady-state assumption, the load
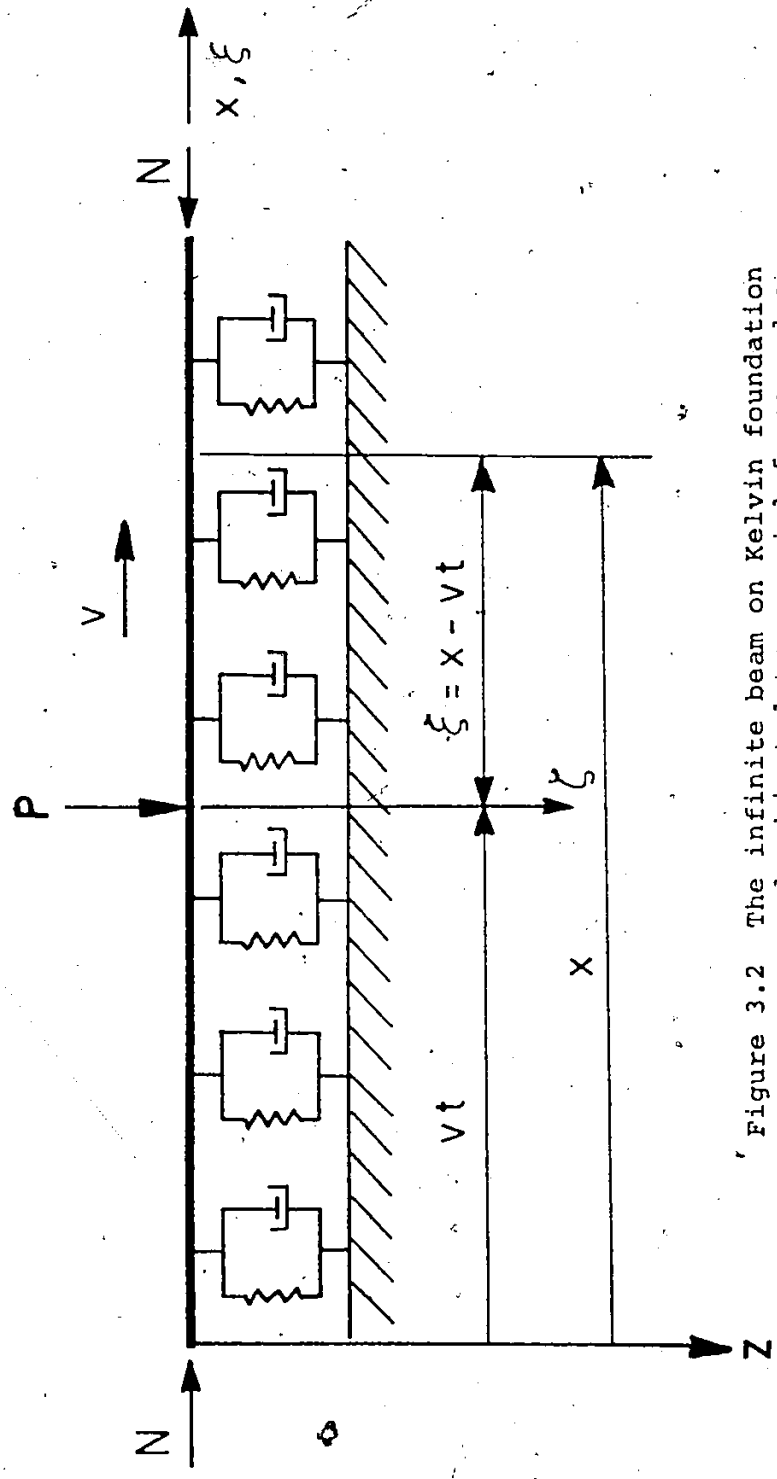
Figure 3.2 The infinite beam on Kelvin foundation and subjected to an axial force and a moving load

moves horizontally but does not experience any acceleration in the vertical direction. Thus P in equation (3.26) represents only the static intensity of the load.

It is useful to note that equation (3.26) is identical to the differential equation of motion of a beam which rests on a damped elastic foundation, subjected to an axial force $(N+mv^2)$ and a lateral load P at $\xi=0$. Dividing through by (EI) equation (3.26) becomes:

$$\eta^{iv} + \frac{N+mv^2}{EI} \eta'' - \frac{cv}{EI} \eta' + \frac{k}{EI} \eta = \frac{P\,\delta\,(\xi)}{EI} \qquad (3.27)$$

Setting:

$$4\alpha_1^2 = \frac{N+mv^2}{EI}$$

$$\theta = \text{speed ratio} = \frac{v}{v_{cr}} = \frac{v}{\sqrt{\sqrt{\frac{4kEI}{m^2}} - \frac{N}{m}}}$$

$$\beta = \text{damping ratio} = \frac{c}{c_{cr}}$$

$$c_{cr} = 2\,k\,m \text{ (as for a simple mass spring system)}$$

$$4\omega^4 = \frac{k}{EI}$$

$$\phi = \frac{c_{cr}\,v_{cr}}{8EI} = \frac{\sqrt{km}}{EI} \sqrt{\frac{\sqrt{\frac{4kEI}{m^2}} - \frac{N}{m}}{8}}$$

Substituting back in equation (3.27), the homogeneous form of the equation becomes:

$$\eta^{iv} + 4\alpha_1^2 \eta'' - 8\theta\phi\beta \eta' + 4\omega^4 \eta = 0 \qquad (3.28)$$

If a concentrated load is assumed at the origin (at $\xi=0$), equation (3.27) may be solved by the use of Green's function, assuming zero deflection and slope at infinity and zero change in deflection, slope, and moment across the origin. A discontinuity in shear across the origin of value $-\frac{P}{EI}$ is used as the last boundary condition. The solution of equation (3.28) is developed in Appendix (A) with the aid of these boundary conditions. It is useful to recall that when $N \geq N_{cr}$, the stable beam shape is not straight and hence the differential equation (3.28) is not applicable. In this investigation we analyze only the case when $N < N_{cr}$, the problem of immediate practical importance.

The solutions for the region ahead and region behind the load in the moving reference coordinates (ξ, y, ζ) are given by equation (A.12) in the Appendix. In the fixed coordinates (x, y, z) the solutions are obtained by transformation:

For $x \geq vt$:

$$Y_a = \frac{dP\ e^{-d(x-vt)}}{EI} \left[\frac{1}{4(2d^4 + 2\alpha_1^2 d^2 - \theta\phi\beta d) + \frac{\theta\phi\beta}{d}(4d^2 + 4\frac{\theta\phi\beta}{d})} \right]$$

$$\left[\frac{-(\theta\phi\beta - d^3)}{d^2\sqrt{2\alpha_1^2 + d^2 - \frac{2\theta\phi}{d}}}\ \sin \sqrt{2\alpha_1^2 + d^2 - \frac{2\theta\phi\beta}{d}}\ (x-vt) \right.$$

$$+ \cos \sqrt{2\alpha_1^2 + d^2 + \frac{2\theta\phi\beta}{d}} \ (x-vt) \Bigg] \tag{3.29a}$$

For $x \leqslant vt$

$$Y_b = \frac{dP \ e^{d(x-vt)}}{EI} \left[\frac{1}{4(2d^4 + 2\alpha_1^2 d^2 - \theta\phi\beta d) + \frac{\theta\phi\beta}{d}(4d^2 + 4\frac{\theta\phi\beta}{d})} \right]$$

$$\left[\frac{-(\theta\phi\beta + d^3)}{d^2\sqrt{2\alpha_1^2 + d^2 - \frac{2\theta\phi\beta}{d}}} \sin \sqrt{2\alpha_1^2 + d^2 - \frac{2\theta\phi\beta}{d}} \ (x-vt) \right.$$

$$+ \cos \sqrt{2\alpha_1^2 + d^2 + \frac{2\theta\phi\beta}{d}} \ (x-vt) \Bigg] \tag{3.29b}$$

where d is the positive real root of equation (A.9)

In the limiting case of no damping the solutions for the vertical deflections ahead and behind the load become:

For $x \geqslant vt$:

$$Y_a = \frac{P \ e^{-\{\sqrt{\omega^2 - \alpha_1^2}(x-vt)\}}}{8 \ EI \ \omega^2 \ \sqrt{\omega^2 - \alpha_1^2}} \left[\frac{\sqrt{\omega^2 - \alpha_1^2}}{\sqrt{\omega^2 + \alpha_1^2}} \sin \sqrt{\omega^2 - \alpha_1^2}(x-vt) \right.$$

$$\left. + \cos \sqrt{\omega^2 - \alpha_1^2}(x-vt) \right]$$

and for $x \leqslant vt$:

$$Y_b = \frac{P \ e^{+\{\sqrt{\omega^2 - \alpha_1^2}(x-vt)\}}}{8 \ EI \ \omega^2 \ \sqrt{\omega^2 - \alpha_1^2}} \left[\frac{-\sqrt{\omega^2 - \alpha_1^2}}{\sqrt{\omega^2 + \alpha_1^2}} \sin \sqrt{\omega^2 + \alpha_1^2}(x-vt) \right.$$

$$\left. + \cos \sqrt{\omega^2 + \alpha_1^2}(x-vt) \right] \Bigg\} \tag{3.30}$$

Hence the wave caused by P, and which moves with P at a constant velocity v, is symmetrical with respect to P for any $N < N_{cr}$. In the presence of damping, the wave is not symmetrical.

3.3 Numerical Solutions and Results

For the case of the general solution, the mathematical formulation of the problem is quite general and no steady-state assumptions were made. It was noted, however, that the resulting integral solutions given by equations (3.9), (3.11), and (3.12) are, in general, difficult to evaluate in closed form and known solutions were obtained for special cases of interest. To be able to solve all cases of interest, an alternative approach is to numerically solve the equations resulting from the general analysis. A general computer program was developed to integrate the equations resulting from the analysis. It is obvious that numerical solutions of equations (3.9), (3.11), and (3.12) are not free of a different type of difficulty. Singularities, accurate evaluation of the Bessel function expressions and the integrals ... etc., are numerical difficulties that have to be watched for. The program was first tested for some cases for which solutions were known or found in closed form. Figure 3.3 illustrates the comparison of the results obtained from the numerical solution with the one obtained from the exact
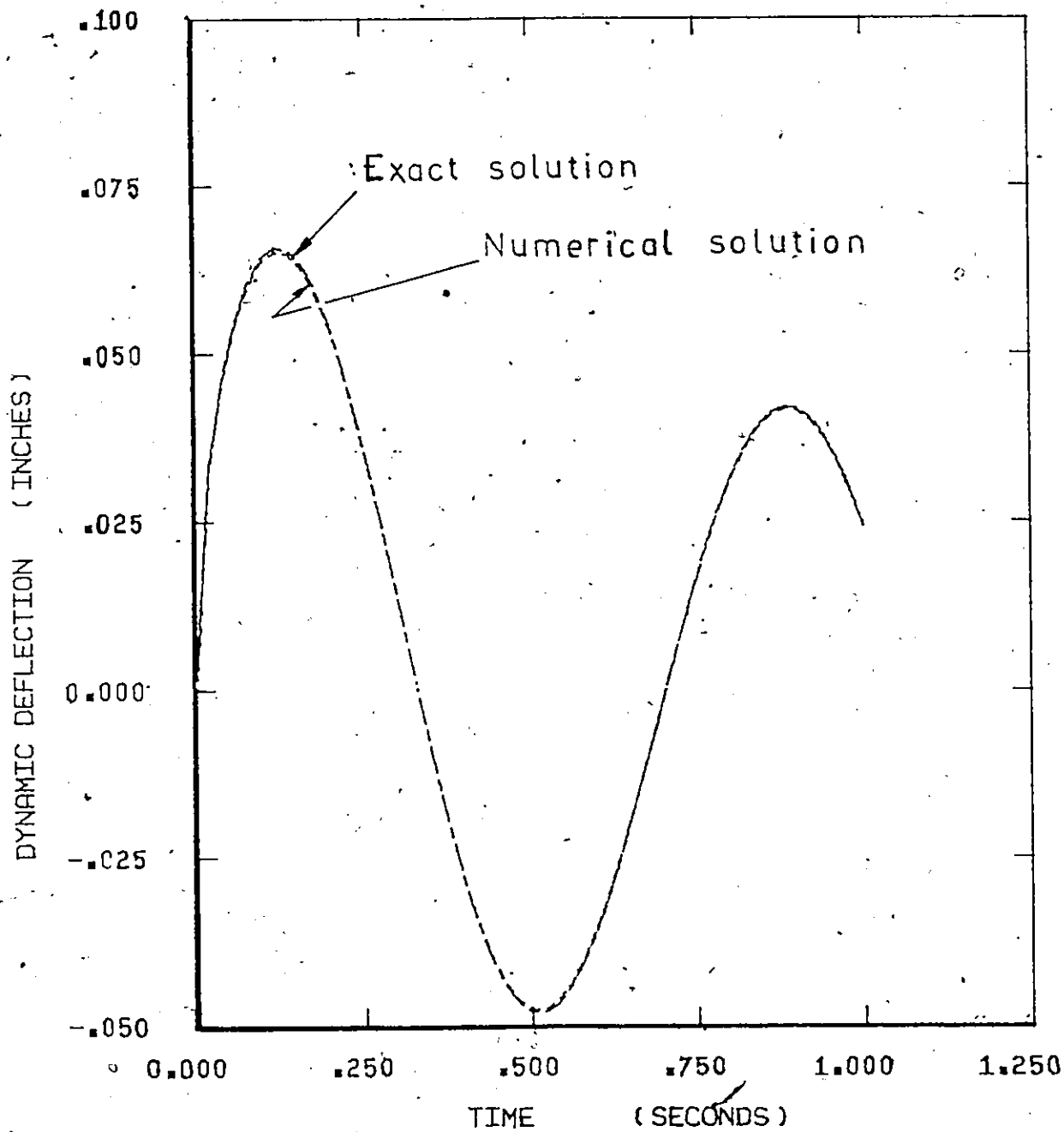
Figure 3.3   Comparison of numerical and
exact solutions for q(x,t)=
P δ(x) δ(t)

solution obtained earlier for the same case of transient

impact loading, $q(x,t) = P \delta(x) \delta(t)$, (with no damping or

axial load in the beam).

Figure 3.4 represents the solution versus time

for the case of the infinite beam subjected to a constant

concentrated load $P \delta(x)$, with no axial force in the beam,

but in order to converge to steady-state results a small

amount of damping is included. It is shown that the

response for large values of time converges to the steady-

state response which in this case is the result obtained

by equation (3.19).

The computer results obtained for the case of a

concentrated moving load with a velocity v and an

acceleration ρ i.e., for $q(x,t) = P \delta(x-vt \pm \rho t^2)$

indicated that the acceleration has little effect on the

dynamic deflection of the beam.

For the numerical integration two different

algorithms were used. The first algorithm is based on

Clenshaw – Curtis quadrature developed by Gentleman [73].

The second algorithm is based on Simpson quadrature used

adaptively [74]. The two algorithms proved to be efficient

and accurate in most cases.

The effects of the damping, the axial force and

the velocity of the moving loads on the dynamic deflection

of the railway track are illustrated in Figures 3.5 to 3.9.
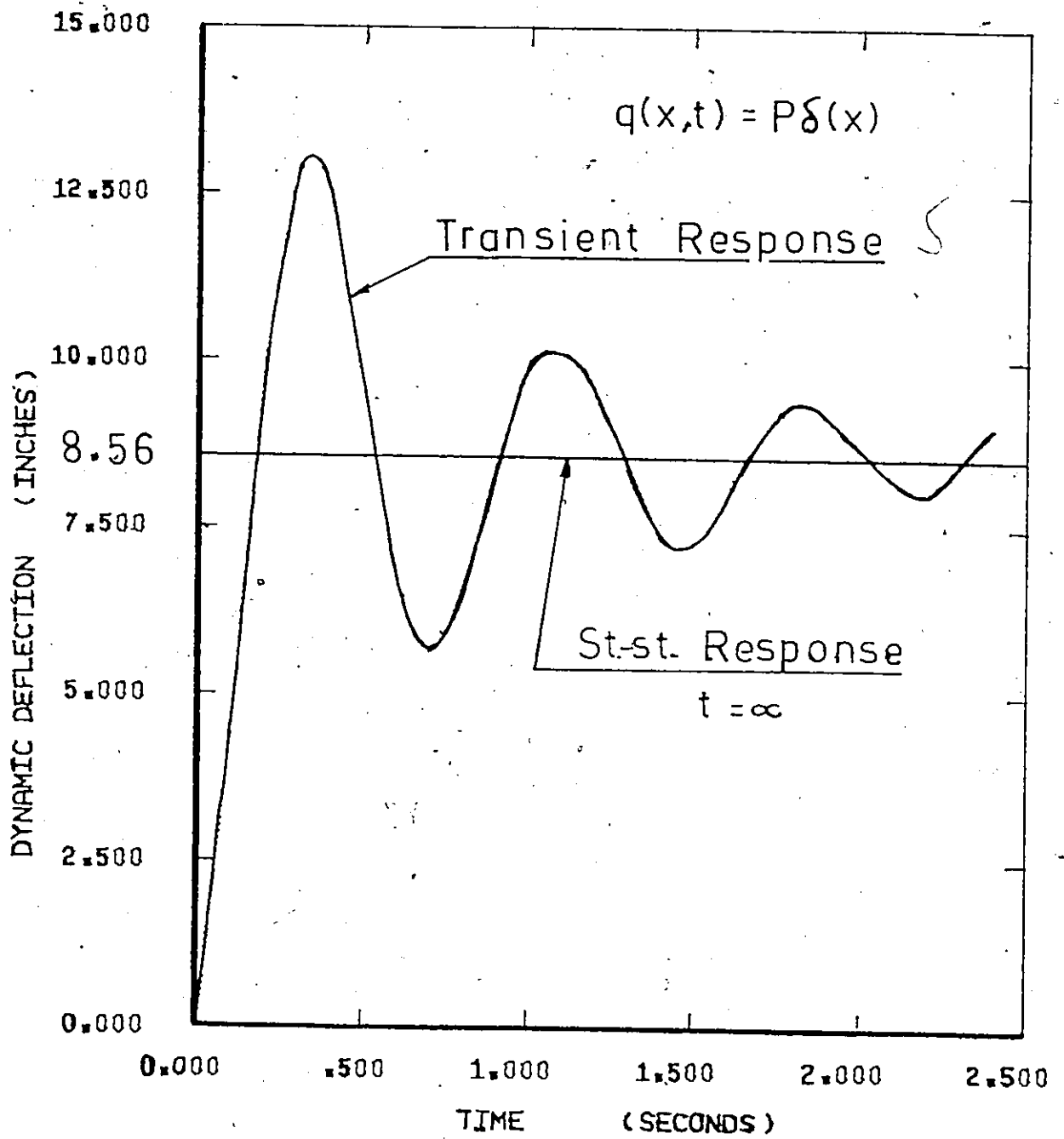
Figure 3.4   Response to a constant load
q(x, t) = P δ(x)

These results are computer plotted after evaluation of the
dynamic deflections given by equations (3.29a) and 3.29b).
The ordinate in all these figures is the deflection of the
conventional railway track with wooden ties. The
illustrated results show that the presence of damping in
the foundation results in an unsymmetric dynamic deflection
of the rail. Due to phase shift the point of largest
deflection occurs slightly behind the point of application
of the moving load. The deflection ahead of the point of
maximum deflection is always larger than the deflection
behind it. As the damping increases, the amplitude of the
maximum deflection decreases and the shift increases. This
is shown in Figure 3.5 for values of damping ratios of 10%
and 20% for the case of no axial force and in Figure 3.6
when an axial load in the rail is present. In both cases
comparison is shown with the limiting case of no damping
$(\beta = 0)$. It is interesting to note that in the presence
of damping the amplitude of the deflection profile ahead
is always larger and the frequency of the wave is higher
than the frequency behind the point of maximum deflection.
The effect of axial load on the dynamic deflection
of the rail is shown in Figure 3.7. It is shown that when
a compressive force exists, the maximum deflection is
larger than in the case of no axial compression, and the
frequency of the deflection wave is higher. In contrast,
when a tension force exists, the maximum deflection is
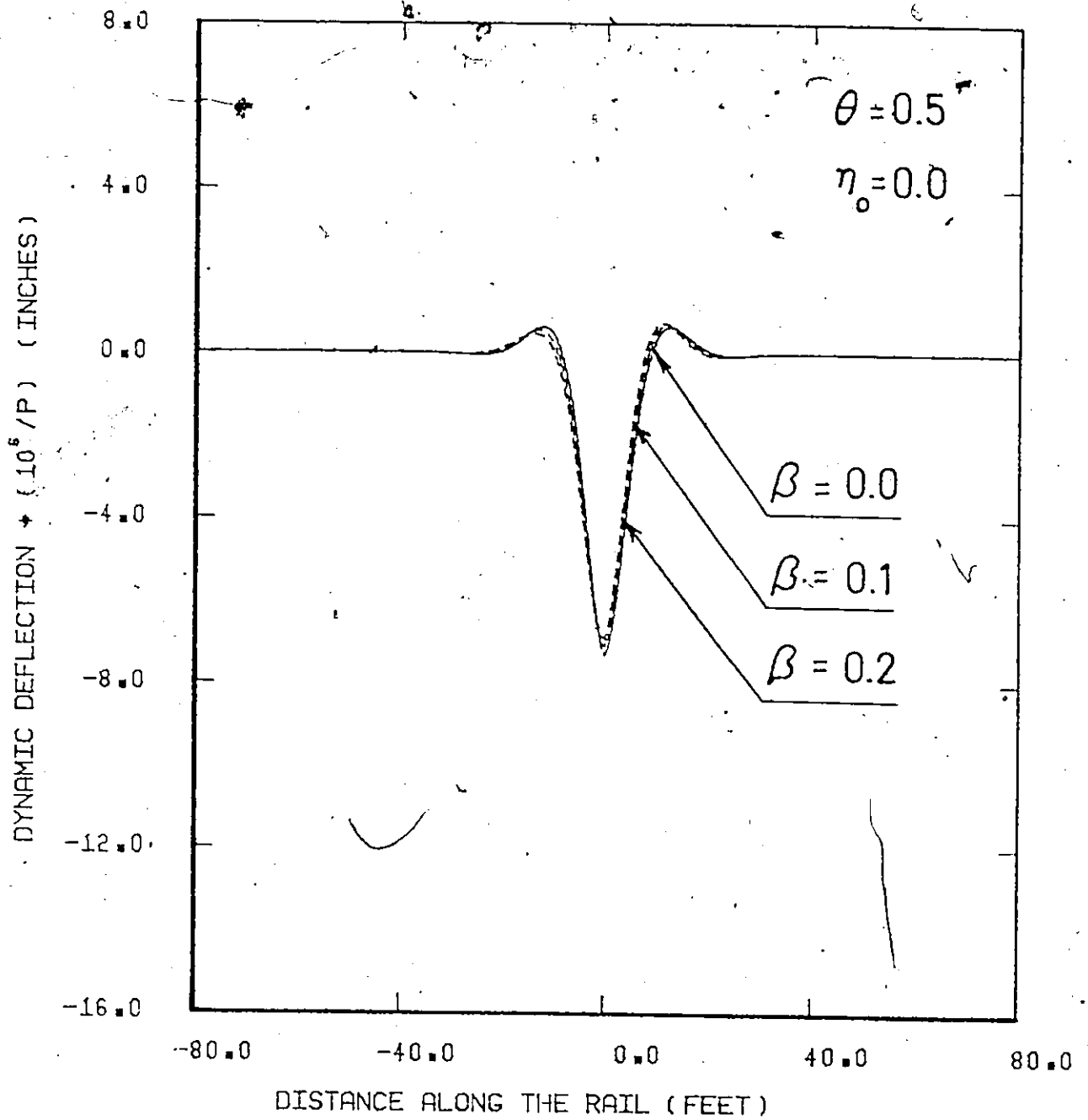
Figure 3.5 Effect of damping on the dynamic deflection of the rail (for no axial force)
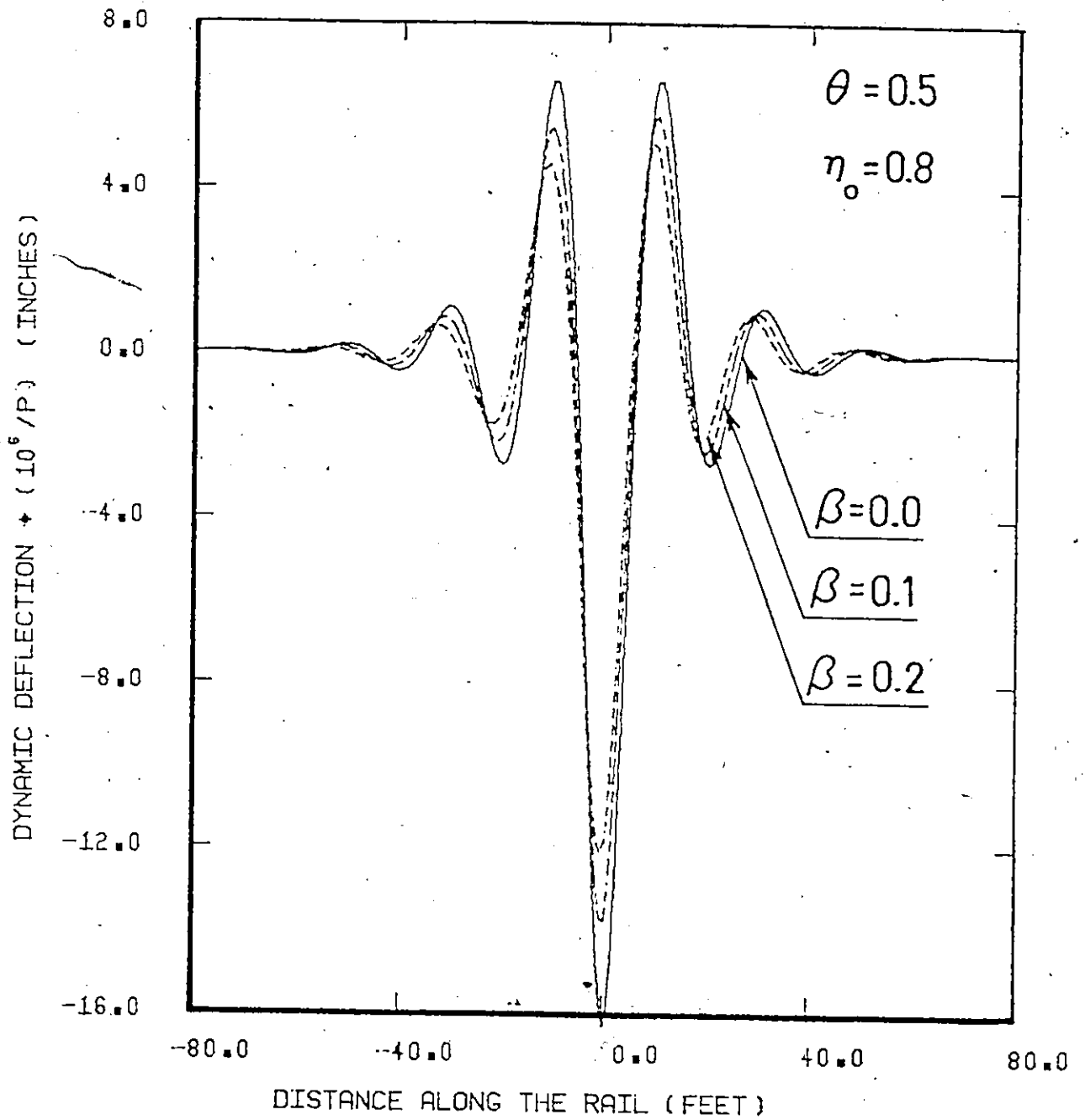
Figure 3.6   Effect of damping on the dynamic
deflection of the rail (in the
presence of an axial force)
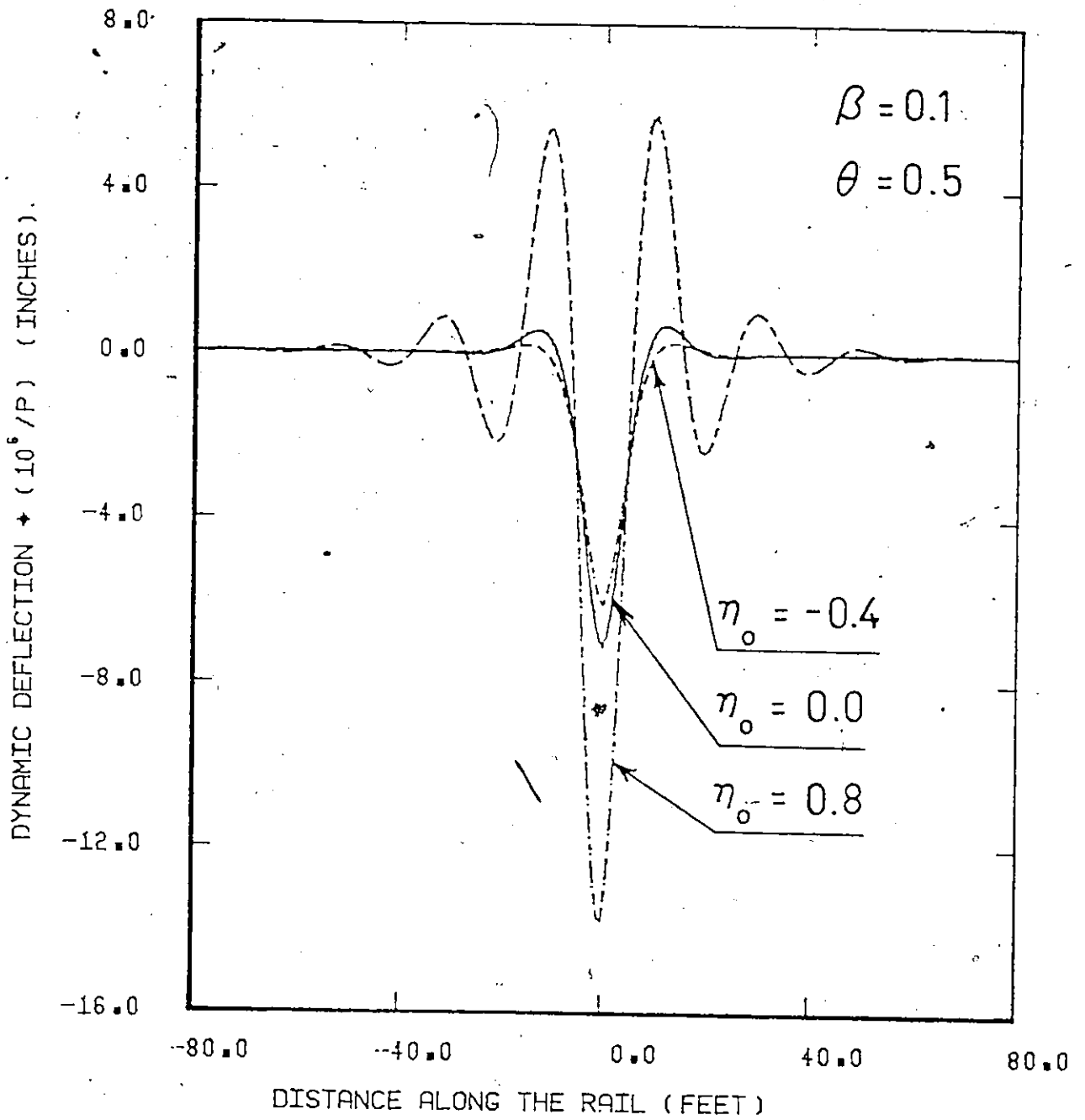
Figure 3.7 Effect of axial force on the dynamic deflection of the rail

smaller than in the case of no axial compression, and the
frequency of the deflection wave is lower. Figures 3.8 and
3.9 show the effect of velocity of the moving load on the
dynamic deflection of the rail in the presence and absence
of damping respectively. It is seen that the increase in
the deflection as the velocity ratio increases is quite
small.

The negligible effect of the velocity of the moving
load on the dynamic deflection is a result of particular
importance. This suggests that it is not necessary to
consider the wave type expression to study the effect of
track elasticity on the dynamics of railway vehicles.
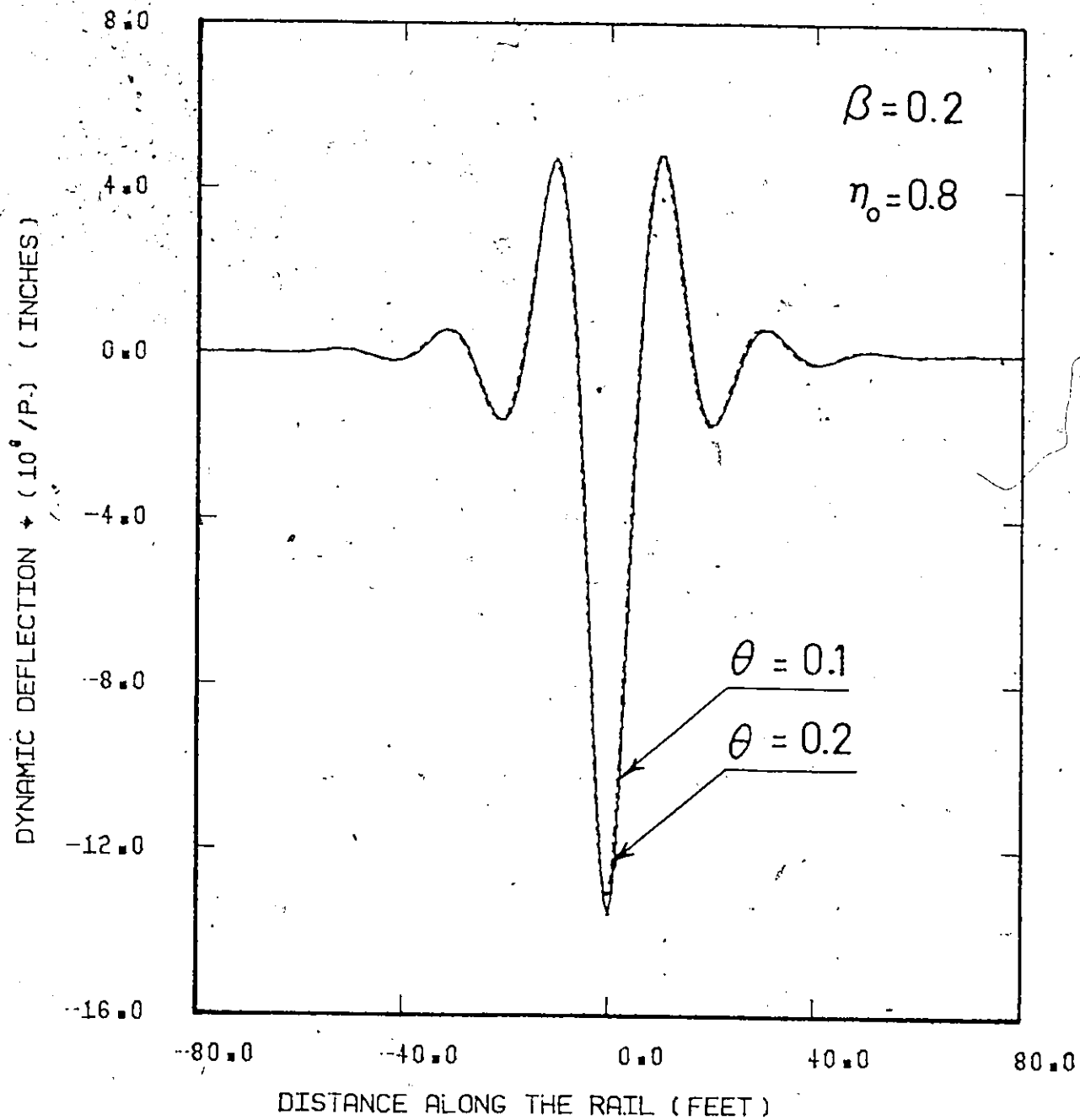
Figure 3.8 Effect of velocity on the dynamic
deflection of the rail (in the
presence of damping)
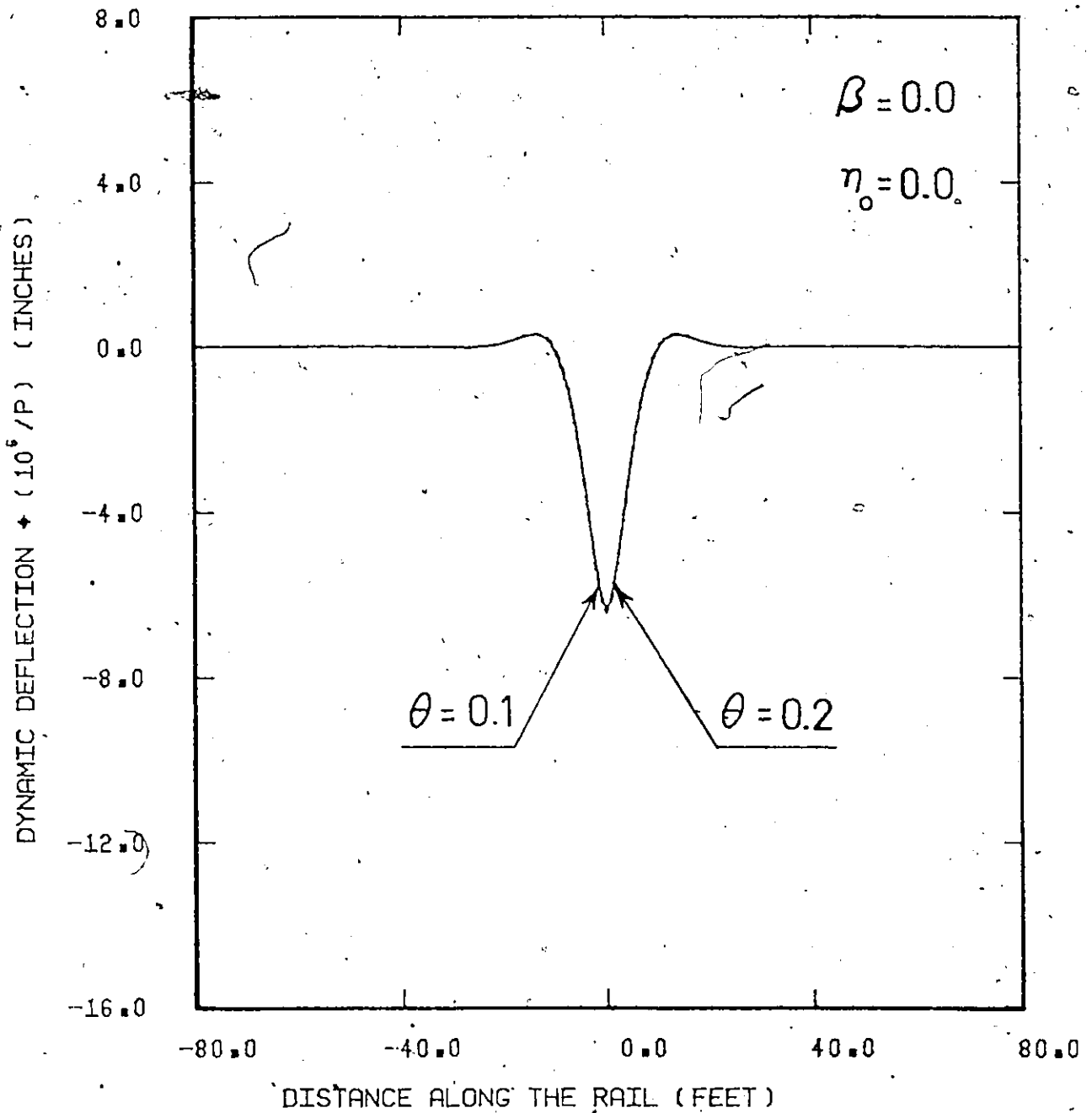
Figure 3.9 Effect of velocity on the
dynamic deflection of the rail
(in the absence of damping)

CHAPTER 4

VEHICLE/TRACK DYNAMICS

Over the last decade there has been an increasing effort devoted to research and development concerned with railway vehicles. Most of the research work reported in the literature is concerned with the dynamic stability analysis of single, conventional railway vehicles. The dynamic stability of railway vehicles is indeed an important aspect of the dynamics of railway vehicles. Below the critical speed, the lateral and vertical motions of railway vehicles are determined by track geometry. The response of railway vehicles to rail irregularities and the minimization of the vibrations transmitted to passenger positions received little attention until recently. The new interest is motivated by the concern about passenger comfort for high speed rail transit systems.

In addition to supporting the vehicle, the rail vehicle suspension is designed such as to provide guidance with adequate stability range and to provide effective vibration isolation such that passengers experience a comfortable ride and freight is not damaged.

Recently, it has been recognized that guidance, dynamic stability and dynamic response to rail

irregularities analyses are intimately related, and a new approach to railway vehicle design was possible. This approach recognizes that, in the first instance, the aim should be to design the vehicle and its suspension so that guidance is achieved by the forces acting between the wheel treads and the rails. Therefore flange contact is avoided in normal running conditions. With this approach it has been possible to develop a theory for the dynamics of railway vehicles based on a linearized analysis. This approach, which is adopted here, enables the consideration of a significantly large number of degrees of freedom. This is of prime importance because simplified models in which some of the degrees of freedom are neglected do not, in general, lead to realistic results.

Dynamic coupling occurs between a railway vehicle and the track due to the reaction forces acting between the wheels and the track, and the elasticity of the track and the foundation. It has become apparent that track elasticity can influence the dynamic behaviour of the railway vehicle, yet in most of the research work in the area of railway vehicle dynamics reported so far, the track is regarded simply as a rigid structure, providing the reactions to the loads of passing vehicles.

In this chapter the models used for the analyses of the vehicle dynamics (on rigid track) and for the

coupled vehicle/track dynamics will be described. The
equations of motion are derived, and the results obtained
for the coupled vehicle/track model are presented and
compared with those obtained for the case of an infinitely
rigid track. The objectives here are, first, to present
methods for the dynamic analysis of the vehicle/track
model, and second to compare the dynamic behaviour of that
model with that of the vehicle on a rigid track. Particular
emphasis is on the effect of vertical track elasticity on
the lateral dynamic stability, and on the response of the
vehicle to vertical track elasticity.

4.1 Description of the Vehicle/Track Model

The mathematical model for the coupled vehicle/
track dynamics is shown in Figure 4.1. The model for the
railway vehicle is that of a six-axle locomotive of the
type commonly used in North America. The model consists
of fifteen rigid bodies: the locomotive body (chassis),
two frames (trucks), six motors and six wheelsets. The
suspension of the body (the secondaries) is usually very
stiff in the vertical direction in order to stabilize the
truck frames against the locomotive body and thereby
minimize the deflection of the former in the pitching mode.
At the same time it must permit the necessary lateral and
rotational movements in the horizontal plane. The ultimate
form of body suspension might employ a horizontal sliding

surface which would be infinitely stiff vertically, but

these present the disadvantage of being wearing components

and requiring oil bath lubrication. An ideal alternative

was found in laminated rubber sidebearers which consist

of several layers of rubber bonded to intermediate steel

plates [75]. The locomotive body is supported on such

sidebearers which provide a stiff spring effect in the

vertical direction while permitting movement in the

horizontal directions against a relatively low resistance,

the rate of which can be selected from a fairly wide range

as required. A resiliently mounted centre pivot is used

in conjunction with the sidebearers, thus avoiding

metallic contact between the body and the frames. Further-

more; the several inches of rubber provide a complete

break in the metallic structure of the locomotive's

suspension and thus make a good noise barrier.

Because the body is supported freely, it can

oscillate in all six modes, i.e., along the three

principal axes through their centres of gravity

    (i)   longitudinal or "fore and aft" oscillation

           (in the u direction)

    (ii)   lateral oscillation (in the v direction)

    (iii)   vertical or "bouncing" oscillation (in

           the w direction)

and rotate about these three axes:
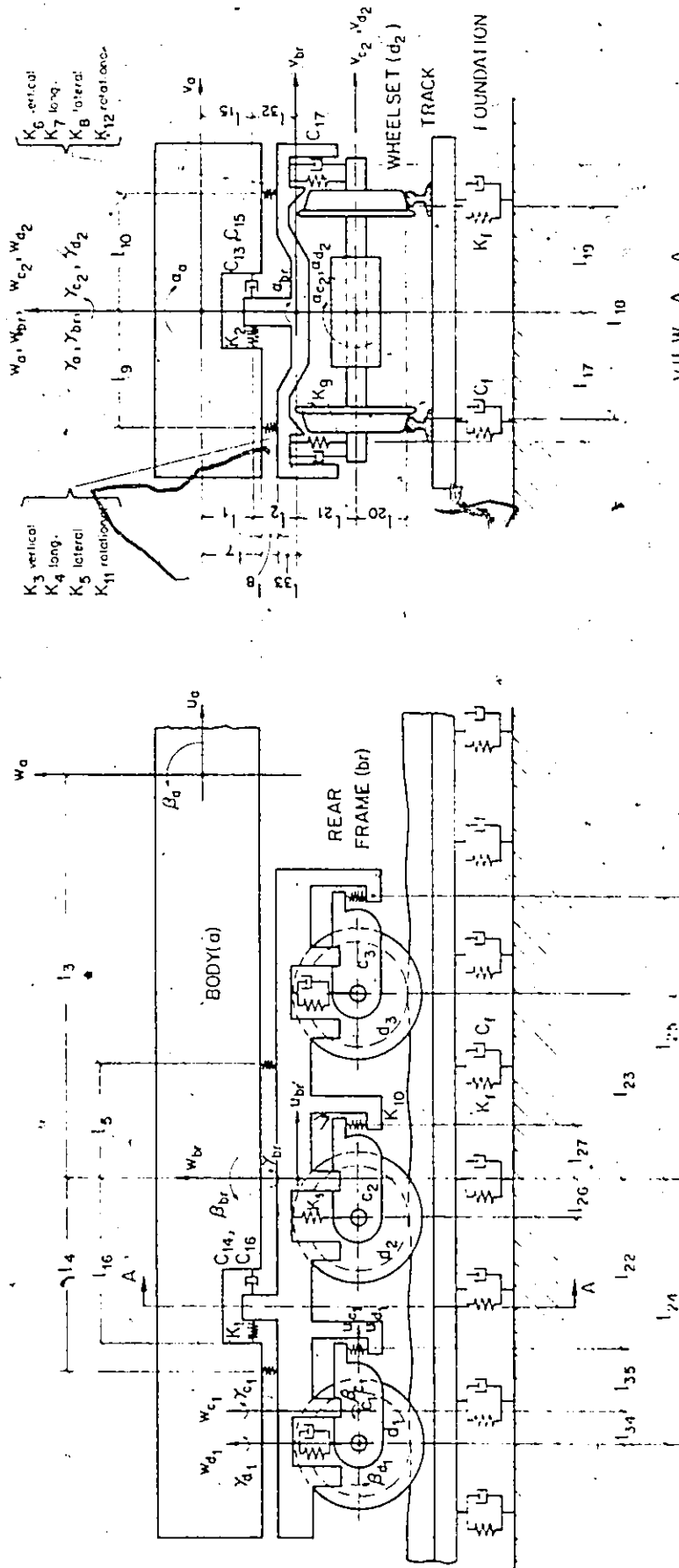
Figure 4.1 Mathematical model for the coupled vehicle/track dynamics

98

(i)   about the longitudinal u-axis or "roll" (in the α direction)

(ii)   about the lateral v-axis or "pitch" (in the β direction)

(iii) about the vertical w-axis or "yaw" (in the γ direction)

The primary suspension, which is the one between the wheelsets axle bearings and the frames consists of coil springs and shock absorbers. If the secondaries are very stiff as described above, then the major vertical springing must be provided by the primary suspension. Low-rate springs also suit the requirements of low-weight transfer by being able to accomodate variations in track level or pitching of the frames with a minimum variation in axles loading [75].

Wheelsets are restrained with respect to the frames in both the longitudinal and in the lateral directions. The driving mechanism is arranged with all the motors on the same side of their respective axles. A traction motor is supported on the axle from one side and on a rubber nose support on the other side. A rubber nose support is used to prevent motor nose lug failure due to sudden torque impulses. This assembly is such that rotation of the motor about the axle center line is the only allowable relative motion between the motor and the

wheelset.

The railway track is modelled, as described earlier, as an infinite beam continuously supported on an elastic damped foundation of the Kelvin type. In order to simulate the coupled dynamic behaviour of the vehicle/track model, the mathematical simulation of the track involves the replacement of the infinitely long continuous model of the track by an equivalent lumped-parameter system composed of discrete masses, springs and dampers. The discretization is possible because it was found in chapter 3 that the velocity effects can be neglected, and that it is not necessary to consider the wave type equation for the simulation of the dynamic response of the track in the vertical direction. For this study of the dynamic effect of the track elasticity, it was concluded that the track can be adequately represented by a single degree of freedom system with a lumped mass, stiffness and damping which will have the same natural frequency as that of the distributed system. A lumped mass-spring-damper system under each wheelset, which corresponds to a certain effective rail length, allows two additional degrees of freedom per wheelset, vertical displacement and roll. The wheelsets are assumed to remain in contact with the track at all times, which is the case in normal running conditions.

Because of symmetry, the equations describing the lateral motions of the system (these include the lateral, roll and yaw displacements), are uncoupled from the equations describing the longitudinal motions (these include the longitudinal, vertical and pitch displacements). With this observation in mind, the solutions for the lateral motions will be treated separately from the solutions for the vertical modes of vibrations. For the coupled vehicle/track model the total number of degrees of freedom is 42, fifteen for the lateral dynamics and twenty-seven generalized coordinates for the vertical dynamics. For the dynamics of the railway vehicle on rigid tracks the total number of degrees of freedom is reduced to 30, nine for the lateral dynamics and twenty-one for the vertical dynamics. Figure 4.2 illustrates the model for the six-axle locomotive on rigid track.

For both the coupled vehicle/track model and the model of the vehicle on rigid tracks, the complete mathematical modelling includes the effects of the wheel/rail profile, the gravity stiffness effects and the creep forces. Several assumptions are made in deriving the equations of motion. The vehicle components are treated as perfectly rigid, and the elasticity is lumped in the suspension elements. Aerodynamic and coupling forces on the vehicle are assumed to be negligible. The
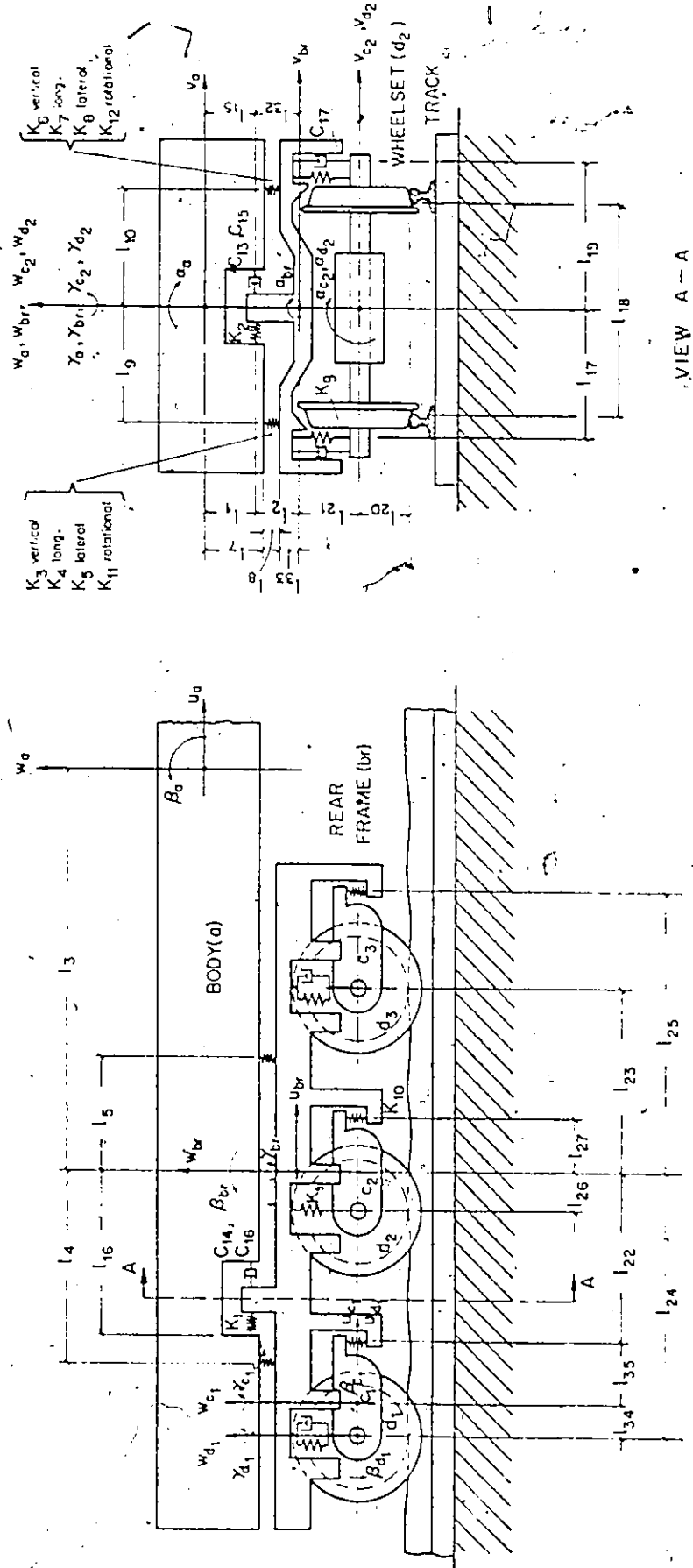
Figure 4.2   Mathematical model for the six-axle
locomotive

axles are assumed to run freely in their bearings with no
lateral or longitudinal play. All displacements are
assumed to be small.

4.2 Derivation of the Equations of Motion

The equations of motion are derived in this section
for the coupled vehicle/track model. The kinematics.
problem is solved first following the approach described
in reference [41]. In this approach displacements and
velocities are found for the mass center of each rigid
body in the system and for each point on the bodies where
an active force acts. Inertia forces are also found for
each coordinate. The active forces are all forces acting
on the bodies except those contact forces between bodies
that are applied at points where the relative velocity
between the bodies has no component parallel to the line
of action of the force. The active forces are due to
linear springs and dampers. The non-active forces are the
internal reactions which will be eliminated from the
equations of motion. This elimination process is followed
by the transformation of the resulting equations to the
generalized coordinates system as described in Appendix (B).

The motion of a railway vehicle can not be
adequately explained by a model that assumes pure rolling
of the wheels on the rail, because there is relative motion
between the two surfaces at their contact. Consequently,

the tangential forces acting on the contact areas, which
are of fundamental importance, must be included in the
analyses. These forces are due to the creep phenomenon
and are non-conservative in nature. In order to analyse
the forces acting between the wheel and rail the wheel-
rail geometry and the wheel/rail interaction forces have
to be studied. In addition to the suspension forces and
the creep forces, "gravity stiffness" effects will be
considered and the corresponding gravity forces are
included in the equations of motion.

4.2.1 Wheel/Rail Interaction and Gravity Stiffness Effects

The gravity stiffness effects and corresponding
gravity forces are due to the lateral, roll and yaw
displacements of the wheelset. When a wheelset is displaced
laterally a small distance, the normal reaction forces
between the rails and the wheels change their direction.
Since they are large forces, approximately equal to half
the axle load, a small change in direction can lead to a
significant lateral force on the wheelset. This lateral
restoring force is due to the increase in potential energy
due to the rise of the wheelset center of gravity and
will depend on the shape of the wheel tread and the rail
head profile. Similarly, the yaw gravity stiffness which
is defined as the change of the net torque on the wheelset
per unit of yaw displacement is a function of axle loading

and wheel-rail contact geometry, and for conventional
wheels and rails, comes out as a negative stiffness term
that acts to further displace the wheelset. Gilchrist
et.al. [18] indicate that for new wheels the gravitational
stiffness is negligible. Some authors [33] neglect gravity
stiffness completely.

Lateral gravity stiffness and yaw gravity stiffness
are present for the model of the wheelset on both flexible
and rigid tracks. In addition in the former case, a
displacement in roll of the track, gives rise to a new
negative stiffness term that acts to displace the wheelset.

In order to derive expressions for the forces
acting between wheels and rails it is necessary to consider
the mutual geometry of the wheel tread and rail head and
the wheel/rail kinematics. The most important kinematic
parameter is the effective conicity which is defined as
the rate of change of rolling radii with the lateral
displacement of the wheelset. For a purely coned wheel
the effective conicity is simply equal to the cone angle
(usually 1/20 taper). For purely coned wheels the area
of contact with the rail is small and the contact stresses
are high. Local wear occurs and this produces hollowness
of the tread profile. After an initial period of rapid
wear, the wear is distributed over the whole tread to
give the "worn" profile which thereafter remains fairly

constant.

Linearized theories of wheel-rail kinematics are given in [16,19,26,30,32,34,41,77,78]. Usually the geometric parameters are obtained from the wheel/rail kinematics assuming the wheel tread and rail head profile to be circular arcs of different radii as shown in Figure 4.3. The assumption that the length and width of the contact area between wheel and rail is quite small compared with the displacements of the wheelset is also made. Consequently, the small area is treated as a point. However in deriving the expressions for the creep coefficients, the contact area is treated as finite. The geometric relationships can be very complex, and estimates for equivalent linear values of the effective conicity and other parameters have been obtained using different methods including measurements of existing wheel/rail combinations [16,18,29,78]. When the wheels are centralized, both tread circles have the same radius r_0. When the wheelset is displaced laterally, contact occurs at new points, and the angles made by the contact planes are changed. These angles θ_r and θ_ℓ are affected in the case of the flexible track with the rotation of the track as illustrated in Figure 4.3. Following Wickens [16] for the linearized expression relating the change in the angles made by the contact plane with the horizontal resulting from the lateral displacement of the wheelset, the following
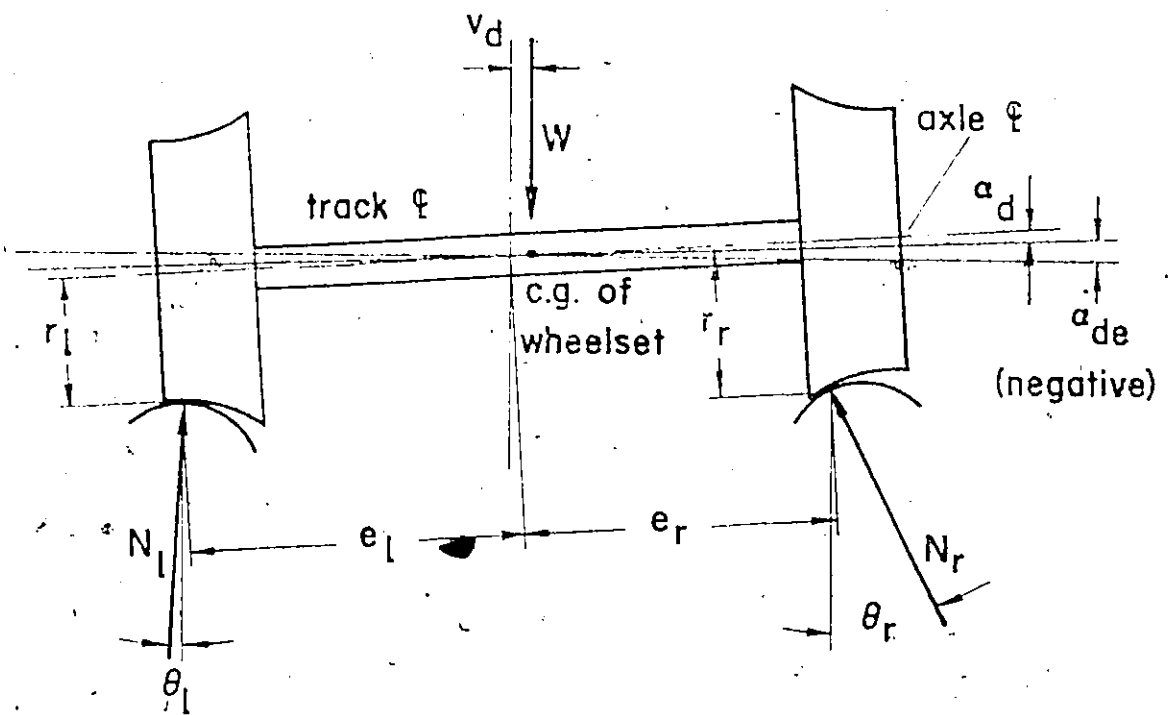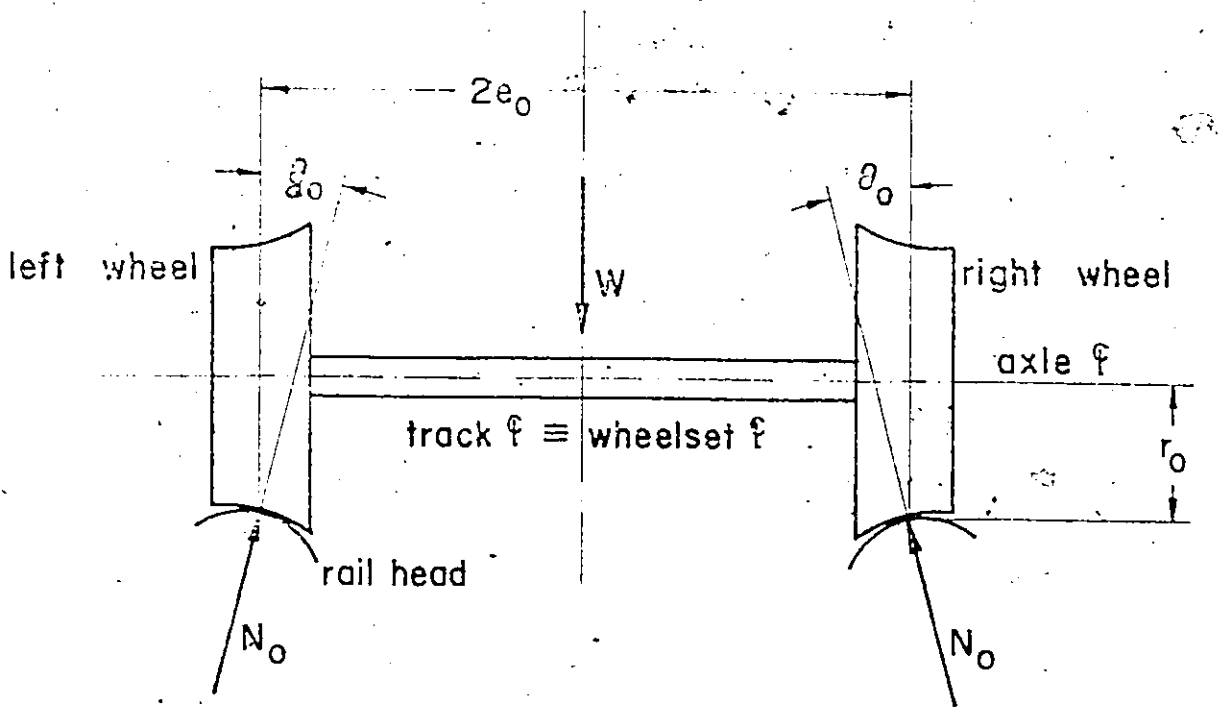
Figure 4.3   Wheel-rail interaction before and after lateral movement of wheelset and roll displacement of track

expressions are obtained.

$$\theta_r = \theta_0 + \varepsilon \frac{v_d}{e_0} - \alpha_{de} \qquad (4.1)$$

and

$$\theta_\ell = \theta_0 - \varepsilon \frac{v_d}{e_0} + \alpha_{de} \qquad (4.2)$$

where θ_0 is the angle between the contact plane and horizontal when the wheelset is in central position with no track rotation

θ_r, θ_ℓ are the angles between the contact planes and the horizontal after lateral movement of the wheelset and/or rotation of the track

v_d is the lateral displacement of the wheelset

α_{de} is the roll displacement of the wheelset/track

ε is the rate of change of contact plane slope with lateral displacement of the wheelset (for new wheels ε becomes λ)

e_0 half the lateral distance between the wheel-rail contact points

From equations (4.1) and (4.2), it is seen that both θ_r and θ_ℓ are equal to θ_0 if the lateral displacement of the wheelset is zero for a horizontal track.

Similarly, the distances between the wheelset center-line and the contact points can be expressed as

$$e_r = e_0 - \eta\, v_d \qquad (4.3)$$

$$e_\ell = e_0 + \eta\, v_d \qquad (4.4)$$

where η is a correction factor equal to the change in the distance between the center-line of the track and the contact point for a unit lateral displacement.

The tread radii of the wheels are given by

$$r_r = r_0 + \lambda\, v_d \qquad (4.5)$$

$$r_\ell = r_0 - \lambda\, v_d \qquad (4.6)$$

where r_0 is the wheel circle radius, when the wheelset is in central position

r_r, r_ℓ are the radii of tread circles, when the wheelset is displaced laterally

and λ is the effective conicity which is defined as the rate of change of rolling radius with lateral displacement of the wheelset.

In addition the complex non-linear constraint between the rolling motion of the wheelset and its lateral displacement is linearized as follows

$$\alpha_d = -\psi\, v_d \qquad (4.7)$$

where ψ is defined as rate of change of the angle of the wheelset center-line to the horizontal with the lateral displacement of the wheelset.

An expression for ψ can be found from studies of the wheel-rail contact geometry assuming the wheel tread and rail head profiles to be circular arcs. From reference [29] or [78]:

$$\psi = \frac{\theta_0}{e_0 - r_0\,\theta_0} \qquad (4.8)$$

The value of θ_0 is small (≈ 0.05) and the value of ψ obtained from equation (4.8) is even much smaller. Apparently for this reason some research workers [77] neglect ψ altogether.

Typical values for the parameters ε, λ, θ_0, η and ψ are given by Wickens [16] and by Joly [78].

4.2.2 Creep Forces

Creep and corresponding creep forces between wheel and rail is of fundamental importance in the study of dynamics of railway vehicles. In railway vehicles non-conservative forces arise from the phenomenon of creep. Consequently the tangential forces acting on the contact area, because of the relative motion between the two surfaces at their contact, must be included among the acting forces.

The problem of determining the tangential forces between two elastic bodies in rolling contact has been studied by a number of researchers. Although the theory of creep has advanced considerably, exact solutions for

the general problem have not yet been found. Approximate
theories are now fairly well established but the
difficulty of obtaining working data for real vehicles
still exists. Johnson [8] divides the rolling problem
into three categories: free rolling, rolling under
tangential forces and rolling with spin. In free rolling
the resultant force transmitted between the contact
surfaces is perpendicular to the plane of contact, without
spin between the bodies. In rolling under tangential
forces, the transmitted force is not normal to the contact
plane. Rolling with spin occurs when the bodies move
with an angular velocity relative to each other about an
axis normal to the contact surface. The actual rolling
of a wheel on a rail includes each of these categories.
However, the resistance to motion in free rolling is small
compared with the other tangential forces. Note that the
components of the tangential forces in the longitudinal
directions do not include the steady state propelling
force. They are variations about this force.

The constitutive relationships for creep and spin
on a single wheel are:

$$\left.\begin{array}{l} T_x = - f_1 \, \xi_x. \\[2mm] T_y = - f_2 \, \xi_y - f_{23} \, \xi_\gamma \\[2mm] M_z = - f_{32} \, \xi_y - f_3 \, \xi_\gamma \end{array}\right\} \qquad (4.9)$$

where

T_x, T_y are the longitudinal and lateral creep forces

M_z is the moment about the spin axis

$f_1, f_2,$
f_3, f_{23} are a complete set of creep-spin coefficients.
$\quad$ According to Kalker's theory $f_{32} = - f_{23}$
and f_{32}

ξ_x, ξ_y are the longitudinal and lateral creepages

ξ_γ is the spin

Carter [5] originally proposed the following relationship to predict the creep forces:

$$\text{Tangential creep forces} = - f \left[\frac{\text{creep or relative slip velocity in direction of force}}{\text{rolling velocity}} \right]$$

where f is the creep coefficient given by an empirical equation [4]:

$$f = 3500 \ (r_0 \ N)^{1/2} \tag{4.10}$$

where r_0 is the radius of the wheel,

and N is the vertical pressure between the wheel and the rail.

The formulation (4.10) assumes that $f_1 = f_2$ and neglects f_{23} and f_{32}. Clark and Law [33] and Marcotte [79] used this evaluation. Cooperrider [77] used different

values for the longitudinal and lateral creep coefficients derived from Vermeulen and Johnson [10] but neglects the spin and coupling coefficients. Wickens [30], Gilchrist et.al. [18] and others [34, 41, 76] used the work of Vermeulen and Johnson [10] and Kalker [11] for longitudinal and lateral coefficients and of Johnson [9] for the rotational coefficients. A similar practice is adopted here.

The creepage is defined by Kalker [11] as the difference in the circumferential velocity of the wheel and the rail in the longitudinal and lateral directions divided by the rolling velocity. Spin is defined as the difference between the angular velocities about an axis perpendicular to the contact area divided by the rolling velocity. Using these definitions for the wheel/rail model of a wheelset and with S the forward speed of the railway vehicle and λ the effective conicity (defined as the rate of change of rolling radius with the lateral displacement of the wheelset), the creep forces for the right wheel are given by:

(i) longitudinal creep:

In a small interval of time dt, the actual forward displacement at the wheel tread is:

$$S \; dt + d \; u_d + e_0 \; d \; \gamma_d$$

The pure rolling forward displacement is:

$$r_r \frac{S}{r_0} dt - r_r d\beta_d .$$

Hence the longitudinal creep displacement in time dt =

$$(r_0 + \lambda v_d) d\beta_d + du_d + e_0 \, d\gamma_d - \lambda v_d \frac{S \, dt}{r_0} \qquad (4.11)$$

The first two terms represent slip induced by the difference between the axle longitudinal displacement and the displacement corresponding to the angular rotation of the axle. The third term is slip induced by angular displacement and the fourth term is slip induced by the forward steady state displacement S dt due to the rolling radius deviating from the mean r_0.

To get the creep velocity we divide the terms in expression (4.11) by dt and get the limit as dt approaches zero.

$$creep = (r_0 + \lambda v_d) \dot{\beta}_d + \dot{u}_d + e_0 \, \dot{\gamma}_d - \lambda v_d \frac{S}{r_0}$$

The nonlinear term is assumed negligible and dividing the longitudinal creep velocity by the velocity attributable to rolling we get the longitudinal creepage

$$\xi_{xr} = (r_0 \, \dot{\beta}_d + \dot{u}_d + e_0 \, \dot{\gamma}_d - \lambda v_d \frac{S}{r_0})/S \qquad (4.12)$$

The longitudinal creep force on the right wheel is obtained using equations (4.9) and (4.12)

$$T_{xr} = - f_1 (\frac{r_0}{S} \dot{\beta}_d + \frac{1}{S} \dot{u}_d + \frac{e_0}{S} \dot{\gamma}_d - \frac{\lambda}{r_0} v_d) \qquad (4.13)$$

(ii) lateral creep:

The actual lateral displacement in time dt is given by: $d\,v_d - r_0\,d\,\alpha_d$.

∴. The pure rolling lateral displacement, which is the lateral component of the forward displacement is: $-S\,dt\,\gamma_d$

Hence the lateral creepage is given by

$$\xi_{yr} = (\dot{v}_d - r_0\,\dot{\alpha}_d + S_o\,\gamma_d)/S \qquad (4.14)$$

and the rotational creepage (spin) is

$$\xi_{\gamma r} = \dot{\gamma}_d/S \qquad (4.15)$$

Using equations (4.9), (4.14) and (4.15), the lateral creep force at the right wheel is found to be

$$T_{yr} = -f_2(\frac{1}{S}\dot{v}_d - \frac{r_0}{S}\dot{\alpha}_d + \gamma_d) - f_{23}\frac{1}{S}\dot{\gamma}_d \qquad (4.16)$$

(iii) rotational creep:

The torque due to spin is given by

$$M_{zr} = -f_{32}(\frac{1}{S}\dot{v}_d - \frac{r_0}{S}\dot{\alpha}_d + \gamma_d) - f_3\frac{1}{S}\dot{\gamma}_{d1} \qquad (4.17)$$

In a similar manner the creep forces at the left wheel are found:

$$T_{x\ell} = -f_1(\frac{r_0}{S}\dot{\beta}_d + \frac{1}{S}\dot{u}_d - \frac{e_0}{S}\dot{\gamma}_d + \frac{\lambda}{r_0}v_d) \qquad (4.18)$$

The expressions giving the lateral creep force and creep torque for the left wheels ($T_{y\ell}$ and $M_{z\ell}$) are similar to the ones obtained for the lateral creep force and creep torque for the right wheel (T_{xr} and M_{zr}) given by equations (4.16) and (4.17) respectively. The creep

forces and torques acting on the wheelset are obtained
from the summation of the forces and torques due to creep
and spin at the right and left wheels.

For the determination of the creep coefficients
the contact surface between the rail and the wheel is
considered to be an ellipse. The length of the major and
minor axes of the ellipse and the distribution of the
normal load between the bodies across the contact area are
found by Hertz's solution [80] for the pressure between
two bodies in contact, an assumption made in nearly all
analyses of this rolling contact problem.

For a wheel in contact with a rail when both are
of the same material, the length of the axes, a and b are
[80]:

$$a = m \sqrt[3]{\frac{3}{2} \frac{N}{E} \frac{(1-\nu^2)}{(A+B)}} \qquad (4.19)$$

and

$$b = n \sqrt[3]{\frac{3}{2} \frac{N}{E} \frac{(1-\nu^2)}{(A+B)}} \qquad (4.20)$$

where N   is the normal load between the two bodies (wheel
          and rail)

E   is the modulus of elasticity

ν is the Poisson's ratio for the bodies

m,n   are functions of the ratio $(B-A)/(A+B)$ given in
      a table on page 416 in [80]

A,B are constants depending on the magnitude of the principal curvatures of the surfaces in contact and on the angle between the planes of principal curvature of the two surfaces [80].

Vermeulen and Johnson [10] assumed that the non-slip region is a geometrically similar ellipse tangent to the leading boundary of the contact ellipse. And the relations between the longitudinal and lateral creep ratios or creepages and the longitudinal and lateral creep forces respectively are given by the following expressions:

$$\xi_x = -\frac{3}{G\pi ab}\mu N \, \phi[1 - (1 - \frac{T_x}{\mu N})^{1/3}] \qquad (4.21)$$

$$\xi_y = -\frac{3}{G\pi ab}\mu N \, \psi_1[1 - (1 - \frac{T_y}{\mu N})^{1/3}] \qquad (4.22)$$

where T_x is the tangential force in the direction of rolling,

T_y is the transverse tangential force,

N is the normal force between the two surfaces,

G is the modulus of rigidity,

μ is the coefficient of friction,

ξ_x, ξ_y are the longitudinal and lateral creepage and

ϕ, ψ_1 are functions of the ratio $\frac{a}{b}$ and Poisson's ratio ν. Their values can be obtained from

Figure 2 in reference [10] or from the table
on page 208 of reference [81].

For small values of tangential forces (T_x, T_y)
compared with the limiting friction force μN, the creep
relations (4.21) and (4.22) become [81]:

$$\xi_x = - \frac{\phi}{G\pi ab} \, T_x \qquad\qquad (4.23)$$

$$\xi_y = - \frac{\psi_1}{G\pi ab} \, T_y \qquad\qquad (4.24)$$

To get the longitudinal creep coefficient we use
equation (4.23) knowing that

$$T_x = - f_1 \, \xi_x$$

hence

$$f_1 = \frac{G\pi ab}{\phi} \qquad\qquad (4.25)$$

similarly

$$f_2 = \frac{G\pi ab}{\psi_1} \qquad\qquad (4.26)$$

A correction factor is usually used in conjunction
with the values of f_1, f_2 given by equations (4.25) and
(4.26) respectively to account for the discrepency in the
experimental and analytical results as suggested in
reference [81].

For the determination of the creep coefficients
relating spin with transverse tangential force and moment
about the spin axis, Johnson [9] considered the problem of

the effect of spin upon the rolling motion of an elastic
sphere on a plane. Johnson reports agreement between his
theory and quantitative measurements over a wide range of
creep. Equations (26) and (27) in reference [9] express
the following relations

$$\xi_y = \frac{2}{3} \frac{(2 - \nu)}{(3 - 2\nu)} \ c \ \xi_\gamma \qquad (4.27)$$

and

$$M_z = - \frac{32}{9} \frac{(2 - \nu)}{(3 - 2\nu)} \ G \ c^4 \ \xi_\gamma \qquad (4.28)$$

where c is the radius of the circular contact area. For
an elliptical area of contact c can be approximated to be
$\sqrt{ab}$ where a and b are the semi-axes for the ellipse. For
the area of contact between wheel and rail, the ratio of
the two axes of the ellipse is nearly unity, and therefore
equations (4.27) and (4.28) are considered to be quite
satisfactory.

The creep coefficient relating the creep torque to
the spin is from equation (4.28)

$$f_3 = \frac{32}{9} \frac{(2 - \nu)}{(3 - 2\nu)} \ G \ c^4 \qquad (4.29)$$

The coupled creep coefficient is defined by

$$\text{lateral force} = - f_{23} \ \xi_\gamma \qquad (4.30)$$

but the lateral force is also given by

$$\text{lateral force} = - f_2 \ \xi_y \qquad (4.31)$$

Using equation (4.27), (4.30) and (4.31), one finds the relation between f_2 and f_{23}

$$f_{23} = \frac{2}{3} \frac{(2 - \nu)}{(3 - 2\nu)} c \ f_2 = 0.469 \ c \ f_2 \qquad (4.32)$$

It should be noted that the choice of the reference coordinates for the full model of the railway vehicle on rigid track and for the coupled vehicle/track model was such that the expressions derived in both cases for the longitudinal and lateral creepages and spin are identical. Therefore the corresponding expressions for the creep forces and moments acting on the wheelsets are the same in both cases. For the gravity forces, the expressions are different.

4.2.3 Lumped Parameter Model of Track

The simulation of the track for the coupled vehicle/ track dynamics, involves the representation of the infinitely long structure by an equivalent lumped parameter system composed of discrete masses, springs and dampers. This is possible because it was found that the velocity effects on the dynamic response of the track can be neglected. In this representation, the vertical elasticity of the track is considered by including a lumped parameter system of an effective lumped stiffness K_e and an effective mass m_e. The error involved in this approximation is negligible especially for low frequencies in comparison

with the fundamental type of free vibration of the rail on an elastic foundation. This frequency can be calculated in a very simple manner by taking into consideration the fact that the fundamental type of vibration consists of an oscillation of the rail as an absolutely rigid body in the vertical direction.

$$\omega_0 = \sqrt{\frac{k}{m}} \tag{4.33}$$

This can also be obtained from the equation giving the natural frequencies of a finite beam of length ℓ on an elastic foundation [82]

$$\omega_j^2 = \frac{a^2 \pi^4}{\ell^4} (j^4 + \imath) \tag{4.34}$$

as ℓ tends to infinity

where $a^2 = \dfrac{EI}{m}$

$$\imath = \frac{k}{EI} \frac{\ell^4}{\pi^4}$$

and ω_j is the natural frequency for the jth mode of vibration

Equation (4.33) can also be rewritten to give the frequency in hertz:

$$f_0 = \frac{1}{2\pi} \omega_0 = \frac{1}{2\pi} \sqrt{\frac{k}{m}} \tag{4.35}$$

For typical physical parameters for the conventional track f_0 is found to be approximately 62 hertz.

If ℓ_e is the effective length of rail which will give an effective lumped mass m_e corresponding to the natural frequency of the distributed system, the value of ℓ_e and m_e can be determined by writing equation (4.35) in the form

$$2\pi f_0 = \left[\frac{k\,\ell_e}{m\,\ell_e}\right]^{1/2} = \left[\frac{K_e}{m_e}\right]^{1/2} \tag{4.36}$$

For an infinite beam on elastic foundation [51]:

$$K_e = \frac{P}{y(0)} = \frac{2\,k}{\omega} \tag{4.37}$$

where $y(0)$ is the deflection of the beam under the load P and

$$\omega = \left(\frac{k}{4EI}\right)^{1/4} \tag{4.38}$$

which gives the lumped system parameter

$$\ell_e = 2/\omega \tag{4.39}$$

The damping C_e is calculated as for a single degree of freedom system given a certain percentage. Meacham [65,66] showed that both the damping and the mass of the track structure can be neglected so long as the frequencies are less than $0.3\,f_0$ with little loss of accuracy in the dynamic deflections. In the present analysis however, these effects are included.

4.2.4 Equations of Motion

The derivation of the equations of motion for all masses except the wheelsets is quite straight forward. For the wheelsets, in addition to the active forces due to the suspension system and the inertia forces, the creep forces and gravity forces have to be included. For wheelset number 1, the equations are:

(i) Longitudinal - Motor/Wheelset:

$$(m_c + m_d)\ddot{u}_{d1} + (\frac{2f_1}{S})\dot{u}_{d1} + (\frac{2\ell_{20}}{S})\dot{\beta}_{d1}$$

$$+ (RA_1) = 0 \qquad (4.40)$$

(ii) Vertical - Track/Wheelset:

$$(m_d + m_e)\ddot{w}_{d1} + (-2K_9)w_{br} + (2K_9 + K_e)w_{d1}$$

$$+ (2\ell_{24}K_9)\beta_{br} + (-C_{17}-C_{18})\dot{w}_{br}$$

$$+ (C_{17}+C_{18}+C_e)\dot{w}_{d1} + \ell_{24}(C_{17}+C_{18})\dot{\beta}_{br}$$

$$- (RW_1) = 0 \qquad (4.41)$$

(iii) Pitch - Wheelset:

$$- I_{d\beta}\ddot{\beta}_{d1} + (\frac{2\ell_{20}f_1}{S})\dot{u}_{d1} + (\frac{2\ell_{20}^2 f_1}{S})\dot{\beta}_{d1} = 0 \qquad (4.42)$$

(iv) Lateral - Wheelset:

$$m_d\ddot{v}_{d1} + (2f_2)\gamma_{d1} + (\frac{2f_2}{S})\dot{v}_{d1} + (-\frac{2\ell_{20}f_2}{S})\dot{\alpha}_{d1}$$

$$+ (\frac{2f_{23}}{S})\dot{\gamma}_{d1} + N_{r1}(\theta_0 + \frac{2\epsilon v_{d1}}{\ell_{18}} - \alpha_{de1})$$

$$- N_{\ell 1} \left(\theta_0 - \frac{2\epsilon v_{d1}}{\ell_{18}} + \alpha_{del} \right) + (RB_1)$$

$$+ (RV_1) = 0 \qquad (4.43)$$

But

$$N_{r1} \left(\theta_0 + \frac{2\epsilon v_{d1}}{\ell_{18}} - \alpha_{del} \right) - N_{\ell 1} \left(\theta_0 - \frac{2\epsilon v_{d1}}{\ell_{18}} + \alpha_{del} \right)$$

can be rewritten as:

$$(N_{r1} - N_{\ell 1}) \, \theta_0 + (N_{r1} + N_{\ell 1}) \left(\frac{2\epsilon v_{d1}}{\ell_{18}} - \alpha_{del} \right)$$

However $(N_{r1} + N_{\ell 1}) \simeq W$ and equation (4.43) can be rewritten as:

$$m_d \ddot{v}_{d1} + (2f_2) \gamma_{d1} + \left(\frac{2f_2}{S} \right) \dot{v}_{d1} + \left(-\frac{2\ell_{20} f_2}{S} \right) \dot{\alpha}_{d1}$$

$$+ \left(\frac{2f_{23}}{S} \right) \dot{\gamma}_{d1} + \left(\frac{2W\epsilon}{\ell_{18}} \right) v_{d1} + (-W) \alpha_{del}$$

$$+ (N_{r1} - N_{\ell 1}) \theta_0 + (RB_1) + (RV_1) = 0 \qquad (4.44)$$

where the quantity $\frac{2W\epsilon}{\ell_{18}}$ is the so called lateral gravitational stiffness.

(v) Roll - Motor/Wheelset:

$$(I_{c\alpha} + I_{d\alpha}) \ddot{\alpha}_{d1} + (-2\ell_{17}^2 K_9) \alpha_{br} + (2\ell_{17}^2 K_9) \alpha_{d1}$$

$$+ [\ell_{19}^2 (-C_{17} - C_{18})] \dot{\alpha}_{br} + [\ell_{19}^2 (C_{17} + C_{18}) \dot{\alpha}_{d1}$$

$$+ (-2\ell_{20} f_2) \gamma_{d1} + \left(-\frac{2\ell_{20} f_2}{S} \right) \dot{v}_{d1}$$

$$+ \left(\frac{2\ell_{20}^2 f_2}{S} \right) \dot{\alpha}_{d1} + \left(-\frac{2\ell_{20} f_{23}}{S} \right) \dot{\gamma}_{d1}$$

$$+ \left(\frac{\ell_{18}}{2} - \eta \, v_{d1} \right) N_{r1} - \left(\frac{\ell_{18}}{2} + \eta \, v_{d1} \right) N_{\ell 1}$$

$$+ \ell_{20}(\theta_0 - \frac{2\varepsilon v_{dl}}{\ell_{18}} + \alpha_{del})N_{\ell 1} - \ell_{20}(\theta_0 + \frac{2\varepsilon v_{dl}}{\ell_{18}}$$

$$- \alpha_{del})N_{r1} = 0 \qquad (4.45)$$

Combining the terms in N_{r1} and $N_{\ell 1}$ as done before we get

$$(I_{c\alpha} + I_{d\alpha})\ddot{\alpha}_{dl} + (-2\ell_{17}^2 K_9)\alpha_{br} + (2\ell_{17}^2 K_9)\alpha_{dl}$$

$$+ [\ell_{19}^2(-C_{17} - C_{18})]\dot{\alpha}_{br} + [\ell_{19}^2(C_{17} + C_{18})]\dot{\alpha}_{dl}$$

$$+ (-2\ell_{20}f_2)\gamma_{dl} + (-\frac{2\ell_{20}f_2}{S})\dot{v}_{dl}$$

$$+ (\frac{2\ell_{20}^2 f_2}{S})\dot{\alpha}_{dl} + (-\frac{2\ell_{20}f_{23}}{S})\dot{\gamma}_{dl}$$

$$+ (-\eta W + \frac{2\ell_{20}\varepsilon W}{\ell_{18}})v_{dl} + (\ell_{20}W)\alpha_{del}$$

$$+ (\frac{\ell_{18}}{2} - \ell_{20}\hat{\theta}_0)(N_{r1} - N_{\ell 1}) = 0 \qquad (4.46)$$

(vi) Yaw - Wheelset:

$$I_{d\gamma}\ddot{\gamma}_{dl} + (-\frac{\ell_{18}\lambda f_1}{\ell_{20}})v_{dl} + (2f_{32})\gamma_{dl} + (\frac{2f_{32}}{S})\dot{v}_{dl}$$

$$+ (-\frac{2\ell_{20}f_{32}}{S})\dot{\alpha}_{dl} + (\frac{\ell_{18}^2 f_1}{2S} + \frac{2f_3}{S})\dot{\gamma}_{dl}$$

$$+ [-(\theta_0 - \frac{2\varepsilon v_{dl}}{\ell_{18}} + \alpha_{del})\frac{\ell_{18}}{2} N_{\ell 1}]\gamma_{dl}$$

$$+ [-(\theta_0 + \frac{2\varepsilon v_{dl}}{\ell_{18}} - \alpha_{del})\frac{\ell_{18}}{2} N_{r1}]\gamma_{dl}$$

$$+ (RM_1) + (R\gamma_1) = 0 \qquad (4.47)$$

Substituting for $N_{\ell 1} + N_{r1} = W$ and neglecting $(N_{\ell 1} - N_{r1})$ $\frac{\varepsilon v_{dl}}{\ell_{18}}$, equation (4.47) becomes:

$$I_{d\gamma}\ddot{\gamma}_{d1} + (-\frac{\ell_{18}\lambda f_1}{\ell_{20}})v_{d1} + (2f_{32} - W\frac{\ell_{18}}{2}\theta_0)\gamma_{d1}$$

$$+ (\frac{2f_{32}}{S})\dot{v}_{d1} + (-\frac{2\ell_{20}f_{32}}{S})\ddot{\alpha}_{d1} + (\frac{\ell_{18}^2 f_1}{2S}$$

$$+ \frac{2f_3}{S})\dot{\gamma}_{d1} + (RM_1) + (R\gamma_1) = 0$$

$$(4.48)$$

where $-\frac{\ell_{18}}{2}\theta_0 W$ is the yaw gravitational stiffness which

is a negative stiffness that acts to further displace the

wheelset.

(vii) Roll - Track/Motor/Wheelset:

$$(I_{c\alpha}+I_{d\alpha}+\frac{1}{4}\ell_{18}^2 m_e)\ddot{\alpha}_{del} + (-W)v_{d1} + (-2\ell_{17}^2 K_9)\alpha_{br}$$

$$+ (2\ell_{17}^2 K_9 + \frac{1}{2}\ell_{18}^2 K_e')\alpha_{del} + [\ell_{19}^2(-C_{17}-C_{18})]\dot{\alpha}_{br}$$

$$+ [\ell_{19}^2(C_{17}+C_{18}) + \frac{1}{2}\ell_{18}^2 C_e']\dot{\alpha}_{del} = 0 \qquad (4.49)$$

The other wheelsets have similar equations of

motion. Combining these equations for the wheelsets with

the equations for the other masses of the system, we get

all the equations of motion which are given in detail in

Appendix (B). In that Appendix the process of elimination

of internal reactions and the transformation of the

equations to the generalized coordinates system are

described in detail.

Because of the symmetry, the equations describing

the lateral motions of the system (these include the

lateral displacement·(v), the roll (α) and the yaw (γ)) are uncoupled from the equations of motion of the longitudinal modes (longitudinal (u), vertical (w), and pitch (β) displacements).

The equations of motion for the lateral vibrations are given in part (B.1) of Appendix (B) and those for the longitudinal vibrations in part (B.2) of the same appendix. The equations in the generalized coordinates have the general form

$$[M]\{\ddot{x}\} + [C]\{\dot{x}\} + [K]\{x\} = \{0\} \qquad (4.50)$$

where [M] is the mass matrix

[C] is the damping matrix

[K] is the stiffness matrix

and {x} is the vector of the independent displacements.

For the lateral vibration of the coupled vehicle/ track model equation (4.50) is a 15 by 15 matrix equation. For the longitudinal vibration of the same model equation (4.50) represents a 27 by 27 matrix equation. Because of the introduction of the non-conservative creep forces and gravity forces, the mass, stiffness and damping matrices are not symmetric.

The equations were derived for the coupled vehicle/ track model. The equations of motion for the model of the vehicle on rigid track can be obtained if all the terms in w_{dj} and α_{dej} (j = 1,...,6), in the given equations,

are neglected, i.e., by eliminating the rows and columns
in the matrix equations, corresponding to these zero
displacement.

4.3 Solutions and Results

4.3.1 Dynamic Stability

The dynamic stability of the railway vehicle
model is investigated by studying the character of the
solutions, more precisely by studying the roots of the
characteristic equation associated with the equations of
motion of the system.

The creep forces are of fundamental importance in
the dynamic stability analysis of railway vehicles. Creep
can modify the transient response of a railway vehicle
appreciably. At high speeds the system is dynamically
unstable and so there is a critical speed dependent upon
the elastic restoring forces, damping in the system, the
creep forces and the gravity forces. Motions at speeds
above the critical speed are limited by the wheel flanges
and slipping at the treads.

For a multi-degree of freedom system, studying the
character of the solution leads to an eigenvalue problem.
The solution of the eigenvalue problem in the presence of
damping in the system results in complex conjugate
eigenvalues with negative real part for all roots if the

system is stable. The dynamic stability is then investigated using root-locus plots.

First it is required to transform the equations governing the lateral motion of the system to a standard form, required for the computations of the charactertistic roots. The procedure used is to transform the n second order differential equations into 2n first order differential equations. The n second order differential equations governing the lateral motions of the system, are given in their general form by the matrix equation (4.50). Equation (4.50) can be rewritten in the following form:

$$
D \left\{ \begin{array}{c} x \\ \hline \dot{x} \end{array} \right\} = \left[\begin{array}{c|c} 0 & [I] \\ \hline -[M^{-1}][K] & -[M^{-1}][C] \end{array} \right] \left\{ \begin{array}{c} x \\ \hline \dot{x} \end{array} \right\}
\tag{4.51}
$$

where all the quantities in equation (4.51) are submatrices except D which is the differential operator; and x is the vector of displacements.

Now let:
$$
\{v\} = \left\{ \begin{array}{c} x \\ \hline \dot{x} \end{array} \right\}
\tag{4.52}
$$

and
$$
G = \left[\begin{array}{c|c} 0 & [I] \\ \hline -[M^{-1}][K] & -[M^{-1}][C] \end{array} \right]
\tag{4.53}
$$

Substituting from equation (4.52) and (4.53), equation (4.51) becomes:

$$D \{ \upsilon \} = [G] \{ \psi \} \qquad (4.54)$$

Assume a solution in the form

$$\{ \upsilon \} = \{ T\, e^{st} \} \qquad (4.55)$$

and substitute in equation (4.54), getting

$$s \{ T \} = [G] \{ T \} \qquad (4.56)$$

or

$$(s\, [I] - [G]) \{ T \} = 0 \qquad (4.57)$$

which is the algebraic eigenvalue problem. The matrix [G] is a 2n x 2n matrix with real coefficients. The roots of [G] are the eigenvalues and may be obtained numerically using a computer library subroutine. The solutions are complex in the form:

$$s_j = \mu_j \pm i\, \omega_{dj} \qquad (4.58)$$

for the jth root,

where μ_j is the real part of the root and is equal zero
for zero damping associated with the jth root

and ω_{dj} is the damped natural frequency.

From equations (4.55) and (4.58) it is found that a general element of the vector υ is

$$\upsilon_j = A\, e^{\mu_j t} \cos(\omega_{dj} t + \psi) \qquad (4.59)$$

If any μ_j is positive, the displacement u_j becomes unstable. Hunting for the railway vehicle can be investigated by determining the eigenvalues of the matrix [G]. The procedure is to solve for all eigenvalues for increasing values of forward speed until a μ_j becomes positive, indicating instability and the critical speed.

The root locus plots for the railway vehicle under consideration moving on rigid track and on flexible track are shown in Figure 4.4, corresponding to the conventional wooden ties track structure. The results show that track elasticity tends to increase the linear critical speed at which hunting occurs. The increase for the track parameters used is small, however the results indicate that the increase in vertical track elasticity provides an inherently more stable ride for the railway vehicle.

4.3.2 Dynamic Response to Track Irregularities

Below the critical speed the lateral and vertical motions of railway vehicles are determined by track geometry. In studies of dynamic response, three general quantities of interest exist: the definition of the input, the determination of the transfer function and assessment of the resulting output. The transfer function is determined from the equations of motion derived in a similar manner as for the dynamic stability analysis.
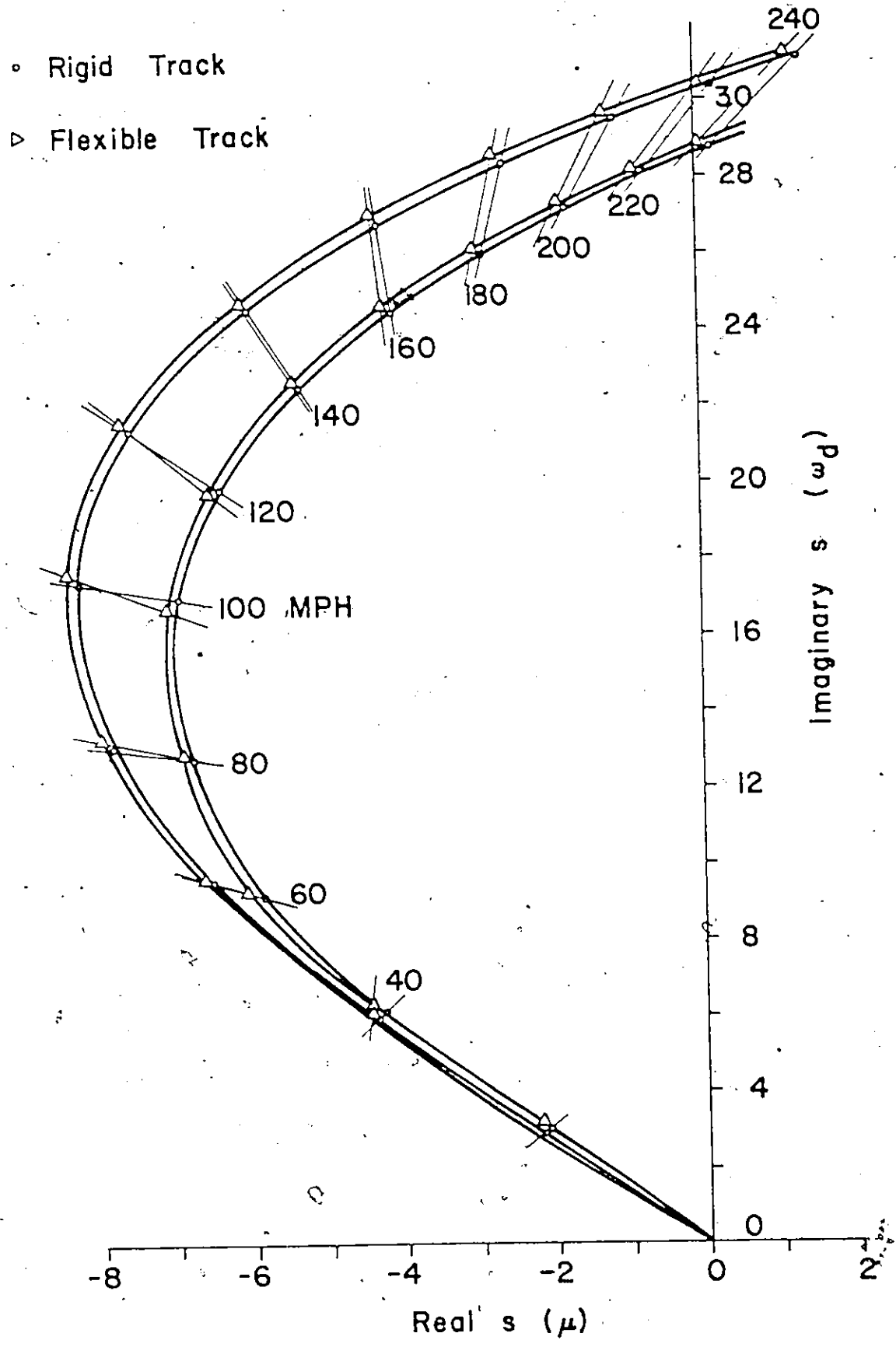
Figure 4.4 Velocity root locus plot for the locomotive on rigid and flexible track

Motions of the vehicle symmetric about the
longitudinal plane of symmetry are excited by vertical
track irregularities, while transverse motions are
excited by lateral track irregularities and cross-level.
The sinusoidal track irregularities are in particular
worth considering because power spectra and auto-
correlation functions obtained from field measurements
indicate the existence of periodic functions [35]. Periodic
excitation of vertical vehicle oscillations results also
from evenly spaced rail joints or rail welds.

When the railway vehicle is moving on the track,
the generalized displacements of the wheelsets are governed
by the laws of creep and the dynamics of the full system.
The system of linear differential equation of motion may
be expressed in the following form:

$$[\bar{M}]\{\ddot{x}\} + [\bar{C}]\{\dot{x}\} + [\bar{K}]\{x\} = \Psi(x,\dot{x}) + F(y,\dot{y},\ddot{y}) \qquad (4.60)$$

where $\Psi(x,\dot{x})$ represents the constraint imposed by the
track (due to creep process, mutual wheel/rail
geometry, gravity stiffness effects and the
forward speed)

$F(y,\dot{y},\ddot{y})$ is the forcing function due to rail
irregularities. For a perfectly straight track
F would simply be a zero vector.

The force Ψ depends on the instantaneously prevailing

values of x and $\dot{x}$. In the linear case, the function
$\Psi(x,\dot{x})$ may be expressed in the form:

$$\Psi(x,\dot{x}) = - ([C']\{\dot{x}\} + [K']\{x\}) \tag{4.61}$$

where the square matrices $\dot{C}'$ and K' are determined by the
process of creepage, the mutual wheel/rail geometry and
by the forward speed S of the railway vehicle. K' and C'
are not symmetric, equation (4.60) can be rewritten in
the form:

$$[M]\{\ddot{x}\} + [C]\{\dot{x}\} + [K]\{x\} = \{F\} \tag{4.62}$$

The L.H.S. of equation (4.62) is the same as for equation
(4.50).

In the present analysis the forcing function
$F(y,\dot{y},\ddot{y})$ has the form

$$F(y,\dot{y},\ddot{y}) = - [\bar{M}]\{\ddot{y}\} - [\bar{C}]\{\dot{y}\} - [\bar{K}]\{y\} \tag{4.63}$$

where $\{y\}$ is the vector of known displacements due to
rail irregularities. To determine this forcing function,
we must go back to the original equations of motion up to
the point where creep forces and gravity forces are
introduced. These are valid for any displacements whether
free or induced. Assume that all displacements have the
general form

$$x = x_r + x_i \tag{4.64}$$

where x_r is the displacement relative to the track due to
creep

and x_i is the induced displacement due to track irregularities.

All displacements x_i are zeros except for the variables describing the motion of the wheelsets and for the frames in the lateral and yaw directions. The rolling motion of the wheelsets relative to the track $[\alpha_{dj}(j=1,\ldots 6)]$ are not independent variables, but they do exist implicitly in the equations due to the lateral displacement of the wheelsets and the mutual wheel/rail geometry.

Because it is assumed that in normal running conditions the wheels are following the rails in the vertical direction and that there is no creep in this direction, the following additional constraints are imposed:

a)   For the case of the rigid track

The relative displacement of the wheels in the vertical direction is zero ($x_r=0$), it follows that $w_{dj} = 0$ ($j=1,\ldots,6$), and rows and columns corresponding to these variables should be deleted reducing the number of degrees of freedom of the system by 6.

The induced vertical displacements of the wheels are due to the vertical track irregularities, i.e.,

$$x_i = \epsilon(t) \qquad (4.65)$$

where $\epsilon(t)$ is an error function due to track irregularities.

b) For the case of the flexible track.

The displacement of the wheels in the vertical direction is due to the vertical displacement of the track and track irregularities which are represented by an input time function $\varepsilon(t)$ corresponding to spatial variation and train speed so that

$$w_w(t) = w_d(t) + \varepsilon(t) \qquad (4.66)$$

where w_w is the vertical displacement of the wheelset

w_d is the vertical displacement of the track

The steady state solutions are obtained using the generalized method of complex algebra. The use of this method simplifies the procedure for solving the system of differential equations. For forced vibration of a linear general multi-degree of freedom system where the impressed force is harmonic, the steady state vibrations are also harmonic with the same frequency. In the presence of damping in the system, phase differences between the resulting motions and the input excitation exist. Hence we solve the system of differential equations given by the matrix equation (4.62), where F is a vector representing the forcing function

$$\{F\} = \{\bar{F}\}\, e^{i\Omega t} \qquad (4.67)$$

where $\bar{F}$ is the vector representing the complex amplitude of the input.

and Ω is the forcing frequency.

Equation (4.62) can be solved by assuming the solution in the form

$$\{x\} = \{\bar{X}\}\, e^{i\Omega t} \qquad\qquad (4.68)$$

where $\bar{X}$ is the vector representing the amplitude of the response in complex form.

Equations (4.62), (4.67) and (4.68) lead to the equation

$$[(K-\Omega^2 M) + i\Omega C]\{\bar{X}\} = \{\bar{F}\} \qquad\qquad (4.69)$$

Where the quantity in square brackets is a square matrix whose elements are complex. If this square matrix is denoted by Z, and provided that Z is nonsingular, the solution of (4.62) will be:

$$\{\bar{X}\} = [Z^{-1}]\{\bar{F}\} \qquad\qquad (4.70)$$

It should be noted that the derivation was done for a multi-degree of freedom system related to an arbitrary set of periodic forces all having the same frequency. If the system is acted upon by forces of different frequencies then the resultant displacement vector will be the sum of the displacement vectors due to the forces at each frequency taking one frequency at a time.

The method outlined provides a systematic way of

finding the displacements due to an applied set of forces with or without damping. For a system having a large number of degrees of freedom, the method is ideally suitable for solution on a digital computer.

The steady state response of the vehicle components to varying input frequencies is computed and computer plotted in each case. The input frequency, which is a function of the wave length of the irregularities and the vehicle forward speed, is increased from zero to 8 hertz corresponding to a forward speed of approximately 200 mph. Typical results for the response obtained for the cases of rigid and flexible tracks are shown in Figures 4.5 to 4.11. Figures 4.5 to 4.7 show the response curves obtained for the body in longitudinal vertical and pitch displacements respectively. Figure 4.8 show the response curves obtained for the vertical amplitude of displacements for the rear frame. Figure 4.9 gives the response of the front frame in pitch motion. Figures 4.10 and 4.11 show the response curves for the pitch mode of oscillation of the motor and wheelset number 3 respectively.

The results show that track elasticity has an appreciable effect on the vibration of the motors and the wheelsets especially at high frequencies. More specifically track elasticity has little effect on the dynamic displacements of the car body in the vertical and pitch
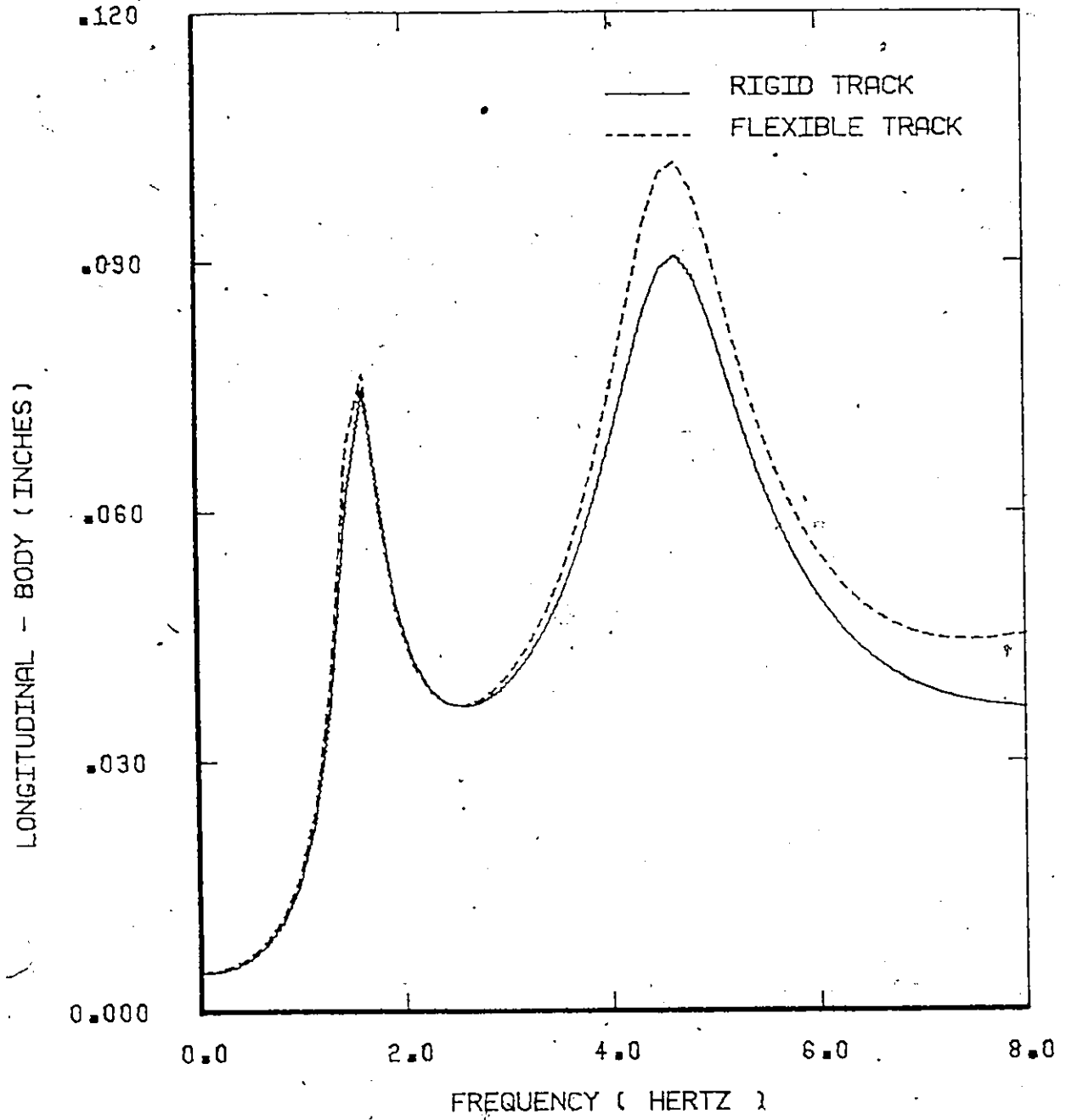
Figure 4.5 Body longitudinal displacement
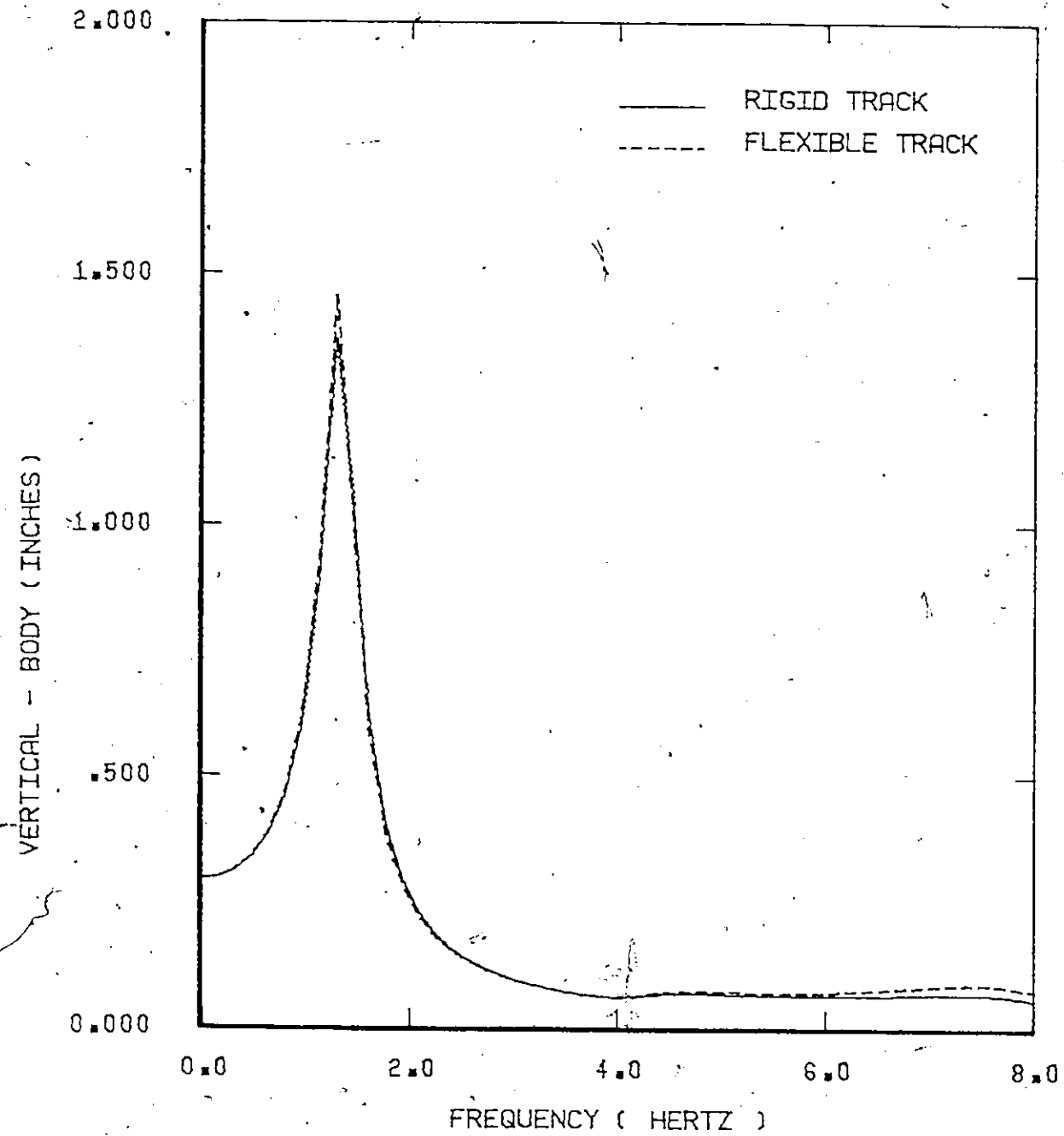
Figure 4.6   Body vertical displacement
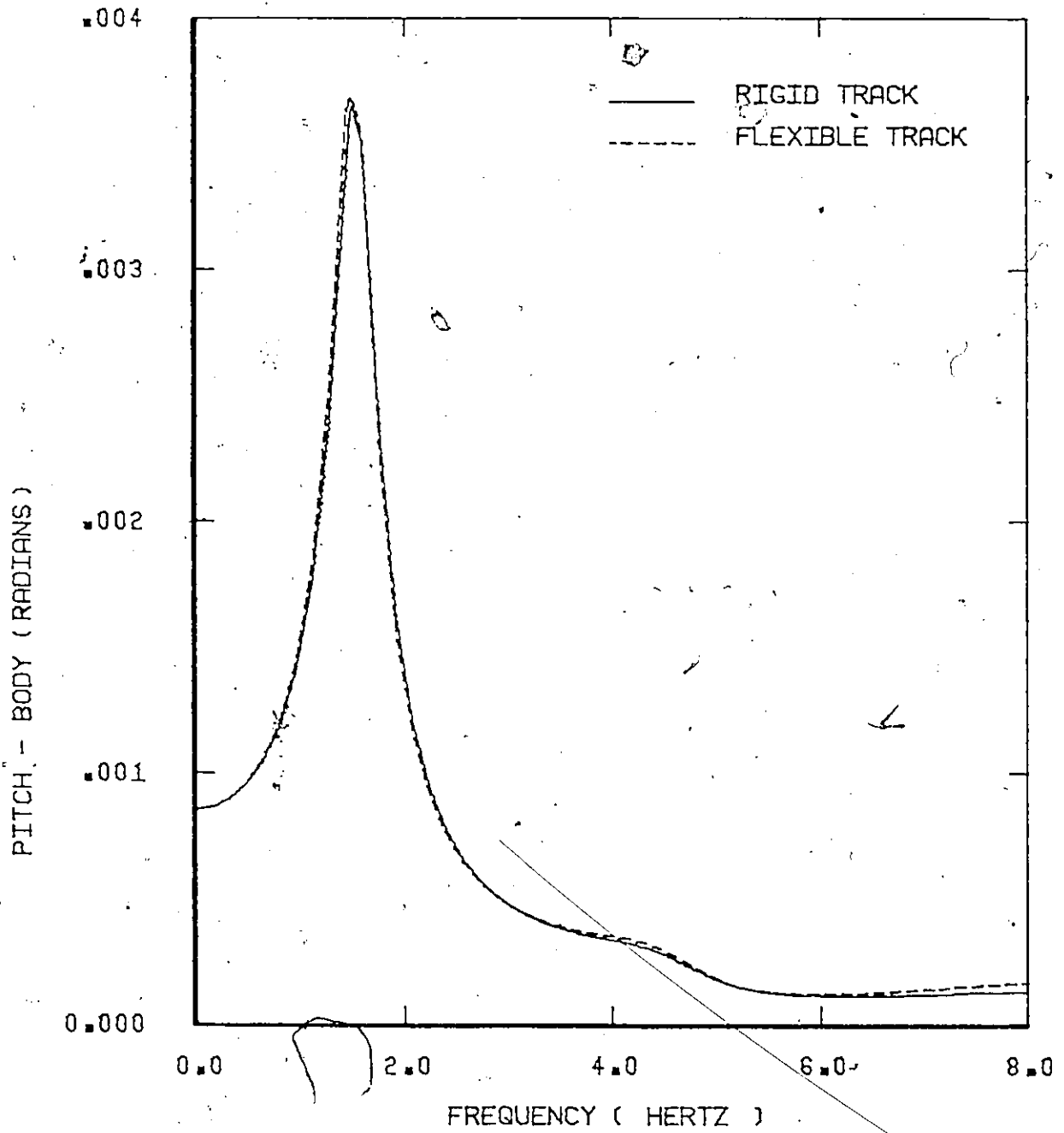
Figure 4.7   Body pitch displacement
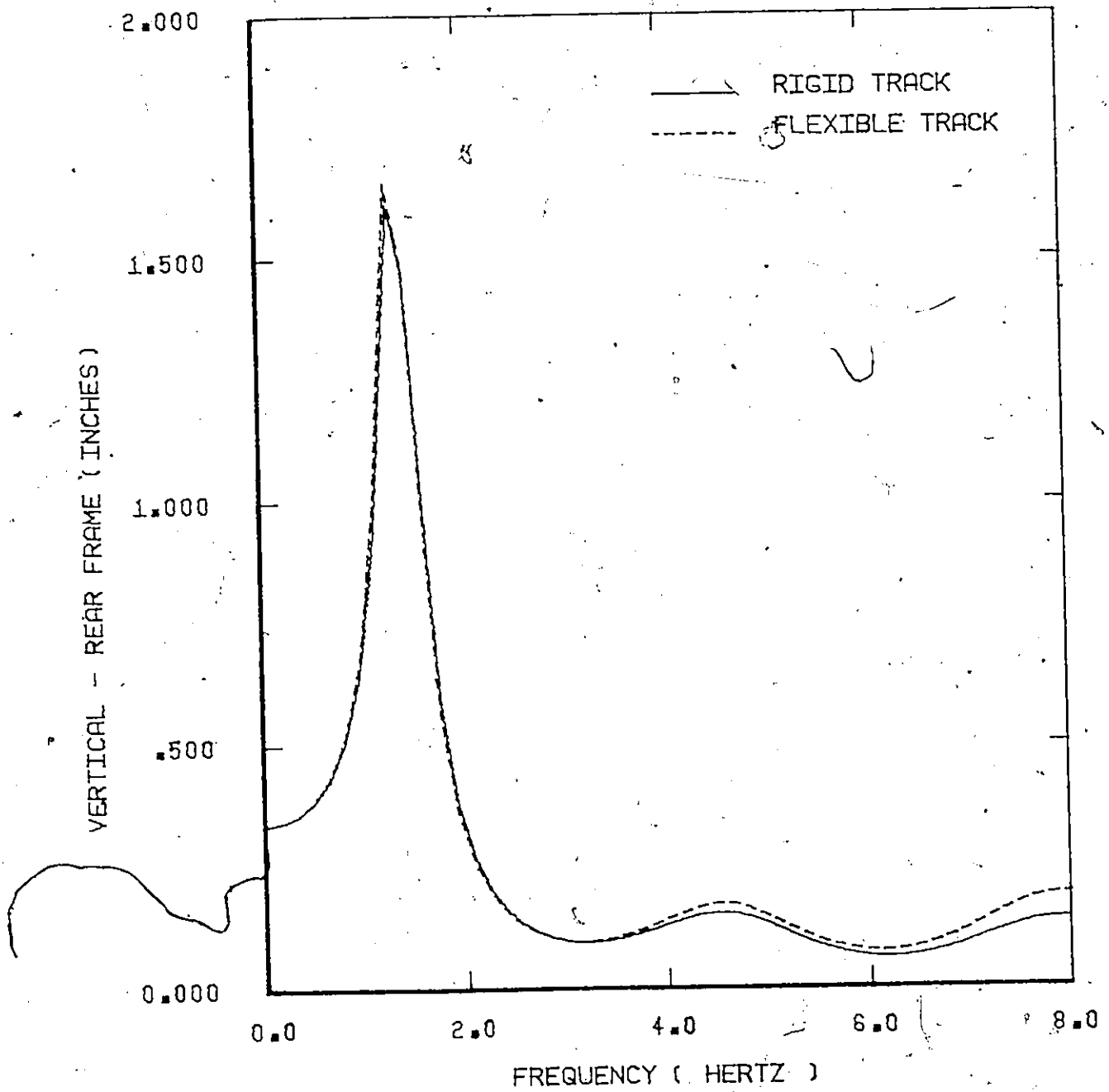
Figure 4.8   Rear frame vertical
              displacement
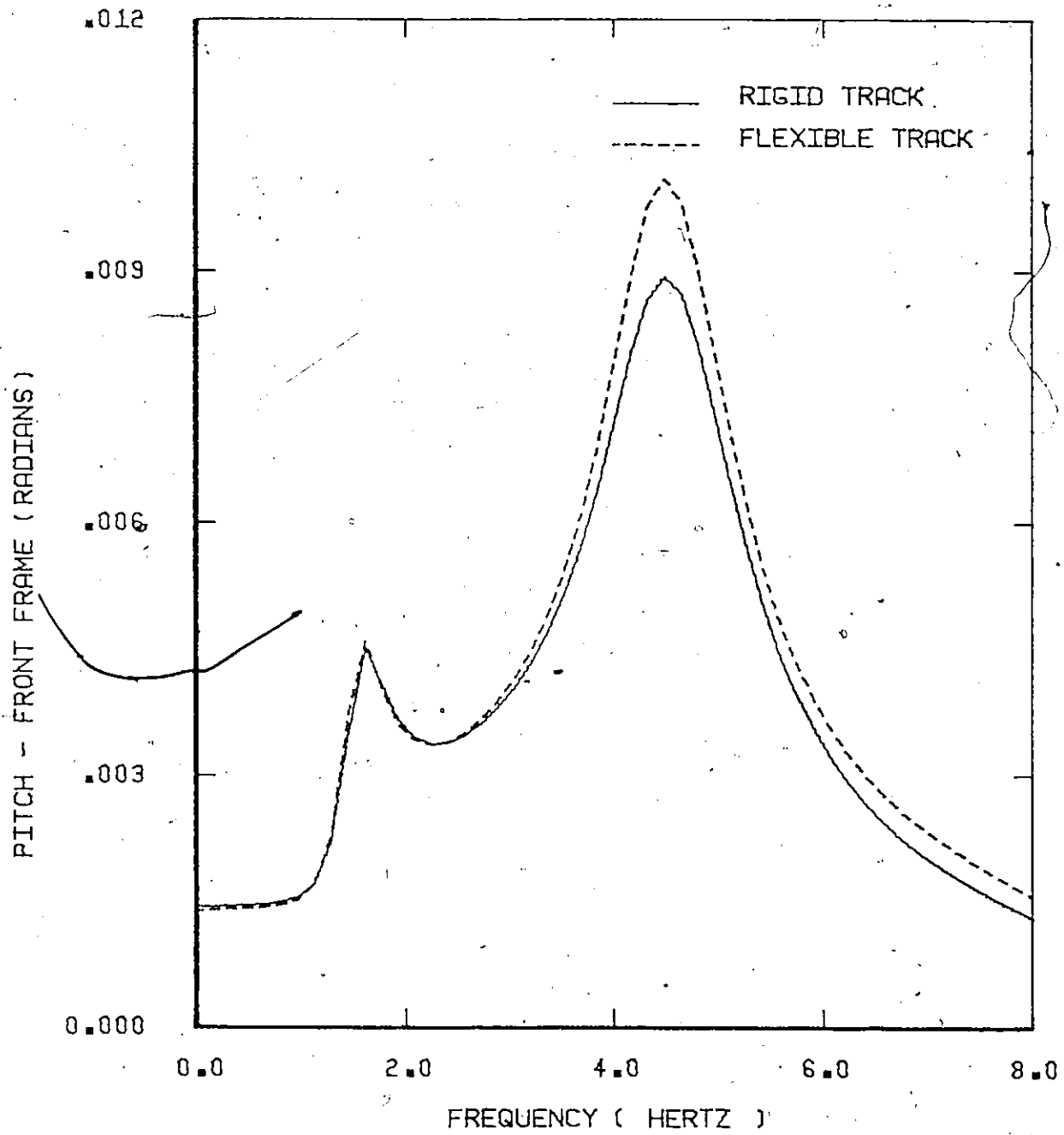
Figure 4.9 Front frame pitch displacement
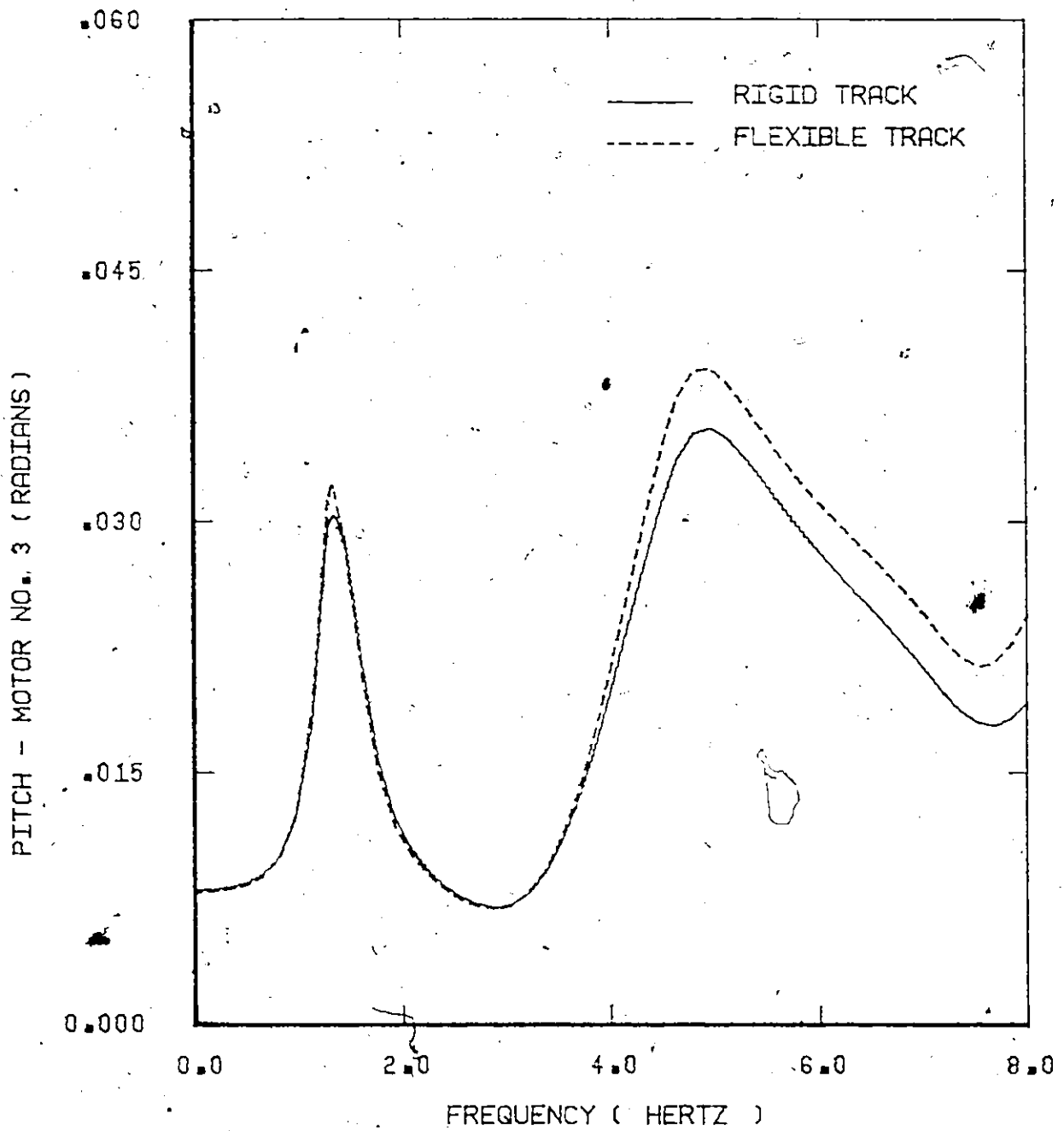
Figure 4.10   Motor No. 3 pitch displacement
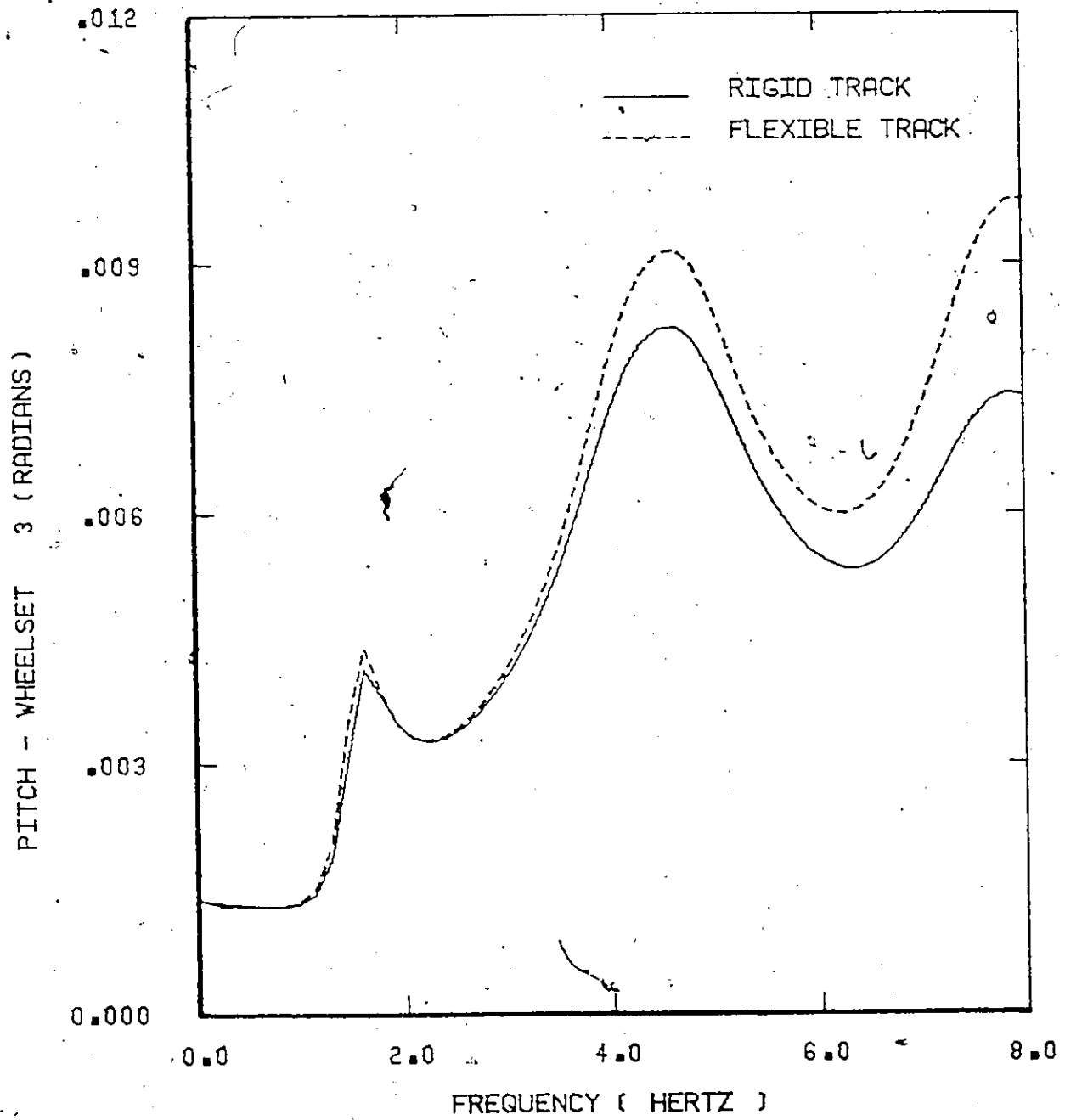
Figure 4.11   Wheelset No. 3 pitch
displacement

displacements, the effect is negligible for low
frequencies. For the vibrations of the body in the
longitudinal mode, the effect is more appreciable at high
frequencies. The effect of the elasticity of the track
on the dynamic displacements of the frames is shown in
Figures 4.8 and 4.9. The effect on the vertical displace-
ment is negligible especially at lower frequencies, for
the pitch displacement the effect is more appreciable
especially near higher resonant responses. The effect of
track elasticity on the vibrations of the motors and the
wheelsets is shown to be appreciable especially at higher
frequencies.

Figure 4.12 illustrates the frequency response
curve for the vertical displacement of the track/wheelset
no. 3. Other wheelsets have similar responses.

The results presented show that track elasticity
results, in general, in higher dynamic displacements for
the vehicle components. For the motors, wheelsets and
pitch of frames the effect is significant especially on
peak responses at high frequencies. In all cases the
track elasticity does not generally affect the shape of
the response curves except for the vertical displacement
of the wheelsets where the response for the case of rigid
track is zero.

It is recommended that the elasticity of the track
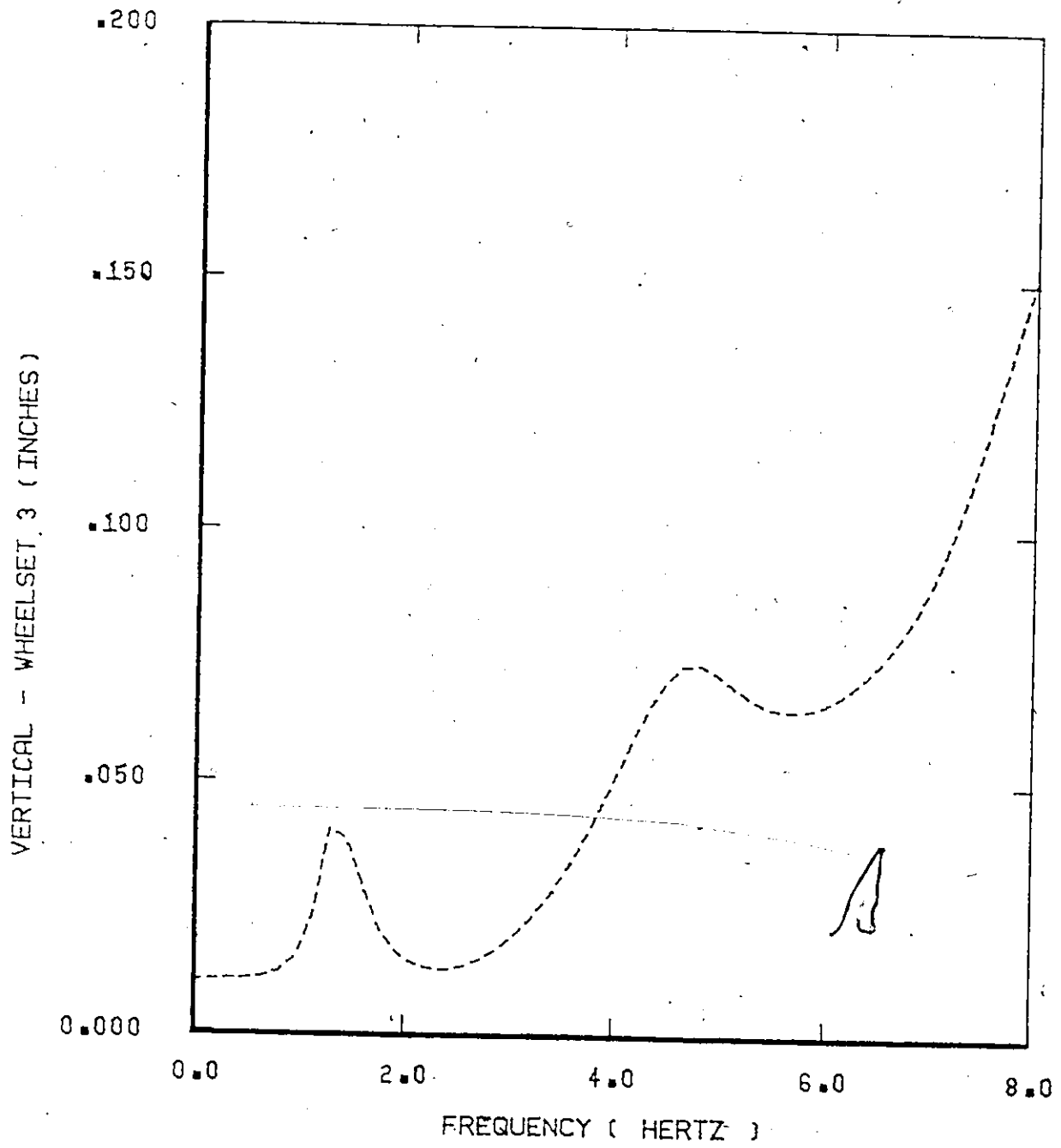
Figure 4.12 / Track/Wheelset No. 3 vertical
displacement

be included in the dynamic response analyses of railway

vehicles to track irregularities especially for proposed

high speed systems.

4.3.3 Minimization of Response to Track Irregularities

The minimization of the response of railway vehicles

due to track irregularities is a topic which received

little attention in the literature until recently. In the

last few years a great deal of effort has been devoted to

trying to improve the riding qualities of railway vehicles.

The aim is to achieve maximum speed and comfort on

existing tracks. The objectives of maximizing the speed

while minimizing the response of vehicle components to

economically attractive track irregularities have always

conflicted to various degrees. The aim is to design an

optimum suspension system capable of attenuating the

vibrations at passenger positions while still maintaining

an adequate margin of dynamic stability.

In most of the research work published in this

area so far, attempts have been made to find near

optimum designs. The optimization process is carried

either in the time domain [42] or in the frequency domain

[44]. The advantage of the solution in the frequency

domain is that the minimization is carried out for all

frequencies within the range of interest. References [43,

44, 45] report some of the research work directed toward

the minimization of the vibrations transmitted due to rail irregularities. In these studies no rigid body pitch motion of the car is allowed and consequently out of phase vertical inputs to front and rear suspensions could not be considered. The general objective of the optimization is to minimize the acceleration of chosen points on the railway car within the frequency domain of interest. Usually, designers used a sensitivity analysis approach to the problem.

A sensitivity analysis is a procedure based on trial and error. If the responses do not fall within prescribed limits, the designer changes the configuration or the elements of the system and the analysis is repeated. This process is time consuming and leaves doubts in the designers mind as to what alternative trials should be terminated. Because a great deal of interaction between the suspension elements exists, the prediction of the contribution of each suspension element considered separately is quite difficult.

In this research a method for the minimization of the response to track irregularities based on a minimax principle and mathematical programming techniques is suggested. The objective of the optimization is to minimize the lateral acceleration transfer function at the cab. A simplified model of the locomotive on rigid track

is used for the illustration of the proposed method. The simplification is made by assuming that the primary suspension and creep forces have little effect on the lateral vibrations of the body. It is known that the response of a dynamic system such as a railway vehicle can be minimized by choosing certain, optimum, values of the damping and stiffness elements in the system.

In any optimization problem, certain parameters called the design variables, the suspension parameters in the present case, are to be found. The optimum parameters optimize (minimize) a certain objective function, satisfy the equations which describe the behaviour of the system and at the same time satisfy certain design constraints.

The objective of the optimization is to minimize the maximum lateral acceleration at the cab, within the frequency domain of interest. For an n degree of freedom system, it is well known that the response or acceleration transfer function f has n or fewer maxima in Ω, the number of maxima depending on the damping in the system; for small enough damping there are exactly n maxima. The frequencies of these maxima correspond to the damped natural frequencies of the system. By solving the eigenvalue problem, the damped natural frequencies can be obtained as given in equation (4.58):

$$s_j = \mu_j \pm i \, \omega_{dj} \qquad (j = 1, \ldots, n)$$

where s_j are the complex conjugate eigenvalues.

A maximum is suppressed at the damping value for which two values of the real part of the roots coalesce.

If the damped natural frequencies ω_{dj} are inserted into the transfer function f, the response maxima are obtained as functions of the independent design variables $(\vec{x})$ only, where f is a real-valued function of the real variable Ω and n_1, n_2,...,n_r are the r stiffness and damping lumped parameters to be optimized. The notation $\vec{x}$ is used to represent the r component vector of the independent design variables. The jth response maximum is

$$f_j (\vec{x}) = f (\omega_{dj} (\vec{x}), \vec{x}) \qquad (4.71)$$

For each value of $\vec{x}$ there are n or fewer f_j, these are defined for all $\vec{x}$ values for which ω_{dj} are defined.

The frequency interval of interest may be infinite or finite, in most practical cases it is finite, in any case, Ω_ℓ and Ω_u denote the lower and upper bounds on the frequency interval respectively. Ω_ℓ may be zero or finite and Ω_u may be infinite or finite.

Let:

$$\left.\begin{array}{l} f_\ell (\vec{x}) = f (\Omega_\ell, \vec{x}) \\[2em] f_u (\vec{x}) = f (\Omega_u, \vec{x}) \end{array}\right\} \qquad (4.72)$$

The reason for including the functions evaluated at the

limits of the frequency interval of interest is that in case all resonances are suppressed in the interval, the optimum parameters vector $\vec{x}$ will be the vector to minimize equation (4.72). It is useful to note that some resonant responses may reappear for large values of damping.

The set of response maxima functions is taken as the set f_j from equation (4.71) together with f_ℓ and f_u from equations (4.72), hence

$$\left\{ f_k \; (\vec{x}) \right\} = \left\{ \begin{array}{c} \{f_j \; (\vec{x})\} \\ f_\ell \; (\vec{x}) \\ f_u \; (\vec{x}) \end{array} \right\} \qquad (4.73)$$

Equation (4.73) defines at most $n \div 2$ functions and no fewer than 2. For each given design variables, values of $\vec{x}$ in the first orthant, one of the elements of the vector f_k will be the largest. The objective function is defined as the maximum of the response maxima, i.e.,

$$U \; (\vec{x}) = \max_k \; \{f_k \; (\vec{x})\} \qquad (4.74)$$

U is a well-defined positive function in the first orthant of $\vec{x}$ space. It can be shown that U is a continuous function everywhere except at corners of the first orthant which represent zero damping in the system, where U is infinite. The optimum stiffness and damping

parameters $\vec{x}_{opt}$ is defined as the vector which minimizes the objective function U:

$$U(\vec{x}_{opt}) = \min_{\vec{x}} U(\vec{x}) = \min_{\vec{x}} \max_{k} \{f_k(\vec{x})\} \qquad (4.75)$$

The response corresponding to x_{opt} is defined as the minimax response for the given function f and frequency interval Ω_ℓ to Ω_u.

To find the optimum parameters vector x_{opt} the minimax principle together with mathematical programming techniques are used. The design constraints, which are bounds on the design variables, and the optimization techniques used for the solution of this problem are discussed in detail in [83].

The response to lateral track irregularities and the lateral acceleration transfer function at the cab is computed for varying input frequencies. The input frequency is increased from zero to 3 cycles per second which corresponds to a forward speed of 150 mph for the known wave length of lateral track irregularities. The cab lateral acceleration before optimization is given in Figure 4.13. The maximum lateral acceleration at the cab within the frequency range of interest is very large.

The values of the existing suspension were used to start the search for the minimax response of the system.
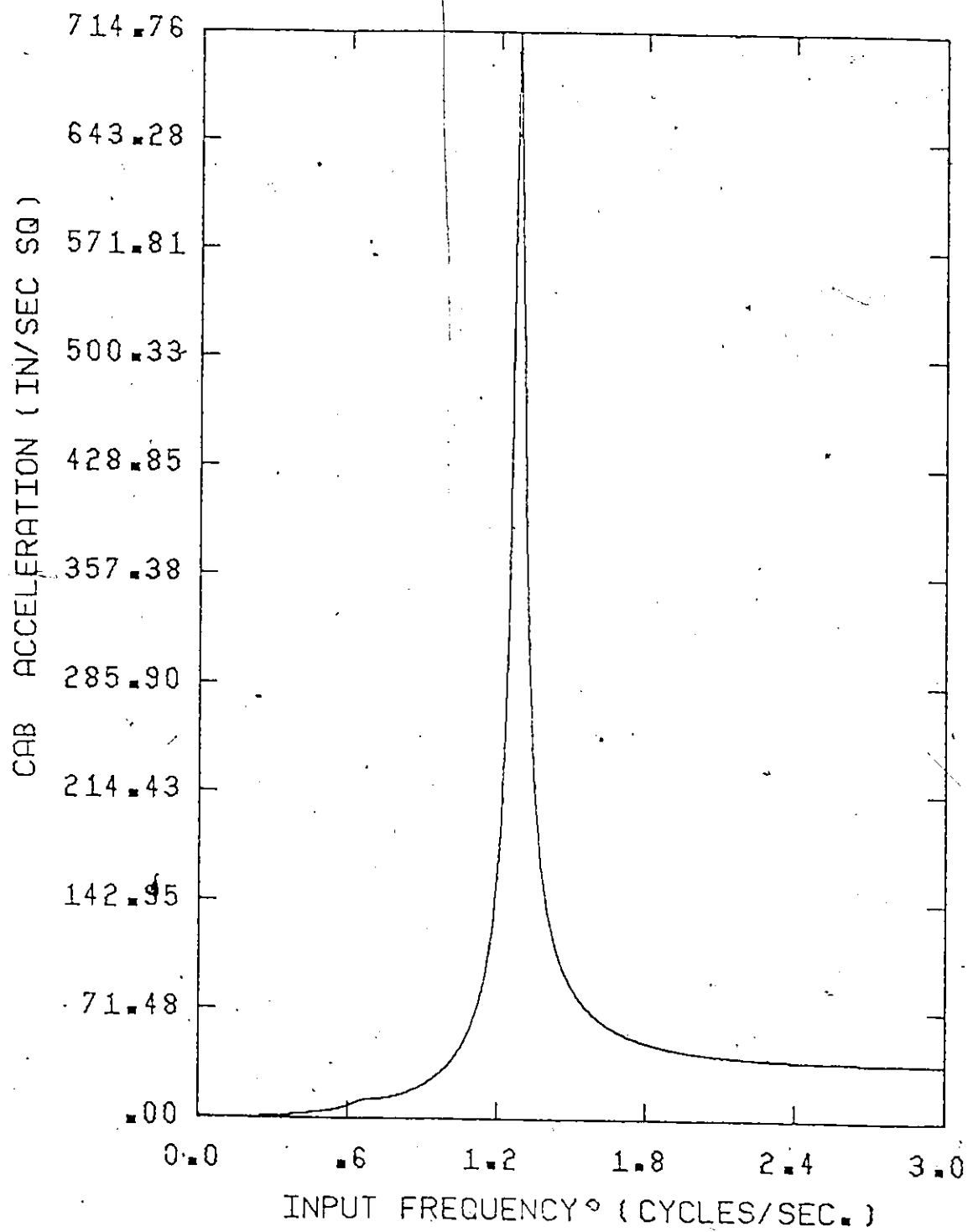
Figure 4.13   Lateral cab acceleration before
             optimization

The procedure was repeated for different starting points. In all cases the constraints were satisfied and the same optimum solution was found.

The acceleration after optimization is given in Figure 4.14. It is shown that the peak acceleration dropped from 714.8 in/sec^2 to 56.2 in/sec^2 after optimization, which is a great improvement. It was also found that the maximum lateral displacement at the cab was 11 in. and 1.3 in. before and after optimization as shown in Figures 4.15 and 4.16 respectively. These results correspond to an amplitude of lateral irregularities of 0.25 inches. A check on the dynamic stability of the locomotive was also made. Figure 4.17 shows the velocity root locus curves before and after optimization. The results indicate a small drop in the value of the critical speed, but the stability is maintained throughout the range of interest.

Figure 4.18 illustrates three dimensional computer plots for the objective function with and without the constraints versus the two most important parameters K_2 and K_3. It is interesting to note that an absolute optimization of such system, i.e., without any bounds on the design variables, tends to assume a value of zero for the stiffnesses involved. For these values the natural frequencies of the system zero and the lateral cab
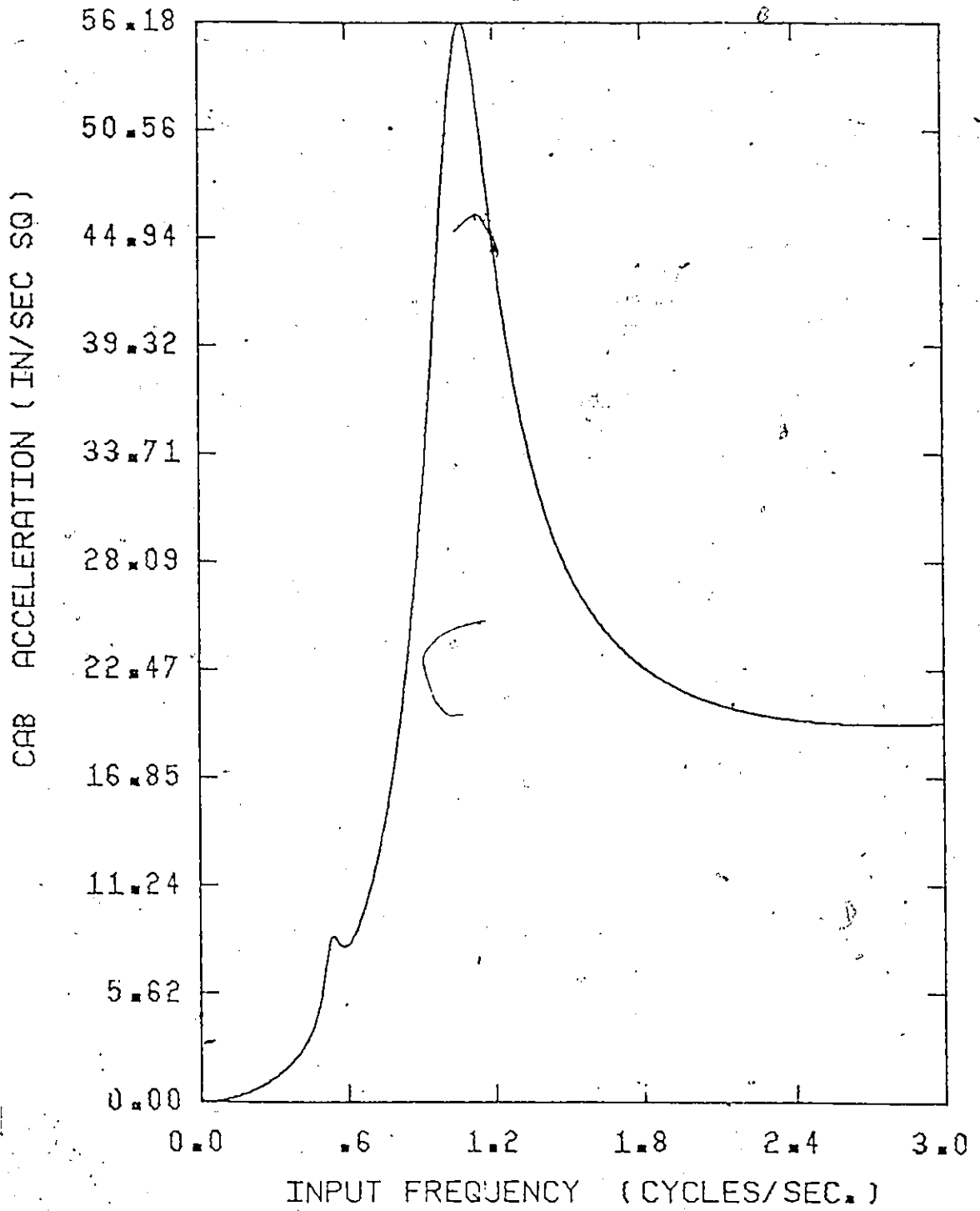
Figure 4.14   Cab lateral acceleration
after optimization
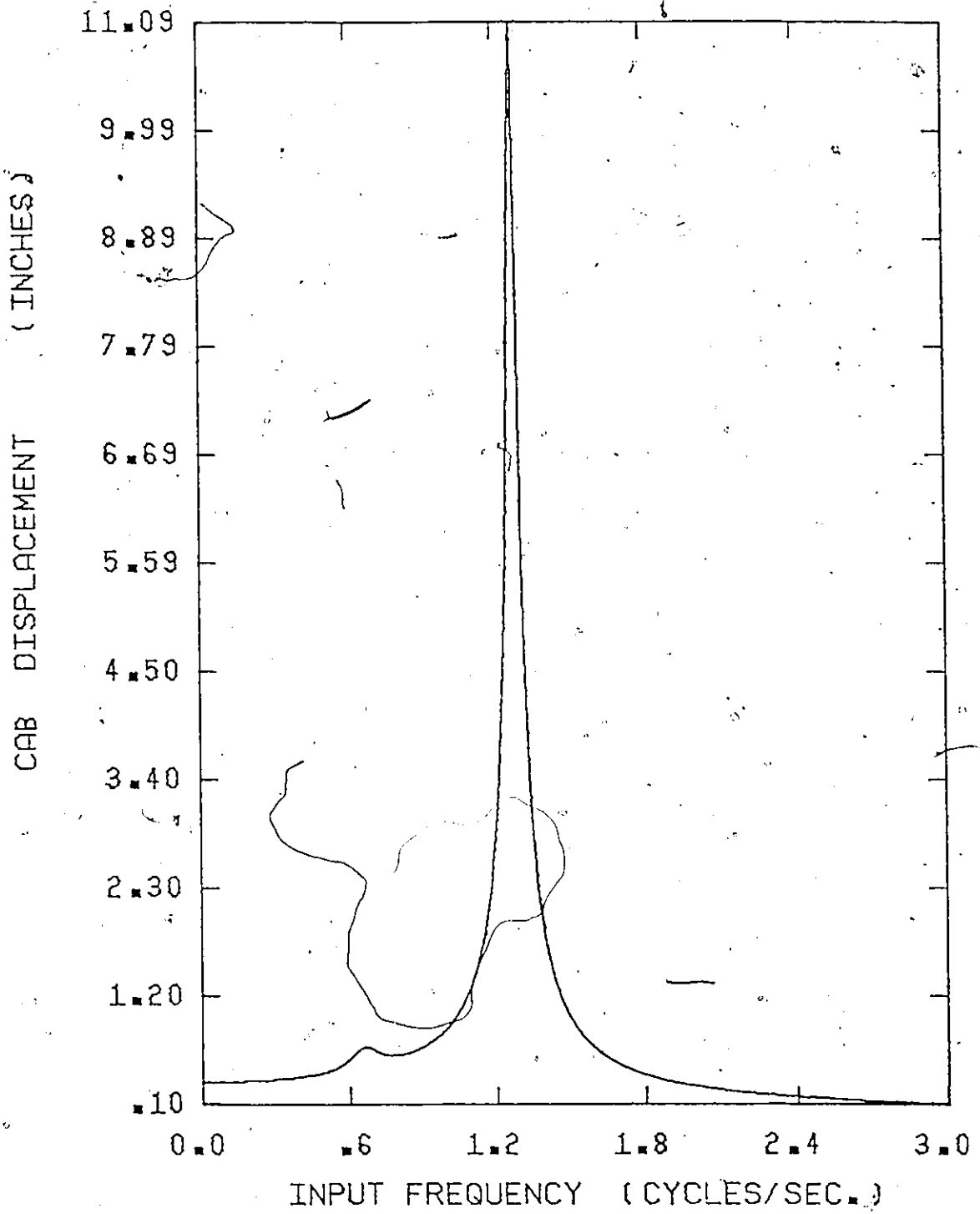
Figure 4.15   Lateral cab displacement
before optimization
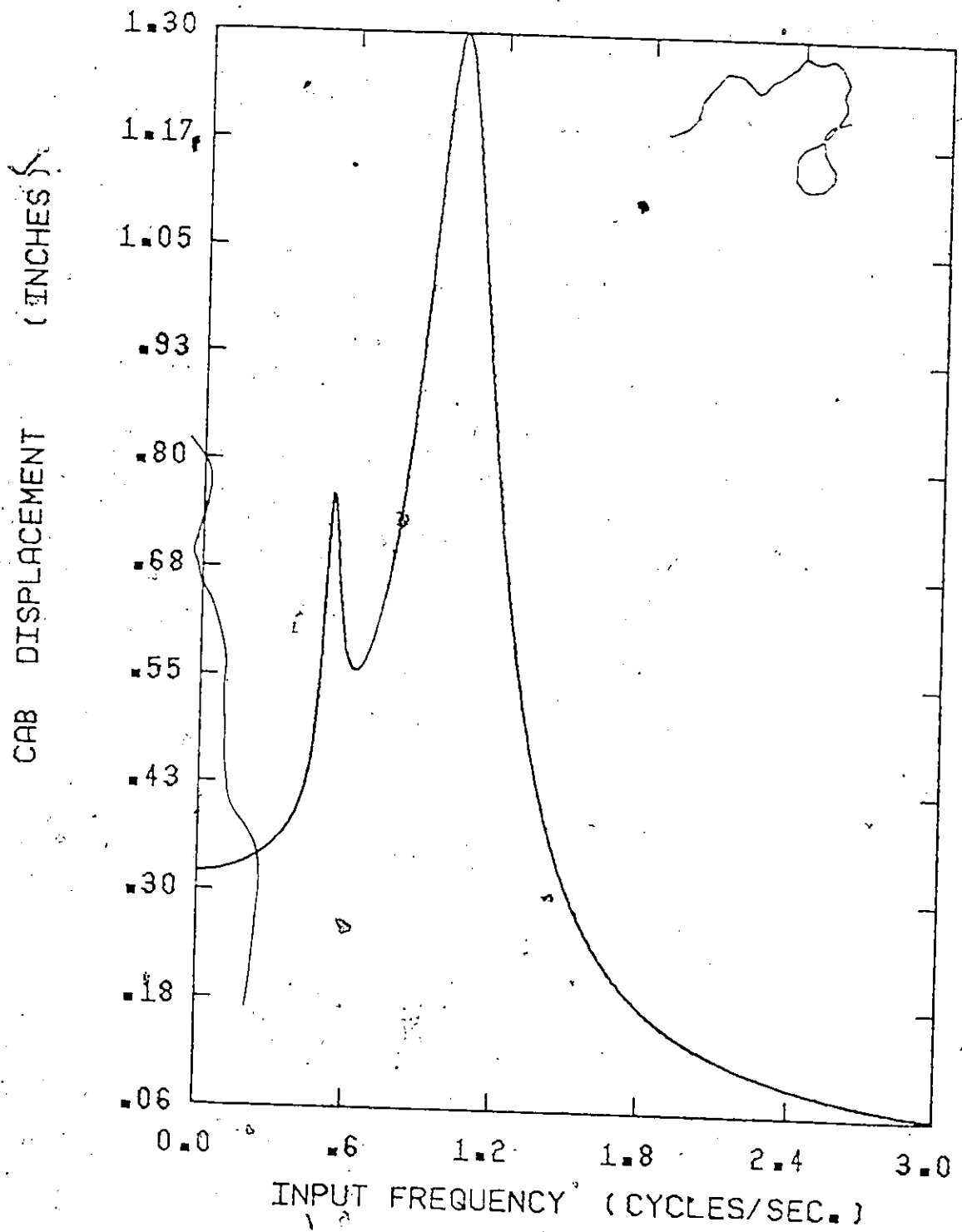
Figure 4.16   Lateral cab displacement
after optimization

° Before Optimization

△ After Optimization
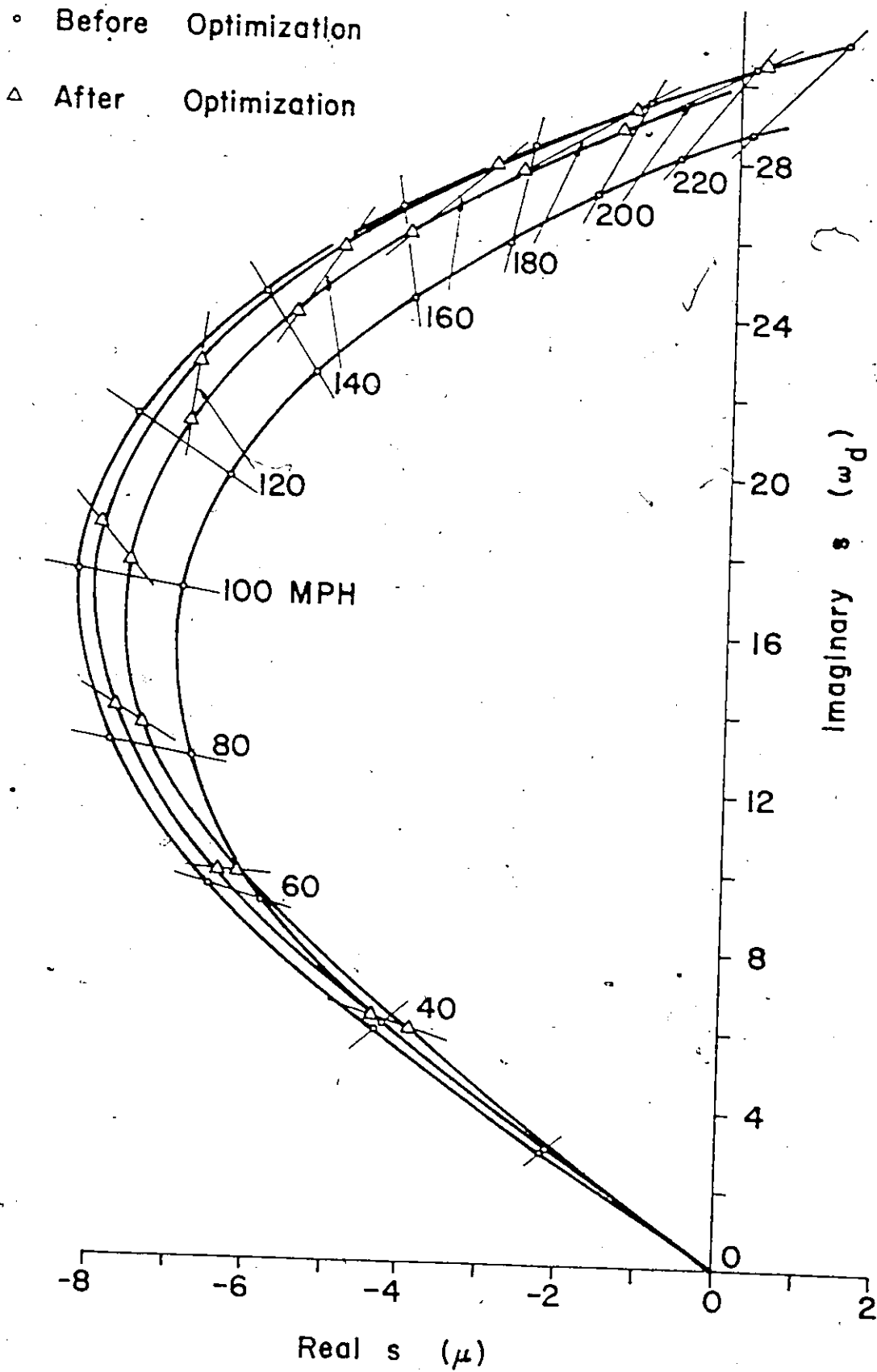
Figure 4.17 Velocity root locus plots before and after optimization
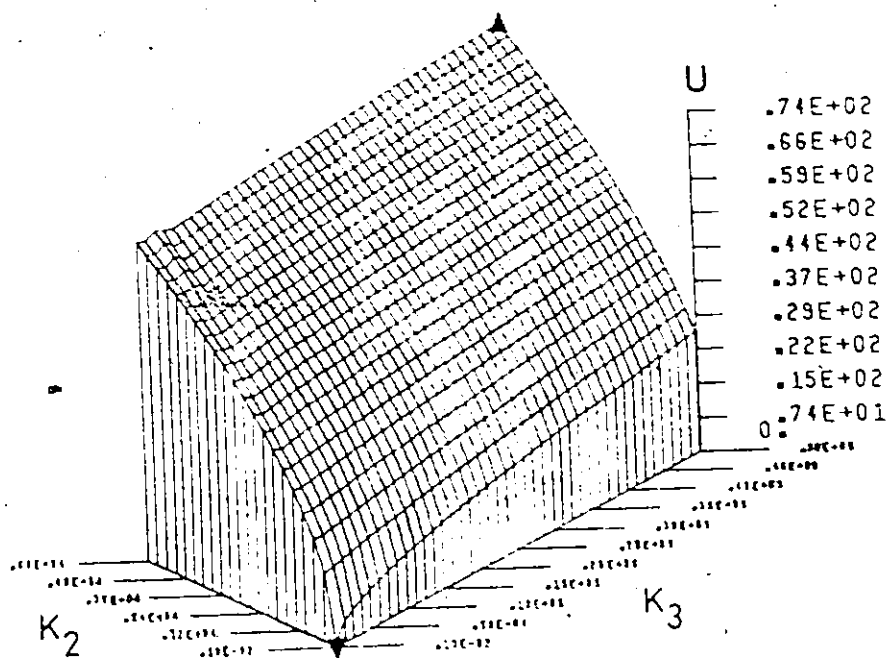
(a) unconstrained objective function
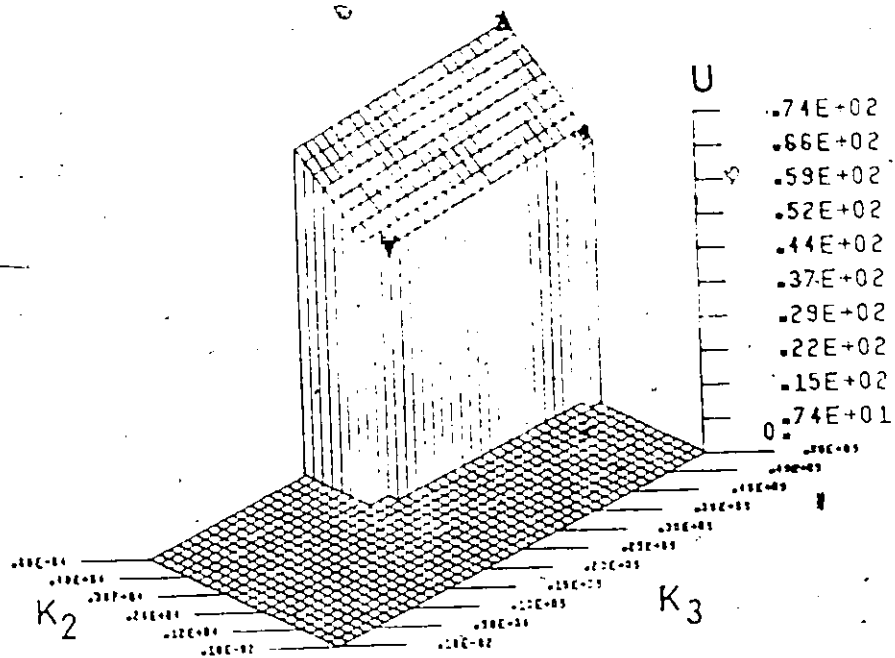
(b) constrained objective function

Figure 4.18 Three dimensional computer plots for the unconstrained and constrained objective functions versus K_2 and K_3

acceleration vanishes., This is however a trivial solution.
For the practical case where the design constraints are
introduced, the optimum solution is found at the
intersection of the constraining surfaces.

CHAPTER 5

SUMMARY AND CONCLUDING REMARKS

The principal factors limiting the speed of trains are related to the dynamic characteristics of both the railway vehicles and the tracks. One of these factors is the sustained lateral oscillations experienced by railway vehicles when the speed is increased. For safe operation, the speed at which this hunting instability occurs should be greater than the operating speed. When this is achieved, the vibration of the railway vehicle components is determined by track geometry. The response to track irregularities can result in passenger discomfort, in the case of passenger trains, or in damage to freight car contents. Another main cause for limiting the speed of trains is the railway track which conceptually did not change for more than a century. As the speeds and loads increased the length of the rails increased, with the elimination of all joints by welding them as a final goal, the tie cross section increased and the tie spacing decreased. At the present time an intensified research effort is devoted to the design and testing of new track structures including the possibility of eliminating the tie spacing altogether by using, instead of discrete ties, a continuous bed.

In this thesis, the dynamic response of the railway track modelled as a continuously supported beam on a Kelvin type foundation and subjected to an axial force and a moving load is studied. The transient and steady state solutions are found for the general case including all linear effects. For the transient response in the case of a general load, the resulting integral solutions are, in general, very difficult to evaluate in a closed form. Closed form solutions were obtained for some special cases of interest, but for other cases, a numerical approach had to be used; and a digital computer program was developed for the solution in the general case of loading.

The results show that the presence of damping results in an unsymmetric dynamic deflection of the rail. Due to phase shift the point of largest deflection occurs slightly behind the point of application of the moving load, and the deflection ahead of the point of maximum deflection is always larger than the deflection behind it. As the damping increases, the amplitude of the maximum deflection decreases and the phase shift increases. When no damping is present, the dynamic deflection profile is symmetric about the line of action of the load. The presence of an axial compression force in the rail is shown to result in a larger amplitude of response to the

moving load compared to the case of no axial force and the frequency of the deflection wave is higher. In contrast, when a tension force exists, the maximum deflection is smaller than the one obtained for no axial force and the frequency of the deflection wave is lower. In the presence of damping the amplitude of the deflection profile ahead is always larger and the frequency of the wave is larger than the amplitude and frequency, respectively, behind the point of maximum deflection. The results also show that an increase in the dynamic deflection due to an increase in the velocity of the moving load is quite small.

Dynamic coupling occurs between a railway vehicle and the track due to the reaction forces acting between the wheels and the track, and the elasticity of the track and the foundation. An analysis for the coupled dynamics of the railway vehicle and the track with particular reference to the lateral stability and the response to vertical track irregularities is presented. The model used for the vehicle is that of a six axle locomotive of the type commonly used in North America. Wheel tread and rail head profile parameters, gravity forces and creep forces are included in the equations of motion. The results obtained show that an increase in track elasticity causes a very small increase in the speed at which hunting occurs, but the vehicle is inherently more stable. The increase in track elasticity results in a larger amplitude of

response to track irregularities. In general, the effect is small for low forcing frequencies but becomes more appreciable as the forcing frequency is increased.

A method for the minimization of the vibrations transmitted due to track irregularities using the minimax principle and mathematical programming techniques is suggested. The method is demonstrated by considering the minimization of the acceleration response at the cab within the frequency range of interest.

The analysis of the continuously supported track subjected to moving loads was done to provide a fundamental understanding for the simultaneous effects of damping in the track and the foundation, an axial force in the rail and the velocity of the moving load on the dynamic deflection of the track. As the tendency is towards higher loads and speeds, the forces exerted by the wheels may cause excessive dynamic deflections of the track. It is therefore of interest to know how these forces will affect the dynamic deflection or if they will cause permanent deformation of the track. An instance of a situation where such knowledge is important is when it is necessary to choose between various designs for railway vehicles transmitting to the track forces having different characteristics. The results obtained are also relevant to present studies of the temperature effects on the

dynamic response and buckling of the continuously welded rails. The negligible effect of the velocity of the moving load on the dynamic deflection is a result of particular importance. This suggested that it is not necessary to consider the wave type expression to study the effect of track elasticity on the dynamics of railway vehicles. For this reason, the modelling of the track for the coupled vehicle/track dynamics involves the representation of the infinitely long structure by a dynamically equivalent lumped parameter model composed of discrete masses, springs and dampers.

In the analysis of the dynamics of the railway vehicle, the difference in the predicted critical speeds for a vehicle running on a flexible track and on rigid track was found to be very small. This suggests that for the study of the lateral stability of a railway vehicle the assumption of a rigid track is adequate. For the response to track irregularities, however, this assumption is inadequate for high forcing frequencies.

The analyses and digital computer simulations are viewed as analytical tools for studying the effect of changing the vehicle and/or track parameters on the dynamic response of both the vehicle and the track. It follows that, in addition to the results and conclusions reached in this research, one of the most important contributions is

that techniques which can be used in the assessment of the dynamic behaviour of new designs of railway vehicles and tracks, have been developed.

BIBLIOGRAPHY

1. Jones, S. "The Impact of Engineering Science on the Economics of Railways", Physics in Technology, Vol. 4, No. 1, (1973).

2. Klingel. Organ Fortschrift Eisenbahn Wes., Vol. 38, (1883), 113-123.

3. Wickens, A.H. "Vehicle Dynamics and Wheel-Rail Interface Problems", Proceedings of the Carnegie-Mellon Conference on High-Speed Ground Transportation, Pittsburgh, Pa., (1969), 157-171.

4. Carter, F.W. "On the Stability of Running Locomotives", Proceedings of the Royal Society of London, Vol. 121, Series A, (1928).

5. -------- "The Running Locomotives with Reference to their Tendency to Derail", The Institution of Civil Engineers, Selected Engineering Paper No. 91, (1930).

6. Langer, B.F. and Shamberger, J.P. "Lateral Oscillations of Rail Vehicles", Transaction A.S.M.E., Vol. 57, (1935).

7. Poritsky, H. "Stresses and Deflections of Cylindrical Bodies in Contact with Application to Contact of Gears and of Locomotive Wheels", Journal of Applied Mech., Trans. A.S.M.E., (1950).

8. Johnson, K.L. "The Effect of a Tangential Contact Force Upon the Rolling Motion of an Elastic Sphere", Journal of Applied Mechanics, Vol. 80, (1958).

9. -------- "Effect of Spin upon the Rolling Motion of an Elastic Sphere on a Plane", Journal of Applied Mechanics, Vol. 80, (1958), 332-338.

10. Vermeulen, P.J. and Johnson, K.Z. "Contact of Nonspherical Elastic Bodies Transmitting Tangential Forces", Trans. A.S.M.E., Journal of Applied Mechanics, Vol. 86, (1964).

11. Kalker, J.J. "On the Rolling Contact of Two Elastic Bodies in the Presence of Dry Friction", Ph.D. Thesis, Delft Tech. University, Delft, (1967).

12. -------- "Rolling with Slip and Spin in the Presence of Dry Friction", Wear, Vol. 9, (1966), 20-38.

13. Haines, D.J. and Ollerton, E. "Contact Stress Distribution on Elliptical Contact Surfaces Subjected to Radial and Tangential Forces", Proc. Inst. of Mech. Engrs. Vol. 77, No. 4, (1963).

14. Nayak, P.R. et.al. "Friction and Creep in Rolling Contact", NTIS Report, PB 196 707, (November 1970).

15. Nayak, P.R. and Tanner, R.B. "Frictional and Vibratory Behaviour of Rolling and Sliding Contacts", NTIS Report, PB-220 625, (July 1972).

16. Wickens, A.H. "The Dynamics of Railway Vehicles on Straight Track: Fundamental Considerations of Lateral Stability", Interaction between Vehicle and Track, The Institution of Mechanical Engineers Proceedings, Vol. 180, Part 3F, (1966), 29-44.

17. Matsudaira, T. "Hunting Problem of High-Speed Railway Vehicles with Special Reference to Bogie Design for the New Tokaido Line", Interaction between Vehicle and Track, The Institution of Mechanical Engineers Proceedings, Vol. 180, Part 3F, (1966), 58-66.

18. Gilchrist, A.O., Hobbs, A.E., King, B.L. and Washby, V. "The Riding of Two Particular Designs of Four-Wheeled Railway Vehicle", Interaction between Vehicle and Track, The Institution of Mechanical Engineers Proceedings, Vol. 180, Part 3F, (1966), 99-113.

19. Blader, F.B. and Kurtz, E.F. Jr. "Dynamic Stability of Cars in Long Freight Trains", A.S.M.E. Paper No. 73-WA/RT-2, (November 1973).

20. De Pater, A.D. "The Approximate Determination of the Hunting Movement of a Railway Vehicle by the Aid of the Method of Krylov and Bogoljulov", Appl. Sci. Res. A., Vol. 10, (1961), 205.

21. Van Bommel, P. "Application de la Théorie de Vibrations Non Linéaires sur le Problème du Mouvement de Lacet d'un Vehicule de Chemin de Fer", Doctoral Thesis, Delft Tech. University, (1964).

22. Law, E.H. and Brand, R.S. "Analysis of the Nonlinear Dynamics of a Railway Vehicle Wheelset", A.S.M.E. Meeting Preprint, 1427, Joint ASCE and A.S.M.E. Transportation Engineering Meeting, (July 26-30, 1971).

23. Cooperrider, N.K. "The Hunting Behaviour of Conventional Railway Trucks", Trans. A.S.M.E., Series B, Vol. 94, No. 2, (May 1972), 752-762.

24. Cain, B.S. "Safe Operation of High-Speed Locomotives", Trans. A.S.M.E., Vol. 57, (1935).

25. -------- Vibration of Road and Rail Vehicles. New York: Pitman, 1940.

26. Wickens, A.H. "The Dynamic Stability of Railway Vehicle Wheelsets and Bogies having Profiled Wheels", Int. J. Solids Structures, Vol. 1, (1965), 319-341.

27. The Institution of Mechanical Engineers. Interaction Between Vehicle and Track. The Institution of Mechanical Engineers, Vol. 180, Part 3F, (1965-66).

28. Müller, C.Th. "Dynamics of Railway Vehicles on Curved Track", Interaction between Vehicle and Track, The Institution of Mechanical Engineers Proceedings, Vol. 180, Part 3F, 45-57.

29. Blader, F.B. "Free Lateral Oscillations in Long Freight Trains", Ph.D. Thesis, Queen's Univ., (1972).

30. Wickens, A.H. "Recent Developments in the Lateral Dynamics of High Speed Railway Vehicles", Monthly Bulletin of the International Railway Congress Association, Vol. 44, No. 12, (1967), 781-803.

31. -------- "General Aspects of the Lateral Dynamics of Railway Vehicles", Trans. A.S.M.E., Journal of Engineering for Industry, Vol. 91 B, (August 1969), 869.

32. Matsudaira, T., Mutsui, N., Arai, S., and Yokose, K. "Problems on Hunting of Railway Vehicles on Test Stand", Trans. A.S.M.E., Journal of Engineering for Industry, Vol. 91 B, (August 1969), 879.

33. Clark, J.W. and Law, E.H. "Investigation of the Truck Hunting Instability Problem of High-Speed Trains", A.S.M.E. Paper, No. 67, Trans. 17, (August 1967).

34. Dokainish, M.A. and Siddall, J.N. "Dynamic Stability Analysis of the Suspension for a Light Weight High-Speed Railway Passenger Car", Report on CARED Project 128, McMaster University, (1969).

35. Hobbs, A.E.W. "The Response of a Restrained Wheelset to Variations in the Alignment of an Ideally Straight Track", British Railways Research Department Report, No. E542, (October 1964).

36. Cooperrider, N.K. "The Lateral Stability of Conventional Railway Passenger Trucks", The Proceedings of the First International Conference on Vehicle Mechanics, Wayne University, Michigan, (1968).

37. British Railways Research Department. "The Dynamics of Four Wheeled Railway Vehicles as Determined by Suspension Design and Track Geometry", British Railways Research Department, Report No. E600, (May 1965).

38. Stassen, H.G. "Random Lateral Motions of Railway Vehicles", Doctoral Thesis, Delft Technological University, Delft, (1967).

39. Sewall, J.L., Parrish, R.V. and Durling, B.J. "Dynamic Response of Railroad Car Models to Vertical and Lateral Rail Inputs", NASA Technical Note, NASA TN D-6375, (November 1971).

40. LaBuschagne, T.J. and Scheffel, H. "Some Aspects of the Interaction between Railway Vehicle and Track", Die Sivielle Ingenieur in Suid Afrika, Vol. 11, No. 10, (October 1969).

41. ElMaraghy, W.H. "On the Effect of Track Irregularities on the Dynamic Response of Railway Vehicles", M.Eng. Thesis, McMaster University, (1972).

42. Potter, R.A. and Willmert, K.D. "Optimum Design of a
        Vehicle Suspension System", A.S.M.E. Paper,
        No. 73-DET-46.

43. Nelson, J.A. and Hapemann, M.J. "A New Transit
    • Propulsion Unit Suspension - Proved on Northeast
        Corridor High-Speed Test Cars", Trans. A.S.M.E.,
        Series B, J. Eng. Ind., Vol. 91, No. 3, (August
        1966), 897-907.

44. Mixson, J.S. and Steiner, R. "Optimization of a
        Simple Dynamic Model of a Railroad Car Under
        Random and Sinusoidal Inputs", Paper presented
        at A.S.M.E. Annual Meeting, Symposium on Random
        Processes in Dynamical Problems, Los Angeles,
        California, (November 1969).

45. Sewall, J.L., Parrish, R.V. and Durling, B.J.
        "Dynamic Response of Railroad Car Models to
        Vertical and Lateral Rail Inputs", NASA Report,
        TN D-6375, (November 1971).

46. Koci, L.F. "Wheel and Rail Loadings from Diesel
        Locomotives", AAR Conference on Track/Train
        Dynamics Interaction, Chicago, (December 1971).

47. Matsudaira, T. "How High Can Train Speed be Increased?
        A Review of Present and Future", Japanese
        Railway Eng., (June 1966).

48. Timoshenko, S.S. "Method of Analysis of Statical and
        Dynamical Stresses in Rail", Proc. 2nd
        International Congress for Applied Mechanics,
        Zurich, (1927), 1-12.

49. Kerr, A.D. "The Continuously Supported Rail
        Subjected to an Axial Force and/a Moving Load",
        Int. J. Mech. Sci., Vol. 14, (1972), 71-78.

50. Richardson, H.H. and Wormley, D.N. "The Coupled
        Dynamics of Transportation Vehicles and Beam-type
        Elevated Guideways", Surveys of Research in
        Transportation Technology, A.S.M.E. AMD, Vol.
        5, (1973).

51. Hetényi, M. Beams on Elastic Foundation. Ann Arbor:
        University of Michigan Press, 1967.

52. Kerr, A.D. "Elastic and Viscoelastic Foundation
        Models", Journal of Applied Mechanics, (September
        1964), 491-498.

53. Birmann, F. "Track Parameters, Static and Dynamic", Interaction between Vehicle and Track, The Institution of Mechanical Engineers Proceedings, Vol. 180, Part 3F (1965-66), 73-85.

54. Timoshenko, S.S. and Langer, B.F. "Stresses in Railroad Track", A.S.M.E. Anthology of Rail Vehicle Dynamics, Vol. III, (1972), 217-234.

55. Criner, H.E. and McCann, G.D. "Rails on Elastic Foundation Under the Influence of High-Speed Travelling Loads", Journal of Applied Mechanics, (1953), 13-22.

56. Kenney, J.T. "Steady-State Vibrations of Beams on Elastic Foundations for Moving Load ", Journal of Applied Mechanics, (1954), 359-364.

57. Mathews, P.M. "Vibrations of Beam on Elastic Foundation", Zeitschrift für Angewandte Matematik und Mechanik, (1958), 105-115.

58. -------- "Vibrations of Beam on Elastic Foundation II", Zeitschrift für Angewandte Matematik und Mechanik, (1959), 13-19.

59. Newland, D.B. "Instability of an Elastically Supported Beam under a Travelling Inertia Load", Mechanical Engineering Science, Vol. 12, No. 5, (1970), 373-374.

60. Nelson, H.D. and Conover, R. "Dynamic Stability of a Beam Carrying Moving Masses", Journal of Applied Mechanics, Trans. A.S.M.E., Series E., Vol. 38, (December 1971), 1003-1006.

61. Benedetti, G.A. "Transverse Vibration and Stability of a Beam Subjected to Moving Mass Loads", Ph.D. Thesis, Arizona State University, (1973).

62. Wilson, J.F. and Biggers, S.B. "Dynamic Interactions Between Long, High-Speed Trains of Air Cushion Vehicles and Their Guideways", Journal of Dynamic Systems, Measurements, and Control, Trans. A.S.M.E., (March 1971), 16-24.

63. Biggers, S.B. and Wilson, J.F. "Dynamic Interactions of High-Speed Tracked Air Cushion Vehicles with their Guideways", Journal of Dynamic Systems, Measurements and Control, Trans. A.S.M.E., (March 1973), 76-85.

64. Kuroda, S. "Dynamic Variation of Wheel Load Attributed to Vertical Deformation of Rail End", Quarterly Report, Railway Technical Research Institute (Tokyo), Vol. 14, No. 3 (September 1973), 143-144.

65. Meacham, H.C. and Ahlbeck, D.R. "A Computer Study of Dynamic Loads Caused by Vehicle-Track Interaction", A.S.M.E. Paper, No. 69-RR-1,(1969).

66. Meacham, H.C. "Analysis of Track Structures", Proc. of the AAR Conference on Track/Train Dynamics Interaction, (December 1971), 300-328.

67. Nowacki, W. Dynamics of Elastic Systems. John Wiley, 1963.

68. Sneddon, I.N. The Use of Integral Transforms. McGraw-Hill Book Company, 1972.

69. Stadler, W. and Shreeves, R.W. "The Transient and Steady-State Response of the Infinite Bernoulli-Euler Beam with Damping and an Elastic Foundation", Quart. J. Mech. and Appl. Math. XXIII, (1970).

70. Erdélyi, A. Tables of Integral Transforms. Vol. 1, McGraw Hill Book Company, 1954.

71. Gradshteyn, I.S. and Ryzhik, I.M. Tables of Integrals, Series and Products, New York: Academic Press, 1965.

72. Watson, G.N. Theory of Bessel Functions. Second Edition, Cambridge University Press, 1952.

73. Gentleman, W.M. "Implementing Clenshaw-Curtis Quadrature", Communications of the ACM, Vol. 15, No. 5, (May 1972).

74. Lyness, J.N. "SQUANK (Simpson Quadrature used Adaptively - Noise Killed) [D1]", Applied Mathematics Division, Argonne National Laboratory, Argonne IL60439.

75. Gaiser, J.A. and Dobson, R.N. "Weight Transfer Reduction in Diesel Electric Locomotives", 1971 Rail Transportation Proceedings, A.S.M.E. Rail Transportation Division.

76. Abramovitz, M. and Stegun, I.A. Handbook of Mathematical Functions. Dover Publications, Inc., 1968.

77. Cooperrider, N.K. "High Speed Dynamics of Conventional Railway Trucks", Ph.D. Thesis, Stanford University, (1968).

78. Joly, R. "Study of the Transverse Stability of a Railway Vehicle Running at High Speed", Rail International, Vol. 3, No. 2, (February 1972), 83.

79. Marcotte, P.P. "Lateral Dynamic Stability of Railway Bogie Vehicles", M.Eng. Thesis, University of Sheffield, (1972).

80. Timoshenko, S. and Goodier, J.N. Theory of Elasticity. McGraw-Hill Book Company, 1970, 414-420.

81. Johnson, K.L. "Adhesion", Proc. Inst. Mech. Engrs., Vol. 178, Pt. 3E, (1963-64), 208-209.

82. Timoshenko, S. and Young, D.H. Vibration Problems in Engineering. D. Van Nostrand Company, 1964.

83. ElMaraghy, W.H., Dokainish, M.A. and Siddall, J.N. "Minimax Optimization of Railway Vehicle Suspensions", A.S.M.E. Paper, No. 74-WA/RT-3, Presented at the 1974 A.S.M.E. Winter Annual Meeting.

APPENDIX (A)

DERIVATION OF SOLUTION FOR THE RESPONSE OF THE

TRACK TO GENERAL AND CONSTANT VELOCITY MOVING LOAD

A.1 Solution for a General Load

Consider the solution of the partial differential equation

$$EI \frac{\partial^4 y}{\partial x^4} + N \frac{\partial^2 y}{\partial x^2} + m \frac{\partial^2 y}{\partial t^2} + c \frac{\partial y}{\partial t} + ky = q(x,t) \qquad \left.\right\} \quad (A.1.1)$$

$$-\infty < x < \infty \qquad t > 0$$

subject to:

(i)   the initial conditions

$$y(x,0) = f(x) \qquad \left.\right\}$$

$$\frac{\partial y(x,0)}{\partial t} = g(x) \qquad (A.1.2)$$

and

(ii)   the boundary conditions

$$y(x,t) \Big|_{|x| \to \infty} \longrightarrow 0 \qquad \left.\right\}$$

$$\frac{\partial^n y(x,t)}{\partial x^n} \Big|_{|x| \to \infty} \longrightarrow 0 \quad (n=1,2,3) \qquad (A.1.3)$$

176

Fourier and Laplace transforms are used to solve equation (A.1.1) subject to the initial and boundary conditions given by (A.1.2) and (A.1.3), respectively.

Note that the second term of equation (A.1.1) could be positive or negative. It is positive if the load is compressive and negative if the load is tensile. For definiteness, assume that in this case the load is tensile and of its magnitude equals to N.

Also let

$$\mathscr{F}[f(x); \alpha] = F(\alpha) \equiv F$$

$$\mathscr{F}[g(x); \alpha] = G(\alpha) \equiv G$$

$$\mathscr{F}[y(x,t); x \to \alpha] = Y(\alpha,t) \equiv Y$$

$$\mathscr{F}[q(x,t); x \to \alpha] = Q(\alpha,t) \equiv Q$$

$$\mathscr{F}[\frac{\partial^2 y(x,t)}{\partial x^2}; x \to \alpha] = -\alpha^2 Y(\alpha,t) \equiv -\alpha^2 Y$$

$$\mathscr{F}[\frac{\partial^4 y(x,t)}{\partial x^4}; x \to \alpha] = \alpha^4 Y(\alpha,t) \equiv \alpha^4 Y$$

Knowing that E, I, N, m, c and k are constants, the Fourier transform for both sides of equation (A.1.1) gives:

$$(EI\ \alpha^4 + N\ \alpha^2 + k)Y(\alpha,t) + c\ \frac{\partial Y(\alpha,t)}{\partial t}$$

$$+ m\ \frac{\partial^2 Y(\alpha,t)}{\partial t^2} = Q(\alpha,t) \qquad (A.1.4)$$

Let

$$\mathscr{L}[Y(\alpha,t); t \to p] = \bar{Y}(\alpha,p) \equiv \bar{Y}$$

$$\mathscr{L}[Q(\alpha,t); t \to p] = \bar{Q}(\alpha,p) \equiv \bar{Q}$$

$$\mathcal{L}[\frac{\partial Y(\alpha,t)}{\partial t}; \; t \to p] = p\, \bar{Y}(\alpha,p) - Y(\alpha,0)$$

$$= p\, \bar{Y} - F$$

$$\mathcal{L}[\frac{\partial^2 Y(\alpha,t)}{\partial t^2}; \; t \to p] = p^2\, \bar{Y}(\alpha,p) - p\, Y(\alpha,0) - Y'(\alpha,0)$$

$$= p^2\, \bar{Y} - p\, F - G$$

The transformed form of equation (A.1.1) becomes

$$(EI\,\alpha^4 + N\,\alpha^2 + k)\bar{Y} + c\,(p\bar{Y}-F) + m\,(p^2\bar{Y}-pF-G) = \bar{Q} \quad \text{(A.1.5)}$$

The capitalization of the respective letters implies the Fourier transformation and the overbar indicates the Laplace transformation.

The transformed equation (A.1.5) can be written as:

$$\bar{Y}(\alpha,p) = \frac{(c + mp)\,F + m\,G + \bar{Q}}{EI\,\alpha^4 + N\,\alpha^2 + k + cp + m\,p^2} \quad \text{(A.1.6)}$$

If we let

$$\zeta = \frac{c}{2m}, \qquad a^2 = \frac{EI}{m}, \qquad b = \frac{N}{2EI}$$

$$\lambda^2 = \omega_0^2 - \zeta^2 - a^2 b^2 \quad \text{and} \quad \omega_0^2 = \frac{k}{m}$$

Equation (A.1.6) can be written in a more suitable form as

$$\bar{Y}(\alpha,p) = \frac{1}{(p+\zeta)^2 + a^2(\alpha^2+b^2) + \lambda^2}[(\zeta F+G) + (p+\zeta)F + \frac{1}{m}\bar{Q}]$$

$$\text{(A.1.7)}$$

The inversion and convolution theorems for Laplace transforms [68] are used to write

$$Y(\alpha,t) = (G+\zeta F)e^{-\zeta t} H(\alpha,t) + F e^{-\zeta t} \frac{\partial H}{\partial t}$$

$$+ \frac{1}{m} \int_0^t Q(\alpha,\tau) e^{-\zeta(t-\tau)} H(\alpha;t-\tau) d\tau$$

(A.1.8)

where

$$H(\alpha,t) = \frac{\sin t. \sqrt{a^2(\alpha^2+b)^2+\lambda^2}}{\sqrt{a^2(\alpha^2+b)^2+\lambda^2}}$$

The application of the convolution theorem for Fourier transforms [68] in conjunction with the inverse transform of H [69], enables writing the final solution for the displacement field y(x,t) in the following integral form:

$$y(x,t) = e^{-\zeta t} \int_{-\infty}^{\infty} [g(\xi) + \zeta f(\xi)] h(x-\xi,t) d\xi$$

$$+ e^{-\zeta t} \int_{-\infty}^{\infty} f(\xi) h_t(x-\xi,t) d\xi$$

$$+ \frac{1}{m} \int_0^t e^{-\zeta(t-\tau)} \int_{-\infty}^{\infty} q(\xi,\tau).h(x-\xi,t-\tau) d\xi d\tau$$

(A.1.9)

where

$$h(x,t) = \frac{1}{\sqrt{4\pi a}} \int_0^t J_0(\lambda\sqrt{t^2-u^2}) \frac{1}{\sqrt{u}} \cos(\frac{x^2}{4au}-abu-\frac{\pi}{4}) du$$

(A.1.10)

and

$$h_t = \frac{\partial h(x,t)}{\partial t}$$

(A.1.11)

For zero initial conditions the solution becomes

$$y(x,t) = \frac{1}{m} \int_0^t e^{-\zeta(t-\tau)} \int_{-\infty}^{\infty} q(\xi,\tau) . h(x-\xi, t-\tau) \, d\xi d\tau \quad (A.1.12)$$

Some special cases for the forcing functions of physical interest are:

(i) $q(x,t) = P \, \delta(x)$

(ii) $q(x,t) = P \, \delta(x) \, \delta(t)$

(iii) $q(x,t) = P \, \delta(t), \quad x_1 \leqslant x \leqslant x_2$

(iv) $q(x,t) = P \, \delta(x-vt)$

(v) $q(x,t) = P \cos \Omega t \, \delta(x-vt)$

(vi) $q(x,t) = P \, f(t) \, \delta(x-vt \pm \rho t^2)$

Assuming the beam to be initially at rest in the equilibrium position, the solutions for these different cases will be obtained using the integral representation for the displacement field given by (A.1.12)

(i) $q(x,t) = P \, \delta(x)$

$$y(x,t) = \frac{P}{m\sqrt{4\pi a}} \int_0^t e^{-\zeta(t-\tau)} \int_0^{t-\tau} J_0(\lambda\sqrt{(t-\tau)^2-u^2}) \frac{1}{\sqrt{u}}$$

$$\cos(\frac{x^2}{4au} - abu - \frac{\pi}{4}) \, du \, d\tau$$

$$(A.1.13)$$

Let $t - \tau = r$, hence

$$y(x,t) = \frac{P}{m\sqrt{4\pi a}} \int_{0}^{t} e^{-\zeta r} \int_{0}^{r} J_0(\lambda\sqrt{r^2-u^2}) \frac{1}{\sqrt{u}}$$

$$\cos(\frac{x^2}{4au}-abu-\frac{\pi}{4}) \; du \; dr \qquad (A.1.14)$$

(ii) $q(x,t) = \delta(x) \; \delta(t)$

$$y(x,t) = \frac{P}{m\sqrt{4\pi a}} \; e^{-\zeta t} \int_{0}^{t} J_0(\lambda\sqrt{t^2-u^2}) \frac{1}{\sqrt{u}}$$

$$\cos(\frac{x^2}{4au}- abu -\frac{\pi}{4}) \; du \qquad (A.1.15)$$

(iii) $q(x,t) = P \; \delta(t), \; x_1 \leqslant x \leqslant x_2$

$$y(x,t) = \frac{P}{m\sqrt{4\pi a}} \; e^{-\zeta t} \int_{0}^{t} \int_{x_1}^{x_2} J_0(\lambda\sqrt{t^2-u^2}) \frac{1}{\sqrt{u}}$$

$$\cos(\frac{x^2}{4au} -abu-\frac{\pi}{4}) \; dx \; du \qquad (A.1.16)$$

(iv) $q(x,t) = P \; \delta(x-vt)$

let $\eta = x-vt$ and $r = t - \tau$

$$y(x,t) = \frac{P}{m\sqrt{4\pi a}} \int_{0}^{t} e^{-\zeta r} \int_{0}^{r} J_0 \; \lambda\sqrt{r^2-u^2} \; \frac{1}{\sqrt{u}}$$

$$\cos(\frac{(\eta+vr)^2}{u} - abu - \frac{\pi}{4}) \; du \; dr$$

$$(A.1.17)$$

(v) $q(x,t) = P \; \cos \Omega \; t \; \delta(x-vt)$

let $\eta = x-vt$ and $r = t - \tau$

$$y(x,t) = \frac{P}{m\sqrt{4\pi a}} \int_0^t e^{-\zeta r} \cos \Omega(t-r) \int_0^r J_0(\lambda\sqrt{r^2-u^2})\frac{1}{\sqrt{u}}$$

$$\cos(\frac{(\eta+vr)^2}{4au} - abu - \frac{\pi}{4}) \, du \, dr$$

(A.1.18)

(vi) $q(x,t) = P\, f(t)\, \delta(x-vt \pm \rho t^2)$

let $\eta = x-vt \pm \rho t^2$ and $r = t - \tau$

$$y(x,t) = \frac{P}{m\sqrt{4\pi a}} \int_0^t e^{-\zeta r} f(t-r) \int_0^r J_0(\lambda\sqrt{r^2-u^2}) \frac{1}{\sqrt{u}} \cdot$$

$$\cos(\frac{(\eta+vr\pm\rho r^2)^2}{4au} - abu - \frac{\pi}{4}) \, du \, dr$$

(A.1.19)

A.2 Solution for a Constant-Velocity Moving Load

Consider the solution of the ordinary differential equation:

$$\eta^{iv} + 4\,\alpha_1^2\,\eta'' - 8\phi\beta\,\eta' + 4\,\omega^4\,\eta = 0 \qquad (A.2.1)$$

where

$$4\alpha_1^2 = \frac{N+mv^2}{EI} \; ; \quad \beta = \frac{c}{c_{cr}} = \frac{c}{\sqrt{km}}$$

$$\theta = \frac{v}{v_{cr}} = \frac{v}{\sqrt{\sqrt{\dfrac{4KEI}{m^2}} - \dfrac{N}{m}}}$$

$$\phi = \frac{\sqrt{km}}{EI} \cdot \frac{\sqrt{\sqrt{\dfrac{4KEI}{m^2}} - \dfrac{N}{m}}}{8}$$

$$4\omega^4 = \frac{k}{EI} \; ; \qquad \omega = \sqrt[4]{\frac{k}{4EI}}$$

Assume a solution of the form

$$\eta = e^{r\xi} \qquad (A.2.2)$$

Substituting in equation (A.2.1) we get:

$$r^4 + 4 \alpha_1^2 \, r^2 - 8\theta\phi\beta \, r + 4\omega^2 = 0 \qquad (A.2.3)$$

By Descartes' rule there is not more than one pair of real roots to this equation. Since interest is in the underdamped portion of the solution let us assume the following two complex conjuguate pairs:

$$\left.\begin{array}{l} r_1 = d+ib_1 \\[6pt] r_2 = d-ib_1 \\[6pt] r_3 = -d+ib_2 \\[6pt] r_4 = -d-ib_2 \end{array}\right\} \qquad (A.2.4)$$

Since the assumed roots must satisfy the following identity:

$$(r-r_1) \, (r-r_2) \, (r-r_3) \, (r-r_4) = 0 \qquad (A.2.5)$$

Combining equations (A.2.4) and (A.2.5) we get:

$$r^4 + (-2d^2+b_1^2+b_2^2) \, r^2 - 2d \, (b_2^2-b_1^2) \, r + (d^2+b_1^2) \, (d^2+b_2^2) = 0$$

$$(A.2.6)$$

Equating coefficients of (A.2.3) and (A.2.6) we get:

$$-2d^2 + b_1^2 + b_2^2 = 4\alpha_1^2$$

$$-2d \, (b_2^2-b_1^2) = -8\theta\phi\beta \qquad (A.2.7)$$

$$(d^2+b_1^2) \, (d^2+b_2^2) = 4\omega^4$$

From the first two equations in (A.2.7) obtain b_1^2 and b_2^2

$$b_1^2 = 2\alpha_1^2 + d^2 - 2\rho\frac{\theta\phi\beta}{d}$$

$$b_2^2 = 2\alpha_1^2 + d^2 + \frac{2\theta\phi\beta}{d}$$

$$\tag{A.2.8}$$

Substitute back in the third equation in (A.2.7) to get

$$d^6 + (2\alpha_1^2)\ d^4 + (\alpha_1^4 - \omega^4)\ d^2 - \theta^2\phi^2\beta^2 = 0 \tag{A.2.9}$$

The positive real root of this last equation is to be used to keep the form of the solution as assumed in equation (A.2.4). The solution of the homogeneous differential equation (A.2.1) written in real form becomes:

$$\eta_a = e^{-d\xi}(C_1\ \sin b_2\xi + C_2\ \cos b_2\xi)$$

$$+ e^{d\xi}\ (A_1\ \sin b_1\xi + A_2\ \cos b_1\xi)$$

for the region ahead of the load, and:

$$\eta_b = e^{d\xi}\ (C_3\ \sin b_1\xi + C_4\ \cos b_1\xi)$$

$$+ e^{-d\xi}\ (A_3\ \sin b_2\xi + A_4\ \cos b_2\xi)$$

for the region behind the load.

It is reasonable to assume that as $\xi \to \infty$, $\eta_a = 0$ and $\xi \to -\infty$, $\eta_b = 0$. Thus

$$A_1 = A_2 = 0 \quad \text{and} \quad A_3 = A_4 = 0$$

and the solutions reduce to:

$$\left.\begin{array}{l} \eta_a = e^{-d\xi} (C_1 \sin b_2\xi + C_2 \cos b_2\xi) \text{ for } \xi \geqslant 0 \\[3mm] \eta_b = e^{d\xi} (C_3 \sin b_1\xi + C_4 \cos b_1\xi) \text{ for } \xi \leqslant 0 \end{array}\right\} \text{(A.2.10)}$$

The remaining four constants C_1, C_2, C_3 and C_4 are determined from the four conditions at $\xi = 0$.

(a) $\lim\limits_{\varepsilon \to 0} [\eta_a (0+\varepsilon) - \eta_b (0-\varepsilon)] = 0$

(b) $\lim\limits_{\varepsilon \to 0} [\eta_a' (0+\varepsilon) - \eta_b' (0-\varepsilon)] = 0$

(c) $\lim\limits_{\varepsilon \to 0} [\eta_a'' (0+\varepsilon) - \eta_b'' (0+\varepsilon)] = 0$

(d) $\lim\limits_{\varepsilon \to 0} [\eta_a''' (0+\varepsilon) - \eta_b''' (0-\varepsilon)] = \dfrac{-P}{EI}$

The solution for the constants gives:

$$\left.\begin{array}{l} C_2 = C_4 = \dfrac{d\,P}{EI\ d^2[4d^2+b_2^2+3b_1^2] + \dfrac{(b_2^2-b_1^2)(4d^2-b_1^2+b_2^2)}{4}} \\[8mm] C_1 = \dfrac{b_1^2 - b_2^2 + 4d^2}{4db_2}\, C_2 \qquad C_3 = \dfrac{b_1^2 - b_2^2 - 4d^2}{4db_1}\, C_2 \end{array}\right\} \text{(A.2.11)}$$

Equations (A.2.9) with (A.2.10) and (A.2.11) give the solution of the differential equation (A.2.1), which can be written as

follows:

$$b_2^2 + 3b_1^2 = 2\alpha_1^2 + d^2 + 2\frac{\theta\phi\beta}{d} + 6\alpha_1^2 + 3d^2 - 6\frac{\theta\phi\beta}{d}$$

$$= 8\alpha_1^2 + 4d^2 - 4\frac{\theta\phi\beta}{d}$$

$$b_2^2 - b_1^2 = 4\frac{\theta\phi\beta}{d}$$

Hence

$$C_2 = C_4 = \frac{d\ P}{EI\ \{[8d^4+8\alpha_1^2d^2-4\theta\phi\beta d] + \frac{\theta\phi\beta}{d}(4d^2+4\frac{\theta\phi\beta}{d})\}}$$

$$b_1^2 - b_2^2 = -\frac{4\theta\phi\beta}{d}$$

$$C_3 = \frac{-\frac{4\theta\phi\beta}{d} - 4d^2}{4\ d\ b_1} \qquad C_2 = -\frac{\theta\phi\beta+d^3}{d^2b_1}\ C_2$$

and

$$C_1 = -\frac{\theta\phi\beta-d^3}{d^2b_2}\ C_2$$

Hence for $\xi \geq 0$

$$\eta_a = \left[\frac{d\ P\ e^{-d\xi}}{EI\{4[2d^4+2\alpha_1^2d^2-\theta\phi\beta d] + \frac{\theta\phi\beta}{d}(4d^2+4\frac{\theta\phi\beta}{d})\}}\right]$$

$$\left[\frac{-(\theta\phi\beta-d^3)}{d^2\ \sqrt{2\alpha_1^2+d^2+\frac{2\theta\phi\beta}{d}}}\ \sin\sqrt{2\alpha_1^2-d^2+\frac{2\theta\phi\beta}{d}}\ \xi +\right.$$

$$\left.\cos\sqrt{2\alpha_1^2+d^2+\frac{2\theta\phi\beta}{d}}\ \xi\right]$$

and for $\xi \leqslant 0$

$$n_b = \left[\frac{d\,P\,e^{d\xi}}{EI\{4[2d^4+2\alpha_1^2 d^2-\theta\phi\beta d] + \frac{\theta\phi\beta}{d}\,(4d^2+4\frac{\theta\phi\beta}{d})\}}\right]$$

$$\left[\frac{-(\theta\phi\beta+d^3)}{d^2\,\sqrt{2\alpha_1^2+d^2-\frac{2\theta\phi\beta}{d}}}\;\sin\sqrt{2\alpha_1^2+d^2-\frac{2\theta\phi\beta}{d}}\;\xi\;+\right.$$

$$\left.\cos\sqrt{2\alpha_1^2+d^2-\frac{2\theta\phi\beta}{d}}\;\xi\right] \qquad (A.2.12)$$

where d is the positive real root of equation (A.2.9). For the limiting case of no damping $\beta = 0$, and equation (A.2.8) simplifies to:

$$d^4 + 2\alpha_1^2 d^2 + \alpha_1^4 - \omega^4 = 0$$

Let:

$$d = \sqrt{\omega^2 - \alpha_1^2} = g \qquad (A.2.13)$$

For $\xi \geqslant 0$

$$n_a = \frac{P\,e^{-g\xi}}{8EI\,g(g^2+\alpha_1^2)}$$

$$\left[\frac{g}{\sqrt{2\alpha_1^2+g^2}}\;\sin\sqrt{2\alpha_1^2+g^2}\;\xi\;+\;\cos\sqrt{2\alpha_1^2+g^2}\;\xi\right]$$

and for $\xi \leqslant 0$

$$n_b = \frac{P\,e^{g\xi}}{8EI\,g(g^2+\alpha_1^2)}$$

$$\left[\frac{-g}{\sqrt{2\alpha_1^2+g^2}}\;\sin\sqrt{2\alpha_1^2+g^2}\;\xi\;+\;\cos\sqrt{2\alpha_1^2+g^2}\;\xi\right]$$

These equations can be rewritten as

$$\eta_a = \frac{P\ e^{-g\xi}}{8EI\omega^2 g} \left[\frac{g}{\sqrt{\omega^2+\alpha_1^2}}\ \sin\ \sqrt{\omega^2+\alpha_1^2}\ \xi\ + \right.$$

$$\left. \cos\ \sqrt{\omega^2+\alpha_1^2}\ \xi \right]$$

and   (A.2.14)

$$\eta_b = \frac{P\ e^{g\xi}}{8EI\omega^2 g} \left[\frac{-g}{\sqrt{\omega^2+\alpha_1^2}}\ \sin\ \sqrt{\omega^2+\alpha_1^2}\ \xi\ + \right.$$

$$\left. \cos\ \sqrt{\omega^2+\alpha_1^2}\ \xi \right]$$

Hence, in the limiting case of no damping, the wave caused
by P, and which moves with P at a constant velocity less
than the critical, is symmetrical with respect to P for any
$N < N_{cr}$.
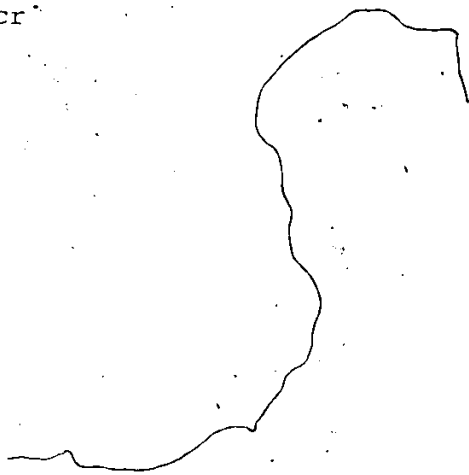
APPENDIX (B)

EQUATIONS OF MOTION FOR THE COUPLED
VEHICLE/TRACK DYNAMICS

In this appendix the equations of motion for the full moving model of the vehicle including the discretized model of the track are given. For the equations describing the motions of the wheelsets, the effects of creep (and the corresponding creep forces) between wheels and rails and the wheel tread/rail profile geometry are considered.

Because of symmetry, the equations describing the lateral motions of the system (these include the lateral displacement (v), the roll (α) and the yaw (γ)) are uncoupled from the equations of motion of the longitudinal modes (longitudinal (-), vertical (w), and pitching (β) displacements).

In the first part of this appendix (Section (B.1)) the equations of motion for the lateral vibrations are given both in detail and in their general forms. The elimination of the internal reactions is described and the transformation matrix [T] relating all the variables with the independent ones is shown in Table (B.1) based on the given equations of constraints. In this case the system is composed of fifteen degrees of freedom. In the generalized coordinates, .

190

the general form of the equations is given by the matrix equation (B.1.50).

In the second part of the appendix (Section (B.2)) the equations governing the longitudinal motions of the system are presented following a similar analysis. In this case the transformation matrix is [D] which is shown in Table (B.2). The system consists of twenty-seven degrees of freedom; and the equations are given in their general form, in the generalized coordinates, by the matrix equation (B.2.44).

Figure B.1 shows the plan view of the secondary suspension and illustrates some of the dimensions and parameters given in the equations (dimensions, angles α_1 and α_2, damping coefficients,...,etc.). The primary suspension consists of coil springs and shock absorbers (C_{17} and C_{18}), because of symmetry, C_{17} and C_{18} have the same numeric value.

192

Figure B.1 Plan view for secondary suspension

B.1 Equations of Motion for Lateral Vibrations

Lateral - Body

$$m_a \ddot{v}_a + (2K_2 + 4K_5 + 4K_8)v_a$$

$$+ (-K_2 - 2K_5 - 2K_8)v_{bf} + (-K_2 - 2K_5 - 2K_8)v_{br}$$

$$+ (-2\ell_1 K_2 - 4\ell_7 K_5 - 4\ell_7 K_8)\alpha_a$$

$$+ (-\ell_2 K_2 - 2\ell_{33} K_5 - 2\ell_{33} K_8)\alpha_{bf}$$

$$+ (-\ell_2 K_2 - 2\ell_{33} K_5 - 2\ell_{33} K_8)\alpha_{br}$$

$$+ (\ell_{16} K_2 + 2\ell_4 K_5 - 2\ell_5 K_8)\gamma_{bf}$$

$$+ (-\ell_{16} K_2 - 2\ell_4 K_5 + 2\ell_5 K_8)\gamma_{br}$$

$$+ (2C_2 + 4C_5 + 4C_8 + 4C_{13}\sin\alpha_1 + 4C_{15}\sin\alpha_2)\dot{v}_a$$

$$+ (-C_2 - 2C_5 - 2C_8 - 2C_{13}\sin\alpha_1 - 2C_{15}\sin\alpha_2)\dot{v}_{bf}$$

$$+ (-C_2 - 2C_5 - 2C_8 - 2C_{13}\sin\alpha_1 - 2C_{15}\sin\alpha_2)\dot{v}_{br}$$

$$+ (-2\ell_1 C_2 - 4\ell_7 C_5 - 4\ell_7 C_8 - 4\ell_{15}C_{13}\sin\alpha_1$$
$$- 4\ell_{15}C_{15}\sin\alpha_2)\dot{\alpha}_a$$

$$+ (-\ell_2 C_2 - 2\ell_{33}C_5 - 2\ell_{33}C_8 - 2\ell_{32}C_{13}\sin\alpha_1$$
$$- 2\ell_{32}C_{15}\sin\alpha_2)\dot{\alpha}_{bf}$$

$$+ (-\ell_2 C_2 - 2\ell_{33}C_5 - 2\ell_{33}C_8 - 2\ell_{32}C_{13}\sin\alpha_1$$
$$- 2\ell_{32}C_{15}\sin\alpha_2)\dot{\alpha}_{br}$$

$$+ [\ell_{16}C_2 + 2\ell_4 C_5 - 2\ell_5 C_8 + 2C_{13}(\ell_{31}\cos\alpha_1 + \ell_{29}\sin\alpha_1)$$
$$+ 2C_{15}(\ell_{30}\cos\alpha_2 + \ell_{28}\sin\alpha_2)]\dot{\gamma}_{bf}$$

$$+ [(-\ell_{16}C_2 - 2\ell_4 C_5 + 2\ell_5 C_8 - 2C_{13}(\ell_{31} \cos\alpha_1 + \ell_{29} \sin\alpha_1)$$

$$- 2C_{15}(\ell_{30} \cos\alpha_2 + \ell_{28} \sin\alpha_2)]\dot{\gamma}_{br} = 0$$

$$(B.1.1)$$

Roll - Body

$$I_{a\alpha}\ddot{\alpha}_a + (-2\ell_1 K_2 - 4\ell_7 K_5 - 4\ell_7 K_8)v_a$$

$$+ (\ell_1 K_2 + 2\ell_7 K_5 + 2\ell_7 K_8)v_{bf} + (\ell_1 K_2 + 2\ell_7 K_5 + 2\ell_7 K_8)v_{br}$$

$$+ (2\ell_1^2 K_2 + 4\ell_7^2 K_5 + 4\ell_7^2 K_8 + 4\ell_9^2 K_3 + 4\ell_{10}^2 K_6)\alpha_a$$

$$+ (\ell_1 \ell_2 K_2 + 2\ell_7 \ell_{33} K_5 + 2\ell_7 \ell_{33} K_8 - 2\ell_9^2 K_3 - 2\ell_{10}^2 K_6)\alpha_{bf}$$

$$+ (\ell_1 \ell_2 K_2 + 2\ell_7 \ell_{33} K_5 + 2\ell_7 \ell_{33} K_8 - 2\ell_9^2 K_3 - 2\ell_{10}^2 K_6)\alpha_{br}$$

$$+ (-\ell_1 \ell_{16} K_2 - 2\ell_7 \ell_4 K_5 + 2\ell_7 \ell_5 K_8)\gamma_{bf}$$

$$+ (\ell_1 \ell_{16} K_2 + 2\ell_7 \ell_5 K_5 - 2\ell_7 \ell_5 K_8)\gamma_{br}$$

$$+ (2\ell_1 C_2 - 4\ell_7 C_5 - 4\ell_7 C_8 - 4\ell_{15}C_{13} \sin \alpha_1$$

$$- 4\ell_{15}C_{15} \sin \alpha_2)\dot{v}_a$$

$$+ (\ell_1 C_2 + 2\ell_7 C_5 + 2\ell_7 C_8 + 2\ell_{15}C_{13} \sin \alpha_1$$

$$+ 2\ell_{15}C_{15} \sin \alpha_2)\dot{v}_{bf}$$

$$+ (\ell_1 C_2 + 2\ell_7 C_5 + 2\ell_7 C_8 + 2\ell_{15}C_{13} \sin \alpha_1$$

$$+ 2\ell_{15}C_{15} \sin \alpha_2)\dot{v}_{br}$$

$$+ (2\ell_1^2 C_2 + 4\ell_7^2 C_5 + 4\ell_7^2 C_8 + 4\ell_9^2 C_3 + 4\ell_{10}^2 C_6$$

$$+ 4\ell_{15}^2 C_{13} \sin\alpha_1 + 4\ell_{15}^2 C_{15} \sin\alpha_2)\dot{\alpha}_a$$

$$+ (\ell_1\ell_2 C_2 + 2\ell_7\ell_{33}C_5 + 2\ell_7\ell_{33}C_8 - 2\ell_9^2 C_3 - 2\ell_{10}^2 C_6$$

$$+ 2\ell_{15}\ell_{32}C_{13} \sin \alpha_1 + 2\ell_{15}\ell_{32}C_{15} \sin \alpha_2)\dot{\alpha}_{bf}$$

$$+ (\ell_1\ell_2 C_2 + 2\ell_7\ell_{33}C_5 + 2\ell_7\ell_{33}C_8 - 2\ell_9^2 C_3 - 2\ell_{10}^2 C_6$$

$$+ 2\ell_{15}\ell_{32}C_{13} \sin \alpha_1 + 2\ell_{15}\ell_{32}C_{15} \sin \alpha_2)\dot{\alpha}_{br}$$

$$+ (-\ell_1\ell_{16}C_2 - 2\ell_7\ell_4 C_5 + 2\ell_7\ell_5 C_8 - 2\ell_{15}C_{13} (\ell_{31} \cos \alpha_1$$

$$+ \ell_{29} \sin \alpha_1) - 2\ell_{15}C_{15}(\ell_{30} \cos \alpha_2 + \ell_{28}\sin \alpha_2))\dot{\gamma}_{bf}$$

$$+ (\ell_1\ell_{16}C_2 + 2\ell_7\ell_4 C_5 - 2\ell_7\ell_5 C_8 + 2\ell_{15}C_{13}(\ell_{31} \cos \alpha_1$$

$$+ \ell_{29} \sin \alpha_1) + 2\ell_{15}C_{17}(\ell_{30} \cos \alpha_2 + \ell_{28} \sin \alpha_2))\dot{\gamma}_{br}=0$$

$$(B.1.2)$$

Yaw - Body

$$I_{a\gamma}\ddot{\gamma}_a + [(\ell_3+\ell_{16})K_2 + 2(\ell_3+\ell_4)K_5 + 2(\ell_3-\ell_5)K_8]v_{bf}$$

$$+ [-(\ell_3+\ell_{16})K_2 - 2(\ell_3+\ell_4)K_5 - 2(\ell_3-\ell_5)K_8]v_{br}$$

$$+ [(\ell_3+\ell_{16})\ell_2 K_2 + 2(\ell_3+\ell_4)\ell_{33}K_5 + 2(\ell_3-\ell_5)\ell_{33}K_8]\alpha_{bf}$$

$$+ [-(\ell_3+\ell_{16})\ell_2 K_2 - 2(\ell_3+\ell_4)\ell_{33}K_5 - 2(\ell_3-\ell_5)\ell_{33}K_8]\alpha_{br}$$

$$+ [2(\ell_3+\ell_{16})^2 K_2 + 4\ell_9^2 K_4 + 4\ell_{10}^2 K_7 + 4(\ell_3+\ell_4)^2 K_5$$

$$+ 4(\ell_3-\ell_5)^2 K_8 + 4K_{11} + 4K_{12}]\gamma_a$$

$$+ [-\ell_{16}(\ell_3+\ell_{16})K_2 - 2\ell_9^2 K_4 - 2\ell_{10}^2 K_7 - 2(\ell_3+\ell_4)\ell_4 K_5$$

$$+ 2(\ell_3-\ell_5)\ell_5 K_8 - 2K_{11} - 2K_{12}]\gamma_{bf}$$

$$+ [-\ell_{16}(\ell_3+\ell_{16})K_2 - 2\ell_9^2 K_4 - 2\ell_{10}^2 K_7 - 2(\ell_3+\ell_4)\ell_4 K_5$$

$$+ 2(\ell_3-\ell_5)\ell_5 K_8 - 2K_{11} - 2K_{12}]\gamma_{br}$$

$$+ [(\ell_3+\ell_{16})C_2 + 2(\ell_3+\ell_4)C_5 + 2(\ell_3-\ell_5)C_8 + 2(\ell_{12}C_{13}$$
$$+\ell_{13}C_{14}) \sin \alpha_1 + 2(\ell_6C_{15}+\ell_{11}C_{16}) \sin \alpha_2]\dot{v}_{bf}$$
$$+ [-(\ell_3+\ell_{16})C_2 - 2(\ell_3+\ell_4)C_5 - 2(\ell_3-\ell_5)C_8 - 2(\ell_{12}C_{13}$$
$$+\ell_{13}C_{14}) \sin \alpha_1 - 2(\ell_6C_{15}+\ell_{11}C_{16}) \sin \alpha_2]\dot{v}_{br}$$
$$+ [(\ell_3+\ell_{16})\ell_2C_2 + 2(\ell_3+\ell_4)\ell_{33}C_5 + 2(\ell_3-\ell_5)\ell_{33}C_8$$
$$+ 2\ell_{32}(\ell_{12}C_{13} + \ell_{13}C_{14}) \sin \alpha_1 + 2\ell_{32}(\ell_6C_{15}$$
$$+\ell_{11}C_{16}) \sin \alpha_2]\dot{\alpha}_{bf}$$
$$+ [-(\ell_3+\ell_{16})\ell_2C_2 - 2(\ell_3+\ell_4)\ell_{33}C_5 - 2(\ell_3-\ell_5)\ell_{33}C_8$$
$$- 2\ell_{32}(\ell_{12}C_{13}+\ell_{13}C_{14}) \sin \alpha_1 - 2\ell_{32}(\ell_6C_{15}$$
$$+\ell_{11}C_{16} \sin \alpha_2]\dot{\alpha}_{br}$$
$$+ [2(\ell_3+\ell_{16})^2C_2 + 4\ell_9^2C_4 + 4\ell_{10}^2C_7 + 4(\ell_3+\ell_4)^2C_5$$
$$+ 4(\ell_3-\ell_5)^2C_8 + 4C_{11} + 4C_{12} + 4(\ell_{13} \cos \alpha_1$$
$$+ \ell_{12} \sin \alpha_1)(\ell_{12}C_{13}+\ell_{13}C_{14}) + 4(\ell_{11} \cos \alpha_2$$
$$+ \ell_6 \sin \alpha_2) (\ell_6C_{15}+\ell_{11}C_{16})]\dot{\gamma}_a$$
$$+ [-\ell_{16}(\ell_3+\ell_{16})C_2 - 2\ell_9^2C_4 - 2\ell_{10}^2C_7 - 2(\ell_3+\ell_4)\ell_4C_5$$
$$+ 2(\ell_3-\ell_5)\ell_5C_8 - 2C_{11} - 2C_{12} - 2(\ell_{31} \cos \alpha_1$$
$$+ \ell_{29} \sin \alpha_1)(\ell_{12}C_{13}+\ell_{13}C_{14}) - 2(\ell_{30} \cos \alpha_2$$
$$+ \ell_{28} \sin \alpha_2)(\ell_6C_{15}+\ell_{11}C_{16})]\dot{\gamma}_{bf}$$
$$+ [-\ell_{16}(\ell_3+\ell_{16})C_2 - 2\ell_9^2C_4 - 2\ell_{10}^2C_7 - 2(\ell_3+\ell_4)\ell_4C_5$$
$$+ 2(\ell_3-\ell_5)\ell_5C_8 - 2C_{11} - 2C_{12} - 2(\ell_{31} \cos \alpha_1$$

$$+ \ell_{29} \sin \alpha_1)(\ell_{12}C_{13}+\ell_{13}C_{14}) - 2(\ell_{30} \cos \alpha_2$$

$$+ \ell_{28} \sin \alpha_2)(\ell_6C_{15}+\ell_{11}C_{16})]\dot{\gamma}_{br} = 0$$

$$(B.1.3)$$

Lateral – Rear Frame

$$m_b\ddot{v}_{br} + (-K_2 - 2K_5 - 2K_8)v_a + (K_2 + 2K_5 + 2K_8)v_{br}$$

$$+ (\ell_1K_2 + 2\ell_7K_5 + 2\ell_7K_8)\alpha_a + (\ell_2K_2 + 2\ell_{33}K_5 + 2\ell_{33}K_8)\alpha_{br}$$

$$+ [-(\ell_3+\ell_{16})K_2 - 2(\ell_3+\ell_4)K_5 - 2(\ell_3-\ell_5)K_8]\gamma_a$$

$$+ (\ell_{16}K_2 + 2\ell_4K_5 - 2\ell_5K_8)\gamma_{br}$$

$$+ (-C_2 - 2C_5 - 2C_8 - 2C_{13} \sin \alpha_1 - 2C_{15} \sin \alpha_2)\dot{v}_a$$

$$+ (C_2 + 2C_5 + 2C_8 + 2C_{13} \sin \alpha_1 + 2C_{15} \sin \alpha_2)\dot{v}_{br}$$

$$+ (\ell_1C_2 + 2\ell_7C_5 + 2\ell_7C_8 + 2\ell_{15}C_{13} \sin \alpha_1$$

$$+ 2\ell_{15}C_{15} \sin \alpha_2)\dot{\alpha}_a$$

$$+ (\ell_2C_2 + 2\ell_{33}C_5 + 2\ell_{33}C_8 + 2\ell_{32}C_{13} \sin \alpha_1$$

$$+ 2\ell_{32}C_{15} \sin \alpha_2)\dot{\alpha}_{br}$$

$$+ [-(\ell_3+\ell_{16})C_2 - 2(\ell_3+\ell_4)C_5 - 2(\ell_3-\ell_5)C_8$$

$$- 2\ell_{13}C_{13} \cos \alpha_1 - 2\ell_{12}C_{13} \sin \alpha_1 - 2\ell_{11}C_{15} \cos \alpha_2$$

$$- 2\ell_6C_{15} \sin \alpha_2]\dot{\gamma}_a$$

$$+ (\ell_{16}C_2 + 2\ell_4C_5 - 2\ell_5C_8 + 2\ell_{31}C_{13} \cos \alpha_1$$

$$+ 2\ell_{29}C_{13} \sin \alpha_1 + 2\ell_{30}C_{15} \cos \alpha_2$$

$$+ 2\ell_{28}C_{15} \sin \alpha_2)\dot{\gamma}_{br}$$

$$- (RB_1 + RB_2 + RB_3) = 0 \qquad (B.1.4)$$

Roll - Rear Frame

$$I_{ba}\dot{\alpha}_{br} + (-\ell_2 K_2 - 2\ell_{33}K_5 - 2\ell_{33}K_8)v_a$$

$$+ (\ell_2 K_2 + 2\ell_{33}K_5 + 2\ell_{33}K_8)v_{br}$$

$$+ (\ell_2\ell_1 K_2 + 2\ell_{33}\ell_7 K_5 + 2\ell_{33}\ell_7 K_8 - 2\ell_9^2 K_3 - 2\ell_{10}^2 K_6)\alpha_a^0$$

$$+ (\ell_2^2 K_2 + 2\ell_{33}^2 K_5 + 2\ell_{33}^2 K_8 + 2\ell_9^2 K_3 + 2\ell_{10}^2 K_6 + 6\ell_{17}^2 K_9)\alpha_{br}$$

$$+ (-2\ell_{17}^2 K_9)\alpha_{d1} + (-2\ell_{17}^2 K_9)\alpha_{d2} + (-2\ell_{17}^2 K_9)\alpha_{d3}$$

$$+ (-2\ell_{17}^2 K_9)\alpha_{de1} + (-2\ell_{17}^2 K_9)\alpha_{de2} + (-2\ell_{17}^2 K_9)\alpha_{de3}$$

$$\div [-\ell_2(\ell_3+\ell_{16})K_2 - 2\ell_{33}(\ell_3+\ell_4)K_5 - 2\ell_{33}(\ell_3-\ell_5)K_8]\gamma_a$$

$$+ (\ell_2\ell_{16}K_2 + 2\ell_{33}\ell_4 K_5 - 2\ell_{33}\ell_5 K_8)\gamma_{br}$$

$$+ (-\ell_2 C_2 - 2\ell_{33}C_5 - 2\ell_{33}C_8 - 2\ell_{32}C_{13}\sin\alpha_1$$
$$- 2\ell_{32}C_{15}\sin\alpha_2)\dot{v}_a$$

$$+ (\ell_2 C_2 + 2\ell_{33}C_5 + 2\ell_{33}C_8 + 2\ell_{32}C_{13}\sin\alpha_1$$
$$+ 2\ell_{32}C_{15}\sin\alpha_2)\dot{v}_{br}$$

$$+ (\ell_2\ell_1 C_2 + 2\ell_{33}\ell_7 C_5 + 2\ell_{33}\ell_7 C_8 - 2\ell_9^2 C_3 - 2\ell_{10}^2 C_6$$
$$+ 2\ell_{32}\ell_{15}C_{13}\sin\alpha_1 + 2\ell_{32}\ell_{15}C_{15}\sin\alpha_2)\dot{\alpha}_a$$

$$+ (\ell_2^2 C_2 + 2\ell_{33}^2 C_5 + 2\ell_{33}^2 C_8 + 2\ell_9^2 C_3 + 2\ell_{10}^2 C_6$$
$$+ 2\ell_{32}^2 C_{13}\sin\alpha_1 + 2\ell_{32}^2 C_{15}\sin\alpha_2 + 2\ell_{19}^2 C_{17}$$
$$+ 4\ell_{19}^2 C_{18})\dot{\alpha}_{br}$$

$$+ (-\ell_{19}^2 C_{17} - \ell_{19}^2 C_{18}) \dot{\alpha}_{d1} + (-2\ell_{19}^2 C_{18}) \dot{\alpha}_{d2}$$

$$+ (-\ell_{19}^2 C_{17} - \ell_{19}^2 C_{18}) \dot{\alpha}_{d3}$$

$$+ (-\ell_{19}^2 C_{17} - \ell_{19}^2 C_{18}) \dot{\alpha}_{de1} + (-2\ell_{19}^2 C_{18}) \dot{\alpha}_{de2}$$

$$+ (-\ell_{19}^2 C_{17} - \ell_{19}^2 C_{18}) \dot{\alpha}_{de3}$$

$$+ [-\ell_2(\ell_3 + \ell_{16}) C_2 - 2\ell_{33}(\ell_3 + \ell_4) C_5 - 2\ell_{33}(\ell_3 - \ell_5) C_8$$

$$- 2\ell_{32}\ell_{13} C_{13} \cos \alpha_1 - 2\ell_{32}\ell_{12} C_{13} \sin \alpha_1$$

$$- 2\ell_{32}\ell_{11} C_{15} \cos \alpha_2 - 2\ell_{32}\ell_6 C_{15} \sin \alpha_2] \dot{\gamma}_a$$

$$+ [\ell_2\ell_{16} C_2 + 2\ell_{33}\ell_4 C_5 - 2\ell_{33}\ell_5 C_8 + 2\ell_{32}\ell_{31} C_{13} \cos \alpha_1$$

$$+ 2\ell_{32}\ell_{29} C_{13} \sin \alpha_1 + 2\ell_{32}\ell_{30} C_{15} \cos \alpha_2$$

$$+ 2\ell_{32}\ell_{28} C_{15} \sin \alpha_2] \dot{\gamma}_{br}$$

$$+ \ell_{21}(RB_1 + RB_2 + RB_3) = 0 \qquad\qquad (B.1.5)$$

Yaw - Rear Frame

$$I_{by}\dot{\gamma}_{br} + (-\ell_{16}K_2 - 2\ell_4 K_5 + 2\ell_5 K_8) v_a$$

$$+ (\ell_{16}K_2 + 2\ell_4 K_5 - 2\ell_5 K_8) v_{br}$$

$$+ (\ell_{16}\ell_1 K_2 + 2\ell_4\ell_7 K_5 - 2\ell_5\ell_7 K_8) \alpha_a$$

$$+ (\ell_{16}\ell_2 K_2 + 2\ell_4\ell_{33} K_5 - 2\ell_5\ell_{33} K_8) \alpha_{br}$$

$$+ [-2\ell_9^2 K_4 - 2\ell_{10}^2 K_7 - \ell_{16}(\ell_3 + \ell_{16}) K_2 - 2\ell_4(\ell_3 + \ell_4) K_5$$

$$+ 2\ell_5(\ell_3 - \ell_5) K_8 - 2K_{11} - 2K_{12}] \gamma_a$$

$$+ [2\ell_9^2 K_4 + 2\ell_{10}^2 K_7 + \ell_{16}^2 K_2 + 2\ell_4^2 K_5 + 2\ell_5^2 K_8 + 2K_{11}$$

$$+ 2K_{12}] \gamma_{br}$$

$$+ [-\ell_{16}C_2 - 2\ell_4C_5 + 2\ell_5C_8 - 2\ell_{31}C_{14} \sin \alpha_1$$

$$-2\ell_{29}C_{13} \sin \alpha_1 - 2\ell_{30}C_{16} \sin \alpha_2 - 2\ell_{28}C_{15} \sin \alpha_2]\dot{v}_a$$

$$+ [\ell_{16}C_2 + 2\ell_4C_5 - 2\ell_5C_8 + 2\ell_{31}C_{14} \sin \alpha_1$$

$$+ 2\ell_{29}C_{13} \sin \alpha_1 + 2\ell_{30}C_{16} \sin \alpha_2 + 2\ell_{28}C_{15} \sin \alpha_2]\dot{v}_{br}$$

$$+ [\ell_{16}\ell_1C_2 + 2\ell_4\ell_7C_5 - 2\ell_5\ell_7C_8 + 2\ell_{31}\ell_{15}C_{14} \sin \alpha_1$$

$$+ 2\ell_{29}\ell_{15}C_{13} \sin \alpha_1 + 2\ell_{30}\ell_{15}C_{16} \sin \alpha_2$$

$$+ 2\ell_{28}\ell_{15}C_{15} \sin \alpha_2]\dot{\alpha}_a$$

$$+ [\ell_{16}\ell_2C_2 + 2\ell_4\ell_{33}C_5 - 2\ell_5\ell_{33}C_8 + 2\ell_{31}\ell_{32}C_{14} \sin \alpha_1$$

$$+ 2\ell_{29}\ell_{32}C_{13} \sin \alpha_1 + 2\ell_{30}\ell_{32}C_{16} \sin \alpha_2$$

$$+ 2\ell_{28}\ell_{32}C_{15} \sin \alpha_2]\dot{\alpha}_{br}$$

$$+ [-2\ell_9^2C_4 - 2\ell_{10}^2C_7 - \ell_{16}(\ell_3+\ell_{16})C_2 - 2\ell_4(\ell_3+\ell_4)C_5$$

$$+ 2\ell_5(\ell_3-\ell_5)C_8 - 2C_{11} - 2C_{12} + (-2\ell_{31}C_{14}$$

$$- 2\ell_{29}C_{13})(\ell_{13} \cos \alpha_1 - \ell_{12} \sin \alpha_1) + (-2\ell_{30}C_{16}$$

$$- 2\ell_{28}C_{15})(\ell_{11} \cos \alpha_2 + \ell_6 \sin \alpha_2)]\dot{\gamma}_a$$

$$+ [2\ell_9^2C_4 + 2\ell_{10}^2C_7 + \ell_{16}^2C_2 + 2\ell_4^2C_5 + 2\ell_5^2C_8 + 2C_{11}$$

$$+ 2C_{12} + (2\ell_{31}C_{14} + 2\ell_{29}C_{13})(\ell_{31} \cos \alpha_1 + \ell_{29} \sin \alpha_1)$$

$$+ (2\ell_{30}C_{16}) + 2\ell_{28}C_{15})(\ell_{30} \cos \alpha_2$$

$$+ \ell_{28} \sin \alpha_2)]\dot{\gamma}_{br}$$

$$- \ell_{24}(RB_1) - \ell_{26}(RB_2) + \ell_{23}(RB_3) - (RM_1 + RM_2$$

$$+ RM_3)=0 \quad (B.1.6)$$

Lateral – Front Frame

$$m_b \ddot{v}_{bf} + (-K_2 - 2K_5 - 2K_8)v_a + (K_2 + 2K_5 + 2K_8)v_{bf}$$

$$+ (\ell_1 K_2 + 2\ell_7 K_5 + 2\ell_7 K_8)\dot{\alpha}_a$$

$$+ (\ell_2 K_2 + 2\ell_{33}K_5 + 2\ell_{33}K_8)\alpha_{bf}$$

$$+ [(\ell_3 + \ell_{16})K_2 + 2(\ell_3 + \ell_4)K_5 + 2(\ell_3 - \ell_5)K_8]\gamma_a$$

$$+ (-\ell_{16}K_2 - 2\ell_4 K_5 + 2\ell_5 K_8)\gamma_{bf}$$

$$+ (-C_2 - 2C_5 - 2C_8 - 2C_{13}\sin\alpha_1 - 2C_{15}\sin\alpha_2)\dot{v}_a$$

$$+ (C_2 + 2C_5 + 2C_8 + 2C_{13}\sin\alpha_1 + 2C_{15}\sin\alpha_2)\dot{v}_{bf}$$

$$+ (\ell_1 C_2 + 2\ell_7 C_5 + 2\ell_7 C_8 + 2\ell_{15}C_{13}\sin\alpha_1$$
$$+ 2\ell_{15}C_{15}\sin\alpha_2)\dot{\alpha}_a$$

$$+ (\ell_2 C_2 + 2\ell_{33}C_5 + 2\ell_{33}C_8 + 2\ell_{32}C_{13}\sin\alpha_1$$
$$+ 2\ell_{32}C_{15}\sin\alpha_2)\dot{\alpha}_{bf}$$

$$+ [(\ell_3 + \ell_{16})C_2 + 2(\ell_3 + \ell_4)C_5 + 2(\ell_3 - \ell_5)C_8 + 2\ell_{13}C_{13}\cos\alpha_1$$
$$+ 2\ell_{12}C_{13}\sin\alpha_1 + 2\ell_{11}C_{15}\cos\alpha_2 + 2\ell_6 C_{15}\sin\alpha_2]\dot{\gamma}_a$$

$$+ [-\ell_{16}C_2 - 2\ell_4 C_5 + 2\ell_5 C_8 - 2\ell_{31}C_{13}\cos\alpha_1$$
$$- 2\ell_{29}C_{13}\sin\alpha_1 - 2\ell_{30}C_{15}\cos\alpha_2 - 2\ell_{28}C_{15}\sin\alpha_2]\dot{\gamma}_{bf}$$

$$- (RB_4 + RB_5 + RB_6) = 0 \tag{B.1.7}$$

Roll - Front Frame

$$I_{b\alpha}\dot{\alpha}_{bf} + (-\ell_2 K_2 - 2\ell_{33}K_5 - 2\ell_{33}K_8)v_a$$

$$+ (\ell_2 K_2 + 2\ell_{33}K_5 + 2\ell_{33}K_8)v_{bf}$$

$$+ (\ell_2\ell_1 K_2 + 2\ell_{33}\ell_7 K_5 + 2\ell_{33}\ell_7 K_8 - 2\ell_9^2 K_3 - 2\ell_{10}^2 K_6)\alpha_a$$

$$+ (\ell_2^2 K_2 + 2\ell_{33}^2 K_5 + 2\ell_{33}^2 K_8 + 2\ell_9^2 K_3 + 2\ell_{10}^2 K_6 + 6\ell_{17}^2 K_9)\alpha_{bf}$$

$$+ (-2\ell_{17}^2 K_9)\alpha_{d4} + (-2\ell_{17}^2 K_9)\alpha_{d5} + (-2\ell_{17}^2 K_9)\alpha_{d6}$$

$$+ (-2\ell_{17}^2 K_9)\alpha_{de4} + (-2\ell_{17}^2 K_9)\alpha_{de5} + (-2\ell_{17}^2 K_9)\alpha_{de6}$$

$$+ [\ell_2(\ell_3+\ell_{16})K_2 + 2\ell_{33}(\ell_3+\ell_4)K_5 + 2\ell_{33}(\ell_3-\ell_5)K_8]\gamma_a$$

$$+ (-\ell_2\ell_{16}K_2 - 2\ell_{33}\ell_4 K_5 + 2\ell_{33}\ell_5 K_8)\gamma_{bf}$$

$$+ (-\ell_2 C_2 - 2\ell_{33}C_5 - 2\ell_{33}C_8 - 2\ell_{32}C_{13} \sin \alpha_1$$
$$- 2\ell_{32}C_{15} \sin \alpha_2)\dot{v}_a$$

$$+ (\ell_2 C_2 + 2\ell_{33}C_5 + 2\ell_{33}C_8 + 2\ell_{32}C_{13} \sin \alpha_1$$
$$+ 2\ell_{32}C_{15} \sin \alpha_2)\dot{v}_{bf}$$

$$+ [\ell_2\ell_1 C_2 + 2\ell_{33}\ell_7 C_5 + 2\ell_{33}\ell_7 C_8 - 2\ell_9^2 C_3 + 2\ell_{10}^2 C_6$$
$$+ 2\ell_{32}\ell_{15}C_{13} \sin \alpha_1 + 2\ell_{32}\ell_{15}C_{15} \sin \alpha_2]\dot{\alpha}_a$$

$$+ [\ell_2^2 C_2 + 2\ell_{33}^2 C_5 + 2\ell_{33}^2 C_8 + 2\ell_9^2 C_3 + 2\ell_{10}^2 C_6$$
$$+ 2\ell_{32}^2 C_{13} \sin \alpha_1 + 2\ell_{32}^2 C_{15} \sin \alpha_2 + 2\ell_{19}^2 C_{17}$$
$$+ 4\ell_{19}^2 C_{18}]\dot{\alpha}_{bf}$$

$$+ (-\ell_{19}^2 C_{17} - \ell_{19}^2 C_{18})\dot{\alpha}_{d4} + (-2\ell_{19}^2 C_{18})\dot{\alpha}_{d5}$$

$$+ (-\ell_{19}^2 C_{17} - \ell_{19}^2 C_{18})\dot{\alpha}_{d6}$$

$$+ (-\ell_{19}^2 C_{17} - \ell_{19}^2 C_{18})\dot{\alpha}_{de4} + (-2\ell_{19}^2 C_{18})\dot{\alpha}_{de5}$$

$$+ (-\ell_{19}^2 C_{17} - \ell_{19}^2 C_{18})\dot{\alpha}_{de6}$$

$$+ [\ell_2(\ell_3+\ell_{16})C_2 + 2\ell_{33}(\ell_3+\ell_4)C_5 + 2\ell_{33}(\ell_3-\ell_5)C_8$$

$$+ 2\ell_{32}\ell_{13}C_{13} \cos \alpha_1 + 2\ell_{32}\ell_{12}C_{13} \sin \alpha_1$$

$$+ 2\ell_{32}\ell_{11}C_{15} \cos \alpha_2 + 2\ell_{32}\ell_6 C_{15} \sin \alpha_2]\dot{\gamma}_a$$

$$+ [-\ell_2\ell_{16}C_2 - 2\ell_{33}\ell_4 C_5 + 2\ell_{33}\ell_5 C_8 - 2\ell_{32}\ell_{31}C_{13} \cos \alpha_1$$

$$- 2\ell_{32}\ell_{29}C_{13} \sin \alpha_1 - 2\ell_{32}\ell_{30}C_{15} \cos \alpha_2$$

$$- 2\ell_{32}\ell_{28}C_{15} \sin \alpha_2]\dot{\gamma}_{bf}$$

$$+ \ell_{21} (RB_4 + RB_5 + RB_6) = 0 \qquad (B.1.8)$$

Yaw - Front Frame

$$I_{b\gamma}\ddot{\gamma}_{bf} + (\ell_{16}K_2 + 2\ell_4 K_5 - 2\ell_5 K_8)v_a$$

$$+ (-\ell_{16}K_2 - 2\ell_4 K_5 + 2\ell_5 K_8)v_{bf}$$

$$+ (-\ell_{16}\ell_1 K_2 - 2\ell_4\ell_7 K_5 + 2\ell_5\ell_7 K_8)\alpha_a + (-\ell_{16}\ell_2 K_2$$

$$- 2\ell_4\ell_{33}K_5 + 2\ell_5\ell_{33}K_8)\alpha_{bf}$$

$$+ [-2\ell_9^2 K_4 - 2\ell_{10}^2 K_7 - \ell_{16}(\ell_3+\ell_{16})K_2 - 2\ell_4(\ell_3+\ell_4)K_5$$

$$+ 2\ell_5(\ell_3-\ell_5)K_8 - 2K_{11} - 2K_{12}]\gamma_a$$

$$+ [2\ell_9^2 K_4 + 2\ell_{10}^2 K_7 + \ell_{16}^2 K_2 + 2\ell_4^2 K_5 + 2\ell_5^2 K_8 + 2K_{11}$$

$$+ 2K_{12}]\gamma_{bf}$$

$$+ (\ell_{16}C_2 + 2\ell_4 C_5 - 2\ell_5 C_8 + 2\ell_{31}C_{14} \sin \alpha_1$$

$$+ 2\ell_{29}C_{13} \sin \alpha_1 + 2\ell_{30}C_{16} \sin \alpha_2 + 2\ell_{28}C_{15} \sin\alpha_2)\dot{v}_a$$

$$+ (-\ell_{16}C_2 - 2\ell_4C_5 + 2\ell_5C_8 - 2\ell_{31}C_{14} \sin \alpha_1$$

$$- 2\ell_{29}C_{13} \sin \alpha_1 - 2\ell_{30}C_{16} \sin \alpha_2$$

$$- 2\ell_{28}C_{15} \sin \alpha_2)\dot{v}_{bf}$$

$$+ (-\ell_{16}\ell_1C_2 - 2\ell_4\ell_7C_5 + 2\ell_5\ell_7C_8 - 2\ell_{31}\ell_{15}C_{14} \sin \alpha_1$$

$$- 2\ell_{29}\ell_{15}C_{13} \sin \alpha_1 - 2\ell_{30}\ell_{15}C_{16} \sin \alpha_2$$

$$- 2\ell_{28}\ell_{15}C_{15} \sin \alpha_2)\dot{\alpha}_a$$

$$+ (-\ell_{16}\ell_2C_2 - 2\ell_4\ell_{33}C_5 + 2\ell_5\ell_{33}C_8 - 2\ell_{31}\ell_{32}C_{14} \sin \alpha_1$$

$$- 2\ell_{29}\ell_{32}C_{13} \sin \alpha_1 - 2\ell_{30}\ell_{32}C_{16} \sin \alpha_2$$

$$- 2\ell_{28}\ell_{32}C_{15} \sin \alpha_2)\dot{\alpha}_{bf}$$

$$+ [-2\ell_9^2C_4 - 2\ell_{10}^2C_7 - \ell_{16}(\ell_3+\ell_{16})C_2 - 2\ell_4(\ell_3+\ell_4)C_5$$

$$+ 2\ell_5(\ell_3-\ell_5)C_8 - 2C_{11} - 2C_{12} + (2\ell_{31}C_{14}$$

$$+ 2\ell_{29}C_{13})(-\ell_{13} \cos \alpha_1 - \ell_{12} \sin \alpha_1) + (2\ell_{30}C_{16}$$

$$+ 2\ell_{28}C_{15})(-\ell_{11} \cos \alpha_2 - \ell_6 \sin \alpha_2)]\dot{\gamma}_a$$

$$+ [2\ell_9^2C_4 + 2\ell_{10}^2C_7 + \ell_{16}^2C_2 + 2\ell_4^2C_5 + 2\ell_5^2C_8 + 2C_{11} + 2C_{12}$$

$$+ (2\ell_{31}C_{14} + 2\ell_{29}C_{13})(\ell_{31} \cos \alpha_1 + \ell_{29} \sin \alpha_1)$$

$$+ (2\ell_{30}C_{16} + 2\ell_{28}C_{15})(\ell_{30} \cos \alpha_2 + \ell_{28} \sin \alpha_2)]\dot{\gamma}_{bf}$$

$$- \ell_{23}(RB_4) + \ell_{26}(RB_5) + \ell_{24}(RB_6) - (RM_4 + RM_5$$

$$+ RM_6) = 0$$

$$\text{(B.1.9)}$$

Lateral - Motor No. 1

$$m_c \ddot{v}_{c1} - (RV_1) = 0 \qquad\qquad (B.1.10)$$

Yaw - Motor No. 1

$$I_{c\gamma} \ddot{\gamma}_{c1} - \ell_{34}(RV_1) - (R\gamma_1) = 0 \qquad (B.1.11)$$

Lateral - Wheelset No. 1

$$m_d \ddot{v}_{d1} + (\frac{2W\varepsilon}{\ell_{18}}) v_{d1} + (-W) \alpha_{de1} + (2f_2) \gamma_{d1} + (\frac{2f_2}{S}) \dot{v}_{d1}$$

$$+ (-\frac{2\ell_{20}f_2}{S}) \dot{\alpha}_{d1} + (\frac{2f_{23}}{S}) \dot{\gamma}_{d1} + (N_{r1} - N_{\ell 1}) \theta_0$$

$$+ (RB_1) + (RV_1) = 0 \qquad (B.1.12)$$

Roll - Motor/Wheelset No. 1

$$(I_{c\alpha} + I_{d\alpha}) \ddot{\alpha}_{d1} + (-2\ell_{17}^2 K_9) \alpha_{br} + (2\ell_{17}^2 K_9) \alpha_{d1}$$

$$+ [\ell_{19}^2(-C_{18} - C_{17})] \dot{\alpha}_{br} + [\ell_{19}^2(C_{18} + C_{17})] \dot{\alpha}_{d1}$$

$$+ (-W\eta + \frac{2\ell_{20}\varepsilon W}{\ell_{18}}) v_{d1} + (\ell_{20}W) \alpha_{de1}$$

$$+ (-2\ell_{20}f_2) \gamma_{d1} + (- \frac{2\ell_{20}f_2}{S}) \dot{v}_{d1}$$

$$+ (\frac{2\ell_{20}^2 f_2}{S}) \dot{\alpha}_{d1} + (- \frac{2\ell_{20}^2 f_{23}}{S}) \dot{\gamma}_{d1}$$

$$+ (\frac{\ell_{18}}{2} - \ell_{20}\theta_0) (N_{r1} - N_{\ell 1}) = 0 \qquad (B.1.13)$$

Yaw - Wheelset No. 1

$$I_{d\gamma}\ddot{\gamma}_{d1} + (\frac{2f_{32}}{S})\dot{v}_{d1} + (-\frac{2\ell_{20}f_{32}}{S})\dot{\alpha}_{d1} + (\frac{\ell_{18}^{2}f_{1}}{.2S}+\frac{2f_{3}}{S})\dot{\gamma}_{d1} - \frac{\ell_{18}\lambda f_{1}}{\ell_{20}}v_{d1}$$

$$+ (2f_{32}-W\frac{\ell_{18}}{2}\theta_{0})\gamma_{d1} + (RM_{1}) + (R\gamma_{1}) = 0 \qquad (B.1.14)$$

Lateral - Motor No. 2

$$m_{c}\ddot{v}_{c2} - (RV_{2}) = 0 \qquad (B.1.15)$$

Yaw - Motor No. 2

$$I_{c\gamma}\ddot{\gamma}_{c2} - \ell_{34}(RV_{2}) - (R\gamma_{2}) = 0 \qquad (B.1.16)$$

Lateral - Wheelset No. 2

$$m_{d}\ddot{v}_{d2} + (\frac{2W\epsilon}{\ell_{18}})v_{d2} + (-W)\alpha_{de2} + (2f_{2})\gamma_{d2} + (\frac{2f_{2}}{S})\dot{v}_{d2}$$

$$+ (-\frac{2\ell_{20}f_{2}}{S})\dot{\alpha}_{d2} + (\frac{2f_{23}}{S})\dot{\gamma}_{d2} + (N_{r2}-N_{\ell2})\theta_{0}$$

$$+ (RB_{2}) + (RV_{2}) = 0 \qquad (B.1.17)$$

Roll - Motor/Wheelset No. 2

$$(I_{c\alpha} + I_{d\alpha})\ddot{\alpha}_{d2} + (-2\ell_{17}^{2}K_{9})\alpha_{br} + (2\ell_{17}^{2}K_{9})\alpha_{d2}$$

$$+ (-2\ell_{19}^{2}C_{18})\dot{\alpha}_{br} + (2\ell_{19}^{2}C_{18})\dot{\alpha}_{d2}$$

$$+ (-Wn + \frac{2\ell_{20}\epsilon W}{\ell_{18}}v_{d2} + (\ell_{20}W)\alpha_{de2}$$

$$+ (-2\ell_{20}f_{2})\gamma_{d2} + (-\frac{2\ell_{20}f_{2}}{S})\dot{v}_{d2}$$

$$+ (\frac{2\ell_{20}^{2}f_{2}}{S})\dot{\alpha}_{d2} + (-\frac{2\ell_{20}f_{23}}{S})\dot{\gamma}_{d2}$$

$$+ (\frac{\ell_{18}}{2} - \ell_{20}\theta_{0})(N_{r2} - N_{\ell2}) = 0 \qquad (B.1.18)$$

Yaw - Wheelset No. 2

$$I_{d\gamma}\ddot{\gamma}_{d2} + (\frac{2f_{23}}{S})\dot{v}_{d2} + (-\frac{2\ell_{20}f_{32}}{S})\dot{\alpha}_{d2} + (\frac{\ell_{18}^2 f_1}{2S} + \frac{2f_3}{S})\dot{\gamma}_{d2} - \frac{\ell_{18}\lambda f_1}{\ell_{20}}v_{d2}$$

$$+ (2f_{32} - W\frac{\ell_{18}}{2}\theta_0)\gamma_{d2} + (RM_2) + (R\gamma_2) = 0 \qquad (B.1.19)$$

Lateral - Motor No. 3

$$m_c\ddot{v}_{c3} - (RV_3) = 0 \qquad (B.1.20)$$

Yaw - Motor No. 3

$$I_{c\gamma}\ddot{\gamma}_{c3} - \ell_{34}(RV_3) - (R\gamma_3) = 0 \qquad (B.1.21)$$

Lateral -- Wheelset No. 3

$$m_d\ddot{v}_{d3} + (\frac{2W\epsilon}{\ell_{18}})v_{d3} + (-W)\alpha_{de3} + (2f_2)\gamma_{d3} + (\frac{2f_2}{S})\dot{v}_{d3}$$

$$+ (-\frac{2\ell_{20}f_2}{S})\dot{\alpha}_{d3} + (\frac{2f_{23}}{S})\dot{\gamma}_{d3} + (N_{r3} - N_{\ell3})\theta_0$$

$$+ (RB_3) + (RV_3) = 0 \qquad (B.1.22)$$

Roll - Motor/Wheelset No. 3

$$(I_{c\alpha} + I_{d\alpha})\ddot{\alpha}_{d3} + (-2\ell_{17}^2 K_9)\alpha_{br} + (2\ell_{17}^2 K_9)\alpha_{d3}$$

$$+ [\ell_{19}^2(-C_{17} - C_{18})]\dot{\alpha}_{br} + [\ell_{19}^2(C_{17} + C_{18})\dot{\alpha}_{d3}$$

$$+ (-Wn + \frac{2\ell_{20}\epsilon W}{\ell_{18}})v_{d3} + (\ell_{20}W)\alpha_{de3}$$

$$+ (-2\ell_{20}f_2)\gamma_{d3} + (-\frac{2\ell_{20}f_2}{S})\dot{v}_{d3}$$

$$+ (\frac{2\ell_{20}^2 f_2}{S})\dot{\alpha}_{d3} + (-\frac{2\ell_{20}f_{23}}{S})\dot{\gamma}_{d3}$$

$$+ (\frac{\ell_{18}}{2} - \ell_{20}\theta_0)(N_{r3} - N_{\ell3}) = 0 \qquad (B.1.23)$$

Yaw – Wheelset No. 3

$$I_{d\gamma}\ddot{\gamma}_{d3} + (\frac{2f_{32}}{S})\dot{v}_{d3} + (-\frac{2\ell_{20}f_{32}}{S})\dot{\alpha}_{d3} + (\frac{\ell_{18}^2 f_1}{2S} + \frac{2f_3}{S})\dot{\gamma}_{d3} - \frac{\ell_{18}\lambda f_1}{\ell_{20}}v_{d3}$$

$$+ (2f_{32} - W\frac{\ell_{18}}{2}\theta_0)\gamma_{d3} + (RM_3) + (R\gamma_3) = 0 \qquad (B.1.24)$$

Lateral – Motor No. 4

$$m_c \ddot{v}_{c4} - (RV_4) = 0 \qquad (B.1.25)$$

Yaw – Motor No. 4

$$I_{c\gamma}\ddot{\gamma}_{c4} + \ell_{34}(RV_4) - (R\gamma_4) = 0 \qquad (B.1.26)$$

Lateral – Wheelset No. 4

$$m_d \ddot{v}_{d4} + (\frac{2W\epsilon}{\ell_{18}})v_{d4} + (-W)\alpha_{de4} + (2f_2)\gamma_{d4} + (\frac{2f_2}{S})\dot{v}_{d4}$$

$$+ (-\frac{2\ell_{20}f_2}{S})\dot{\alpha}_{d4} + (\frac{2f_{23}}{S})\dot{\gamma}_{d4} + (N_{r4} - N_{\ell4})\theta_0$$

$$+ (RB_4) + (RV_4) = 0 \qquad (B.1.27)$$

Roll – Motor/Wheelset No. 4

$$(I_{c\alpha} + I_{d\alpha})\ddot{\alpha}_{d4} + (-2\ell_{17}^2 K_9)\alpha_{bf} + (2\ell_{17}^2 K_9)\alpha_{d4}$$

$$+ [\ell_{19}^2(-C_{18} - C_{17})\dot{\alpha}_{bf} + [\ell_{19}^2(C_{18} + C_{17})\dot{\alpha}_{d4}$$

$$+ (-W\eta + \frac{2\ell_{20}\epsilon W}{\ell_{18}})v_{d4} + (\ell_{20}W)\alpha_{de4}$$

$$+ (-2\ell_{20}f_2)\gamma_{d4} + (-\frac{2\ell_{20}f_2}{S})\dot{v}_{d4}$$

$$+ (\frac{2\ell_{20}^2 f_2}{S})\dot{\alpha}_{d4} + (-\frac{2\ell_{20}f_{23}}{S})\dot{\gamma}_{d4}$$

$$+ (\frac{\ell_{18}}{2} - \ell_{20}\theta_0)(N_{r4} - N_{\ell4}) = 0 \qquad (B.1.28)$$

Yaw – Wheelset No. 4

$$I_{d\gamma}\ddot{\gamma}_{d4} + (\frac{2f_{32}}{S})\dot{v}_{d4} + (-\frac{2\ell_{20}f_{32}}{S})\dot{\alpha}_{d4} + (\frac{\ell_{18}^2 f_1}{2S} + \frac{2f_3}{S})\dot{\gamma}_{d4} - \frac{\ell_{18}\lambda f_1}{\ell_{20}}v_{d4}$$

$$+ (2f_{32} - W\frac{\ell_{18}}{2}\theta_0)\gamma_{d4} + (RM_4) + (RY_4) = 0 \qquad (B.1.29)$$

Lateral – Motor No. 5

$$m_c\ddot{v}_{c5} - (RV_5) = 0 \qquad (B.1.30)$$

Yaw – Motor No. 5

$$I_{c\gamma}\ddot{\gamma}_{c5} + \ell_{34}(RV_5) - (RY_5) = 0 \qquad (B.1.31)$$

Lateral – Wheelset No. 5

$$m_d\ddot{v}_{d5} + (\frac{2W\epsilon}{\ell_{18}})v_{d5} + (-W)\alpha_{de5} + (2f_2)\gamma_{d5} + (\frac{2f_2}{S})\dot{v}_{d5}$$

$$+ (-\frac{2\ell_{20}f_2}{S})\dot{\alpha}_{d5} + (\frac{2f_{23}}{S})\dot{\gamma}_{d5} + (N_{r5} - N_{\ell5})\theta_0$$

$$+ (RB_5) + (RV_5) = 0 \qquad (B.1.32)$$

Roll – Motor/Wheelset No. 5

$$(I_{c\alpha} + I_{d\alpha})\ddot{\alpha}_{d5} + (-2\ell_{17}^2 K_9)\alpha_{bf} + (2\ell_{17}^2 K_9)\alpha_{d5}$$

$$+ (-2\ell_{19}^2 C_{18})\dot{\alpha}_{bf} + (2\ell_{19}^2 C_{18})\dot{\alpha}_{d5}$$

$$+ (-W\eta + \frac{2\ell_{20}\epsilon W}{\ell_{18}})v_{d5} + (\ell_{20}W)\alpha_{de5}$$

$$+ (-2\ell_{20}f_2)\gamma_{d5} + (-\frac{2\ell_{20}f_2}{S})\dot{v}_{d5}$$

$$+ (\frac{2\ell_{20}^2 f_2}{S})\dot{\alpha}_{d5} + (-\frac{2\ell_{20}f_{23}}{S})\dot{\gamma}_{d5}$$

$$+ (\frac{\ell_{18}}{2} - \ell_{20}\theta_0)(N_{r5} - N_{\ell5}) = 0 \qquad (B.1.33)$$

Yaw - Wheelset No. 5

$$I_{d\gamma}\ddot{\gamma}_{d5} + (\frac{2f_{32}}{S})\dot{v}_{d5} + (-\frac{2\ell_{20}f_{32}}{S})\dot{\alpha}_{d5} + (\frac{\ell_{18}^2 f_1}{2S} + \frac{2f_3}{S})\dot{\gamma}_{d5} - \frac{\ell_{18}\lambda f_1}{\ell_{20}}v_{d5}$$

$$+ (2f_{32} - W\frac{\ell_{18}}{2}\theta_0)\gamma_{d5} + (RM_5) + (R\gamma_5) = 0 \qquad (B.1.34)$$

Lateral - Motor No. 6

$$m_c\ddot{v}_{c6} - (RV_6) = 0 \qquad (B.1.35)$$

Yaw - Motor No. 6

$$I_{c\gamma}\ddot{\gamma}_{c6} + \ell_{34}(RV_6) - (R\gamma_6) = 0 \qquad (B.1.36)$$

Lateral - Wheelset No. 6

$$m_d\ddot{v}_{d6} + (\frac{2W\epsilon}{\ell_{18}})v_{d6} + (-W)\alpha_{de6} + (2f_2)\gamma_{d6} + (\frac{2f_2}{S})\dot{v}_{d6}$$

$$+ (-\frac{2\ell_{20}f_2}{S})\dot{\alpha}_{d6} + (\frac{2f_{23}}{S})\dot{\gamma}_{d6} + (N_{r6} - N_{\ell6})\theta_0$$

$$+ (RB_6) + (RV_6) = 0 \qquad (B.1.37)$$

Roll - Motor/Wheelset No. 6

$$(I_{c\alpha} + I_{d\alpha})\ddot{\alpha}_{d6} + (-2\ell_{17}^2 K_9)\alpha_{bf} + (2\ell_{17}^2 K_9)\alpha_{d6}$$

$$+ [\ell_{19}^2(-C_{17} - C_{18})]\dot{\alpha}_{bf} + [\ell_{19}^2(C_{17} + C_{18})\dot{\alpha}_{d6}$$

$$+ (-Wn + \frac{2\ell_{20}\epsilon W}{\ell_{18}})v_{d6} + (\ell_{20}W)\alpha_{de6}$$

$$+ (-2\ell_{20}f_2)\gamma_{d6} + (-\frac{2\ell_{20}f_2}{S})\dot{v}_{d6}$$

$$+ (\frac{2\ell_{20}^2 f_2}{S})\dot{\alpha}_{d6} + (-\frac{2\ell_{20}f_{23}}{S})\dot{\gamma}_{d6}$$

$$+ (\frac{\ell_{18}}{2} - \ell_{20}\theta_0)(N_{r6} - N_{\ell6}) = 0 \qquad (B.1.38)$$

Yaw - Wheelset No. 6

$$I_{d\gamma}\ddot{\gamma}_{d6} + (\frac{2f_{32}}{S})\dot{v}_{d6} + (-\frac{2\ell_{20}f_{32}}{S})\dot{\alpha}_{d6} + (\frac{\ell_{18}}{2S} + \frac{2f_3}{S})\dot{\gamma}_{d6} - \frac{\ell_{18}\lambda f_1}{\ell_{20}}v_{d6}$$

$$+ (2f_{32} - W\frac{\ell_{18}}{2}\theta_0)\gamma_{d6} + (RM_6) + (R\gamma_6) = 0 \qquad (B.1.39)$$

Roll - Track/Motor/Wheelset No. 1

$$(I_{c\alpha} + I_{d\alpha} + \frac{1}{4}\ell_{18}^2 m_e)\ddot{\alpha}_{de1} + (-W)v_{d1} + (-2\ell_{17}^2 K_9)\alpha_{br}$$

$$+ (2\ell_{17}^2 K_9 + \frac{1}{2}\ell_{18}^2 K'_e)\alpha_{de1} + [\ell_{19}^2(-C_{17}-C_{18})]\dot{\alpha}_{br}$$

$$+ [\ell_{19}^2(C_{17}+C_{18}) + \frac{1}{2}\ell_{18}^2 C'_e]\dot{\alpha}_{de1} = 0 \qquad (B.1.40)$$

Roll - Track/Motor/Wheelset No. 2

$$(I_{c\alpha} + I_{d\alpha} + \frac{1}{4}\ell_{18}^2 m_e)\ddot{\alpha}_{de2} + (-W)v_{d2} + (-2\ell_{17}^2 K_9)\alpha_{br}$$

$$+ (2\ell_{17}^2 K_9 + \frac{1}{2}\ell_{18}^2 K'_e)\alpha_{de2} + (-2\ell_{19}^2 C_{18})\dot{\alpha}_{de2}$$

$$+ (2\ell_{19}^2 C_{18} + \frac{1}{2}\ell_{18}^2 C'_e)\dot{\alpha}_{de2} = 0 \qquad (B.1.41)$$

Roll - Track/Motor/Wheelset No. 3

$$(I_{c\alpha} + I_{d\alpha} + \frac{1}{4}\ell_{18}^2 m_e)\ddot{\alpha}_{de3} + (-W)v_{d3} + (-2\ell_{17}^2 K_9)\alpha_{br}$$

$$+ (2\ell_{17}^2 K_9 + \frac{1}{2}\ell_{18}^2 K'_e)\alpha_{de3} + [\ell_{19}^2(-C_{17}-C_{18})]\dot{\alpha}_{br}$$

$$+ [\ell_{19}^2(C_{17}+C_{18}) + \frac{1}{2}\ell_{18}^2 C'_e]\dot{\alpha}_{de3} = 0 \qquad (B.1.42)$$

Roll - Track/Motor/Wheelset No. 4

$$(I_{c\alpha} + I_{d\alpha} + \frac{1}{4}\ell_{18}^2 m_e)\ddot{\alpha}_{de4} + (-W)v_{d4} + (-2\ell_{17}^2 K_9)\alpha_{bf}$$

$$+ (2\ell_{17}^2 K_9 + \frac{1}{2}\ell_{18}^2 K'_e)\alpha_{de4} + [\ell_{19}^2(-C_{17}-C_{18})]\dot{\alpha}_{bf}$$

$$+ [\ell_{19}^2(C_{17}+C_{18}) + \frac{1}{2}\ell_{18}^2 C'_e]\dot{\alpha}_{de4} = 0 \qquad (B.1.43)$$

Roll - Track/Motor/Wheelset No. 5

$$(I_{c\alpha} + I_{d\alpha} + \tfrac{1}{4}\ell_{18}^2 m_e)\ddot{\alpha}_{de5} + (-W)v_{d5} + (-2\ell_{17}^2 K_9)\alpha_{bf}$$

$$+ (2\ell_{17}^2 K_9 + \tfrac{1}{2}\ell_{18}^2 K_e')\alpha_{de5} + (-2\ell_{19}C_{18})\dot{\alpha}_{bf}$$

$$+ (2\ell_{19}^2 C_{18} + \tfrac{1}{2}\ell_{18}^2 C_e')\dot{\alpha}_{de5} = 0 \qquad\qquad (B.1.44)$$

Roll - Track/Motor/Wheelset No. 6

$$(I_{c\alpha} + I_{d\alpha} + \tfrac{1}{4}\ell_{18}^2 m_e)\ddot{\alpha}_{de6} + (-W)v_{d6} + (-2\ell_{17}^2 K_9)\alpha_{bf}$$

$$+ (2\ell_{17}^2 K_9 + \tfrac{1}{2}\ell_{18}^2 K_e')\alpha_{de6} + [\ell_{19}^2(-C_{17}-C_{18})]\dot{\alpha}_{bf}$$

$$+ [\ell_{19}^2(C_{17}+C_{18}) + \tfrac{1}{2}\ell_{18}^2 C_e']\dot{\alpha}_{de6} = 0 \qquad\qquad (B.1.45)$$

The equations describing the lateral motions (equations (B.1.1) to (B.1.45)) are of the general form:

$$[\tilde{A}]\{\ddot{z}\} + [\tilde{C}]\{\dot{z}\} + [\tilde{B}]\{z\} + \{R\} = \{0\} \qquad (B.1.46)$$
$$45 \times 45 \quad 45 \times 1 \qquad\qquad 45 \times 1$$

where $\tilde{A}$ is the inertia matrix

$\tilde{C}$ is the damping matrix

$\tilde{B}$ is the stiffness matrix

and R is the vector of internal reaction given by:

Mode	Equation No.	Reaction
v_a	B.1.1	0
α_a	.2	0
Y_a	.3	0
v_{br}	.4	$-(RB_1 + RB_2 + RB_3)$
α_{br}	.5	$\ell_{21}(RB_1 + RB_2 + RB_3)$

Mode	Equation No.	Reaction
γ_{br}	B.1.6	$= \ell_{24}(RB_1) - \ell_{26}(RB_2) + \ell_{23}(RB_1)$ $- (RM_1 + RM_2 + RM_3)$
v_{bf}	.7	$-(RB_4 + RB_5 + RB_6)$
α_{bf}	.8	$\ell_{21}(RB_4 + RB_5 + RB_6)$
γ_{bf}	.9	$-\ell_{23}(RB_4) + \ell_{26}(RB_5) + \ell_{24}(RB_6)$ $- (RM_4 + RM_5 + RM_6)$
v_{c1}	.10	$-RV_1$
γ_{c1}	.11	$-\ell_{34}(RV_1) - RY_1$
v_{d1}	.12	$RB_1 + RV_1 + (N_{r1} - N_{\ell 1})\theta_0$
α_{d1}	.13	$(\frac{\ell_{18}}{2} - \ell_{20}\theta_0)(N_{r1} - N_{\ell 1})$
γ_{d1}	.14	$RM_1 + RY_1$
v_{c2}	.15	$-RV_2$
γ_{c2}	.16	$-\ell_{34}(RV_2) - RY_2$
v_{d2}	.17	$RB_2 + RV_2 + (N_{r2} - N_{\ell 2})\theta_0$
α_{d2}	.18	$(\frac{\ell_{18}}{2} - \ell_{20}\theta_0)(N_{r2} - N_{\ell 2})$
γ_{d2}	.19	$RM_2 + RY_2$
v_{c3}	.20	$-RV_3$
γ_{c3}	.21	$-\ell_{34}(RV_3) - RY_3$
v_{d3}	.22	$RB_3 + RV_3 + (N_{r3} - N_{\ell 3})\theta_0$
α_{d3}	.23	$(\frac{\ell_{18}}{2} - \ell_{20}\theta_0)(N_{r3} - N_{\ell 3})$
γ_{d3}	.24	$RM_3 + RY_3$
v_{c4}	.25	$-RV_4$
γ_{c4}	.26	$\ell_{34}(RV_4) - RY_4$

Mode	Equation No.	Reaction
v_{d4}	B.1.27	$RB_4 + RV_4 + (N_{r4} - N_{\ell 4})\theta_0$
α_{d4}	.28	$(\frac{\ell_{18}}{2} - \ell_{20}\theta_0)(N_{r4} - N_{\ell 4})$
γ_{d4}	.29	$RM_4 + R\gamma_4$
v_{c5}	.30	$-RV_5$
γ_{c5}	.31	$\ell_{34}(RV_5) - R\gamma_5$
v_{d5}	.32	$RB_5 + RV_5 + (N_{r5} - N_{\ell 5})\theta_0$
α_{d5}	.33	$(\frac{\ell_{18}}{2} - \ell_{20}\theta_0)(N_{r5} - N_{\ell 5})$
γ_{d5}	.34	$RM_5 + R\gamma_5$
v_{c6}	.35	$-RV_6$
γ_{c6}	.36	$\ell_{34}(RV_6) - R\gamma_6$
v_{d6}	.37	$RB_6 + RV_6 + (N_{r6} - N_{\ell 6})\theta_0$
α_{d6}	.38	$(\frac{\ell_{18}}{2} - \ell_{20}\theta_0)(N_{r6} - N_{\ell 6})$
γ_{d6}	.39	$RM_6 + R\gamma_6$
α_{de1}	.40	0
α_{de2}	.41	0
α_{de3}	.42	0
α_{de4}	.43	0
α_{de5}	.44	0
α_{de6}	.45	

The reactions are eliminated from the equation (B.1.46) using the method of substitution as described below. For simplicity the equations are designated by their corresponding

numbers (i.e., 1 refers to equation (B.1.1), 2 to equation (B.1.2),..., and so on).

$$1 = 1$$

$$2 = 2$$

$$3 = 3$$

$$4 = 4 + (10+12+\rho \cdot 13) + (15+17+\rho \cdot 18) + (20+22+\rho \cdot 23)$$

$$5 = 5 - \ell_{21}[(10+12+\rho \cdot 13) + (15+17+\rho \cdot 18) + (20+22+\rho \cdot 23)]$$

$$6 = 6 + [\ell_{24}(10+12+\rho \cdot 13) + \ell_{26}(15+17+\rho \cdot 18) - \ell_{23}(20+22+\rho \cdot 23)]$$
$$- \ell_{34}[(10+15+20) + (11+16+21) + (14+19+24)]$$

$$7 = 7 + (25+27+\rho \cdot 28) + (30+32+\rho \cdot 33) + (35+37+\rho \cdot 38)$$

$$8 = 8 - \ell_{21}[(25+27+\rho \cdot 28) + (30+32+\rho \cdot 33) + (35+37+\rho \cdot 38)]$$

$$9 = 9 + [\ell_{23}(25+27+\rho \cdot 28) - \ell_{26}(30+32+\rho \cdot 33) - \ell_{24}(35+37+\rho \cdot 38)]$$
$$+ \ell_{34}[(25+30+35) + (26+31+36) + (29+34+39)]$$

$$10 = 40$$

$$11 = 41$$

$$12 = 42$$

$$13 = 43$$

$$14 = 44$$

$$15 = 45$$

where

$$\rho = \frac{-\xi_0}{\frac{\ell_{18}}{2} - \ell_{20}\theta_0}$$

After the elimination of the reactions, the system of equations (B.1.46) becomes:

$$[A]_{15 \times 45} \{\ddot{z}\}_{45 \times 1} + [C]\{\dot{z}\} + [B]\{z\} = \{0\} \qquad (B.1.47)$$

That is a system of fifteen equations in fourty-five unknowns, only fifteen of which are independent. The relation between all the unknown displacements and the independent ones will be given by the transformation matrix [T] based on the equations of constraints. The equations defining the constraints are:

(A) Constraints between Wheelsets and Frames

$$v_{d1} = v_{br} - \ell_{21}\alpha_{br} + \ell_{24}\gamma_{br}$$

$$v_{d2} = v_{br} - \ell_{21}\alpha_{br} + \ell_{26}\gamma_{br}$$

$$v_{d3} = v_{br} - \ell_{21}\alpha_{br} - \ell_{23}\gamma_{br}$$

$$v_{d4} = v_{bf} - \ell_{21}\alpha_{bf} + \ell_{23}\gamma_{bf}$$

$$v_{d5} = v_{bf} - \ell_{21}\alpha_{bf} - \ell_{26}\gamma_{bf}$$

$$v_{d6} = v_{bf} - \ell_{21}\alpha_{bf} - \ell_{24}\gamma_{bf}$$

$$\gamma_{d1} = \gamma_{br} \qquad \gamma_{d4} = \gamma_{bf}$$

$$\gamma_{d2} = \gamma_{br} \qquad \gamma_{d5} = \gamma_{bf}$$

$$\gamma_{d3} = \gamma_{br} \qquad \gamma_{d6} = \gamma_{bf}$$

(B) Constraints between Motors and Wheelsets

$$\left.\begin{array}{l} \alpha_{d1} = \alpha_{c1} \\[6pt] \alpha_{d2} = \alpha_{c2} \\[6pt] \alpha_{d3} = \alpha_{c3} \\[6pt] \alpha_{d4} = \alpha_{c4} \\[6pt] \alpha_{d5} = \alpha_{c5} \\[6pt] \alpha_{d6} = \alpha_{c6} \end{array}\right\}$$

These relations have already been satisfied by combining the wheelset and motor equations

$$v_{c1} = v_{br} - \ell_{21}\alpha_{br} + \ell_{24}\gamma_{br} - \ell_{34}\gamma_{c1}$$

$$v_{c2} = v_{br} - \ell_{21}\alpha_{br} + \ell_{26}\gamma_{br} - \ell_{34}\gamma_{c2}$$

$$v_{c3} = v_{br} - \ell_{21}\alpha_{br} - \ell_{23}\gamma_{br} - \ell_{34}\gamma_{c3}$$

$$v_{c4} = v_{bf} - \ell_{21}\alpha_{bf} + \ell_{23}\gamma_{bf} + \ell_{34}\gamma_{c4}$$

$$v_{c5} = v_{bf} - \ell_{21}\alpha_{bf} - \ell_{26}\gamma_{bf} + \ell_{34}\gamma_{c5}$$

$$v_{c6} = v_{bf} - \ell_{21}\alpha_{bf} - \ell_{24}\gamma_{bf} + \ell_{34}\gamma_{c6}$$

$$\gamma_{d1} = \gamma_{c1} \qquad\qquad \gamma_{d4} = \gamma_{c4}$$

$$\gamma_{d2} = \gamma_{c2} \qquad\qquad \gamma_{d5} = \gamma_{c5}$$

$$\gamma_{d3} = \gamma_{c3} \qquad\qquad \gamma_{d6} = \gamma_{c6}$$

(C) Additional Constraints

The constraint between the wheelsets and rails (due to the conicity of the wheels) yields the following constraints:

$$\alpha_{d1} = -\psi\, v_{d1} \qquad\qquad \alpha_{d4} = -\psi\, v_{d4}$$

$$\alpha_{d2} = -\psi\, v_{d2} \qquad\qquad \alpha_{d5} = -\psi\, v_{d5}$$

$$\alpha_{d3} = -\psi\, v_{d3} \qquad\qquad \alpha_{d6} = -\psi\, v_{d6}$$

where v_{di} $(i = 1,\ldots,6)$ is the relative lateral displacement between the wheelsets and the rail.

The Transformation Matrix [T]

This matrix gives the relation between all the variables and the independent variables, based on the equations of constraints. The matrix [T] is given in Table (B.1) where

$$\rho_1 = -\psi \qquad\qquad \rho_2 = \ell_{21}\,\psi$$

$$\rho_3 = -\ell_{24}\,\psi \qquad\qquad \rho_4 = \ell_{24} - \ell_{34}$$

$$\rho_5 = \ell_{26} - \ell_{34} \qquad\qquad \rho_6 = -(\ell_{23} + \ell_{34})$$

$$\rho_7 = -\ell_{26}\,\psi \qquad\qquad \rho_8 = \ell_{23}\,\psi$$

TABLE (A.1)

THE TRANSFORMATION MATRIX [T]

NUMBER	MODE	1 v_a	2 a_a	3 γ_a	4 v_{br}	5 a_{br}	6 γ_{br}	7 v_{bf}	8 a_{bf}	9 γ_{bf}	10 a_{de1}	11 a_{de2}	12 a_{de3}	13 a_{de4}	14 a_{de5}	15 a_{de6}
					G E N E R A L I Z E D					C O O R D I N A T E S						
1	v_a	1														
2	a_a		1													
3	γ_a			1												
4	v_{br}				1											
5	a_{br}					1										
6	γ_{br}						1									
7	v_{bf}															
8	a_{bf}								1							
9	γ_{bf}									1						
10	v_{c1}				1	$-\ell_{21}$	ρ_4									
11	γ_{c1}						1									
12	v_{d1}				1	$-\ell_{21}$	ℓ_{24}									
13	a_{d1}				ρ_1	ρ_2	ρ_3									
14	γ_{d1}						1									
15	v_{c2}				1	$-\ell_{21}$	ρ_5									
16	γ_{c2}						1									
17	v_{d2}				1	$-\ell_{21}$	ℓ_{26}									
18	a_{d2}				ρ_1	ρ_2	ρ_7									
19	γ_{d2}						1									
20	v_{c3}				1	$-\ell_{21}$	ρ_6									
21	γ_{c3}						1									
22	v_{d3}				1	$-\ell_{21}$	$-\ell_{23}$									
23	a_{d3}				ρ_1	ρ_2	ρ_8									
24	γ_{d3}						1									
25	v_{c4}							1	$-\ell_{21}$	$-\rho_6$						
26	γ_{c4}									1						
27	v_{d4}							1	$-\ell_{21}$	ℓ_{23}						
28	a_{d4}							1	ρ_2	$-\rho_8$						
29	γ_{d4}									1						
30	v_{c5}							1	$-\ell_{21}$	$-\rho_5$						
31	γ_{c5}									1						
32	v_{d5}							1	$-\ell_{21}$	$-\ell_{26}$						
33	a_{d5}							1	ρ_2	$-\rho_7$						
34	γ_{d5}									1						
35	v_{c6}							1	$-\ell_{21}$	$-\rho_4$						
36	γ_{c6}									1						
37	v_{d6}							1	$-\ell_{21}$	$-\ell_{24}$						
38	a_{d6}							1	ρ_2	$-\rho_3$						
39	γ_{d6}									1						
40	a_{de1}										1					
41	a_{de2}											1				
42	a_{de3}												1			
43	a_{de4}													1		
44	a_{de5}														1	
45	a_{de6}															1

To eliminate the dependent variables from the
equations of motion, the transformation matrix [T] is used.
This matrix relates all the displacements $\{z\}$ to the
generalized coordinates $\{x\}$ as follows:

$$\underset{45 \times 1}{\{z\}} = \underset{45 \times 15}{[T]} \quad \underset{15 \times 1}{\{x\}} \qquad (B.1.48)$$

Substituting for $\{z\}$ from equation (B.1.48) back in
equation (B.1.47) we get

$$\underset{15 \times 45}{[A]} \quad \underset{45 \times 15}{[T]} \quad \underset{15 \times 1}{\{\ddot{x}\}} + [\dot{C}][T]\{\dot{x}\} + [B][T]\{x\} = \{0\}$$

$$(B.1.49)$$

which after carrying the matrix multiplication gives the
following system of fifteen equations in fifteen
independent coordinates.

$$\underset{15 \times 15}{[AT]} \quad \underset{15 \times 1}{\{\ddot{x}\}} + [CT]\{\dot{x}\} + [BT]\{x\} = \{0\} \qquad (B.1.50)$$

It should be noted that because of the introduction
of the non-conservative creep forces, the inertia, damping
and stiffness matrices ([AT], [CT] and [BT] respectively),
are not symmetric.

B.2 Equations of Motion for Longitudinal Vibrations

Longitudinal - Body

$$m_a \ddot{u}_a + (2K_1 + 4K_4 + 4K_7)u_a + (-K_1 - 2K_4 - 2K_7)u_{bf}$$

$$+ (-K_1 - 2K_4 - 2K_7)u_{br} + (2\ell_1 K_1 + 4\ell_7 K_4 + 4\ell_7 K_7)\beta_a$$

$$+ (\ell_2 K_1 + 2\ell_{33} K_4 + 2\ell_{33} K_7)\beta_{bf}$$

$$+ (\ell_2 K_1 + 2\ell_{33} K_4 + 2\ell_{33} K_7)\beta_{br}$$

$$+ (-C_1 - 2C_4 - 2C_7 - 2C_{14} \cos \alpha_1 - 2C_{16} \cos \alpha_2)\dot{u}_{bf}$$

$$+ (-C_1 - 2C_4 - 2C_7 - 2C_{14} \cos \alpha_1 - 2C_{16} \cos \alpha_2)\dot{u}_{br}$$

$$+ (2\ell_1 C_1 + 4\ell_7 C_4 + 4\ell_7 C_7 + 4\ell_{15} C_{14} \cos \alpha_1$$

$$+ 4\ell_{15} C_{16} \cos \alpha_2)\dot{\beta}_a$$

$$+ (\ell_2 C_1 + 2\ell_{33} C_4 + 2\ell_{33} C_7 + 2\ell_{32} C_{14} \cos \alpha_1$$

$$+ 2\ell_{32} C_{16} \cos \alpha_2)\dot{\beta}_{bf}$$

$$+ (\ell_2 C_1 + 2\ell_{33} C_4 + 2\ell_{33} C_7 + 2\ell_{32} C_{14} \cos \alpha_1$$

$$+ 2\ell_{32} C_{16} \cos \alpha_2)\dot{\beta}_{br}$$

$$+ (2C_1 + 4C_4 + 4C_7 + 4C_{14} \cos \alpha_1 + 4C_{16} \cos \alpha_2)\dot{u}_a = 0$$

$$(B.2.1)$$

Vertical - Body

$$m_a \ddot{w}_a + (4K_3 + 4K_6)w_a + (-2K_3 - 2K_6)w_{bf} + (-2K_3 - 2K_6)w_{br}$$

$$+ (-2\ell_4 K_3 + 2\ell_5 K_6)\beta_{bf} + (2\ell_4 K_3 - 2\ell_5 K_6)\beta_{br}$$

$$+ (4C_3 + 4C_6)\dot{w}_a + (-2C_3 - 2C_6)\dot{w}_{bf} + (-2C_3 - 2C_6)\dot{w}_{br}$$

$$+ (-2\ell_4 C_3 + 2\ell_5 C_6)\dot{\beta}_{bf} + (2\ell_4 C_3 - 2\ell_5 C_6)\dot{\beta}_{br} = 0 \quad (B.2.2)$$

Pitch - Body

$$I_{a\beta}\ddot{\beta}_a + (2\ell_1 K_1 + 4\ell_7 K_4 + 4\ell_7 K_7)u_a$$

$$+ (-\ell_1 K_1 - 2\ell_7 K_4 - 2\ell_7 K_7)u_{bf}$$

$$+ (-\ell_1 K_1 - 2\ell_7 K_4 - 2\ell_7 K_7)u_{br}$$

$$+ (-2(\ell_3+\ell_4)K_3 - 2(\ell_3-\ell_5)K_6)w_{bf}$$

$$+ (+2(\ell_3+\ell_4)K_3 + 2(\ell_3-\ell_5)K_6)w_{br}$$

$$+ (2\ell_1^2 K_1 + 4(\ell_3+\ell_4)^2 K_3 + 4(\ell_3-\ell_5)^2 K_6 + 4\ell_7^2 K_4$$

$$+ 4\ell_7^2 K_7)\beta_a$$

$$+ (\ell_1\ell_2 K_1 - 2\ell_4(\ell_3+\ell_4)K_3 + 2\ell_5(\ell_3-\ell_5)K_6 + 2\ell_7\ell_{33}K_4$$

$$+ 2\ell_7\ell_{33}K_7)\beta_{bf}$$

$$+ (\ell_1\ell_2 K_1 - 2\ell_4(\ell_3+\ell_4)K_3 + 2\ell_5(\ell_3-\ell_5)K_6 + 2\ell_7\ell_{33}K_4$$

$$+ 2\ell_7\ell_{33}K_7)\beta_{br}$$

$$+ (2\ell_1 C_1 + 4\ell_7 C_4 + 4\ell_7 C_7 + 4\ell_{15}C_{14}\cos\alpha_1$$

$$+ 4\ell_{15}C_{16}\cos\alpha_2)\dot{u}_a$$

$$+ (-\ell_1 C_1 - 2\ell_7 C_4 - 2\ell_7 C_7 - 2\ell_{15}C_{14}\cos\alpha_1$$

$$- 2\ell_{15}C_{16}\cos\alpha_2)\dot{u}_{bf}$$

$$+ (-\ell_1 C_1 - 2\ell_7 C_4 - 2\ell_7 C_7 - 2\ell_{15}C_{14}\cos\alpha_1$$

$$- 2\ell_{15}C_{16}\cos\alpha_2)\dot{u}_{br}$$

$$+ (-2(\ell_3+\ell_4)C_3 - 2(\ell_3-\ell_5)C_6)\dot{w}_{bf}$$

$$+ (2(\ell_3+\ell_4)C_3 + 2(\ell_3-\ell_5)C_6)\dot{w}_{br}$$

$$+ [\ell_1 \ell_2 C_1 - 2\ell_4(\ell_3+\ell_4)C_3 + 2\ell_5(\ell_3-\ell_5)C_6 + 2\ell_7 \ell_{33} C_4$$

$$+ 2\ell_7 \ell_{33} C_7 + 2\ell_{15} \ell_{32} C_{14} \cos \alpha_1$$

$$+ 2\ell_{15} \ell_{32} C_{16} \cos \alpha_2] \dot{\beta}_{bf}$$

$$+ [\ell_1 \ell_2 C_1 - 2\ell_4(\ell_3+\ell_4)C_3 + 2\ell_5(\ell_3-\ell_5)C_6 + 2\ell_7 \ell_{33} C_4$$

$$+ 2\ell_7 \ell_{33} C_7 + 2\ell_{15} \ell_{32} C_{14} \cos \alpha_1$$

$$+ 2\ell_{15} \ell_{32} C_{16} \cos \alpha_2] \dot{\beta}_{br}$$

$$+ [2\ell_1^2 C_1 + 4(\ell_3+\ell_4)^2 C_3 + 4(\ell_3-\ell_5)^2 C_6 + 4\ell_7^2 C_4 + 4\ell_7^2 C_7$$

$$+ 4\ell_{15}^2 C_{14} \cos \alpha_1 + 4\ell_{15}^2 C_{16} \cos \alpha_2] \dot{\beta}_a = 0 \quad (B.2.3)$$

Longitudinal - Rear Frame

$$m_b \ddot{u}_{br} + (-K_1 - 2K_4 - 2K_7)u_a + (K_1 + 2K_4 + 2K_7)u_{br}$$

$$+ (-\ell_1 K_1 - 2\ell_7 K_4 - 2\ell_7 K_7)\beta_a$$

$$+ (-\ell_2 K_1 - 2\ell_{33} K_4 - 2\ell_{33} K_7)\beta_{br}$$

$$+ (-C_1 - 2C_4 - 2C_7 - 2C_{14} \cos \alpha_1$$

$$- 2C_{16} \cos \alpha_2)(\dot{u}_a - \dot{u}_{br})$$

$$+ (-\ell_1 C_1 - 2\ell_7 C_4 - 2\ell_7 C_7 - 2\ell_{15} C_{14} \cos \alpha_1$$

$$- 2\ell_{15} C_{16} \cos \alpha_2)\dot{\beta}_a$$

$$+ (-\ell_2 C_1 - 2\ell_{33} C_4 - 2\ell_{33} C_7 - 2\ell_{32} C_{14} \cos \alpha_1$$

$$- 2\ell_{32} C_{16} \cos \alpha_2)\dot{\beta}_{br}$$

$$- (RA_1 + RA_2 + RA_3) = 0 \quad\quad\quad (B.2.4)$$

Vertical - Rear Frame

$$m_b \ddot{w}_{br} + (-2K_3 - 2K_6)w_a + (2K_3 + 2K_6 + 6K_9 + 3K_{10})w_{br}$$

$$+ (-K_{10})w_{c1} + (-K_{10})w_{c2} + (-K_{10})w_{c3} + (-2K_9)w_{d1}$$

$$+ (-2K_9)w_{d2} + [2(\ell_3+\ell_4)K_3 + 2(\ell_3-\ell_5)K_6]\beta_a$$

$$+ (-2K_9)w_{d3}$$

$$+ [-2\ell_4 K_3 + 2\ell_5 K_6 - 2(\ell_{23} + \ell_{26} + \ell_{24})K_9 - (\ell_{25}$$

$$- \ell_{27} + \ell_{22})K_{10}]\beta_{br}$$

$$+ [-\ell_{35}K_{10}]\beta_{c1} + [-\ell_{35}K_{10}]\beta_{c2} + [-\ell_{35}K_{10}]\beta_{c3}$$

$$+ (-2C_3 - 2C_6)\dot{w}_a + (2C_3 + 2C_6 + 2C_{17} + 4C_{18} + 3C_{10})\dot{w}_{br}$$

$$+ (-C_{17} - C_{18})\dot{w}_{d1} + (-2C_{18})\dot{w}_{d2} + (-C_{17} - C_{18})\dot{w}_{d3}$$

$$- (C_{10})\dot{w}_{c1} + (-C_{10})\dot{w}_{c2} + (-C_{10})\dot{w}_{c3}$$

$$+ [2(\ell_3+\ell_4)C_3 + 2(\ell_3-\ell_5)C_6]\dot{\beta}_a$$

$$+ [-2\ell_4 C_3 + 2\ell_5 C_6 + (-\ell_{24}+\ell_{23})C_{17} + (-\ell_{24}-2\ell_{26}+\ell_{23})C_{18}$$

$$+ (\ell_{25}+\ell_{27}-\ell_{22})C_{10}]\dot{\beta}_{br}$$

$$+ (-\ell_{35}C_{10})\dot{\beta}_{c1} + (-\ell_{35}C_{10})\dot{\beta}_{c2} + (-\ell_{35}C_{10})\dot{\beta}_{c3} = 0 \quad (B.2.5)$$

Pitch - Rear Frame

$$I_{b\beta}\ddot{\beta}_{br} + (\ell_2 K_1 + 2\ell_{33}K_4 + 2\ell_{33}K_7)u_a$$

$$+ (-\ell_2 K_1 - 2\ell_{33}K_4 - 2\ell_{33}K_7)u_{br}$$

$$+ [2\ell_4 K_3 - 2\ell_5 K_6]w_a + (\ell_{22}K_{10})w_{c1} + (-\ell_{27}K_{10})w_{c2}$$

$$+ (-\ell_{25}K_{10})w_{c3}$$

$$+ (2\ell_{24}K_9)\dot{w}_{d1} + (2\ell_{26}K_9)\dot{w}_{d2} + (-2\ell_{33}K_9)\dot{w}_{d3}$$

$$+ [-2\ell_4 K_3 + 2\ell_5 K_6 + 2(-\ell_{24}-\ell_{26}+\ell_{23})K_9$$
$$+ (-\ell_{22}+\ell_{27}+\ell_{25})K_{10}]w_{br}$$

$$+ [\ell_2\ell_1 K_1 + 2\ell_{33}\ell_7 K_4 + 2\ell_{33}\ell_7 K_7 - 2\ell_4(\ell_3+\ell_4)K_3$$
$$+ 2\ell_5(\ell_3-\ell_5)K_6]\beta_a$$

$$+ [\ell_2^2 K_1 + 2\ell_{33}^2 K_4 + 2\ell_{33}^2 K_7 + 2\ell_4^2 K_3 + 2\ell_5^2 K_6$$
$$+ 2(\ell_{24}^2+\ell_{26}^2+\ell_{23}^2)K_9 + (\ell_{22}^2+\ell_{27}^2+\ell_{25}^2)K_{10}]\beta_{br}$$

$$+ [\ell_{22}\ell_{35}K_{10}]\beta_{c1} + [-\ell_{27}\ell_{35}K_{10}]\beta_{c2} + [-\ell_{25}\ell_{35}K_{10}]\beta_{c3}$$

$$+ (\ell_2 C_1 + 2\ell_{33}C_4 + 2\ell_{33}C_7 + 2\ell_{32}C_{14}\cos\alpha_1$$
$$+ 2\ell_{32}C_{16}\cos\alpha_2)\dot{u}_a$$

$$+ (-\ell_2 C_1 - 2\ell_{33}C_4 - 2\ell_{33}C_7 - 2\ell_{32}C_{14}\cos\alpha_1$$
$$- 2\ell_{32}C_{16}\cos\alpha_2)\dot{u}_{br}$$

$$+ (2\ell_4 C_3 - 2\ell_5 C_6)\dot{w}_a + [-2\ell_4 C_3 + 2\ell_5 C_6 - \ell_{24}(C_{17}+C_{18})$$
$$- 2\ell_{26}C_{18} + (-\ell_{22}+\ell_{27}+\ell_{25})C_{10} + \ell_{23}(C_{17}+C_{18})]\dot{w}_{br}$$

$$+ \ell_{24}(C_{17}+C_{18})\dot{w}_{d1} + (2\ell_{26}C_{18})\dot{w}_{d2} + (-\ell_{23}(C_{17}+C_{18}))\dot{w}_{d3}$$

$$+ (\ell_{22}C_{10})\dot{w}_{c1} + (-\ell_{27}C_{10})\dot{w}_{c2} + (-\ell_{25}C_{10})\dot{w}_{c3}$$

$$+ (\ell_2\ell_1 C_1 + 2\ell_{33}\ell_7 C_4 + 2\ell_{33}\ell_7 C_7 - 2\ell_4(\ell_3+\ell_4)C_3$$
$$+ 2\ell_5(\ell_3-\ell_5)C_6 + 2\ell_{32}\ell_{15}C_{14}\cos\alpha_1$$
$$+ 2\ell_{32}\ell_{15}C_{16}\cos\alpha_2)\dot{\beta}_a$$

$$+ [\ell_2^2 C_1 + 2\ell_{33}^2 C_4 + 2\ell_{33}^2 C_7 + 2\ell_4^2 C_3 + 2\ell_5^2 C_6$$

$$+ 2\ell_{32}^2 C_{14} \cos \alpha_1 + 2\ell_{32}^2 C_{16} \cos \alpha_2 + \ell_{24}^2 C_{17}$$

$$+ \ell_{24}^2 C_{18} + 2\ell_{26}^2 C_{18} + \ell_{23}^2 C_{17} + \ell_{23}^2 C_{18}$$

$$+ (\ell_{23}^2 + \ell_{27}^2 + \ell_{25}^2) C_{10}] \dot{\beta}_{br}$$

$$+ (\ell_{22}\ell_{35} C_{10}) \dot{\beta}_{c1} + (-\ell_{35}\ell_{27} C_{10}) \dot{\beta}_{c2} + (-\ell_{25}\ell_{35} C_{10}) \dot{\beta}_{c3}$$

$$- \ell_{21}(RA_1 + RA_2 + RA_3) = 0 \qquad (B.2.6)$$

Longitudinal - Front Frame

$$m_b \ddot{u}_{bf} + (-K_1 - 2K_4 - 2K_7) u_a + (K_1 + 2K_4 + 2K_7) u_{bf}$$

$$+ (-\ell_1 K_1 - 2\ell_7 K_4 - 2\ell_7 K_7) \dot{\beta}_a$$

$$+ (-\ell_2 K_1 - 2\ell_{33} K_4 - 2\ell_{33} K_7) \beta_{bf}$$

$$+ (-C_1 - 2C_4 - 2C_7 - 2C_{14} \cos \alpha_1 - 2C_{16} \cos \alpha_2) \dot{u}_a$$

$$+ (C_1 + 2C_4 + 2C_7 + 2C_{14} \cos \alpha_1 + 2C_{16} \cos \alpha_2) \dot{u}_{bf}$$

$$+ (-\ell_1 C_1 - 2\ell_7 C_4 - 2\ell_7 C_7 - 2\ell_{15} C_{14} \cos \alpha_1$$

$$- 2\ell_{15} C_{16} \cos \alpha_2) \dot{\beta}_a$$

$$+ (-\ell_2 C_1 - 2\ell_{33} C_4 - 2\ell_{33} C_7 - 2\ell_{32} C_{14} \cos \alpha_1$$

$$- 2\ell_{32} C_{16} \cos \alpha_2) \dot{\beta}_{bf}$$

$$- (RA_4 + RA_5 + RA_6) = 0 \qquad (B.2.7)$$

Vertical - Front Frame

$$m_b \ddot{w}_{bf} + (-2K_3 - 2K_6) w_a + (2K_3 + 2K_6 + 6K_9 + 3K_{10}) w_{bf}$$

$$+ (-K_{10}) w_{c4} + (-K_{10}) w_{c5} + (-K_{10}) w_{c6}$$

$$+ (-2K_9) w_{d4} + (-2K_9) w_{d5} + (-2K_9) w_{d6}$$

$$+ [-2(\ell_3+\ell_4)K_3 - 2(\ell_3-\ell_5)K_6]\beta_a$$

$$+ [2\ell_4K_3 - 2\ell_5K_6 + 2(-\ell_{23}+\ell_{26}+\ell_{24})K_9$$

$$+ (-\ell_{25}-\ell_{27}+\ell_{22})K_{10}]\beta_{bf}$$

$$+ (\ell_{35}K_{10})\beta_{c4} + (\ell_{35}K_{10})\beta_{c5} + (\ell_{35}K_{10})\beta_{c6}$$

$$+ (-2C_3 - 2C_6)\dot{w}_a + (2C_3 + 2C_6 + 2C_{17} + 4C_{18})\dot{w}_{bf}$$

$$+ (-C_{17}-C_{18})\dot{w}_{d4} + (-2C_{18})\dot{w}_{d5} + (-C_{18}-C_{17})\dot{w}_{d6}$$

$$+ (-C_{10})\dot{w}_{c4} + (-C_{10})\dot{w}_{c5} + (-C_{10})\dot{w}_{c6}$$

$$+ [-2(\ell_3+\ell_4)C_3 - 2(\ell_3-\ell_5)C_6]\dot{\beta}_a$$

$$+ [2\ell_4C_3 - 2\ell_5C_6 + (-\ell_{23}+\ell_{24})C_{17} + (-\ell_{23}+\ell_{26}+\ell_{24})C_{18}$$

$$+ (-\ell_{25}-\ell_{27}+\ell_{22})C_{10}]\dot{\beta}_{bf}$$

$$+ \ell_{35}C_{10}\dot{\beta}_{c4} + \ell_{35}C_{10}\dot{\beta}_{c5} + \ell_{35}C_{10}\dot{\beta}_{c6} = 0 \qquad (B.2.8)$$

Pitch - Front Frame

$$I_{b\beta}\ddot{\beta}_{bf} + (\ell_2K_1 + 2\ell_{33}K_4 + 2\ell_{33}K_7)u_a$$

$$+ (-\ell_2K_1 - 2\ell_{33}K_4 - 2\ell_{33}K_7)u_{bf}$$

$$+ [-2\ell_4K_3 + 2\ell_5K_6]w_a + [2\ell_4K_3 - 2\ell_5K_6$$

$$+ 2(-\ell_{23}+\ell_{26}+\ell_{24})K_9 + (-\ell_{25}-\ell_{27}+\ell_{22})K_{10}]w_{bf}$$

$$+ (\ell_{25}K_{10})w_{c4} + (\ell_{27}K_{10})w_{c5} + (-\ell_{22}K_{10})w_{c6}$$

$$+ (2\ell_{23}K_9)w_{d4} + (-2\ell_{26}K_9)w_{d5} + (-2\ell_{24}K_9)w_{d6}$$

$$+ [\ell_2\ell_1K_1 + 2\ell_{33}\ell_7K_4 + 2\ell_{33}\ell_7K_7 - 2\ell_4(\ell_3+\ell_4)K_3$$

$$+ 2\ell_5(\ell_3 -\ell_5)K_6]\beta_a$$

$$+ [\ell_2^2 K_1 + 2\ell_{33}^2 K_4 + 2\ell_{33}^2 K_7 + 2\ell_4^2 K_4 + 2\ell_5^2 K_6$$

$$+ 2(\ell_{23}^2 + \ell_{26}^2 + \ell_{24}^2) K_9 + (\ell_{25}^2 + \ell_{27}^2 + \ell_{22}^2) K_{10}] \beta_{bf}$$

$$+ [-\ell_{25}\ell_{35} K_{10}] \beta_{c4} + [-\ell_{27}\ell_{35} K_{10}] \beta_{c5} + [\ell_{22}\ell_{35} K_{10}] \beta_{c6}$$

$$+ [\ell_2 C_1 + 2\ell_{33} C_4 + 2\ell_{33} C_7 + 2\ell_{32} C_{14} \cos \alpha_1$$

$$+ 2\ell_{32} C_{16} \cos \alpha_2] \dot{u}_a$$

$$+ (-\ell_2 C_1 - 2\ell_{33} C_4 - 2\ell_{33} C_7 - 2\ell_{32} C_{14} \cos \alpha_1$$

$$- 2\ell_{32} C_{16} \cos \alpha_2) \dot{u}_{bf}$$

$$+ (-2\ell_4 C_3 + 2\ell_5 C_6) \dot{w}_a + [2\ell_4 C_3 - 2\ell_5 C_6 - \ell_{23}(C_{17} + C_{18})$$

$$+ 2\ell_{26} C_{18} + \ell_{24}(C_{17} + C_{18}) + (-\ell_{25} - \ell_{27} + \ell_{22}) C_{10}] \dot{w}_{bf}$$

$$+ [\ell_{23}(C_{17} + C_{18})] \dot{w}_{d4} + (-2\ell_{26} C_{18}) \dot{w}_{d5}$$

$$+ [-\ell_{24}(C_{17} + C_{18})] \dot{w}_{d6}$$

$$+ (\ell_{25} C_{10}) \dot{w}_{c4} + (\ell_{27} C_{10}) \dot{w}_{c5} + (-\ell_{22} C_{10}) \dot{w}_{c6}$$

$$+ [\ell_2 \ell_1 C_1 + 2\ell_{33}\ell_7 C_4 + 2\ell_{33}\ell_7 C_7 - 2\ell_4(\ell_3 + \ell_4) C_3$$

$$+ 2\ell_5(\ell_3 - \ell_5) C_6 + 2\ell_{32}\ell_{15} C_{14} \cos \alpha_1$$

$$+ 2\ell_{32}\ell_{15} C_{16} \cos \alpha_2] \dot{\beta}_a$$

$$+ (-\ell_{35}\ell_{25} C_{10}) \dot{\beta}_{c4} + (-\ell_{35}\ell_{27} C_{10}) \dot{\beta}_{c5} + (\ell_{35}\ell_{22} C_{10}) \dot{\beta}_{c6}$$

$$+ [\ell_2^2 C_1 + 2\ell_{33}^2 C_4 + 2\ell_{33}^2 C_7 + 2\ell_4^2 C_3 + 2\ell_5^2 C_6$$

$$+ 2\ell_{32}^2 C_{14} \cos \alpha_1 + \ell_{25}^2 C_{10} + \ell_{27}^2 C_{10} + \ell_{22}^2 C_{10}$$

$$+ 2\ell_{32}^2 C_{16} \cos \alpha_2 + \ell_{23}^2 C_{17} + \ell_{23}^2 C_{18} + 2\ell_{26}^2 C_{18}$$

$$+ \ell_{24}^2 C_{17} + \ell_{24}^2 C_{18}] \dot{\beta}_{bf}$$

$$- \ell_{21}(RA_4 + RA_5 + RA_6) = 0 \qquad (B.2.9)$$

Vertical – Motor No. 1

$$m_c \ddot{w}_{c1} + (-K_{10})w_{br} + (K_{10})w_{c1} + (\ell_{22}K_{10})\beta_{br} + (\ell_{35}K_{10})\beta_{c1}$$

$$+ (-C_{10})\dot{w}_{br} + (C_{10})\dot{w}_{c1} + (\ell_{22}C_{10})\dot{\beta}_{br} + (\ell_{35}C_{10})\dot{\beta}_{c1}$$

$$+ (RW_1) = 0 \qquad (B.2.10)$$

Pitch – Motor No. 1

$$I_{c\beta}\ddot{\beta}_{c1} + (-\ell_{35}K_{10})w_{br} + (\ell_{35}K_{10})w_{c1} + (\ell_{22}\ell_{35}K_{10})\beta_{br}$$

$$+ (\ell_{35}^2 K_{10})\beta_{c1} + (-\ell_{35}C_{10})\dot{w}_{br} + (\ell_{35}C_{10})\dot{w}_{c1}$$

$$+ (\ell_{22}\ell_{35}C_{10})\dot{\beta}_{br} + (\ell_{35}^2 C_{10})\dot{\beta}_{c1} - \ell_{34}(RW_1) = 0 \qquad (B.2.11)$$

Longitudinal – Motor/Wheelset No. 1

$$(m_c + m_d)\ddot{u}_{d1} + (\frac{2f_1}{S})\dot{u}_{d1} + (\frac{2\ell_{20}f_1}{S})\dot{\beta}_{d1} + (RA_1) = 0 \qquad (B.2.12)$$

Vertical – Track/Wheelset No. 1

$$(m_d + m_e)\ddot{w}_{d1} + (-2K_9)w_{br} + (2K_9 + K_e)w_{d1} + 2(\ell_{24}K_9)\beta_{br}$$

$$+ (-C_{17} - C_{18})\dot{w}_{br} + (C_{17} + C_{18} + C_e)\dot{w}_{d1}$$

$$+ [\ell_{24}(C_{17} + C_{18})]\dot{\beta}_{br} - (RW_1) = 0 \qquad (B.2.13)$$

Pitch – Wheelset No. 1

$$I_{d\beta}\ddot{\beta}_{d1} + (\frac{2\ell_{20}f_1}{S})\dot{u}_{d1} + (\frac{2\ell_{20}^2 f_1}{S})\dot{\beta}_{d1} = 0 \qquad (B.2.14)$$

Vertical Motor No. 2

$$m_c \ddot{w}_{c2} + (-K_{10})w_{br} + (K_{10})w_{c2} + (-\ell_{27}K_{10})\beta_{br} + (\ell_{35}K_{10})\beta_{c2}$$

$$+ (-C_{10})\dot{w}_{br} + (C_{10})\dot{w}_{c2} + (-\ell_{27}C_{10})\dot{\beta}_{br} + (\ell_{35}C_{10})\dot{\beta}_{c2}$$

$$+ (RW_2) = 0 \qquad (B.2.15)$$

Pitch - Motor No. 2

$$I_{c\beta}\ddot{\beta}_{c2} + (-\ell_{35}K_{10})w_{br} + (\ell_{35}K_{10})w_{c2} + (-\ell_{35}\ell_{27}K_{10})\beta_{br}$$

$$+ (\ell^2_{35}K_{10})\beta_{c2} + (-\ell_{35}C_{10})\dot{w}_{br} + (\ell_{35}C_{10})\dot{w}_{c2}$$

$$+ (-\ell_{35}\ell_{27}C_{10})\dot{\beta}_{br} + (\ell^2_{35}C_{10})\dot{\beta}_{c2} - \ell_{34}(RW_2) = 0$$

$$(B.2.16)$$

Longitudinal - Motor/Wheelset No. 2

$$(m_c + m_d)\ddot{u}_{d2} + (\frac{2f_1}{S})\dot{u}_{d2} + (\frac{2\ell_{20}f_1}{S})\dot{\beta}_{d2} + (RA_2) = 0 \qquad (B.2.17)$$

Vertical - Track/Wheelset No. 2

$$(m_d + m_e)\ddot{w}_{d2} + (-2K_9)w_{br} + (2K_9+K_e)w_{d2} + (2\ell_{26}K_9)\beta_{br}$$

$$+ (-2C_{18})\dot{w}_{br} + (2C_{18}+C_e)\dot{w}_{d2} + (2\ell_{26}C_{18})\dot{\beta}_{br}$$

$$- (RW_2) = 0 \qquad (B.2.18)$$

Pitch - Wheelset No. 2

$$I_{d\beta}\ddot{\beta}_{d2} + (\frac{2\ell_{20}f_1}{S})\dot{u}_{d2} + (\frac{2\ell^2_{20}f_1}{S})\dot{\beta}_{d2} = 0 \qquad (B.2.19)$$

Vertical - Motor No. 3

$$m_c\ddot{w}_{c3} + (-K_{10})w_{br} + (K_{10})w_{c3} + (-\ell_{25}K_{10})\beta_{br} + (\ell_{35}K_{10})\beta_{c3}$$

$$+ (-C_{10})\dot{w}_{br} + (C_{10})\dot{w}_{c3} + (-\ell_{25}C_{10})\dot{\beta}_{br} + (\ell_{35}C_{10})\dot{\beta}_{c3}$$

$$+ (RW_3) = 0 \qquad (B.2.20)$$

Pitch - Motor No. 3

$$I_{c\beta}\ddot{\beta}_{c3} + (-\ell_{35}K_{10})w_{br} + (\ell_{35}K_{10})w_{c3} + (-\ell_{35}\ell_{25}K_{10})\beta_{br}$$

$$+ (\ell^2_{35}K_{10})\beta_{c3} + (-\ell_{35}C_{10})\dot{w}_{br} + (\ell_{35}C_{10})\dot{w}_{c3}$$

$$+ (-\ell_{35}\ell_{25}C_{10})\dot{\beta}_{br} + (\ell^2_{35}C_{10})\dot{\beta}_{c3} - \ell_{34}(RW_3) = 0$$

$$(B.2.21)$$

Longitudinal - Motor/Wheelset No. 3

$$(m_c + m_d)\ddot{u}_{d3} + (\frac{2f_1}{S})\dot{u}_{d3} + (\frac{2\ell_{20}f_1}{S})\dot{\beta}_{d3} + (PA_3) = 0 \qquad (B.2.22)$$

Vertical - Track/Wheelset No. 3

$$(m_d + m_e)\ddot{w}_{d3} + (-2K_9)w_{br} + (2K_9+K_3)w_{d3} + (-2\ell_{23}K_9)\beta_{br}$$

$$+ (-C_{17}-C_{18})\dot{w}_{br} + (C_{17}+C_{18}+C_e)\dot{w}_{d3}$$

$$+ [-\ell_{23}(C_{17}+C_{18})]\dot{\beta}_{br} - (RW_3) = 0 \qquad (B.2.23)$$

Pitch - Wheelset No. 3

$$I_{d\beta}\ddot{\beta}_{d3} + (\frac{2\ell_{20}f_1}{S})\dot{u}_{d3} + (\frac{2\ell_{20}^2f_1}{S})\dot{\beta}_{d3} = 0 \qquad (B.2.24)$$

Vertical - Motor No. 4

$$m_c\ddot{w}_{c4} + (-K_{10})w_{bf} + (K_{10})w_{c4} + (\ell_{25}K_{10})\beta_{bf} + (-\ell_{35}K_{10})\beta_{c4}$$

$$+ (-C_{10})\dot{w}_{bf} + (C_{10})\dot{w}_{c4} + (\ell_{25}C_{10})\dot{\beta}_{bf} + (-\ell_{35}C_{10})\dot{\beta}_{c4}$$

$$+ (RW_4) = 0 \qquad (B.2.25)$$

Pitch - Motor No. 4

$$I_{c\beta}\ddot{\beta}_{c4} + (\ell_{35}K_{10})w_{bf} + (-\ell_{35}K_{10})w_{c4} + (-\ell_{35}\ell_{25}K_{10})\beta_{bf}$$

$$+ (\ell_{35}^2K_{10})\beta_{c4} + (\ell_{35}C_{10})\dot{w}_{bf} + (-\ell_{35}C_{10})\dot{w}_{c4}$$

$$+ (-\ell_{35}\ell_{25}C_{10})\dot{\beta}_{bf} + (\ell_{35}^2C_{10})\dot{\beta}_{c4} + \ell_{34}(RW_4)=0 \qquad (B.2.26)$$

Longitudinal - Motor/Wheelset No. 4

$$(m_c + m_d)\ddot{u}_{d4} + (\frac{2f_1}{S})\dot{u}_{d4} + (\frac{2\ell_{20}f_1}{S})\dot{\beta}_{d4} + (RA_4) = 0 \qquad (B.2.27)$$

Vertical - Track/Wheelset No. 4

$$(m_d + m_e)\ddot{w}_{d4} + (-2K_9)w_{bf} + (2K_9+K_e)w_{d4} + (2\ell_{23}K_9)\beta_{bf}$$

$$+ (-C_{18}-C_{17})\dot{w}_{bf} + (C_{18}+C_{17}+C_e)\dot{w}_{d4}$$

$$+ [\ell_{23}(C_{18}+C_{17})]\dot{\beta}_{bf} - (RW_4) = 0 \qquad (B.2.28)$$

Pitch - Wheelset No. 4

$$I_{d\beta}\ddot{\beta}_{d4} + (\frac{2\ell_{20}f_1}{S})\dot{u}_{d4} + (\frac{2\ell_{20}^2 f_1}{S})\dot{\beta}_{d4} = 0 \qquad (B.2.29)$$

Vertical - Motor No. 5

$$m_c\ddot{w}_{c5} + (-K_{10})w_{bf} + (K_{10})w_{c5} + (\ell_{27}K_{10})\beta_{bf} + (-\ell_{35}K_{10})\beta_{c5}$$

$$+ (-C_{10})\dot{w}_{bf} + (C_{10})\dot{w}_{c5} + (\ell_{27}C_{10})\dot{\beta}_{bf} + (-\ell_{35}C_{10})\dot{\beta}_{c5}$$

$$+ (RW_5) = 0 \qquad (B.2.30)$$

Pitch - Motor No. 5

$$I_{c\beta}\ddot{\beta}_{c5} + (\ell_{35}K_{10})w_{bf} + (-\ell_{35}K_{10})w_{c5} + (-\ell_{35}\ell_{27}K_{10})\beta_{bf}$$

$$+ (\ell_{35}^2 K_{10})\beta_{c5} + (\ell_{35}C_{10})\dot{w}_{bf} + (-\ell_{35}C_{10})\dot{w}_{c5}$$

$$+ (-\ell_{35}\ell_{27}C_{10})\dot{\beta}_{bf} + (\ell_{35}^2 C_{10})\dot{\beta}_{c5} + \ell_{34}(RW_5) = 0 \quad (B.2.31)$$

Longitudinal - Motor/Wheelset No. 5

$$(m_c + m_d)\ddot{u}_{d5} + (\frac{2f_1}{S})\dot{u}_{d5} + (\frac{2\ell_{20}f_1}{S})\dot{\beta}_{d5} + (RA_5) = 0 \qquad (B.2.32)$$

Vertical - Track/Wheelset No. 5

$$(m_d + m_e)\ddot{w}_{d5} + (-2K_9)w_{bf} + (2K_9+K_e)w_{d5} + (-2\ell_{26}K_9)\beta_{bf}$$

$$+ (-2C_{18})\dot{w}_{bf} + (2C_{18}+C_e)\dot{w}_{d5} + (-2\ell_{26}C_{18})\dot{\beta}_{bf}$$

$$- (RW_5) = 0 \qquad (B.2.33)$$

Pitch - Wheelset No. 5

$$I_{d\beta}\ddot{\beta}_{d5} + (\frac{2\ell_{20}f_1}{S})\dot{u}_{d5} + (\frac{2\ell_{20}^2 f_1}{S})\dot{\beta}_{d5} = 0 \qquad (B.2.34)$$

Vertical - Motor No. 6

$$m_c\ddot{w}_{c6} + (-K_{10})w_{bf} + (K_{10})w_{c6} + (-\ell_{22}K_{10})\beta_{bf} + (-\ell_{35}K_{10})\beta_{c6}$$

$$+ (-C_{10})\dot{w}_{bf} + (C_{10})\dot{w}_{c6} + (-\ell_{22}C_{10})\dot{\beta}_{bf} + (-\ell_{35}C_{10})\dot{\beta}_{c6}$$

$$+ (RW_6) = 0 \qquad (B.2.35)$$

Pitch - Motor No. 6

$$I_{c\beta}\ddot{\beta}_{c6} + (\ell_{35}K_{10})w_{bf} + (-\ell_{35}K_{10})w_{c6} + (\ell_{35}\ell_{22}K_{10})\beta_{bf}$$

$$+ (\ell_{35}^2 K_{10})\beta_{c6} + (\ell_{35}C_{10})\dot{w}_{bf} + (-\ell_{35}C_{10})\dot{w}_{c6}$$

$$+ (\ell_{35}\ell_{22}C_{10})\dot{\beta}_{bf} + (\ell_{35}^2 C_{10})\dot{\beta}_{c6} + \ell_{34}(RW_6) = 0 \quad (B.2.36)$$

Longitudinal - Motor/Wheelset No. 6

$$(m_c + m_d)\ddot{u}_{d6} + (\frac{2f_1}{S})\dot{u}_{d6} + (\frac{2\ell_{20}f_1}{S.})\dot{\beta}_{d6} + (RA_6) = 0 \qquad (B.2.37)$$

Vertical - Track/Wheelset No. 6

$$(m_d + m_e)\ddot{w}_{d6} + (-2K_9)w_{bf} + (2K_9+K_e)w_{d6} + (-2\ell_{24}K_9)\beta_{bf}$$

$$+ (-C_{17}-C_{18})\dot{w}_{bf} + (C_{17}+C_{18}+C_e)\dot{w}_{d6}$$

$$+ [\ell_{24}(-C_{17}-C_{18})]\dot{\beta}_{bf} - (RW_6) = 0 \qquad (B.2.38)$$

Pitch - Wheelset No. 6

$$I_{d\beta}\ddot{\beta}_{d6} + (\frac{2\ell_{20}f_1}{S})\dot{u}_{d6} + (\frac{2\ell_{20}^2 f_1}{S})\dot{\beta}_{d6} = 0 \qquad (B.2.39)$$

The equations describing the longitudinal motions (equations (B.2.1) to (B.2.39)) are of the general form:

$$[\tilde{A}] \{\ddot{z}\} + [\tilde{C}]\{\dot{z}\} + [\tilde{B}]\{z\} + \{R\} = \{0\} \qquad (B.2.40)$$

$$\underset{39 \times 39}{} \quad \underset{39 \times 1}{} \quad \underset{39 \times 1}{}$$

where $\tilde{A}$ is the inertia matrix

$\tilde{C}$ is the damping matrix

$\tilde{B}$ is the stiffness matrix

and R is the vector of internal reactions given by:

Mode	Equation No.	Reaction
u_a	B.2.1	0
w_a	.2	0
β_a	.3	0
u_{br}	.4	$-(RA_1+RA_2+RA_3)$
w_{br}	.5	0
β_{br}	.6	$-\ell_{21}(RA_1+RA_2+RA_3)$
u_{bf}	.7	$-(RA_4+RA_5+RA_6)$
w_{bf}	.8	0
β_{bf}	.9	$-\ell_{21}(RA_4+RA_5+RA_6)$
w_{cl}	.10	RW_1
β_{cl}	.11	$-\ell_{34}(RW_1)$
u_{dl}	.12	RA_1
w_{dl}	.13	$-RW_1$
β_{dl}	.14	0
w_{c2}	.15	RW_2

Mode	Equation No.	Reaction
β_{c2}	B.2.16	$-\ell_{34}(RW_2)$
u_{d2}	.17	RA_2
w_{d2}	.18	$-RW_2$
β_{d2}	.19	$0.$
w_{c3}	.20	RW_3
β_{c3}	.21	$-\ell_{34}(RW_3)$
u_{d3}	.22	RA_3
w_{d3}	.23	$-RW_3$
β_{d3}	.24	0
w_{c4}	.25	RW_4
β_{c4}	.26	$\ell_{34}(RW_4)$
u_{d4}	.27	RA_4
w_{d4}	.28	$-RW_4$
β_{d4}	.29	0
w_{c5}	.30	RW_5
β_{c5}	.31	$\ell_{34}(RW_5)$
u_{d5}	.32	RA_5
w_{d5}	.33	$-RW_5$
β_{d5}	.34	0
w_{c6}	.35	RW_6
β_{c6}	.36	$\ell_{34}(RW_6)$
u_{d6}	.37	RA_6
w_{d6}	.38	$-RW_6$
β_{d6}	.39	0

The reactions are eliminated from the equations using the method of substitution as described below. For simplicity the equations are designated by their corresponding numbers (i.e., 1 refers to equation (B.2.1), 2 to equation (B.2.2),..., and so on).

$$1 = 1$$
$$2 = 2$$
$$3 = 3$$
$$4 = 4 + (12+17+22)$$
$$5 = 5$$
$$6 = 6 + \ell_{21}(12+17+22)$$
$$7 = 7 + (27+32+37)$$
$$8 = 8$$
$$9 = 9 + \ell_{21}(27+32+37)$$
$$10 = 11 + \ell_{34}(10)$$
$$11 = 10 + 13$$
$$12 = 14$$
$$13 = 16 + \ell_{34}(15)$$
$$14 = 15 + 18$$
$$15 = 19$$
$$16 = 21 + \ell_{34}(20)$$
$$17 = 20 + 23$$
$$18 = 24$$
$$19 = 26 - \ell_{34}(25)$$
$$20 = 25 + 28$$

$$21 = 29$$

$$22 = 31 - \ell_{34}(30)$$

$$23 = 30 + 33$$

$$24 = 34$$

$$25 = 36 - \ell_{34}(35)$$

$$26 = 35 + 38$$

$$27 = 39.$$

After the elimination of the internal reactions, the system of equations (B.2.40) becomes

$$\underset{27 \times 39}{[A\ ]} \underset{39 \times 1}{\{\ddot{z}\}} + [C\ ]\{\dot{z}\} + [B\ ]\{z\} = \{0\} \tag{B.2.41}$$

That is a system of twenty-seven equations in thirty-nine unknowns, only twenty-seven of which are independent. The relation between all the unknown displacements and the independent ones will be given by the transformation matrix [D] based on the equations of constraints. The equations defining the constraints are:

(A)   <u>Constraints between Wheelsets and Frames</u>

$$u_{d1} = u_{br} + \ell_{21}\beta_{br}$$

$$u_{d2} = u_{br} + \ell_{21}\beta_{br}$$

$$u_{d3} = u_{br} + \ell_{21}\beta_{br}$$

$$u_{d4} = u_{bf} + \ell_{21}\beta_{bf}$$

$$u_{d5} = u_{bf} + \ell_{21}\beta_{bf}$$

$$u_{d6} = u_{bf} + \ell_{21}\beta_{bf}$$

(B)   Constraints between Motors and Wheelsets

$$u_{d1} = u_{c1}$$

$$u_{d2} = u_{c2}$$

$$u_{d3} = u_{c3}$$

$$u_{d4} = u_{c4}$$

$$u_{d5} = u_{c5}$$

$$u_{d6} = u_{c6}$$

These relations have already been satisfied by combining the wheelset and motor equations

$$w_{c1} = w_{d1} + \ell_{34}\beta_{c1}$$

$$w_{c2} = w_{d2} + \ell_{34}\beta_{c2}$$

$$w_{c3} = w_{d3} + \ell_{34}\beta_{c3}$$

$$w_{c4} = w_{d4} - \ell_{34}\beta_{c4}$$

$$w_{c5} = w_{d5} - \ell_{34}\beta_{c5}$$

$$w_{c6} = w_{d6} - \ell_{34}\beta_{c6}$$

The Transformation Matrix [D]

This matrix gives the relation between all the variables and the independent variables, based on the equations of constraints.   The matrix [D] is given in Table (B.2).

The relation between all the displacements $\{z\}$ and the generalized coordinates $\{x\}$ is given by

TABLE (B.2)

THE TRANSFORMATION MATRIX [D]

GENERALIZED COORDINATES

COORD.	1 u_a	2 v_a	3 θ_a	4 u_{br}	5 w_{br}	6 θ_{br}	7 u_{bf}	8 w_{bf}	9 θ_{bf}	10 u_{c1}	11 w_{c1}	12 θ_{c1}	13 u_{c2}	14 w_{d2}	15 θ_{d2}	16 θ_{c3}	17 w_{d3}	18 θ_{d3}	19 θ_{c4}	20 w_{d4}	21 θ_{d4}	22 θ_{c5}	23 w_{d5}	24 θ_{d5}	25 θ_{c6}	26 w_{d6}	27 θ_{d6}
1 u_a	1																										
2 v_a		1																									
3 θ_a			1																								
4 u_{br}				1																							
5 w_{br}					1																						
6 θ_{br}						1																					
7 u_{bf}							1																				
8 w_{bf}								1																			
9 θ_{bf}									1																		
10 w_{c1}					l_{21}					$-l_{34}$																	
11 θ_{c1}											1																
12 u_{d1}				1								1															
13 w_{d1}																											
14 θ_{d1}																											
15 w_{c2}						l_{21}							$-l_{34}$														
16 θ_{c2}																											
17 u_{d2}														1													
18 w_{d2}																											
19 θ_{d2}																											
20 w_{c3}						$-l_{21}$																					
21 θ_{c3}																											
22 u_{d3}																											
23 w_{d3}																											
24 θ_{d3}																											
25 w_{c4}									$-l_{21}$										$-l_{34}$								
26 θ_{c4}							1																				
27 u_{d4}																											
28 w_{d4}																											
29 θ_{d4}																											
30 w_{c5}									l_{21}																		
31 θ_{c5}																											
32 u_{d5}																							1				
33 w_{d5}																								1			
34 θ_{d5}																											
35 w_{c6}									l_{21}																$-l_{34}$	1	
36 θ_{c6}																											
37 u_{d6}																											
38 w_{d6}																											1
39 θ_{d6}																											1

$$\{z\} = [D] \{x\}$$
$$39 \times 1 \quad 39 \times 27 \quad 27 \times 1 \qquad (B.2.42)$$

Substituting for $\{z\}$ from equation (B.2.42) back in equation (B.2.41) we get

$$[A] \quad [D] \quad \{x\} + [C][D]\{\dot{x}\} + [B][D]\{x\} = \{0\} \quad (B.2.43)$$
$$27 \times 39 \quad 39 \times 27 \quad 27 \times 1$$

Which after carrying the matrix multiplication gives the following system of twenty-seven equations in twenty-seven independent coordinates.

$$[AD] \quad \{\ddot{x}\} + [CD]\{\dot{x}\} + [BD]\{x\} = \{0\} \qquad (B.2.44)$$
$$27 \times 27 \quad 27 \times 1$$

It should be noted that here too, the inertia damping and stiffness matrices ([AD], [CD] and [BD] respectively), are not symmetric due to the presence of the non-conservative creep forces.